

# **NON-NEWTONIAN LOSSES THROUGH DIAPHRAGM VALVES**

**By**

**DIEUDONNE MATANG'A KAZADI**  
**BSc (Chemical Engineering) University of Lubumbashi**

Dissertation submitted in fulfilment of the degree  
**MAGISTER TECHNOLOGIAE**  
In the Department of Chemical Engineering  
(Flow Process Research Centre)  
Cape Peninsula University of Technology

**Supervisor: Dr. Veruscha Pienaar**  
**Co-supervisor: Prof. Paul T Slatter**

**August 2005**

## ABSTRACT

The prediction of head losses in a pipe system is very important because head losses affect the performance of fluid machinery such as pumps. In a pipe system, two kinds of losses are observed: major losses and minor losses. In Newtonian and non-Newtonian flow, major losses are those that are due to friction in straight pipes and minor losses are those that are due to pipe fittings such as contractions, expansions, bends and valves. Minor losses must be accurately predicted in a pipe system because they are not negligible and can sometimes outweigh major losses (Edwards *et al.*, 1985). There is presently little data for the prediction of non-Newtonian head losses in pipe fittings in the literature and little consensus amongst researchers (Pienaar *et al.*, 2004).

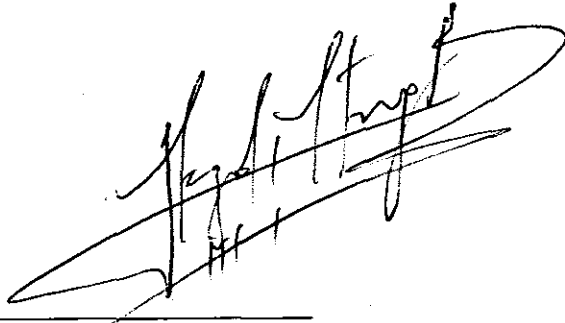
In the case of diaphragm valves, usually, only one loss coefficient value is given in turbulent flow or in laminar flow with no reference to a specific size of the valve, assuming geometrical similarity that would lead to dynamic similarity. However, no one has done a systematic study of various sizes of diaphragm valves from the same manufacturer to establish if this is true. This could be the main reason for discrepancies found in the literature (Hooper, 1981; Perry & Chilton, 1973; Miller, 1978 and Pienaar *et al.*, 2004). This work addresses this issue.

A literature review on the flow of Newtonian and non-Newtonian fluids has been presented. The work of Hooper (1981) on diaphragm valves and the works of Edwards *et al.*, (1985), Banerjee *et al.*, (1994) and Turian *et al.*, (1997) for non-Newtonian fluids in globe and gate valves were found to be relevant to this work. An experimental facility referred to as the Valve test rig was built and commissioned. Diaphragm valves of 40, 50, 65, 80, 100 millimetre nominal bore diameters from the same manufacturer were used. The tests were carried out on these valves in the fully open position. Seven different Newtonian and non-Newtonian materials were tested in each valve. The experimental results are presented in the form of valve loss coefficient ( $k_v$ ) against the Slatter Reynolds number ( $Re_3$ ).

Loss coefficients obtained in this investigation confirmed the general qualitative trend given in the literature that in laminar flow the loss coefficient increases significantly with the decreases of Reynolds number and is a hyperbolic function of Reynolds number. In turbulent flow, the loss coefficient is constant, for any type of fluid, Newtonian or non-Newtonian. It also confirms the general theory that in fittings in general and valves in particular, the transition from laminar to turbulent occurs earlier than in straight pipes. This work also shows that the Slatter Reynolds number is a useful tool and compared to other Reynolds numbers (the Newtonian Reynolds number and the Metzner and Reed generalised Reynolds number), can be used for design purposes. From our analysis, it was established that geometric and dynamic similarity was not achieved in the diaphragm valves tested.

## DECLARATION

I, Dieudonné Matang'a Kazadi hereby declare that this thesis represent my own unaided work and has not been submitted for a degree at another university. Further more it represents my own opinions and not necessarily those of the Cape Peninsula University of Technology.

A handwritten signature in black ink, appearing to read 'Dieudonné Matang'a Kazadi', written over a horizontal line.

Dieudonné Matang'a Kazadi

## DEDICATION

I dedicate this work to my parents: Papa Kasongo and Maman Milemba who continuously insisted that I studied and encouraged me during my studies.

To my wife Therese (Théthé) and son Ronald Kazadi for their encouragement, moral support and affection.

To my brothers, sisters and all my future children.

### *Psalm 23:*

*“The Lord is my shepherd; I shall not want. He maketh me to lie down in green pastures; he leadeth me beside still waters. He restoreth my soul; he leadeth me in paths of righteousness for his name's sake. Yea, though I walk through the valley of the shadow of death, I will fear no evil: for thou art with thy rod; thy staff, and me they comfort me. Thou preparest a table before me in the presence of mine enemies; thou hast anointed my head with oil; my cup runneth over. Surely, goodness and loving-kindness shall follow me all the days of my life; and I will dwell in the house of the Lord for the length of the days”.*

## ACKNOWLEDGEMENTS

I thank Prof. P. Slatter for the opportunity he gave me to complete my studies within his research unit.

I thank Dr. V. Pienaar for accepting to supervise this work, and for all her support during the completion of my studies. I also thank all the staff, colleagues and students of the Flow Process Research Centre for their assistance, encouragement and friendship during the completion of this work.

Thank you also to the Cape Peninsula University of Technology through its R&D Department and the NRF for their financial assistance without which I could not have completed this work.

Thank you to Thandiwe Caroline Ngamlana of the writing centre for editing this work.

## TABLE OF CONTENTS

ABSTRACT .....	I
DECLARATION .....	III
DEDICATION.....	IV
ACKNOWLEDGEMENTS.....	V
TABLE OF CONTENTS .....	VI
LIST OF TABLES.....	X
LIST OF FIGURES.....	X
NOMENCLATURE.....	XIII
 <b>CHAPTER 1</b>	
INTRODUCTION .....	1.1
1.1 Introduction.....	1.1
1.2 Statement of research problem.....	1.1
1.3 Objectives of the Study.....	1.2
1.4 Research design and methodology.....	1.2
1.5 Delineation.....	1.2
1.6 Importance and Benefits .....	1.3
 <b>CHAPTER 2</b>	
LITERATURE REVIEW.....	2.1
2.1 INTRODUCTION.....	2.1
2.2 Classification of fluids.....	2.1
2.2.1 Newtonian Fluids.....	2.1
2.2.2 Non-Newtonian Fluids.....	2.2

2.2.3 Time Independent Non-Newtonian Fluids.....	2.3
2.2.4 Time Dependent Non-Newtonian Fluids.....	2.5
2.2.5 Rheology.....	2.7
<b>2.3 FLOW IN STRAIGHT PIPES.....</b>	<b>2.10</b>
2.3.1 Shear Stress Distribution in a Straight Pipe.....	2.10
2.3.2 Energy Loss in Straight Pipe.....	2.10
2.3.3 Newtonian Transition from Laminar to Turbulent and Reynolds Number .....	2.11
2.3.4 Newtonian Laminar Flow in Straight Pipes.....	2.11
2.3.5 Newtonian Turbulent Flow in Straight Pipes.....	2.12
2.3.6 Non-Newtonian Flow in Straight Pipes .....	2.15
2.3.7 Non –Newtonian Transition from Laminar to Turbulent Flow and Non-Newtonian Reynolds Numbers.....	2.15
2.3.8 Non –Newtonian Laminar Flow in Straight Pipes.....	2.19
<b>2.4 Rheological characterisation.....</b>	<b>2.21</b>
<b>2.5 Flow in Pipe Fittings and Valves.....</b>	<b>2.24</b>
2.5.1 Classification of Fittings.....	2.24
2.5.2 Determination of Newtonian and Non-Newtonian Losses Across Pipe Fittings and Valves .....	2.24
<b>2.6 FLOW IN VALVES .....</b>	<b>2.26</b>
2.6.1 Definition of Valves.....	2.26
2.6.2 Classification of Valves.....	2.26
2.6.3 Diaphragm Valves .....	2.27
2.6.4 Newtonian and non-Newtonian flow in valves.....	2.31
<b>2.7 DYNAMIC SIMILARITY .....</b>	<b>2.43</b>
2.7.1 Geometric Similarity.....	2.43
2.7.2 Kinematic Similarity.....	2.43
2.7.3 Dynamic Similarity.....	2.44
2.7.4 The Application of Dynamic similarity for Non-Newtonian Fluid Flows in Valves .....	2.44
<b>2.8 Conclusion .....</b>	<b>2.45</b>
<b>2.9 RESEARCH ASPECT IDENTIFIED .....</b>	<b>2.46</b>
 <b>CHAPTER 3</b>	
<b>EXPERIMENTAL WORK.....</b>	<b>3.1</b>
<b>3.1 INTRODUCTION .....</b>	<b>3.1</b>
<b>3.2 DESCRIPTION OF THE TEST LOOP.....</b>	<b>3.1</b>



3.3 INSTRUMENTATION .....	3.3
3.3.1 Pipes & Valves.....	3.3
3.3.2 Pressure Lines, Pressure Lines Board, Tappings and Pods .....	3.8
3.3.3 Pressure Transducers .....	3.10
3.3.4 The Hand Held Communicator.....	3.10
3.3.5 The Data Acquisition Unit or Data Logger.....	3.10
3.3.6 Computer and Software .....	3.11
3.3.7 Flow meters.....	3.11
3.3.8 Tank and Mixer.....	3.11
3.3.9 Pump .....	3.11
3.3.10 Manometers.....	3.11
3.3.11 Pressure Gauges .....	3.12
3.3.12 Temperature probes .....	3.12
3.4 EXPERIMENTAL PROCEDURE .....	3.12
3.4.1 Calibration.....	3.12
3.4.2 Experimental Test Method (Valve Pressure Drop Test and Straight Pipe Test or Tube Viscometry) .....	3.18
3.5 EXPERIMENTAL ERRORS .....	3.23
3.5.1 Error Theory.....	3.23
3.5.2 Gross Errors .....	3.23
3.5.3 Systematic or Cumulative Errors .....	3.23
3.5.4 Random Errors .....	3.24
3.5.5 Precision and Accuracy.....	3.24
3.5.6 Evaluation of Errors.....	3.24
3.5.7 Error in Measurable Variables .....	3.25
3.5.8 Axial Distance.....	3.25
3.5.9 Weight.....	3.25
3.5.10 Flow Rate.....	3.26
3.5.11 Pressure.....	3.26
3.5.12 Error in derived variables.....	3.26
3.6 MATERIALS TESTED.....	3.35
3.6.1 Introduction.....	3.35
3.6.2 Water.....	3.35
3.6.3 Carboxyl Methyl Cellulose Solution (CMC).....	3.37
3.6.4 Kaolin Slurry.....	3.39
3.7 CONCLUSION.....	3.43
<b>CHAPTER 4</b>	
<b>ANALYSIS OF RESULTS .....</b>	<b>4.1</b>
4.1 Introduction.....	4.1

4.2 Rheological characterisation.....	4.1
4.2.1 Newtonian fluids.....	4.1
4.2.2 Non-Newtonian fluids.....	4.3
4.3 Flow in straight pipes.....	4.7
4.4 Loss coefficients .....	4.9
4.4.1 Procedure for calculating the valve loss coefficient .....	4.9
4.4.2 Graphical presentation of the valve loss coefficient $k_v$ versus Reynolds number .....	4.12
4.5 Effect of Reynolds number on the valve loss coefficient .....	4.19
4.6 Conclusion .....	4.22

## CHAPTER 5

<b>DISCUSSION AND EVALUATION OF RESULTS.....</b>	<b>5.1</b>
5.1 Introduction.....	5.1
5.2 The Literature review.....	5.1
5.3 Experimental test loop .....	5.2
5.4 Instrumentation and machine.....	5.2
5.5 The experimental method .....	5.3
5.6 Materials tested .....	5.3
5.7 Rheological characterisation.....	5.4
5.8 Loss coefficients .....	5.4
5.9 Comparison with literature and originality of this work.....	5.5
5.10 Similarities analysis .....	5.8
5.11 Conclusion .....	5.11

## CHAPTER 6

<b>SUMMARY, CONTRIBUTIONS AND RECOMMENDATIONS.....</b>	<b>6.1</b>
6.1 Introduction.....	6.1
6.2 Summary .....	6.1

6.3 Contributions.....	6.2
6.4 Recommendations.....	6.3
REFERENCES .....	1
APPENDICES.....	1

## LIST OF TABLES

Table 2. 1 Rheological Models available in the literature. (Chhabra & Richardson, 1985) .....	2.8
Table 2. 2 Valves (Pienaar <i>et al.</i> , 2001).....	2.41
Table 2. 3 Loss coefficients for turbulent flow through diaphragm valves (Perry & Chilton, 1973).....	2.42
Table 3. 1 Nominal and internal Dimension of Pipes and Valves.....	3.3
Table 3. 2 Internal dimensions of diaphragm valves tested.....	3.6
Table 3. 3 Calibration constants for different transducers.....	3.15
Table 3. 4 Expected Highest errors and experimental errors in the measurements of the Valve test- rig pipe diameters.....	3.27
Table 3. 6 Highest Expected errors of the Valve loss coefficient.....	3.32
Table 3. 8 Errors of the Valve loss coefficient.....	3.34
Table 3. 9 Physical properties of dry kaolin.....	3.40
Table 3. 10 Chemical properties of dry kaolin.....	3.40
Table 4. 1 Properties of glycerine 100% tested.....	4.2
Table 4. 2 Properties of glycerine 75% tested.....	4.3
Table 4. 3 Fluid properties of CMC 5% tested.....	4.4
Table 4. 4 Fluid properties of CMC 8% tested.....	4.4
Table 4. 5 Fluids properties of Kaolin 10% tested.....	4.6
Table 4. 6 Fluids properties of Kaolin 13% tested.....	4.6
Table 4. 7 Summary of $C_v$ and $k_v$ values obtained in this work.....	4.19
Table 5. 1 Transition by intersection for the different valves.....	5.5
Table 5. 2 Comparison of loss coefficients of this work with literature.....	5.6

## LIST OF FIGURES

Figure 2. 1 Newtonian fluid flow curve.....	2.2
Figure 2. 2 Non-Newtonian fluids flow curves (Paterson & Cooke, 1999).....	2.6
Figure 2. 4 Definition of the loss coefficient (Miller, 1978).....	2.26
Figure 2. 5 The weir or dam type diaphragm valve.....	2.30

Figure 2. 6 The straight-through type diaphragm valve .....	2.30
Figure 2. 7 Typical representation of $k_v$ vs. $Re$ for a fitting (Pienaar <i>et al</i> , 2001).....	2.32
Figure 2. 8 Diagram illustrating the calculation of valve loss coefficient .....	2.34
Figure 2. 9 Loss coefficient vs. valve opening (Miller, 1978).....	2.41
Figure 2. 10 Diagram illustrating the calculation of valve loss coefficient .....	4.11
Figure 3. 2 Diaphragm valve .....	3.4
Figure 3. 3 Connection of diaphragm valves with pipes. ....	3.4
Figure 3. 4 Internal structure of the valve in the fully open position.....	3.5
Figure 3. 5 Internal dimension of the 80 mm nominal bore diaphragm valve.....	3.6
Figure 3. 6 Schematic diagram of the Pressure Lines Board .....	3.9
Figure 3. 7 Connection of the PLB (the rectangular central part) to Pods and Pressure Transducers. ....	3.9
Figure 3. 8 Calibration regression lines of the DP cell of 6kPa span range showing calibration regression lines for 0-6kPa range and 0-1kPa range.....	3.13
Figure 3. 9 Calibration regression line of a Point pressure transducer of 130 kPa.....	3.14
Figure 3. 10 Calibration regression line of Load Cell .....	3.16
Figure 3. 11 Calibration regression line for the Krohne flow meter.....	3.17
Figure 3. 12 Over view of the Valve test- rig direction valves. Valves (1&2) are on-off valves to direct the mainstream flow .....	3.20
Figure 3. 13 DP Cells position in the American Standard Method .....	3.22
Figure 3. 14 Comparison of variation of principal parameters of the Valve test rig .....	3.30
Figure 3. 15 Comparison of water test results with Colebrook & White equation.....	3.36
Figure 3. 16 Comparison of water test results with Colebrook & White equation in double logarithmic scale .....	3.37
Figure 3. 17 Typical valve pressure drop curve of water in a 40 mm Diaphragm valve ( $V=1.79$ m/s and $Re_3=75753.99$ ) .....	3.37
Figure 3. 18 Straight pipe test of CMC 5% in three pipe diameters.....	3.38
Figure 3. 19 Typical valve pressure drop curve of CMC 5% in a 40 mm nominal bore Diaphragm valve ( $V=3.04$ m/s and $Re_3=0.042$ ) .....	3.39
Figure 3. 20 Particle Size Distribution (PSD) Graph for kaolin powder.....	3.41
Figure 3. 21 Straight pipe test for kaolin 10% in three pipes diameters.....	3.42
Figure 3. 22 Typical valve pressure drop curve of kaolin 13% in a 65 mm Diaphragm valve ( $V=0.029$ m/s and $Re_3=4.30$ ) .....	3.43
Figure 4. 1 Flow curve of Glycerine 100% at an average temperature of 21 °C.....	4.2
Figure 4. 2 Flow curve of CMC 5% .....	4.4
Figure 4. 3 Flow curve of kaolin 13 % .....	4.6
Figure 4. 4 Comparison of experimental values of the friction factor in laminar flow for different fluids in straight pipe of diameter 42.12 mm ID pipe. ....	4.8
Figure 4. 10 Comparison of loss coefficient using $Re_3$ and $Re_{MR}$ for a Pseudoplastic fluid. .....	4.20
Figure 4. 11 Comparison of loss coefficient using $Re_3$ and $Re_{MR}$ for a yield pseudoplastic fluid. ....	4.22

---

Figure 5. 1 Comparison of this work turbulent flow valve loss coefficients to valve loss coefficients found in the literature .....	5.7
Figure 5. 2 Variation of loss coefficient in laminar and turbulent flow .....	5.9
Figure 5. 3 Diaphragm valve loss coefficients for CMC 8% in laminar flow .....	5.10
Figure 5. 4 Diaphragm valves loss coefficients for water in turbulent flow.....	5.10

## NOMENCLATURE

Symbol	Description	Unit
a	acceleration	$m/s^2$
A	cross sectional area	$m^2$
$C_v$	laminar flow valve loss coefficient	-
D	internal pipe diameter	m
E	sum of mean error squared	-
f	Fanning friction factor	-
g	gravitational acceleration	$m/s^2$
H	head	m
I	intercept	-
K	fluid consistency index	$Pa.s^n$
$K'$	apparent fluid consistency index	$Pa.s^n$
k	hydraulic roughness	m
$k_{\text{fitt}}$	fitting loss coefficient	-
$k_v$	valve loss coefficient	-
L	pipe length	m
$L_e$	equivalent length	m
M	mass	kg
m	slope	-
N	number of data points	-
n	flow behaviour index	-
$n'$	apparent flow behaviour index	-
p	pressure or static pressure	Pa
Q	volumetric flow rate	$m^3/s$
R	radius	m
$Re$	Reynolds number	-
$Re_{\text{crit}}$	Critical Reynolds number at the transition	-
$Re_{MR}$	Metzner & Reed Reynolds number	-
$Re_3$	Slatter Reynolds number	-

$r$	correlation coefficient	-
$r$	radius from the centre line	-
$t$	time	s
$u$	point velocity	m/s
$V$	average velocity	m/s
$z$	elevation from datum	m
$\alpha$	kinetic energy correction factor	-
$\gamma$	shear rate	$s^{-1}$
$\Delta$	difference	-
$\mu$	dynamic viscosity	Pa.s
$\mu'$	apparent or secant viscosity	Pa.s
$\rho$	fluid or slurry density	$kgm^{-3}$
$t$	shear stress	Pa
$\tau_0$	wall shear stress	Pa
$\tau_y$	yield stress	Pa
$\sigma$	standard deviation	-

### Subscripts

o	at the wall
ann	annulus
calc	calculated
US	upstream
DS	downstream
fitt	fitting
v	valve
obs	observed

max	maximum
m	model
p	prototype



# CHAPTER 1

## CHAPTER 1 INTRODUCTION

### 1.1 INTRODUCTION

The prediction of head losses in a pipe system is very important because head losses affect the performance of fluid machinery such as pumps. In a pipe system, two kinds of losses are observed: major losses and minor losses. In Newtonian and non-Newtonian flow, major losses are those that are due to friction in straight pipes and minor losses are those that are due to pipe fittings such as contractions, expansions, bends and valves. Minor losses must be accurately predicted in a pipe system because they are not negligible and can sometimes outweigh major losses (Edwards *et al.*, 1985). There is presently little data for the prediction of non-Newtonian head losses in pipe fittings in the literature and little consensus among researchers (Pienaar *et al.*, 2004).

In the case of diaphragm valves, usually, only one loss coefficient value is given in turbulent flow or in laminar flow with no reference to a specific size of the valve, assuming geometrical similarity that would lead to dynamic similarity. However, no one has done a systematic study of various sizes of diaphragm valves from the same manufacturer to establish if this is true. This could be the main reason for discrepancies found in the literature (Hooper, 1981; Perry & Chilton, 1973; Miller, 1978 and Pienaar *et al.*, 2004). This work addresses this issue.

This investigation gives loss coefficients data for diaphragm valves and analyses dynamic similarities of diaphragm valves, using the hydraulic grade line (HGL) approach, in the different flow regimes. The diaphragm valve is used owing to its importance and wide usage in the industry dealing with slurries (Brown & Heywood, 1991). This work also contributes to the commissioning, optimisation and verification of the reliability of the new state-of-the-art valve test rig.

### 1.2 STATEMENT OF RESEARCH PROBLEM

There is no experimental loss coefficient data available for a range of diaphragm valves of different sizes from the same manufacturer for both Newtonian and non-Newtonian fluids in laminar, transitional and turbulent flow regimes.

### 1.3 OBJECTIVES OF THE STUDY

The objectives of this study were:

- To commission the Valve test rig.
- To determine the loss coefficients for diaphragm valves of 40, 50, 65, 80 and 100 millimetre nominal bore diameter, in laminar, transitional and turbulent flow for both Newtonian and non-Newtonian fluids using the valve test rig.
- To evaluate dynamic similarity.

### 1.4 RESEARCH DESIGN AND METHODOLOGY

The experimental tests were carried out in the slurry laboratory of the Flow Process Research Centre at the Cape Peninsula University of Technology in Cape Town using the Valve test rig.

Diaphragm valves of 40, 50, 65, 80, 100 millimetre nominal bore diameter were used. The tests were carried out on these valves in the fully open position.

Different materials at different concentrations were used: water and glycerine (100% and 75% volume concentrations) as Newtonian fluids and carboxyl methyl cellulose (CMC)(5% and 8% weight concentrations) and kaolin slurries (10% and 13% volume concentrations) as non-Newtonian materials.

These materials were rheologically characterised by tube viscometry. The hydraulic grade line (HGL) approach was used to determine the valve loss coefficients. In this later approach, each test section as it will be explained later, consisted of two removable pipes of the same diameter in series joined by a diaphragm valve. On each pipe, upstream and downstream of the valve were tapping points where the static pressure drop was measured along the test section. The results for each test were presented in the form of valve loss coefficient ( $k_v$ ) against the Slatter Reynolds number ( $Re_3$ ).

### 1.5 DELINEATION

This work was limited to Newtonian and non-Newtonian fluids flowing through diaphragm valves in laminar, transitional and turbulent flow regimes. Only national trading company (NATCO) diaphragm valves were investigated in the fully open

position. These 5 diaphragm valves were tested in the fully open position only due to time factor and also due to the workload as one of the objectives of this work was to commission the test rig.

Fluids, which have time-dependent and settling behaviour, were not investigated.

## **1.6 IMPORTANCE AND BENEFITS**

This work provides loss coefficients data in laminar, transitional and turbulent flow regimes for non-Newtonian slurries flowing through 5 different sizes diaphragm valves from the same manufacturer. This data can be used directly for practical plant design. It also provides a dynamic similarity study and contributes to the commissioning, optimisation and verification of the reliability of the new Valve test rig.

# CHAPTER 2

## CHAPTER 2 LITERATURE REVIEW

### 2.1 INTRODUCTION

In this chapter, fundamental concepts on fluid classification and fluid rheological characterisation are presented. The relevant theory on fluid flow in straight pipes, pipe fittings and valves is also presented. Both of these are presented in laminar and turbulent flow regimes, with the emphasis on non-Newtonian fluids. The need for an in-depth understanding of the flow phenomena of non-Newtonian fluids through valves is very important in this work, especially through diaphragm valves. This explains the emphasis on flow through diaphragm valves. The theory on dynamic similarity of geometrically similar valves is also presented and its application for non-Newtonian flow in valves.

### 2.2 CLASSIFICATION OF FLUIDS

Generally fluids are classified according to the way they respond to externally applied pressure or to the effects produced on them by the action of shear stress. In this investigation all the fluids tested are assumed to be incompressible fluids and the effects produced by the action of a shear stress is of high interest (Chhabra & Richardson, 1999). These fluids include single-phase liquids, solutions, and pseudo-homogenous mixtures such as slurries that may be treated as a continuum if they are stable (Govier & Aziz, 1972)

In general, fluids belong to one of the three main categories: Newtonian fluids, non-Newtonian fluids and settling slurries (Brown & Heywood, 1991).

#### 2.2.1 Newtonian Fluids

A Newtonian fluid is one in which an infinitesimal shear stress will initiate flow and for which the shear stress is directly proportional to the shear rate.

The flow curve of a Newtonian fluid at a certain temperature and pressure is a straight line passing through the origin. The slope of the flow curve is constant and is the viscosity of the fluid (Chhabra & Richardson, 1999).

The Newtonian fluid flow curve equation is:

$$\tau = \mu_N \dot{\gamma} \quad (2.1)$$

where  $\mu_N$  is the Newtonian viscosity.

Some common examples of Newtonian fluids are: water, mineral oil, glycerine and glycerine-water mixture. Figure 2.1 illustrates the flow curve of a Newtonian fluid.

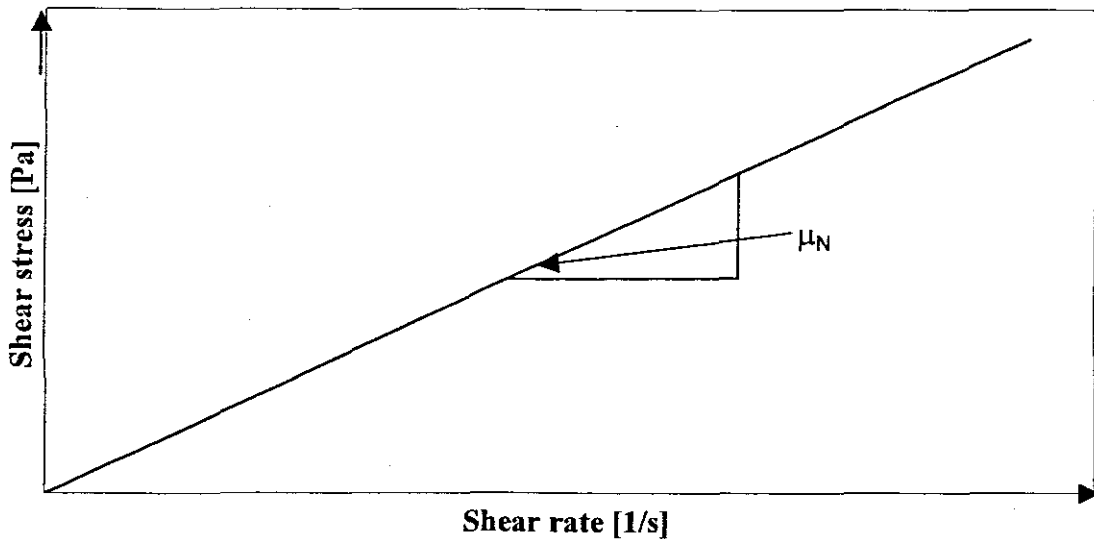


Figure 2. 1 Newtonian fluid flow curve

### 2.2.2 Non-Newtonian Fluids

A fluid is said to be non-Newtonian when the relationship between the shear stress and shear rate is non-linear or does not pass through the origin (Chhabra & Richardson, 1999). Non-Newtonian fluids are classified into three main categories:

- Time independent non-Newtonian fluids (pseudoplastic, dilatant, Bingham plastic and yield pseudoplastic fluids)
- Time dependent non-Newtonian fluids (thixotropic and rheopectic fluids) and
- Viscoelastic fluids.

Time dependant non-Newtonian fluids and viscoelastic fluids are not in the scope of this investigation.

### 2.2.3 Time Independent Non-Newtonian Fluids

Time independent non-Newtonian fluids are fluids for which the shear rate at any point is determined only by the value of the shear stress at that point at that instant (Chhabra & Richardson, 1999).

The constitutive equation of time independent fluids can be written as:

$$\dot{\gamma}_{yx} = f(\tau_{yx}) \quad (2.2)$$

or its inverse form:

$$\tau_{yx} = f^{-1}(\dot{\gamma}_{yx}) \quad (2.3)$$

Time independent non-Newtonian fluids are classified into three main categories:

- Pseudoplastic or shear thinning fluids
- Dilatant or shear thickening fluids and
- Viscoplastic fluids (Bingham plastic and yield pseudoplastic)

#### 2.2.3.1 Pseudoplastic or Shear Thinning Fluids

Pseudoplastic or shear thinning fluids are time independent non-Newtonian fluids in which the apparent viscosity decreases with increasing shear rate (Chhabra & Richardson, 1999). For these fluids, an infinitesimal shear stress will initiate flow, the flow curve passes through the origin.

Generally these fluids are modelled using the power law model equation, which is a two parameter equation:

$$\tau = K\dot{\gamma}^n \quad (2.4)$$

where  $K$  is the fluid consistency index in  $\text{Pa}\cdot\text{s}^n$  and  $n$  is the flow behaviour index or power law exponent and  $n < 1$ .



### 2.2.3.2 Dilatant or Shear Thickening Fluids

Dilatant or shear thickening fluids are time independent non-Newtonian fluids in which the apparent viscosity increases with increasing shear rate. In this case, as for pseudoplastic fluids, an infinitesimal shear stress will initiate flow, the flow curve passes through the origin.

Generally these fluids are also modelled using the power law model equation (2.4).

But in this case the flow behaviour index or power law exponent  $n$  is greater than one ( $n > 1$ ).

### 2.2.3.3 Viscoplastic Fluids

Viscoplastic fluids are fluids characterised by a yield stress ( $\tau_y$ ), which must first be exceeded before the fluid deforms or flows (Chhabra & Richardson, 1999).

Such materials will deform elastically when the applied shear stress is lesser than the yield stress. In this category they are classified Bingham plastic fluids and yield pseudoplastic fluids.

- *Bingham Plastic Fluids (BP)*

Bingham plastic fluids are fluids that require a non-zero shear stress in order to initiate a significant flow. The flow curve of Bingham plastic fluids does not pass through the origin and there is a linear relationship between shear stress in excess of the yield stress and the resulting shear rate (Chhabra & Richardson, 1999).

The Bingham plastic model is described by a two parameter equation:

$$\tau = \tau_{yB} + \mu_B \dot{\gamma} \quad (2.5)$$

Where  $\tau_{yB}$  is the Bingham yield stress and  $\mu_B$  is the Bingham plastic viscosity.

- *Yield Pseudoplastic Fluids (YPP)*

Yield pseudoplastic fluids are fluids that require a non-zero shear stress in order to initiate flow. In yield pseudoplastic fluids the increase in shear stress with shear rate in excess of the yield stress decreases with increasing shear rate (Chhabra & Richardson, 1999).

The flow curve does not pass through the origin and is non-linear.

Yield pseudoplastic fluids can be modelled using the Herschel–Bulkley equation, this model is a three parameter equation:

$$\tau = \tau_{\text{YHB}} + K\dot{\gamma}^n \quad (2.6)$$

where  $\tau_{\text{YHB}}$  is the Herschel-Bulkley yield stress  $K$  is the fluid consistency index and  $n$  the flow behaviour index.

#### 2.2.4 Time Dependent Non-Newtonian Fluids

Time dependent non-Newtonian fluids are fluids that have an apparent viscosity that varies with the shear rate and the time of application of the shear rate (Chhabra & Richardson, 1999).

Time dependent non-Newtonian fluids are also classified into two categories: Thixotropic and rheopectic.

##### 2.2.4.1 Thixotropic Fluids

Thixotropic fluids are fluids when sheared at constant shear rate, their apparent viscosity decreases with the time of shearing (Chhabra & Richardson, 1999).

##### 2.2.4.2 Rheopectic Fluids

A fluid is said to be rheopectic when its apparent viscosity increases with time of shearing. Figure 2.2 illustrates the flow curves of different non-Newtonian fluids as classified above.

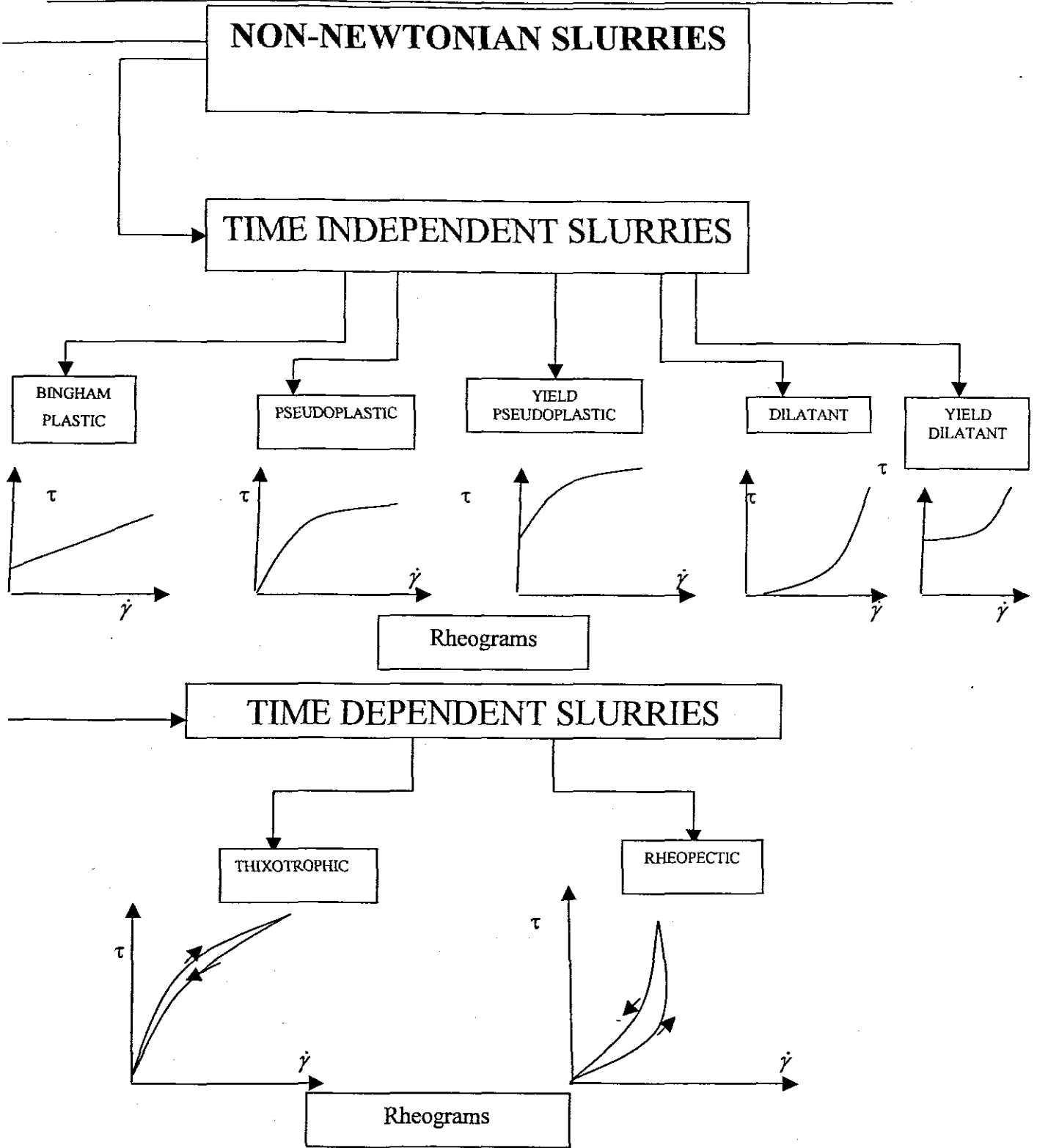


Figure 2. 2 Non-Newtonian fluids flow curves (Paterson & Cooke, 1999)

### 2.2.4.3 Settling Slurries

Settling slurries are solutions or pseudo-homogeneous mixtures where particles in suspension settle very quickly relatively to their residence time in the pipeline (Brown & Heywood, 1991) or a mixture in which solid and liquid phases are separated and the liquid properties are generally considered to be unaltered by the presence of solids. Particles are supported by turbulent mixing and antiparticle collisions (Paterson & Cooke, 1999)

## 2.2.5 Rheology

### 2.2.5.1 Definition

Rheology is defined as the viscous characteristics of a fluid or homogeneous solid-liquid mixture (Chhabra & Slatter, 2002).

### 2.2.5.2 Rheological Models

Various rheological models may describe the viscous characteristic of fluids. In this investigation the following models were used:

- The Newtonian model
- The Pseudoplastic model or Oswald-de-Waele model
- The Bingham plastic model and
- The Herschel-Bulkley or yield pseudoplastic model.

### 2.2.5.3 Rheological Characterisation

Rheological characterisation in the context of this work is the choice of a convenient rheological model that fit better the experimental data. The choice of a suitable rheological model is very important in the characterisation of non-Newtonian fluids and there is divided opinions on which rheological model to use in the literature to model laminar flow.

The choice of models is in fact extremely important not only for rheological characterisation in laminar flow but even more important in turbulent flow predictions (Hanks & Ricks, 1975). The reason for this is that the data is usually extrapolated (Thomas & Wilson, 1987) to much higher shear stresses for turbulent flow predictions than can be measured in laminar flow, even in small diameters (Shook & Rocco, 1991). Table 2.1 gives different rheological model available in the literature, showing the depth of the field of Rheology.

**Table 2. 1 Rheological Models available in the literature. (Chhabra & Richardson, 1985)**

Fluid model	Constitutive equation	Number of Parameters	Parameters
Newtonian	$\tau = \mu \left( -\frac{du}{dr} \right)$	1	$\mu$
Bingham plastic	$\tau = \tau_y + K \left( -\frac{du}{dr} \right)$	2	$\tau_y$ and K
Casson	$\sqrt{\tau} = \sqrt{\tau_y} + \sqrt{\mu_c \left( -\frac{du}{dr} \right)}$	2	$\tau_y$ and $\mu_c$
e-function	$\mu = \mu_o \exp \left[ m \left( -\frac{du}{dr} \right) \right]$	2	$\mu_o$ and m
Oswald de Waele or power-law (pseudoplastic)	$\tau = K \left( -\frac{du}{dr} \right)^n$	2	K and n
Ellis	$\mu = \frac{\mu_o}{1 + \left( \frac{\tau}{\tau_{1/2}} \right)^{\alpha-1}}$	3	$\mu_o, \alpha$ and $\tau_{1/2}$
Herschel-Bulkley or Yield pseudoplastic	$\tau = \tau_y + K \left( -\frac{du}{dr} \right)^n$	3	$\tau_y, n$ and K
Carreau	$\frac{\mu - \mu_o}{\mu_o \mu_\infty} = \left[ 1 + \left( \lambda \left( -\frac{du}{dr} \right) \right)^2 \right]^{\frac{n-1}{2}}$	4	$\mu_\infty, \mu_o, \lambda$ and n
Cross	$\frac{\mu - \mu_\infty}{\mu_o \mu_\infty} = \left[ 1 + \left( \lambda \left( -\frac{du}{dr} \right) \right)^2 \right]^{\frac{n-1}{2}}$	4	$\mu_\infty, \mu_o, \lambda$ and n

Cross and Carreau models are mainly used for polymer solutions, zero shear viscosity is usually associated with very low flow, shear rate  $10^{-3} \text{ s}^{-1}$  (Malkin, 1994).

For suspensions, yield pseudoplastic, Bingham plastic and power law models are more appropriate (Malkin, 1994). Also because the effects produced by the action of a shear stress is of high interest in pipe flow (Chhabra & Richardson, 1999), these equations are also used in this work because, in pipe flow the shear rate is directly calculated.

#### 2.2.5.4 The Yield Pseudoplastic Model

The yield pseudoplastic model will be used in this work to characterise all fluids as it is explained in section 2.3.8. The yield pseudoplastic model (YPP) incorporates the features of all models used in this work: The rheogram curvature of the pseudoplastic model and the yield stress for the Bingham plastic.

The yield pseudoplastic model is very sensitive to small variations in the rheological parameters and requires a sufficient amount of good laminar data to ensure reproducibility of the model to different data sets (Johnson, 1982).

The constitutive equation of the yield pseudoplastic model is given by equation (2.6):

$$\tau = \tau_{yHB} + K\dot{\gamma}^n \quad (2.6)$$

This equation is a three parameters equation:

- The yield stress ( $\tau_{yHB}$ )
- The fluid flow behaviour index ( $n$ )
- The fluid consistency index ( $K$ )

Rheometry or viscometry deals with the establishment of a relationship between shear stress and shear rate. This is required to establish the rheological parameters such as  $\tau_{yHB}$ ,  $K$ , and  $n$ , which are used for the specific fluid.

## 2.3 FLOW IN STRAIGHT PIPES

### 2.3.1 Shear Stress Distribution in a Straight Pipe

The shear stress distribution in a pipe is given by the relationship:

$$\tau = \frac{\Delta p r}{2L} \quad (2.7)$$

where:  $\Delta p$  is the pressure gradient in the portion of a straight pipe of length  $L$  and the radial distance  $r$  (Chhabra & Richardson, 1999).

At the pipe wall equation (2.7) becomes:

$$\tau_o = \frac{\Delta p D}{4L} \quad (2.8)$$

where  $D$  is the pipe diameter.

### 2.3.2 Energy Loss in Straight Pipe

When a fluid flows in a straight pipe the dissipation of energy manifests itself as head loss and can be calculated using the Darcy-Weisbach formula (Massey, 1970):

$$\Delta H = \frac{4fL}{D} \left( \frac{V^2}{2g} \right) \quad (2.9)$$

Where  $f$  is the Fanning friction factor defined as (Massey, 1970):

$$f = \frac{2\tau_o}{\rho V^2} \quad (2.10)$$

The velocity  $V$  is obtained from the continuity equation and is given by:

$$V = \frac{Q}{A} \quad (2.11)$$

Equations (2.7), (2.8), (2.9), (2.10) and (2.11) do not depend on the nature of the fluid (Newtonian or non-Newtonian) or on the nature of the flow (laminar or turbulent). They depend on the homogeneity of the fluid and on the development of the flow (Massey, 1970).

### 2.3.3 Newtonian Transition from Laminar to Turbulent and Reynolds Number

There are two types of flow: laminar or streamline flow and the turbulent flow. Laminar flow occurs at lower velocities, the fluid particles are moving in straight lines, but the velocity with which the particles move along one line is not the same as along another line (Massey, 1970).

In turbulent flow, the path of individual fluid particles are not straight anymore but are sinuous, intertwining and crossing each other in a disorderly manner so that a mixing of the fluid takes place (Massey, 1970).

Experimental work has shown that the transition from laminar to turbulent flow happens at some fixed value of a dimensionless group called Reynolds number (Massey, 1970).

The Reynolds number is the ratio of the inertial to viscous forces and is given for Newtonian fluids by:

$$Re = \frac{\rho VD}{\mu} \quad (2.12)$$

where  $\rho$  is the fluid density,  $V$  the fluid velocity,  $D$  the pipe diameter and  $\mu$  the fluid viscosity.

The general accepted point of transition from laminar to turbulent flow is  $Re=2100$ . But the transition can happen at a Reynolds number higher than 2100 or lower than 2100 depending on the vibrating nature of the surroundings (Massey, 1970).

### 2.3.4 Newtonian Laminar Flow in Straight Pipes

#### 2.3.4.1 Velocity Distribution

The velocity distribution in a pipe in laminar flow (if there is no slip or hold up effect at the pipe wall) is (Massey, 1970):

$$u = \frac{\tau_o}{2\mu R} (R^2 - r^2) \quad (2.13)$$

$u$  is maximum for  $r=0$  and is:

$$u_{\max} = \frac{\tau_o R}{2\mu} \quad (2.14)$$



And the mean velocity is:

$$V = \frac{u_{\max}}{2} \quad (2.15)$$

$$V = \frac{\tau_o R}{4\mu} \quad (2.16)$$

#### 2.3.4.2 Hagen-Poiseuille Formula

For an incompressible Newtonian fluid in laminar flow, the Hagen-Poiseuille formula is (Massey, 1970):

$$Q = \frac{\pi \tau_o R^3}{4\mu} \quad (2.17)$$

#### 2.3.4.3 Friction Factor

In general the friction factor is determined using equation (2.10). The friction factor is generally a function of both the Reynolds number and the pipe wall roughness. In Newtonian laminar flow, the pipe wall roughness has no effect on the friction factor and the friction factor is given by (Massey, 1970):

$$f = \frac{16}{Re} \quad (2.18)$$

#### 2.3.5 Newtonian Turbulent Flow in Straight Pipes

Turbulent flow is a flow characterised by large, random, swirling or eddy motions.

Particle path cross and velocity (both direction and magnitude) and pressure fluctuate on a continuous and random basis.

Turbulent flow is very complex and a consistent mathematical analysis is not yet done and predictions are obtained empirically from experiments (Massey, 1970).

The friction factor in turbulent flow is a function of the Reynolds number and the pipe wall roughness  $k$ . It can be obtained using the Colebrook and White equation (Massey, 1970):

$$\frac{1}{\sqrt{f}} = -4 \log \left[ \frac{k}{3,7D} + \frac{1,26}{Re\sqrt{f}} \right] \quad (2.19)$$

It must be noted that the Moody diagram presents the friction factor  $f$  vs.  $Re$  and is a useful tool when it comes to the friction factor determination.

Fig 2.3 gives the Moody diagram.

In a case of a smooth pipe and for Reynolds numbers between 3000 and 100000, the Blasius equation is used to determine the friction factor (Massey, 1970).

$$f = \frac{0.079}{(Re)^{0.25}} \quad (2.20)$$

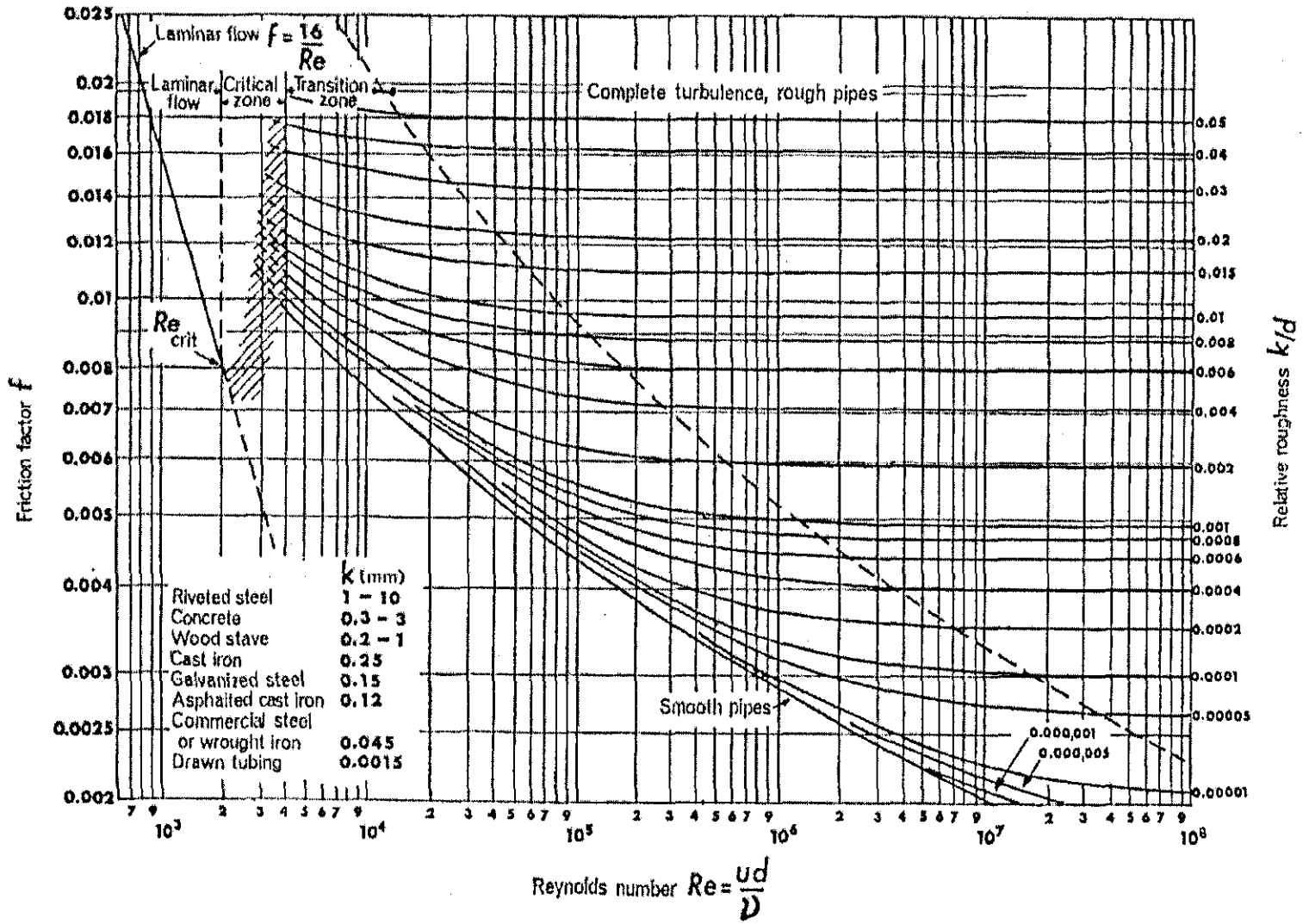


Figure 2. 3 The Moody Diagram (Massey, 1970)

### 2.3.6 Non-Newtonian Flow in Straight Pipes

The fundamental relationships (2.7), (2.8), (2.9), (2.10) and (2.11) on the shear rate, energy loss in pipes and velocity are also valid for non-Newtonian fluids as stated earlier in sections 2.3.1 and 2.3.2.

### 2.3.7 Non-Newtonian Transition from Laminar to Turbulent Flow and Non-Newtonian Reynolds Numbers

In this section, the different criteria for the determination of flow regime for non-Newtonian fluids are presented.

In non-Newtonian flow as in Newtonian flow there are also two kinds of flow: laminar and turbulent. Many criteria have been established for the determination of the nature of flow. Although this investigation uses the Slatter Reynolds number, other non-Newtonian Reynolds numbers and criteria relevant to this work are also presented. The Slatter Reynolds number is favoured because it can describe the behaviour of a wide range of non-Newtonian fluids (Chhabra & Slatter, 2002).

#### 2.3.7.1 Newtonian Approximation

In the Newtonian approximation method, in order to evaluate the transition from laminar to turbulent flow, the Newtonian Reynolds number is used but because a non-Newtonian fluid has a variable viscosity, the apparent or secant viscosity is used and in equation (2.12) the term viscosity  $\mu$  is replaced by  $\mu'$  the apparent or secant viscosity and equation (2.12) becomes:

$$Re_{Newt} = \frac{\rho V D}{\mu'} \quad (2.21)$$

with the apparent viscosity:

$$\mu' = \frac{\tau_o}{\left[ -\frac{du}{dr} \right]_o} \quad (2.22)$$

where:  $\left[-\frac{du}{dr}\right]_o$  is the velocity gradient at the pipe wall.

### 2.3.7.2 Metzner & Reed Generalised Reynolds Number

It has been demonstrated that for laminar pipe flow of any given time independent fluid that  $8V/D$  is some unique function of  $\tau_o$  only (Metzner & Reed, 1955). This may be expressed as:

$$\tau_o = \frac{D \Delta P}{4L} = K' \left( \frac{8V}{D} \right)^{n'} \quad (2.23)$$

where in the most general case  $K'$  and  $n'$  are not constants, but vary with  $8V/D$ . Thus on logarithmic plot of  $\tau_o$  versus  $8V/D$ , Equation (2.23) is simply the equation of the tangent to the curve at a given value of  $8V/D$ ,  $n'$  being the slope of this tangent and  $K'$  its intercept on the ordinate at  $8V/D$  equal to unity (Skelland, 1967).

Metzner & Reed (1955) developed a generalised Reynolds number from the considerations above as:

$$Re_{MR} = \frac{8 \rho V^2}{K' \left( \frac{8V}{D} \right)^{n'}} \quad (2.24)$$

This relation may be rewritten after transformation as:

$$Re_{MR} = \frac{\rho V^{2-n'} D^{n'}}{8^{n'-1} K'} \quad (2.25)$$

In practice,  $n'$  is the tangent of the double logarithmic plot of  $\tau_o$  versus  $(8V/D)$  at any particular value of  $\tau_o$  or  $8V/D$ .  $\log K'$  is the intercept on the y-axis.

$$n' = \frac{d(\log \tau_o)}{d\left(\log \frac{8V}{D}\right)} \quad (2.26)$$

It has been found experimentally that for many fluids  $K'$  and  $n'$  are constant over any range of  $\tau_o$  or  $8V/D$  for which the power law is valid. This is not the case in general (the log-log plot is not always a straight line) and care must be taken to ensure that the range of application is narrow. The quantity  $n'$  characterises the degree of non-Newtonian behaviour for a given fluid. The greater the departure of  $n'$  from unity the more non-

Newtonian is the fluid. The quantity  $K'$  is a measure of the consistency of the fluid, the larger the value of  $K'$  the thicker or less mobile is the fluid (Metzner & Reed, 1955).

For power law fluids or pseudoplastic models:

$$K' = K \left( \frac{3n+1}{4n} \right)^n \text{ and } n=n' \quad (2.27)$$

Thus (2.25) becomes:

$$Re_{MR} = \frac{\rho V^{2-n} D^n}{8^{n-1} K \left( \frac{3n+1}{4n} \right)^n} \quad (2.28)$$

For a Bingham plastic fluid (Skelland, 1967):

$$n' = 1 - \frac{4 \tau_y}{3 \tau_o} \quad (2.29)$$

$$K' = \tau_o \left[ \frac{\eta}{\tau_o \left[ 1 - 4/3(\tau_y/\tau_o) + 1/3(\tau_y/\tau_o)^4 \right]} \right]^{n'} \quad (2.30)$$

For yield pseudoplastic fluids, no relationship has been derived for yield pseudoplastic fluids and this has been done as part of this work. It has been demonstrated in this work that (see Appendix 5):

$$n' = \frac{1}{-3 + \frac{(1+n) \tau_o}{n (\tau_o - \tau_y)} + \frac{2\tau_o(1+n)(\tau_o + 2n\tau_o + n\tau_y)}{(1+n)(1+2n)(\tau_o - \tau_y)^2 + 2\tau_y(\tau_o - \tau_y)(1+n)(1+3n) + \tau_y^2(1+2n)(1+3n)}} \quad (2.31)$$

and

$$K' = \tau_o / \left\{ \left[ \frac{4n}{K^n \tau_o^3} (\tau_o - \tau_y)^{1+n} \left[ \frac{(\tau_o - \tau_y)^2}{1+3n} + \frac{2\tau_y(\tau_o - \tau_y)}{1+2n} + \frac{\tau_y^2}{1+n} \right] \right]^{n'} \right\} \quad (2.32)$$

### 2.3.7.3 Slatter Reynolds Number

The Slatter Reynolds number takes directly in to account the yield stress of non-Newtonian fluids but other non-Newtonian Reynolds numbers do not take directly into account the yield stress. An unsheared core is formed in laminar pipe flow of a fluid with a yield stress. Slatter has proposed a Reynolds number which seeks to express the ratio of inertial forces to viscous shear forces in the sheared portion of the flow (Shook *et al*, 2002).

The Slatter Reynolds number is given by:

$$Re_3 = \frac{8 \rho V_{ann}^2}{\tau_y + K \left( \frac{8 V_{ann}}{D_{shear}} \right)^n} \quad (2.33)$$

For fluid with a yield stress there is a plug flow at the centre of the pipe in laminar flow and the radius of the plug is:

$$r_{plug} = \frac{\tau_y}{\tau_o} R \quad (2.34)$$

The sheared diameter is:

$$D_{shear} = D - D_{plug} \quad (2.35)$$

$$\text{where: } D_{plug} = 2r_{plug} \quad (2.36)$$

The mean velocity of the annulus is:

$$V_{ann} = \frac{Q_{ann}}{A_{ann}} \quad (2.37)$$

$$\text{where } Q_{ann} = Q - Q_{plug} \quad (2.38)$$

$$\text{and } Q_{plug} = u_{plug} \cdot A_{plug} \quad (2.39)$$

Where  $u_{plug}$  is given by equation (2.41) in section 2.3.8.

The transitional value of the Slatter Reynolds number from laminar to turbulent flow in straight pipes is  $Re_3 = 2100$  (Shook *et al*, 2002).

The Slatter Reynolds number can accommodate different rheological models: the Newtonian model, the power law model, the Bingham plastic model and the yield pseudoplastic model, as it will be demonstrated in this investigation.

#### 2.3.7.4 Intersection and Deviation Methods

- *Intersection Method*

This is a practical method. It uses the intersection of the laminar and turbulent flow loci to predict the critical point.

The degree of accuracy of this method depends on the turbulent flow model used and this method is also incompatible with Newtonian fluids (Chhabra & Slatter, 2002)

- *Deviation Method*

This method uses the point from which data starts deviating from the laminar flow line to define the transition region and that deviation happens before the intersection.

This method is relevant for this study because in most cases, the transition from laminar to turbulent regime in pipe fittings and valves occurs earlier than in straight pipe flow (Pienaar *et al.*, 2001) and can be detected using the deviation or intersection method.

#### 2.3.8 Non –Newtonian Laminar Flow in Straight Pipes

The following rheological relationship can be accommodated in the yield pseudoplastic model equation (2.6):

Yield dilatant     ( $\tau_y > 0$  and  $n > 1$ )

Bingham plastic   ( $\tau_y > 0$  and  $n = 1$ )

Dilatant            ( $\tau_y = 0$  and  $n > 1$ )

Newtonian         ( $\tau_y = 0$  and  $n = 1$ )

Pseudoplastic     ( $\tau_y = 0$  and  $n < 1$ )

In laminar flow, the velocity distribution of a yield pseudoplastic fluid is for  $R > r > r_{plug}$ :



$$u = \frac{R}{K^n \tau_o} \frac{n}{n+1} \left[ (\tau_o - \tau_y)^{\frac{n+1}{n}} - (\tau - \tau_y)^{\frac{n+1}{n}} \right] \quad (2.40)$$

When  $0 < r < r_{\text{plug}}$  the fluid moves as a plug at a uniform plug velocity  $u_{\text{plug}}$ :

$$u_{\text{plug}} = \frac{R}{K^n \tau_o} \frac{n}{n+1} (\tau_o - \tau_y)^{\frac{n+1}{n}} \quad (2.41)$$

The volumetric discharge  $Q$  and the average velocity are obtained from the relation:

$$\frac{32Q}{\pi D^3} = \frac{8V}{D} = \frac{4n}{K^n \tau_o^3} (\tau_o - \tau_y)^{\frac{1+n}{n}} \left[ \frac{(\tau_o - \tau_y)^2}{1+3n} + \frac{2\tau_y(\tau_o - \tau_y)}{1+2n} + \frac{\tau_y^2}{1+n} \right] \quad (2.42)$$

With  $\tau_o$  as defined by equation (2.8) and  $V=Q/A$  equation (2.11)

For a Newtonian fluid  $K=\mu$  and  $n=1$ , equation (2.42) becomes:

$$\tau_o = \mu \frac{8V}{D} \quad (2.43)$$

Equation (2.43) shows that wall shear rate at pipe wall for a Newtonian fluid is  $\frac{8V}{D}$ . For

non-Newtonian fluid  $\frac{8V}{D}$  is called the pseudo shear rate or nominal shear rate. The plot

of  $\tau_o$  versus  $\frac{8V}{D}$  is called the pseudo-shear diagram. It is of great importance in non-

Newtonian fluid flow in general and in this investigation in particular.

### 2.3.8.1 The Rabinowitsch-Mooney Relation

The true shear rate can be obtained from the pseudo shear rate of a non-Newtonian fluid, by multiplying the pseudo shear rate by the Rabinowitsch –Mooney relation:

$$\left[ -\frac{du}{dr} \right]_o = \frac{8V}{D} \left[ \frac{3n' + 1}{4n'} \right] \quad (2.44)$$

$n'$  is calculated as:

$$n' = \frac{d(\text{Log} \tau_o)}{d\left(\text{Log} \frac{8V}{D}\right)} \quad (2.26)$$

The coefficient  $n'$  is obtained as the slope of a double logarithmic plot of  $\tau_o$  versus  $8V/D$ . In the case the rheological parameters of the fluid are known ( $\tau_y$ ,  $K$  and  $n$ ),  $n'$  can be obtained directly using relations (2.27) for pseudoplastic fluids, (2.29) for Bingham plastic fluids and (2.31) for yield pseudoplastic fluids.

### 2.3.8.2 Friction Factor for Non-Newtonian Fluids

In the case of inelastic non-Newtonian fluids, the fanning friction factor in laminar flow is given by (Chhabra & Richardson, 1999):

$$f = \frac{16}{Re_{MR}} \quad (2.45)$$

with  $f$  given by equation (2.10).

Slatter (1999) also developed a friction factor for non-Newtonian fluids with a yield stress:

$$f_{ann} = \frac{2\tau_o}{\rho V_{ann}^2} \quad (2.46)$$

In this case the transition is considered to occur when  $f_{ann}$  equals 16/2100.

## 2.4 RHEOLOGICAL CHARACTERISATION

The rheological characterisation of non-Newtonian fluids is not easy (Chhabra & Richardson, 1999), and can be done using a rheometer or a tube viscometer. In the context of this investigation, tube viscometry was used because the experimental test loop could also be used as an in-line tube viscometer having a range of 5 different pipe diameters.

### Rotational viscometry

The instrument used to measure viscous properties of non-Newtonian fluids in this case is known as a rheometer. The rheometer usually consists of a concentric bob and cup, one of which is rotated to produce shear in the test fluid that is in the gap between the bob and

the cup. The shear stress is determined by measuring the applied torque on one of the elements.

The rheometer is a very sophisticated instrument and is capable of measuring the full range of rheological phenomena. The rheometers can be found using one of the many geometries, among others: Concentric cylinders, cone and plate, parallel disks. And the main measurements are angular velocity and applied torque. The software connected to these instruments converts these signals into shear rate and shear stress (Chhabra & Slatter, 2002)

### Tube viscometry

In a tube viscometer the test fluid flows at a controlled, measured rate through a tube of known diameter and the pressure drop over a known length of the tube is measured.

Data from tube viscometer yields a series of coordinates of pseudo shear rate and wall shear stresses ( $8V/D$ ,  $\tau_0$ ) these data must be processed in order to give the required rheology.

Assuming a yield pseudoplastic rheology (2.6):

$$\frac{32Q}{\pi D^3} = \frac{8V}{D} = \frac{4n}{K^n \tau_0^3} (\tau_0 - \tau_y)^{1+n} \left[ \frac{(\tau_0 - \tau_y)^2}{1+3n} + \frac{2\tau_y(\tau_0 - \tau_y)}{1+2n} + \frac{\tau_y^2}{1+n} \right] \quad (2.42)$$

The following technique was used (Slatter, 1994):

A pseudo shear diagram was plotted using the pseudo shear rate ( $8V/D$ ) as abscissa and shear stress ( $D\Delta p/4L$ ) as ordinate. Data points in laminar flow only from all tubes are used. The best curve is fitted to the data by eye. A realistic value of  $\tau_y$  is set according to the data as the ordinate intercept. The value of  $\tau_y$  is then adjusted until the error function is minimised. The error function  $E$  is the root square of difference between observed data and calculated as:

$$E = \sqrt{\frac{\sum_{i=1}^N \left[ \left( \frac{8V}{D} \right)_{i_{obs}} - \left( \frac{8V}{D} \right)_{i_{CALC}} \right]^2}{N-1}} \quad (2.47)$$

and  $K$  value for minimum error  $K_{min}$  is given by:

$$K_{\text{MIN}} = 1 / \left[ \frac{2 \sum_{i=1}^N \left( \frac{8V}{D} \right)_i / 8}{n \sum_{i=1}^N (\tau_o - \tau_y)^{1+n} \left[ \frac{(\tau_o - \tau_y)^2}{1+3n} + \frac{2\tau_y(\tau_{oi} - \tau_y)}{1+2n} + \frac{\tau_y^2}{1+n} \right]} \right]^n \quad (2.48)$$

Errors in tube viscometry:

- **Wall slip:** this effect occurs when the layers of particles near the wall are more dilute than the bulk flow (Heywood & Richardson, 1978). As a result the viscosity near the wall will be reduced and apparent slip will occur. Chhabra & Richardson (1999) warn that serious errors could occur when the wall slip is not accounted for. To account for the wall slip, more than one diameter tube should be tested. Their laminar flow data should coincide if there is no wall slip. If they do not coincide then the slip velocity must be calculated for each tube and deducted from the measured mean velocity (Heywood & Richardson, 1978).
- **Entrance and exit losses:** it is important that the entrance and exit losses in the tubes that are used are minimised. This is possible by making sure that the flow is fully developed before differential pressure readings are taken.

## 2.5 FLOW IN PIPE FITTINGS AND VALVES

In this section, the relevant theory on Newtonian and non-Newtonian losses in pipe fittings and valves is given in both laminar and turbulent flow regimes.

### 2.5.1 Classification of Fittings

Fittings are generally classified in one of the categories below:

- Branching fittings, e.g.: tees, crosses, side outlet elbows, etc.
- Reducing or expending fittings: in which there is a change in the cross section of the pipe e.g.: contraction, expansion, etc.
- Deflecting fittings in which there is a change in the direction of flow e.g.: bends, elbows, return bends and
- Combined or hybrid fittings are a combination of the aforementioned e.g. valves. Other fittings do not offer any resistance to flow such as couplings and unions. (Crane Co., 1981)

### 2.5.2 Determination of Newtonian and Non-Newtonian Losses Across Pipe Fittings and Valves

#### 2.5.2.1 Losses Across Fittings

The Bernoulli formula gives the macroscopic mechanical energy balance for a pipe system and gives the total head loss in the system and is used in the determination of different losses in the system (Massey, 1970).

The Bernoulli formula for a system of two pipes in series connected by a fitting, can be written as follows:

$$z_1 + \frac{\alpha_1 V_1^2}{2g} + \frac{p_1}{\rho g} = z_2 + \frac{\alpha_2 V_2^2}{2g} + \frac{p_2}{\rho g} + H_1 + H_{\text{fit}} + H_2 \quad (2.49)$$

where  $z$  is the elevation of the datum,  $\alpha$  is the kinetic energy correction factor,  $p$  is the static pressure and,  $H$  the head loss.

Subscripts 1 and 2 are for upstream and downstream pipes respectively.

$H_{\text{fit}}$  is the fitting head loss in metres and is predicted using the formula (Massey, 1970):

$$H_{\text{fit}} = k_{\text{fit}} \frac{V^2}{2g} \quad (2.50)$$

For a valve it is written:

$$H_v = k_v \frac{V^2}{2g} \quad (2.51)$$

where  $k_{\text{fit}}$  or  $k_v$  is the fitting or valve head loss coefficient and is defined as the non-dimensionalised difference in overall pressure between the ends of two long straight pipes when there is no fitting and when the real fitting is installed (Miller, 1978). This is shown graphically on Figure 2.4 for a valve.

$$k_{\text{fit}} = H_{\text{fit}} \frac{2g}{V^2} \quad (2.52)$$

or:

$$k_{\text{fit}} = \frac{\Delta p_{\text{fit}}}{1/2\rho V^2} \quad (2.53)$$

The loss coefficient can be calculated in two ways, by including or excluding the length of the fitting.

If the length of the fitting is excluded,  $k_{\text{fit}}$  is called  $k_{\text{gross}}$  and is obtained by the equation (Turian *et al*, 1997):

$$k_{\text{gross}} = \frac{1}{\frac{\rho V^2}{2}} \left[ -\Delta p - \frac{\rho V^2}{2} \frac{4f}{D} (L_u + L_d) \right] \quad (2.54)$$

If the length of the fitting is included,  $k_{\text{fit}}$  is called  $k_{\text{net}}$  and is obtained by the equation (Turian *et al*, 1997):

$$k_{\text{net}} = \frac{1}{\frac{\rho V^2}{2}} \left[ -\Delta p - \frac{\rho V^2}{2} \frac{4f}{D} (L_u + L_{\text{fit}} + L_d) \right] \quad (2.55)$$

With the exception of abrupt contractions and expansions, all other fittings have a physical length. The length of the test valve was included in all calculations in this work.

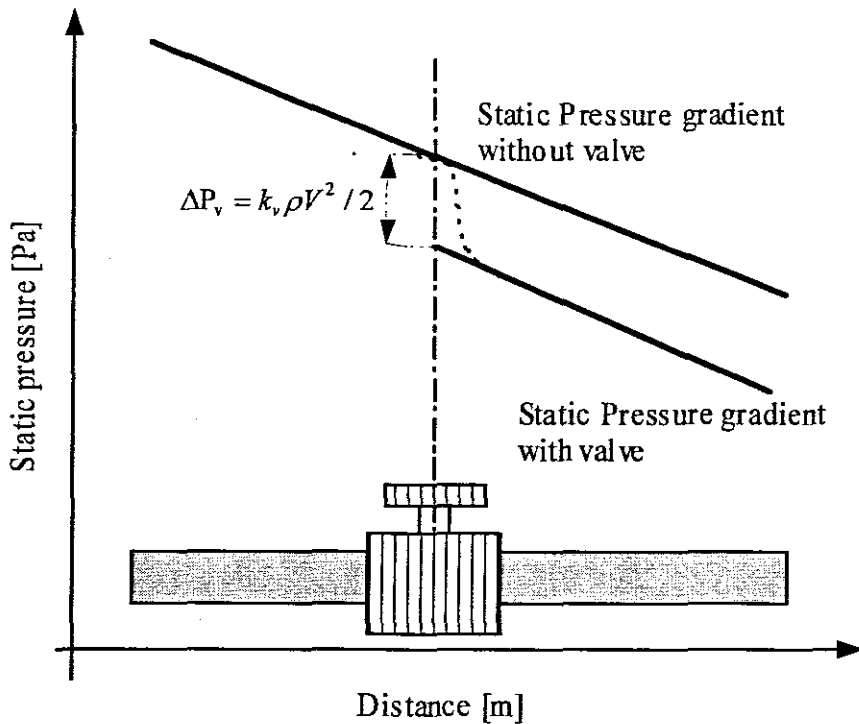


Figure 2. 4 Definition of the loss coefficient (Miller, 1978)

## 2.6 FLOW IN VALVES

### 2.6.1 Definition of Valves

In the industry generally valves are used to isolate, regulate or direct the flow (Lahlou, 2002). From an engineering perspective, a valve is a contraction followed by an expansion (Mc Neil & Morris, 1995).

### 2.6.2 Classification of Valves

According to their resistance to fluid flow, valves are classified either as low resistance valves or high resistance valves. Low resistance valves are those in which there is only a change in the flow cross section and high resistance valves are those where there are both changes in the flow cross section and direction (Crane Co., 1981).

In the industry dealing with non-Newtonian fluids or slurries, valves are used mostly for isolation purposes and rarely for regulating or throttling. However in applications such as polymer processing, valves are used as throttling devices (Mc Neil & Morris, 1995).

It is not possible to do any systematic classification, due to the great variety of valve designs. However, there are five basic valve designs: gate, ball, plug, butterfly, diaphragm and pinch (Heywood, 1999). There are designs intended for a particular application or that combine certain features of other valves for improved performance. These are known as hybrid valves.

According to their mode of operation, valves can be classified as: manual valves, check valves, pressure relieve valves and control valves (Lahlou, 2002).

Diaphragm valves are the objects of this study and a thorough description is given in section 2.6.3 due to their wide usage in the slurry industry and in the mineral processing industry (Brown & Heywood, 1991)

The selection of the right valve in a piping system is crucial because poor selection can lead to problems: excessive high initial and maintenance costs, downtime, leakage, poor performance, dangerous vibration and excessive noise. Many variables are to be considered when doing a slurry valve selection. Slurry valve selection is complex and is not in the scope of this investigation. However the first rule is to avoid the need for valves whenever possible. The need for a valve must be carefully scrutinised. It must also be said that high resistance valves in general are unsuitable for slurry service (Brown & Heywood, 1991).

### 2.6.3 Diaphragm Valves

The diaphragm valve has a valve body assembly with a single flexible diaphragm, which isolates the actuating mechanism from the flowing fluid.

There are two basic designs: the weir or dam and straight through types.

The body can be manufactured from cast iron, bronze, gunmetal or stainless steel. It can be lined with various elastomers, polymers or glass for highly corrosive and/or abrasive applications.

Diaphragms are in elastomeric material or polytetrafluoroethylene (PTFE) with an elastomer backing. Because the diaphragm isolates the moving parts in the bonnet from the flowing fluid, the bonnet assembly can be manufactured from cast iron or plastic-coated materials. Cast iron is used for most applications. This is because it renders the



valve suitable for handling aggressive fluids including those containing suspended solids as well as clean fluid applications (AEA Technology, 1996).

Diaphragm valves can normally operate within a wide temperature range depending on the valve material choice. The application of both types is limited to about 10 bars maximum (lower in large valves) with temperatures and products limited by the diaphragm and optional body linings (typically 100 °C).

The weir or dam type diaphragm valve (Figure 2.5) has a body with a transverse weir above which a flexible diaphragm is mounted. Tight closure of the diaphragm valve is obtained when the diaphragm is screwed down by means of a hand wheel, pneumatic or electric actuator until it touches the weir.

The movement of the diaphragm, even from the fully open to the fully closed position, is relatively short; the result is a long diaphragm life and low maintenance. This type of valve is suitable for throttling applications and is by definition a high resistance valve because there are changes in both the diameter of the cross section and the flow direction.

The straight-through type diaphragm valve (Figure 2.6) may have a parallel or tapered bore through the body. A wedge-shaped diaphragm completes the closure. The method of sealing requires a longer diaphragm movement, which tends to result in a shorter diaphragm life.

The full bore opening offers minimum resistance to flow in the open position and this valve is by definition a low resistance valve because there is change only in the cross section diameter. However, the material choice for the diaphragm is much more limited.

The advantages of the diaphragm valve reside in the fact that the operating mechanism, called the compressor, is above the diaphragm, not in contact with the flowing fluid. Its unlined solid-alloy bodies are relatively less expensive than those of some other types of valves because of the smaller metal mass.

No packing is required. The interior is very smooth and can be easily cleaned.

As limitations, larger sizes of this valve become more difficult and expensive to produce. The valve leaks upon the failure of the diaphragm due, for instance, to excessive cycling.

Diaphragm valves are particularly suitable for less arduous slurry service (Brown & Heywood, 1991). With particularly abrasive slurries, the weir type may be subject to erosive wear and the passage constriction is some times undesirable with large particle slurries.

The straight-through type is better suited for use with high solids content, coarse particles, high viscosity and low pressure, low temperature abrasive slurry systems. It can be found in the brewing, chemical processing, dairy, food, minerals processing, paper and pulp, power generation and water industries (AEA Technology, 1996).

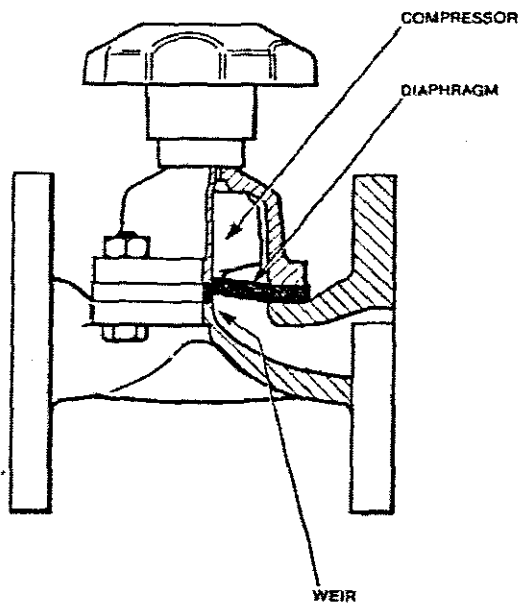


Figure 2. 5 The weir or dam type diaphragm valve

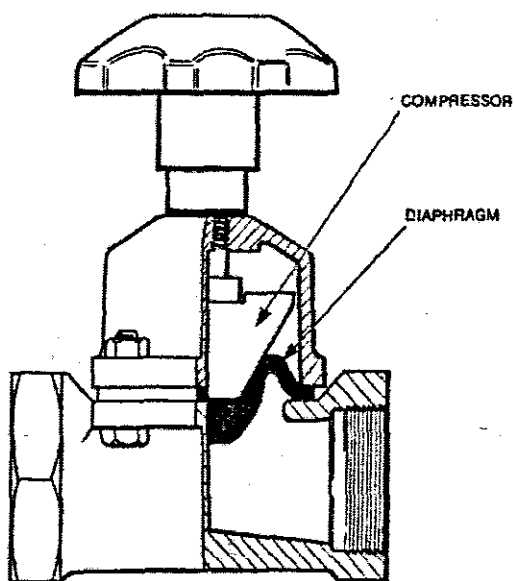


Figure 2. 6 The straight-through type diaphragm valve

## 2.6.4 Newtonian and non-Newtonian flow in valves

### 2.6.4.1 Pressure Drop in Valves

The loss of pressure due to a valve consists of three parts (Turian *et al*, 1997):

1. The pressure drop within the valve itself due to the viscous stresses that cause internal friction and separates flows.
2. The pressure drop in the upstream pipe in excess of that which would normally occur if there were no valve in the line. This effect is small.
3. The pressure drop in the downstream pipe in excess of that which would normally occur if there were no valve in the line. This effect may be comparatively large.

### 2.6.4.2 Valve Loss Coefficient

Friction losses for valves are obtained using equation (2.51) where

$k_v$  is the valve loss coefficient or resistance coefficient and is defined as the number of velocity heads lost due to a valve.

The head loss is independent of the Reynolds number for turbulent flow through valves, because inertia forces dominate. It is clear that the loss coefficient in turbulent flow is independent of the Reynolds number. In laminar flow the valve loss coefficient is Reynolds number dependent and in laminar flow is defined as  $C_v$ , the laminar flow valve loss coefficient (Pienaar *et al.*, 2001):

$$C_v = k_v \cdot Re \quad (2.56)$$

The loss coefficient is usually presented as a function of the Reynolds number. The loss coefficient is on the y-axis and the Reynolds number on the x-axis on logarithmic scale. In laminar flow the loss coefficient is a hyperbolic function of the Reynolds number and it increases significantly as the Reynolds number decreases. Figure 2.7 gives a typical presentation of  $k_v$  vs  $Re$ .

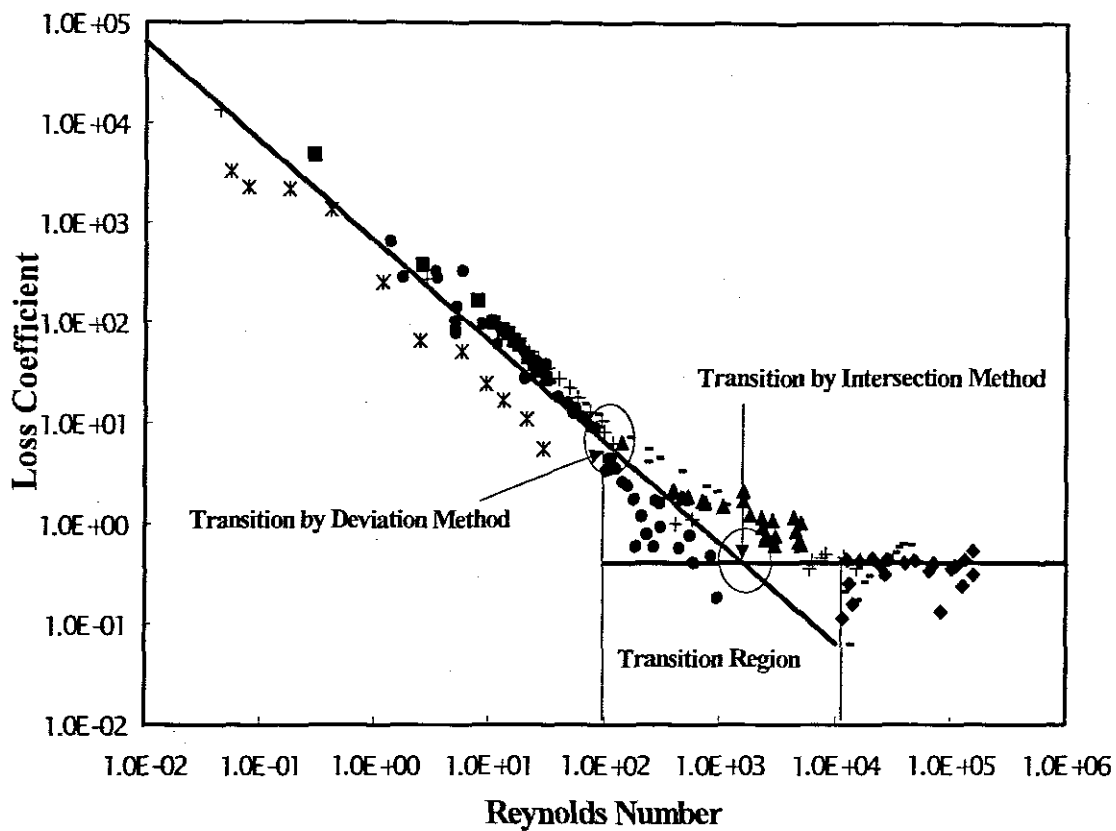


Figure 2. 7 Typical representation of  $k_v$  vs.  $Re$  for a fitting (Pienaar *et al*, 2001)

Figure 2.7 shows the transition from laminar to turbulent flow. Some authors define it as the intersection of the laminar loss coefficient and turbulent loss coefficient loci and others as a point where the experimental data start to deviate from the laminar flow line (Pienaar *et al*, 2001).

#### Determination of the laminar valve loss coefficient.

The laminar loss coefficient in equation (2.56) is determined from experimental data in the laminar flow region by the least square method.

It is obtained by minimising the logarithmic least square:

$$\text{Minimum} \sum \left( \text{Log} \frac{C_v}{\text{Re}} - \text{Log} k_{v/\text{obs}} \right)^2 \quad (2.57)$$

## Methodology

Generally, there are two methods used in the determination of valves or fittings loss coefficient: The hydraulic grade line (HGL) approach and the total pressure method.

Banerjee *et al.*, (1994) and Baudouin, (2003) adopted the hydraulic grade line approach for the determination of loss coefficients, the first for loss coefficients in valves and the latter for loss coefficients in sudden contractions. It consists of measuring and plotting the static pressure gradients upstream and downstream of the valve in the region of fully developed flow far from the valve plan to avoid disturbance of the flow due to the presence of the valve.

The valve pressure loss is obtained as an extrapolation to the valve plane of the pressure gradients measured in the fully developed flow regions upstream and downstream of the valve.

To measure static pressure at different points upstream and downstream of the valve, Banerjee *et al.* (1994) used U-tube manometers containing mercury beneath water connected to pressure tapings. Baudouin (2003) used point pressure transducers and differential pressure cells connected to pressure tapings.

Turian *et al.*, (1997) and Pienaar (1998) used the total pressure method to determine the loss coefficient through fittings and valves. Two pipes in series were joined by a fitting or valve. The method consists of measuring the pressure gradient between two points in the region of fully developed flow in straight pipes around the fitting or valve. Thus knowing the losses in the straight pipe portions one can deduct the fitting or valve loss.

This investigation adopted the hydraulic grade line approach because the experimental loop used was specially designed to accommodate this approach.

The technique for the determination of the valve pressure drop by the hydraulic grade line approach is explained in Figure 2.8 below and will be explained in detail later in chapter 4 (4.4.1).

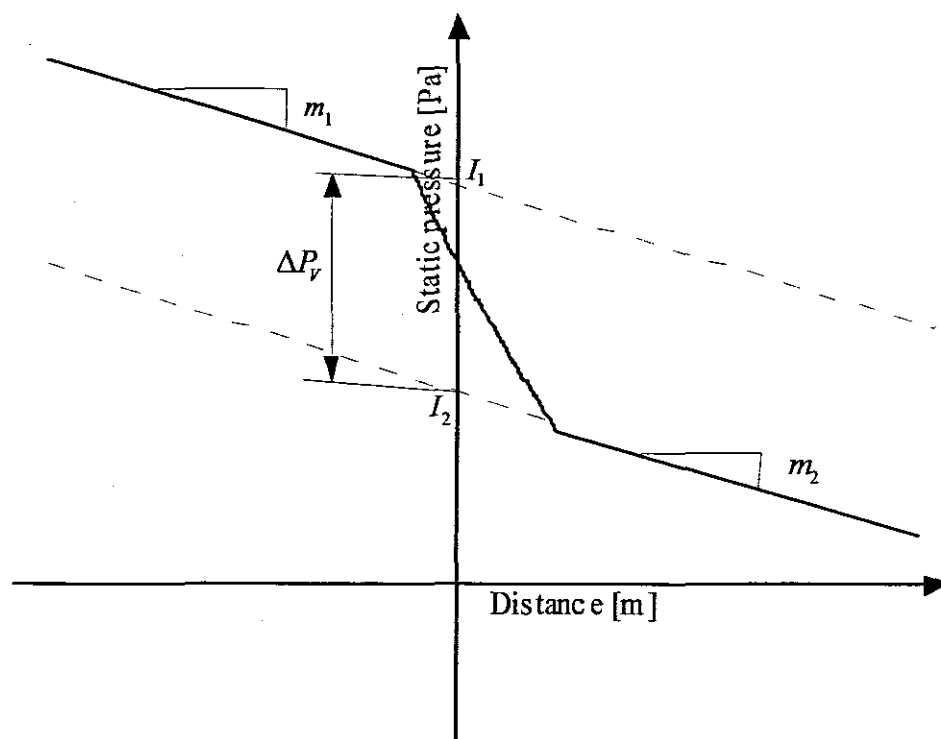


**Figure 2. 8 Diagram illustrating the calculation of valve loss coefficient**

On a graph, static pressure ( $P$ ) vs. axial distance ( $X$ ) points of coordinates ( $P_i, X_i$ ) are plotted from the experimental data. For the two pipes upstream and downstream of the test valve, the curves of static pressure drops follow a linear law and are straight lines.

The coordinates of the point upstream of the test valve plane which is the  $y$ -axis in this case, are used to calculate, by linear regression the slope  $m_1$  and intercept  $I_1$  of the line upstream of the valve. The coordinates of the points downstream of the valve are used to calculate also by linear regression, the slope  $m_2$  and intercept  $I_2$  of the line downstream of the valve.

In the case of valves, the pipes upstream and downstream of the test valve have the same diameters, the two hydraulic grade lines upstream and downstream of the test valve are parallel,  $m_1$  and  $m_2$  are equal and the pressure drop due to the test valve is given by:

$$\Delta p_v = I_1 - I_2 \quad (2.58)$$

And using equation (2.51):

$$k_v = \frac{\Delta p_v}{1/2\rho V^2} \quad (2.59)$$

$$k_v = \frac{(I_1 - I_2)}{\frac{1}{2}\rho V^2} \quad (2.60)$$

### Equivalent length

Alternatively, the valve loss coefficient can be expressed in terms of the equivalent length of straight pipe of the same diameter and having the same loss as the valve. The equivalent length is expressed in numbers of pipe diameters, ( $Le/D$ ) and is obtained by equating the Darcy-Weisbach formula, equation (2.9) to equation (2.51):

$$\left(\frac{Le}{D}\right) = \frac{k_v}{4f} \quad (2.61)$$

The drawback of this method is the fact that the equivalent length for a given fitting is not constant, but depends on Reynolds number and roughness, as well as size and geometry. Therefore, the use of equivalent length method requires consideration of all these factors (Hooper, 1981).

It has been shown using dimensional analysis that  $k_v$  for incompressible Newtonian fluids is a dimensionless function of  $Re$  and of dimensionless geometric ratios characteristic of the valve (Turian *et al.*, 1997):

$$k_v = \text{fn} (Re, \text{geometric ratios}) \quad (2.62)$$

This relation suggests that the resistance coefficient is the same for all sizes of a given type of valve provided dynamic similarity is enforced for instance equality of Reynolds number and geometric similarity are maintained (Turian *et al.*, 1997).

#### 2.6.4.3 Flow Coefficient

In some branches of the valve industry, particularly for control valves, the capacity of the valve is expressed in terms of a flow coefficient.



However there is no agreement on the definition of a flow coefficient in terms of SI units. In the USA and UK the flow coefficient in use is designated by  $C_{\text{valve}}$  and in other European countries by  $K_{\text{valve}}$  and are defined as:

$C_{\text{valve}}$  is the rate of flow of water, in either US or UK gallons per minute, at 60°F, at a pressure drop of one pound per square inch across the valve.

$K_{\text{valve}}$  is the rate of flow of water in cubic metres per hour at a pressure drop of one kilogram force per square centimetre across the valve (Crane Co., 1981).

$$C_{\text{valve}} = 0.0694 Q \sqrt{\frac{\rho}{\Delta p(999)}} \quad (\text{in US gallons}) \quad (2.63)$$

where:

$Q$  is the flow rate in litres per min.

$\rho$  is the density of the fluid in  $\text{kg/m}^3$

$\Delta p$  is pressure gradient in bar.

It must be said that  $C_{\text{valve}}$  is generally a fixed value for a specific type and size of a valve regardless of the operating conditions. In practice however this is true in the turbulent flow regime only where  $k_v$  is not a function of Reynolds number (Jadallah, 1980).

#### 2.6.4.4 Previous work on losses in valves

Substantial work has been done on the prediction of minor losses in pipe systems. In this section a brief review of work relevant to this investigation is presented. The different types of valves tested found in the literature are presented in Table 2.2 and for diaphragm valves in turbulent flow in Table 2.3.

The work of Edwards *et al.* (1985), Banerjee *et al.* (1994), and Turian *et al.* (1978), are all based on gate and globe valves not on diaphragm valves. They are relevant to this work by their methodology and mode of presentation of results.

- Edwards *et al.*, (1985), tested a range of Newtonian and non-Newtonian fluid flow through gate, and globe valves of 25 and 50 millimetres fully opened. They found that it is possible to present the data as a relationship between the loss coefficient and a generalised Reynolds number. They observed that in the laminar flow region, the loss coefficient is inversely proportional to the Reynolds number and can be obtained as:

$$k_v = \frac{C_v}{Re} \quad (2.64)$$

This is the same as equation (2.56). At higher Reynolds numbers a rapid transition is observed to a region in which the loss coefficient becomes constant, at about  $Re=130$ . In the case of gate valves, for various test fluids and for the two sizes used, the data falls together, and the analysis of experimental data gave the correlation:

$$k_v = \frac{273}{Re} \quad (2.65)$$

For globe valves the data for the two dimensions do not fall together. The transition from laminar flow is very rapid and occurs at a low Reynolds number of about 10. For the particular design of globe valves tested, in the fully open position, the following correlations were obtained:

For 25 millimetres valve:  $Re < 12$

$$k_v = \frac{1460}{Re} \quad (2.66)$$

$$Re > 12 \quad k_v = 122 \quad (2.67)$$

For a 50 millimetres valve:  $Re < 15$

$$k_v = \frac{384}{Re} \quad (2.68)$$

$$Re > 15 \quad k_v = 25.4 \quad (2.69)$$

- Banerjee *et al.*, (1994), presented experimental data on the pressure drop across 12.5 millimetres globe and gate valves in the horizontal plane for pseudoplastic fluids in laminar flow. They used generalised correlations in terms of various physical and dynamic variables for the prediction of the frictional pressure drop for each valve.

Three effects were studied:

1. The effect of pressure drop across the valve by plotting static pressure against length for a designated fluid.
2. The effect of the valve opening on pressure drop across the valve by plotting pressure drop against volumetric flow rate at different opening position: The pressure drop increases with an increase in volumetric flow rate for a constant opening. As the opening became smaller, the curve became steeper.

3. The effect of the non-Newtonian characteristics on pressure across the valves by plotting pressure drop across the valve against the volumetric flow rate for different concentration of slurries. At a particular opening of the valve, the pressure drop decreases as the flow behaviour index increases.

The dimensional analysis of the experimental data, suggested the following relationship:

$$\frac{\Delta p}{\rho V^2} = f(\text{Re}, \alpha) \quad (2.70)$$

The functional relationships developed using the above equation through multivariable linear regression analysis were as follows:

**Correlation for globe valve:**

$$\frac{\Delta p}{\rho V^2} = 8.266 \text{Re}^{-0.061 \pm 0.013} \alpha^{-0.797 \pm 0.030} \quad (2.71)$$

After plotting this the values of  $\frac{\Delta p}{\rho V^2}$  predicted using the equation above and the experimental values, the correlation coefficient and variance of estimate are 0.9496 and  $1.326 \times 10^{-2}$ .

**Correlation for gate valve:**

$$\frac{\Delta p}{\rho V^2} = 1.905 \text{Re}^{-0.197 \pm 0.046} \alpha^{-1.987 \pm 0.091} \quad (2.72)$$

After plotting this the values of  $\frac{\Delta p}{\rho V^2}$  predicted using the equation above and the experimental values, the correlation coefficient and variance of estimate are 0.9344 and  $1.106 \times 10^{-2}$ .

- Turian *et al.*, (1997), determined losses for the flow of concentrated slurries of laterite and gypsum solutions through 25 and 50 millimetres globe and gate valves. The loss coefficients were found to be inversely proportional to the generalised Reynolds number for laminar flow and to approach constant asymptotic values for turbulent flow, through gate and globe valves,

The following correlations were obtained:

For the 25 millimetres gate valve the transition from laminar to turbulent flow was observed between  $Re=100$  and  $Re=1000$  and  $k_v=320/Re$  and after the transition, in turbulent flow,  $k_v=0,797$ .

For the 50 millimetres gate valve the transition from laminar to turbulent flow was observed between  $Re=1000$  and  $Re=10000$  and  $k_v=320/Re$  for the laminar region and after the transition, in turbulent flow,  $k_v=0,168$ .

For the 25 millimetres globe valve, the transition from laminar to turbulent flow was observed earlier for  $Re<100$  and the correlation obtained was  $k_v=10,039$  for turbulent flow.

For the 50 millimetres globe valve also the transition was observed earlier for  $Re<100$  and the correlation obtained was  $k_v=6,719$ .

- Hooper, (1981) using the two-K method defined a dimensionless factor  $K$ , as the excess head loss in a pipe fitting, expressed in velocity heads.  $K$  does not depend on the roughness of the fitting (or attached pipe) or the size of the system, but is a function of the Reynolds number and the exact geometry of the fitting and is given by:

$$K = \frac{K_1}{Re_{MR}} + K_\infty \left( 1 + \frac{1}{D} \right) \quad (2.73)$$

where:  $K_1$  is  $K$  for the fitting at  $Re_{MR}=1$ ,  $K_\infty$  is  $K$  for a large fitting at  $Re_{MR}=\infty$  and  $D$  the pipe internal diameter. He found that:  $K_1 = 1000$  and  $K_\infty = 2$  for a dam or weir type diaphragm valve. Doing the analogy with the definition in this study, it can be said that  $C_v=1000$  and  $k_v=2$ .

- Pienaar *et al.*, (2004) tested a 40 mm nominal bore diameter diaphragm valve over a Reynolds number range of 1 to 50000 using various Newtonian and non-Newtonian fluids and obtained  $C_v=1000$  and  $k_v=2.5$ .
- Miller, (1978) classified the valve loss coefficients in three classes:

**Class 1 or definitive loss coefficients:** Loss coefficients in this class are based on experimental data usually from two or more sources or from research programmes, which have been crosschecked against other work. The loss coefficients are considered definitive.

In practice the loss coefficients in class 1 are usually not directly applicable, because of the severe restraints imposed on inlet and outlet conditions and geometrical accuracy

**Class 2 or adequate loss coefficient for design purposes:** Experimentally derived loss coefficients from isolated research programmes where no detailed crosschecking is possible against other sources.

Estimated loss coefficients from two or more research programmes whose results do not agree with what could be expected to be the experimental accuracy

Loss coefficients from class 1 converted to apply outside the strict limitations imposed in class 1 coefficients and for which experimental information is available to predict the effects of departing from class 1 conditions.

**Class 3 or suggested loss coefficient:** Experimentally derived values from less reliable sources

Loss coefficients from class 1 and 2 converted to apply outside their range of application and about which there is little or no information to predict the effects of departing from the conditions under which they were derived.

Loss coefficients in diaphragm valves are classified as class 3 and are given in turbulent flow; these loss coefficients can be obtained from the figure below for both weir and straight through diaphragm valves (Figure 2.9)

In fully open position in turbulent flow, the loss coefficient is approximately 0.8 for the straight-through diaphragm valve.

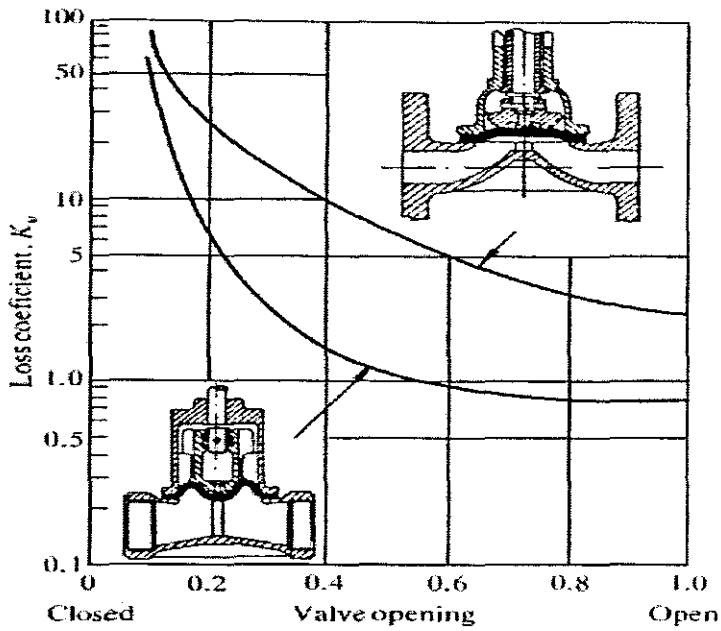


Figure 2. 9 Loss coefficient vs. valve opening (Miller, 1978)

Table 2. 2 Valves (Pienaar *et al.*, 2001)

TYPE	SIZE [mm]	REFERENCE	$C_v$
Gate	25	Turian <i>et al.</i> , 1998	
	50	Turian <i>et al.</i> , 1998	320
	25	Edwards <i>et al.</i> , 1985	273
	50	Edwards <i>et al.</i> , 1985	273
Globe	25	Turian <i>et al.</i> , 1998	
	50	Turian <i>et al.</i> , 1998	
	25	Edwards <i>et al.</i> , 1985	1460
	50	Edwards <i>et al.</i> , 1985	384
3-way plug	-	Steffe <i>et al.</i> , 1984	
Check valves			
Ball			
Horizontal lift			
Bronze disc swing		Kittredge & Rowley, 1957	
Composition disc swing	12.5		
Diaphragm	-	Hooper, 1981	1000

**Table 2.3 Loss coefficients for turbulent flow through diaphragm valves (Perry & Chilton, 1973)**

Operating mode	Loss coefficient, $k_v$
Open	2.3
$\frac{3}{4}$ open	2.6
$\frac{1}{2}$ open	4.3
$\frac{1}{4}$ open	21

## 2.7 DYNAMIC SIMILARITY

In this section, the theory related to the establishment of dynamic similarity and its application to the flow of non-Newtonian fluids flow in valves is presented.

### 2.7.1 Geometric Similarity

Geometric similarity is similarity of shape (Massey, 1970) and is the first requirement for the establishment of physical similarity. If two systems are geometrically similar the ratio of any length in one system to the corresponding length in the other system is everywhere the same and this ratio is called the scale factor.

Geometric similarity exists between a model and a prototype if the ratios of all corresponding dimensions in model and prototype are equal (Giles, 1977):

$$\frac{L_{\text{model}}}{L_{\text{prototype}}} = L_{\text{ratio}} \quad \text{or} \quad \frac{L_m}{L_p} = L_r \quad (2.74)$$

$$\text{and} \quad \frac{A_{\text{model}}}{A_{\text{prototype}}} = \frac{L_{\text{model}}^2}{L_{\text{prototype}}^2} = L_{\text{ratio}}^2 = L_r^2 \quad (2.75)$$

### 2.7.2 Kinematic Similarity

Kinematic similarity is similarity of motion (Massey, 1970). This implies first, geometric similarity and then similarity of time intervals in the motion.

Kinematic similarity exists between a model and a prototype if the paths of homologous moving particles are geometrically similar and if the ratios of the velocities of homologous particles are equal (Giles, 1977):

$$\text{Velocity ratio:} \quad \frac{V_m}{V_p} = \frac{L_m/\Gamma_m}{L_p/\Gamma_p} = \frac{L_r}{T_r} \quad (2.76)$$

$$\text{Acceleration ratio:} \quad \frac{a_m}{a_p} = \frac{L_m/\Gamma_m^2}{L_p/\Gamma_p^2} = \frac{L_r}{T_r^2} \quad (2.77)$$



$$\text{Discharge ratio: } \frac{Q_m}{Q_p} = \frac{L_m^3/\Gamma_m}{L_p^3/\Gamma_p} = \frac{L_r^3}{L_r} \quad (2.78)$$

### 2.7.3 Dynamic Similarity

Dynamic similarity is similarity of forces (Massey, 1970). Dynamic similarity exists between geometrically and kinematically similar systems if the ratios of all homogenous forces in model and prototype are the same.

In the case of a fluid flowing in a closed conduit, as in this investigation, in a pipe, the dominant forces are the viscous and inertial forces, other forces like the pressure force, the surface tension force are negligible and do not affect the flow.

The only interesting ratio in this case is the ratio:

$$\left| \frac{\text{Inertial force}}{\text{Viscous force}} \right| = \frac{\rho V l}{\mu} \quad \text{which for a Newtonian pipe flow is the Reynolds number } Re \text{ and}$$

is in this case, equation (2.12):

$$Re = \frac{\rho V D}{\mu} \quad (2.12)$$

Thus two flows passing geometrically similar boundaries are dynamically similar if the only forces affecting those flows are only viscous, pressure and inertia forces, if the magnitude ratio of inertia and viscous forces at corresponding points are the same. Since this ratio is proportional to the Reynolds number, two systems are dynamically similar when the Reynolds number of the two systems based on corresponding characteristic lengths and velocity are the same for the two flows (Massey, 1978).

### 2.7.4 The Application of Dynamic similarity for Non-Newtonian Fluid Flows in Valves

If only one kind of forces are dominant, apart from inertia and pressure forces, then complete dynamic similarity is achieved simply by making the values of the appropriate dimensionless parameter the same for model and prototype, in this case the Reynolds number (Massey, 1978).

For the case of a Newtonian fluid, the Reynolds number is easily obtained and is used to establish dynamic similarity, but for non-Newtonian fluids, the task is not simple because of other parameters like the yield stress and the rheogram curvature, which must be well established.

For the flow of non-Newtonian fluids in valves, viscous forces are dominant and forces due to weight and surface tension do not play a role. The dimensionless group known as the Reynolds number is of prime importance and two systems are dynamically similar if their Reynolds numbers are the same. Unlike the Newtonian model, where the rheology is characterised by only one parameter the viscosity, the non-Newtonian model is characterised by three parameters: the yield stress, the fluid consistency index and the flow behaviour index. The Slatter Reynolds number accounts specifically for the yield stress together with the other two parameters and can be used to establish dynamic similarity (Slatter & Pienaar, 1999).

To conclude, two non-Newtonian flows in geometrically similar valves are similar if their Slatter Reynolds numbers are the same.

As said earlier, the first requirement for physical similarity is geometric similarity, thus this similarity establishment will be carried on the same type of valves from the same manufacturer otherwise it will be meaningless (Slatter & Pienaar, 1999).

## 2.8 CONCLUSION

Far from being comprehensive, this chapter attempts to present the necessary theory on Newtonian and non-Newtonian fluid flow in straight pipes, pipe fittings and valves, but with an emphasis on non-Newtonian materials flowing in valves especially in diaphragm valves.

From the literature review, it was found that data on diaphragm valves are scarce. Perry & Chilton (1973) give some values of the loss coefficient in diaphragm valves for Newtonian fluids in turbulent flow. Miller (1978) gives a graph of  $k_v$  vs opening of the valve for the determination of an approximate loss coefficient in turbulent flow. Hooper (1981) presents loss coefficient data for a dam or weir type diaphragm valve in the laminar and turbulent flow regimes. Pienaar *et al.* (2004) present data for one size diaphragm valve in both laminar and turbulent flow.

As said earlier, the work of Edwards *et al.* (1985), Banerjee *et al.* (1994), and Turian *et al.* (1978), are all based on gate and globe valves, not on diaphragm valves. However, they are relevant to this work by their methodology and mode of presentation of results.

## 2.9 RESEARCH ASPECT IDENTIFIED

After the completion of the literature review it has been obvious that there is a need for much more data on loss coefficients through diaphragm valves for both Newtonian and non-Newtonian fluids and there is also a need to evaluate existing data. Data on diaphragm valves are scarce and are only approximations. Hooper (1981); Miller (1978) and Perry & Chilton (1973) give the loss coefficient without specifying the dimension of the valve. Hooper (1981) gives the laminar loss coefficient  $C_v$  and the loss coefficient in turbulent flow. Perry & Chilton (1973) and Miller (1978) give only the loss coefficient in turbulent flow for Newtonian fluids. Miller classifies loss coefficients in diaphragm valves as class 3 data, i.e. data from less reliable sources. Data from other type of valves has been converted to apply to diaphragm valves and about which there is little or no information to predict the effects of departing from the conditions under which they were derived (Miller, 1978).

It also became apparent that there is a need to define experimental procedures in the determination of loss coefficients in valves because the value of the loss coefficient is dependent on the experimental procedure used and definitions (Chhabra & Slatter, 2002).

# CHAPTER 3

## CHAPTER 3 EXPERIMENTAL WORK

### 3.1 INTRODUCTION

This chapter describes the experimental test loop. It also provides an in-depth geometric analysis of the type of diaphragm valve tested. The description and calibration of the instrumentation used in the test work, the experimental procedure of the test work, the description of all materials tested and the general theory on errors are also given. Raw results from experimental tests are also presented.

The experimental test loop used is the new Valve test rig. After the construction of the test loop and the calibration of the different instrumentations, commissioning was successfully done by running water tests in all the pipes, followed by tests with non-Newtonian slurries.

### 3.2 DESCRIPTION OF THE TEST LOOP

The test loop used is the new state-of-the-art Valve test rig. The Valve test rig is 22m long and 2,6m high. It consists of a storage and mixing tank of 1,75 m<sup>3</sup> with a header or weigh tank of 500 litres on top. The fluid is forced in the test loop by a positive displacement pump. Before reaching the test sections, the fluid passes a surge damper, then through a heat exchanger. The fluid passes through two magnetic flow meters in parallel; one for the lines of 50 and 63 millimetre outside diameters and the other one for the lines of 75, 90 and 110 millimetre outside diameters. The test section consists of 6 lines of 50, 63, 75, 90 and two 110 millimetre outside diameters respectively. At every entry of a test line there is a diaphragm control valve to direct the fluid. The fluid exits all test lines through a manifold. For each test line there are two pipes of 10 metres long joined in series by a diaphragm valve. Figure 3.1 gives a schematic diagram of the Valve test rig.

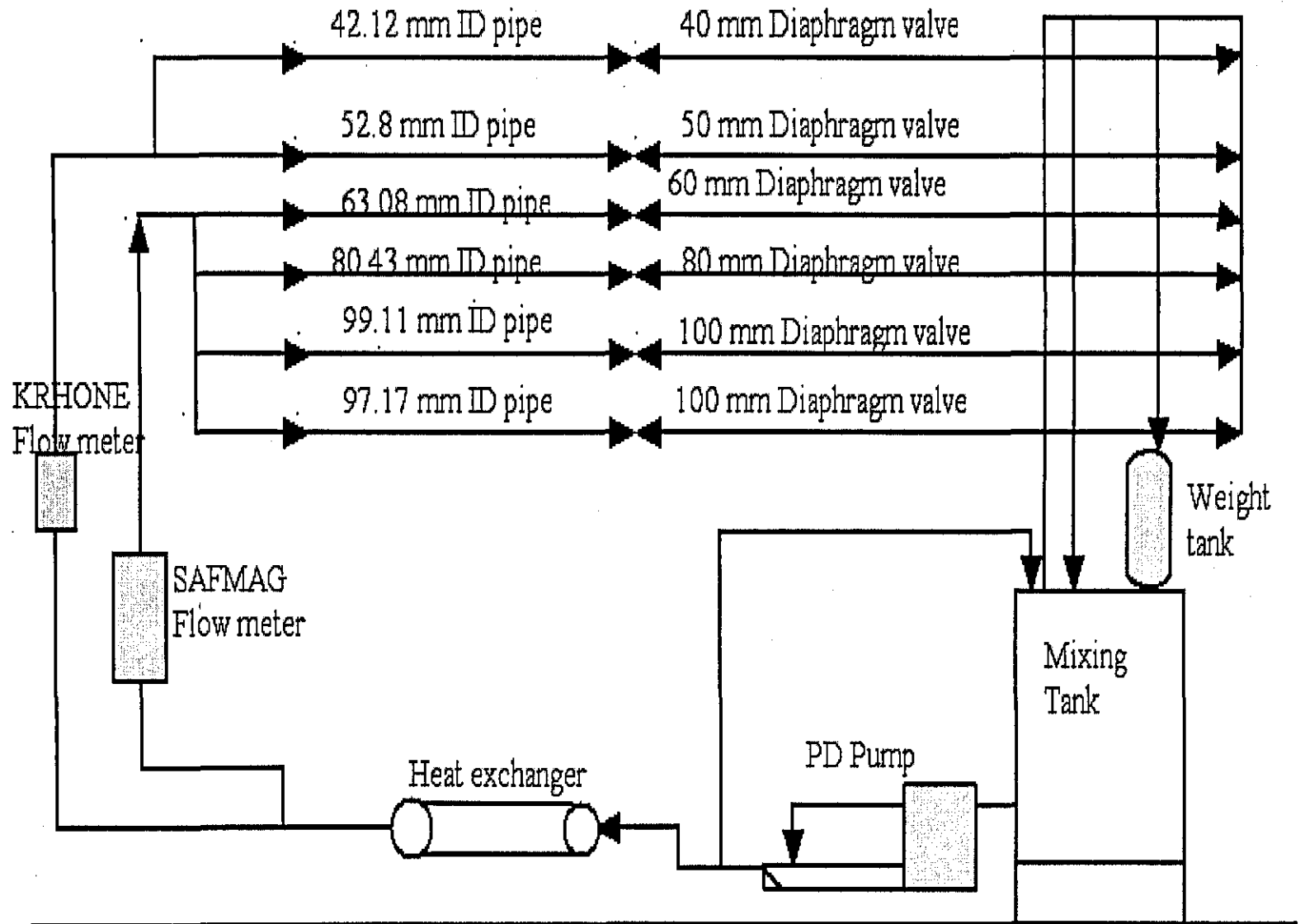


Figure 3. 1 Schematic diagram of the Valve test rig

### 3.3 INSTRUMENTATION

This section describes the instruments connected to the test loop when running different tests in order to collect experimental data.

#### 3.3.1 Pipes and Valves

The pipes used for the test loop were all PVC pipes clear or non-clear with negligible roughness.

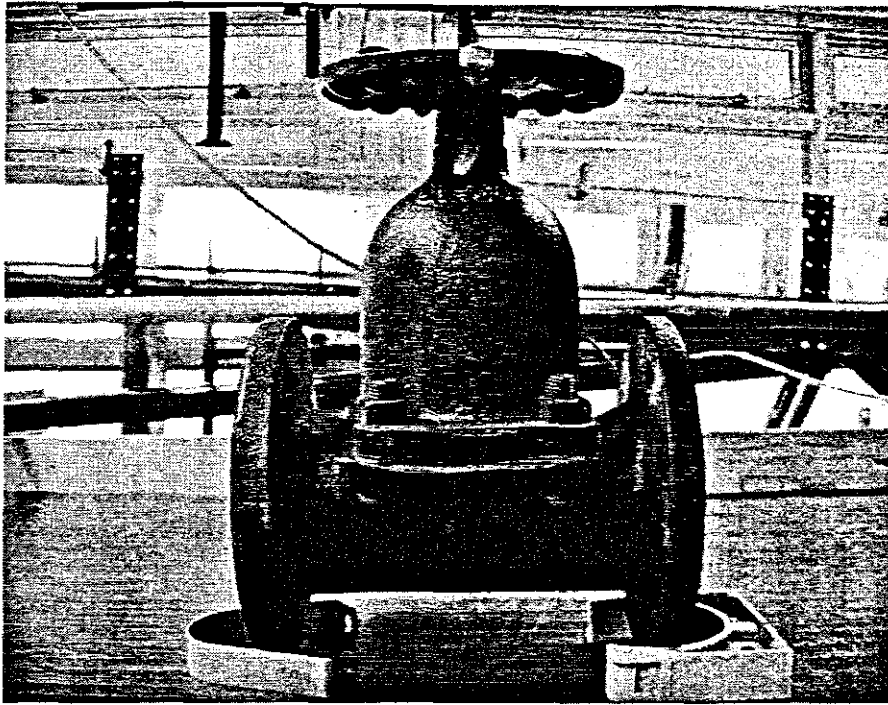
The valves used for determining the loss coefficient are the NATCO straight-through diaphragm valves of 40, 50, 65, 80 and 100 millimetre nominal bore diameter and are low resistance valves.

Table 3.1 gives the outside diameters (OD) or nominal diameter of the six test lines and their internal diameters (ID) as were determined experimentally. The experimental method for the determination of ID is explained later in this Chapter 3 (3.5.12.1).

**Table 3. 1 Nominal and internal dimension of pipes and valves.**

Test Line Number	Outside Diameter [mm]	Internal Diameter [mm]	Valve Dimension [mm]
1 (Top)	50	42.12	40
2 (2nd Top)	63	52.8	50
3 (3rd Top)	75	63.08	65
4 (4th Top)	90	80.43	80
5 (2nd Bottom)	110	99.11	100
6 (Bottom)	110	97.17	100

Figure 3.2 gives an external view of the diaphragm valve used and Fig.3.3 shows the way these diaphragm valves were connected to pipes, Fig.3.4 shows the internal structure of the diaphragm valves at the fully open position.



**Figure 3. 2 Diaphragm valve**

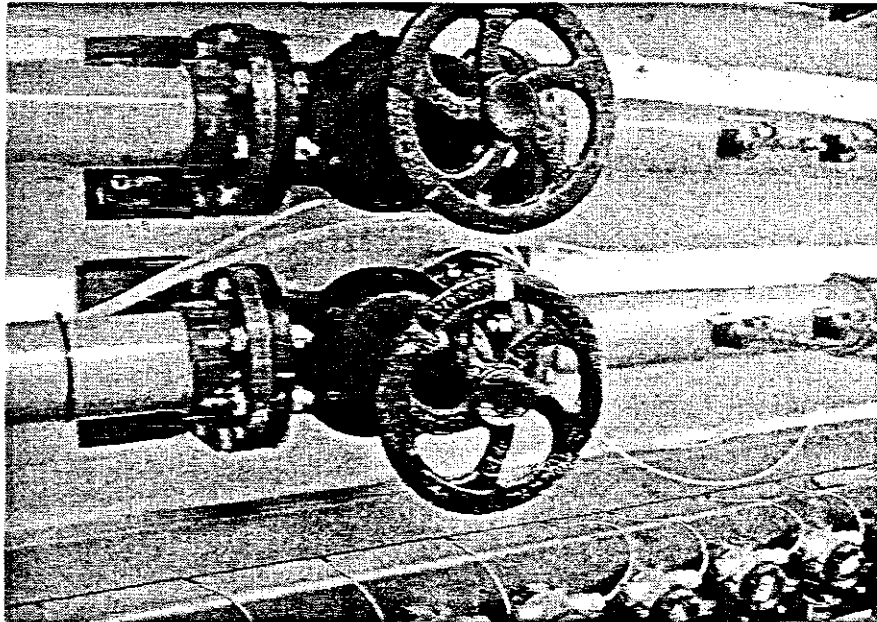


**Figure 3. 3 Connection of diaphragm valves with pipes.**



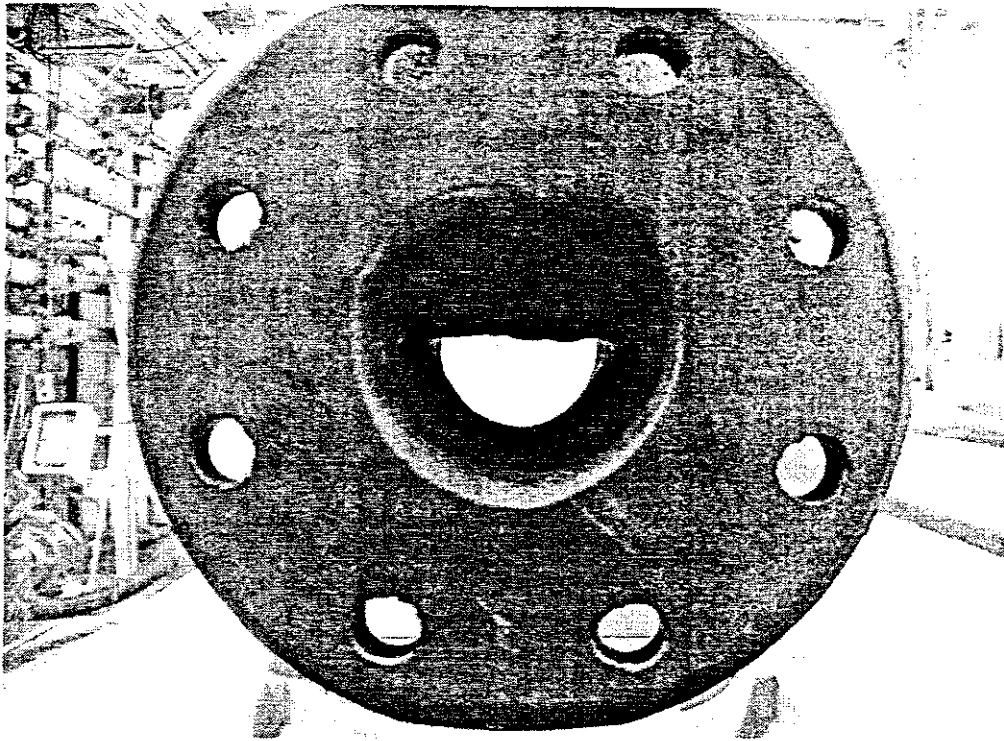


**Figure 3. 4 Internal structure of the valve in the fully open position.**

The diaphragm valves tested are also characterised by some internal dimensions characteristics that are: Cross section dimensions (Width & Depth), Diaphragm dimension (Height, width, Per rev) and bore dimension (A, B and C). Figure 3.5 gives such approximate dimensions for an 80 mm nominal bore diameter diaphragm valve. The diaphragm valve manufacturer supplied the information given in Table 3.2 and Figure 3.5. It is obvious that the dimensions are not always exactly the same for each nominal bore size valve. They are within a certain tolerance as specified by the manufacturer.

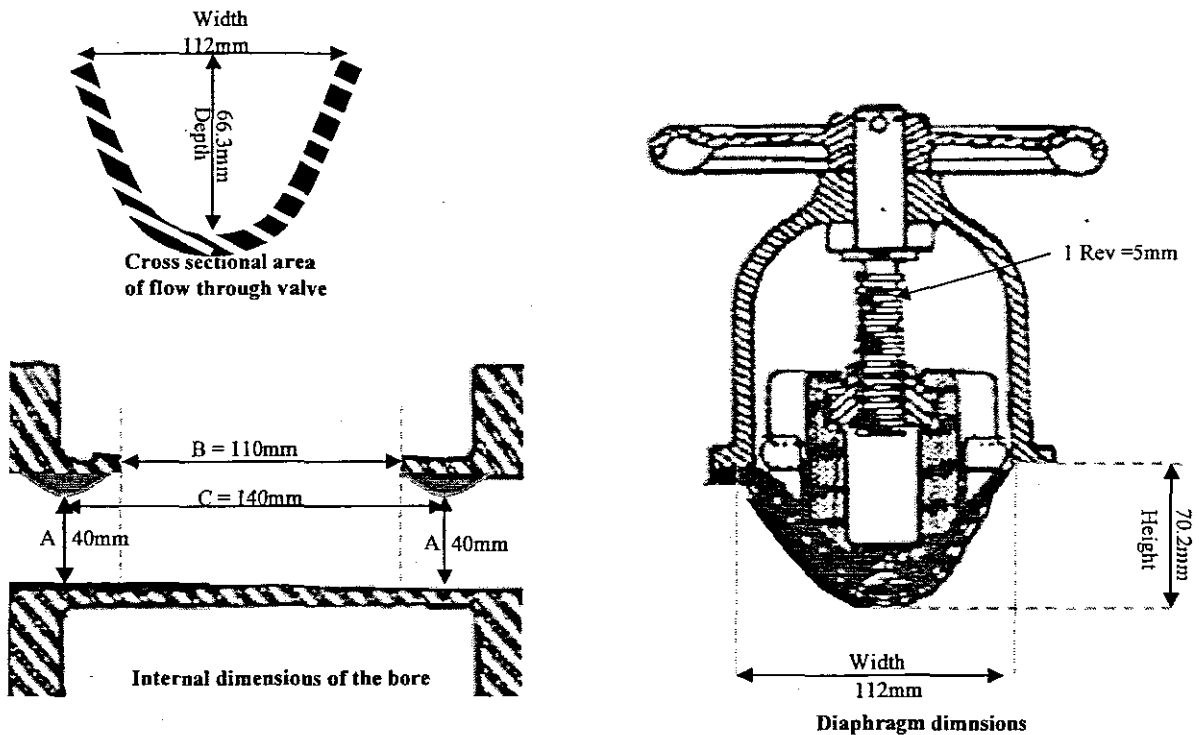


Figure 3. 5 Internal dimension of the 80 mm nominal bore diaphragm valve.

Table 3.2 gives such dimensions (in mm) for all 5 sizes of diaphragm valve tested and Table 3.3 gives such dimensions for all 5 sizes in a dimensionless form, dividing all dimensions of a given valve by the nominal bore size.

Table 3. 2 Internal dimensions of diaphragm valves tested

Bore size	Cross section area		Diaphragm Dimension			Bore dimension		
	Depth	Width	Height	Width	Per Rev	A	B	C
40	35.26	42.78	36.00	47.38	3.00	26.18	45.02	65.34
50	46.65	64.26	47.00	66.34	4.50	36.26	66.71	81.00
65	62.42	90.82	63.00	92.14	5.00	40.00	88.00	125.00
80	68.92	112.00	69.00	114.20	5.70	42.26	111.00	140.50
100	74.72	124.46	75.00	129.92	6.50	62.14	128.00	150.40

Table 3.3 Dimensionless Internal dimensions of diaphragm valves tested

Bore size	Cross section area		Diaphragm Dimension			Bore dimension		
	Depth	Width	Height	Width	Per Rev	A	B	C
1	0.88	1.07	0.90	1.18	0.08	0.65	1.13	1.63
1	0.93	1.29	0.94	1.33	0.09	0.73	1.33	1.62
1	0.96	1.40	0.97	1.42	0.08	0.62	1.35	1.92
1	0.86	1.40	0.86	1.43	0.07	0.53	1.39	1.76
1	0.75	1.24	0.75	1.30	0.07	0.62	1.28	1.50

From these data, a geometric similarity analysis was done based on the fact that geometric similarity exist between a model and a prototype if the ratios of all corresponding dimensions in model and prototype are equal:

$$\frac{L_{\text{model}}}{L_{\text{prototype}}} = L_{\text{ratio}} \quad (2.74)$$

Taking every size as a prototype and comparing with all other sizes and also by analysing the dimensionless sizes of the diaphragm valves tested, it was found that no geometric similarity could be observed between the 5 sizes of diaphragm valves used.

From Fig.3.4, it can be observed that the type of diaphragm valves used has a tapered or narrowed bore through the body of the valve. The full bore opening is characterised by an obstruction of the diaphragm through the opening and the size of the obstruction varies from size to size and is respectively 4.74, 3.35, 2.58, 11.03, 25.28 millimetres for the 40, 50, 65, 80 and 100 millimetres bore nominal diameter. And the scale factor of the height of the obstruction on the nominal bore diameter is 0.12, 0.067, 0.04, 0.14, 0.25 for the 40, 50, 65, 80 and 100 millimetres bore nominal diameter. Once again, no geometric similarity was found. All dimensions above mentioned are tabulated in Table 3.4.

**Table 3.4 Obstruction size and scale ration for the diaphragm valves tested**

Bore size	Obstruction size	Obstruction/Bore size
40	4.74	0.12
50	3.32	0.07
65	2.58	0.04
80	11.03	0.14
100	25.28	0.25

### 3.3.2 Pressure lines, pressure lines board, tappings and pods

Nylon tubes of 3 mm internal diameter were used as pressure lines. They were connected to the test section by tappings via pods and the pressure lines board (PLB) to pressure transducers.

Each test line had tappings at various positions from which the experimenter could choose according to the type of the experimental test to be run.

The pressure line board (PLB) as designed by the author of this investigation, is a hydraulic circuit that allows to select points where the static pressure can be read off. It is also used to set the technique to be used while running the experimental tests. As it will be explained later in this chapter there were six techniques using the PLB and the nine point pressure transducers and two differential pressure transducers to run experimental tests on the Valve test rig: automatic mode (AM), manual single (MS), manual all (MA), American standard method (ASM), straight pipe test (SPT), HGL DP Cell mode. The PLB is a very useful tool and consists of a circuit of nylon tubes and ball valves on a perspex board. The nylon tubes are classified in four pressure lines (PL1, 2, 3 and 4) and the ball valves in: deviation valves (D), isolation valves (I), exit valves (E), bypass valves (B) and connecting valves (C). Deviation valves allow to isolate the PLB and to work in automatic mode with all the pressure transducers at the same time. The isolation valves allow to separate two or more given tappings from other tappings. The exit valves allow to isolate a given tapping from the other tappings. The bypass valves allow to isolate a pressure line and the Connecting valves allow to connect a given PL to a pressure transducer. Figure 3.6 gives a schematic diagram of the pressure lines board and Figure 3.7 gives the connection of the PLB (the rectangular central part) to the test line and to pressure transducers.

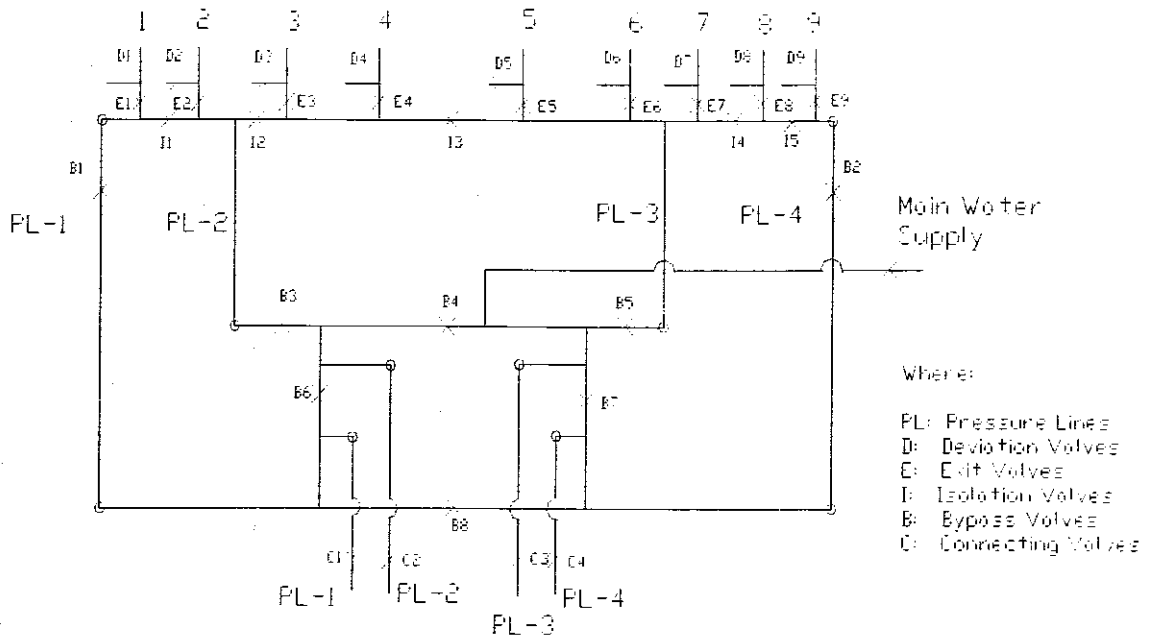


**Figure 3. 6 Schematic diagram of the pressure lines board**

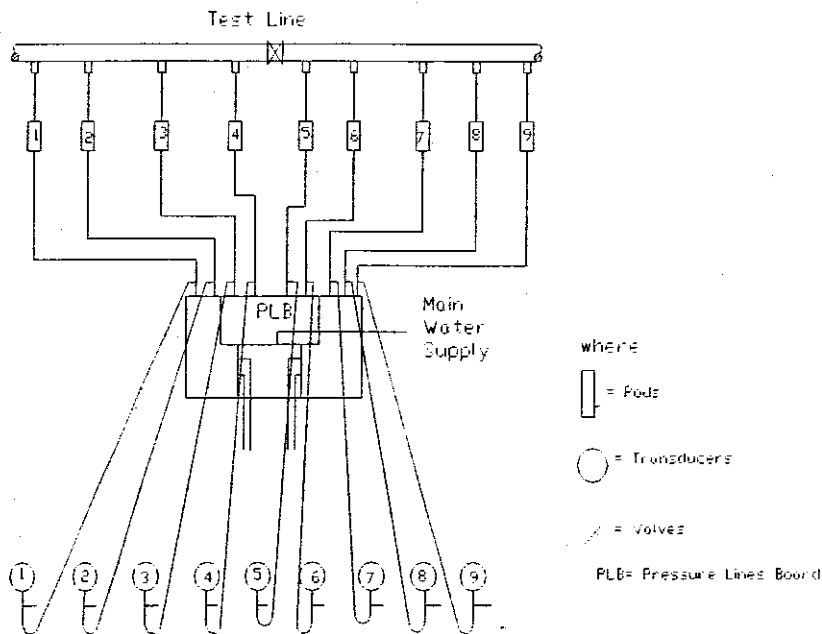


**Figure 3. 7 Connection of the PLB (the rectangular central part) to pods and pressure transducers.**

### 3.3.3 Pressure Transducers

Two kinds of pressure transducers were used:

- a) The Point Pressure Transducer (PPT): It is used to measure static pressure at a given point in the test line.
- b) The Differential Pressure Transducer (DP Cell): It is used to measure the difference of static pressure between two points.

At the time of the completion of this investigation, the Valve test rig had nine PPT and two DP Cells in operation. The nine PPT's have a range span of 130 kPa and are mostly used to run the tests in: automatic mode, manual mode, manual mode all. The two DP Cells, has the range span of 130 kPa and 6 kPa respectively. They are mostly used to run test in the HGL DP cell mode, Straight pipe test and American standard Method. These pressure transducers are connected to the PLB by means of nylon tubes as shown in Figure 3.7 and to the data acquisition unit (DAU) by means of electrical cables.

Included in Appendix 1 is a picture of the pressure transducers used (point pressure transducer and differential pressure transducer).

### 3.3.4 The Hand Held Communicator

The type of hand held communicator (HHC) used is the FXW 10 AY1- A3. It is a portable instrument with many features and is used for the zeroing, calibration, change of unit, range setting, span and damping time setting of both the differential pressure transducer (DPT or DP Cell) and the point pressure transducer (PPT). The hand held communicator is also a display unit of pressure transducers and the two instruments are twins as one cannot be used successfully without the other.

Included in Appendix 1 is shown the picture of the hand held communicator.

### 3.3.5 The data acquisition unit or data logger

The data acquisition unit used is the model HP 34970A, which is equipped with many channels and it converts electrical signals from pressure transducers, temperature sensors, flow meters and load cell connected to it into digital signals that are logged to the computer.

Included in Appendix 1 is the picture of the Data Acquisition Unit.

### 3.3.6 Computer and Software

A Celeron 300 was used for data capturing and processing. Test programs were written in Visual Basic 6. The data capturing, analysis and processing was done in Microsoft Excel.

### 3.3.7 Flow meters

Two magnetic flow meters were used during test work and they were both mounted vertically:

- A Krohne IFC 010D of 50 millimetre internal diameter
- A Safmag 100A2NESSR0032 of 110 millimetre internal diameter.

Include in Appendix 1 is the pictures of the flow meters.

### 3.3.8 Tank and Mixer

The 1.75 m<sup>3</sup> storage tank was fitted with a mixer of the type SEW EURODRIVE ARF 57 DT 90L4 with power of 3 kW. It also has on top a header or weight tank of 500 litre capacity for the calibration of flow meters and flow rate determination in the flow region where the flow meter reading becomes inaccurate.

Included in Appendix 1 is the picture of the mixing tank and the weight tank on top.

### 3.3.9 Pump

The pump used is an Orbit reversible positive displacement pump of the type B4001 CI EN8 NIT with a power of 5,5 kW, with a helical rotor. This pump is fitted with a variable speed drive, which allows shifting the speed of rotation of the pump rotor.

Included in Appendix 1 is the picture of the Pump used.

### 3.3.10 Manometers

Two U-tube manometers were used for calibration of the pressure transducers:

- A mercury- water manometer was used for the calibration of higher pressure ranges.
- A water air manometer was used to calibrate lower pressure ranges.

### 3.3.11 Pressure Gauges

Digital pressure gauges were used mostly to verify the pressure readings of the hand held communicator and that of the computer programme output after the calibration coefficients have been included.

### 3.3.12 Temperature probes

The temperature of the slurry was measured at two positions in the Valve test rig using temperature probes. The first position was: at the end of the heat exchanger and the second at the mainstream flow exit. Both temperature probes were linked to the data acquisition unit that reads the temperature in degrees Celsius. As the data acquisition reads the temperature directly, no signal calibration was required.

## 3.4 EXPERIMENTAL PROCEDURE

### 3.4.1 Calibration

The calibration of the instruments was done for two major reasons: firstly in order to get reliable results and secondly in order to transform the electrical signal from the instruments in a digital signal to be read to the computer workstation. The computer program needs some calibration constants called signal calibration.

#### 3.4.1.1 DP Cells

Two DP Cells were used during the test works. One of the range span of 130 kPa and another of the range span of 6 kPa.

The calibration of the differential pressure transducers was done in the following manner:

-Prior to everything, the DP Cell is manually zeroed and than electronically zeroed with the Hand Held Communicator when there is no external pressure applied to both sides of the DP Cell.

-Than the DP Cell is connected to the manometer so that the high and low sides are respectively connected to the high and low side of the U-tube manometer



-All the air bubbles are flushed from the lines using the main water supply connected to pressure lines of the DP Cell.

-A differential pressure within the range limit is set up in the U-tube manometer.

-The differential pressure is read digitally using the Hand Held Communicator at the same time the DP Cell DC voltage output is read from the Data logger.

-The differential pressure is then decreased uniformly in 5 parts and the previous step is repeated until the equilibrium is attained.

The calibration line is obtained by performing a linear regression on the pressure difference and the transducer DC voltage output. The coefficient of correlation  $R^2$  should be at least 0.999. Figure 3.8 shows an example of the calibration regression lines of the DP cell of 6 kPa span range for two ranges.

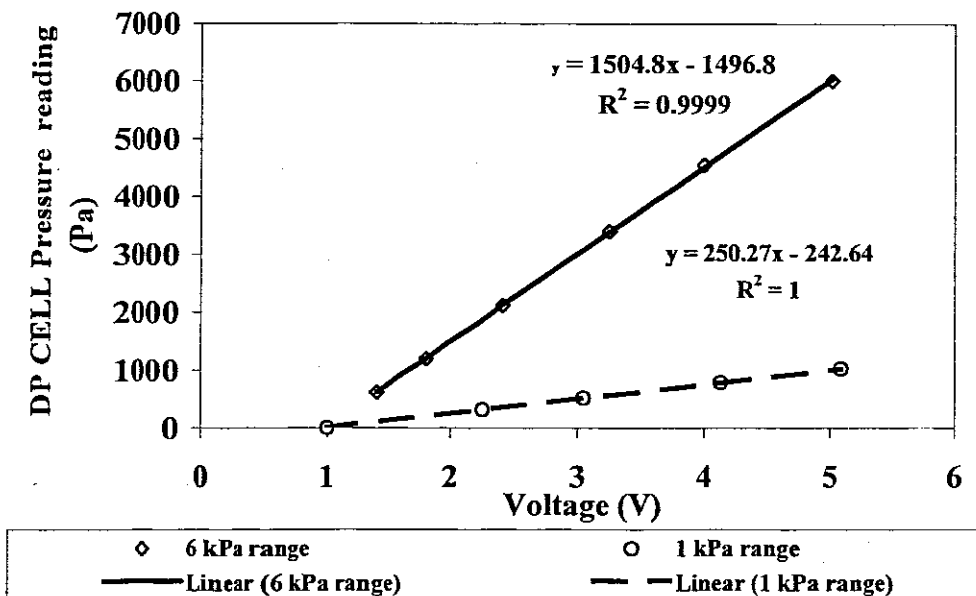


Figure 3. 8 Calibration regression lines of the DP cell of 6kPa span range showing calibration regression lines for 0-6kPa range and 0-1kPa range

#### 3.4.1.2 Point pressure transducer

The calibration of the Point Pressure Transducer was done in the same way as for the DP Cell described above with the only difference being that the pressure line of the PPT was connected to the high side of the U-tube manometer. The differential pressure was read between the higher meniscus and the centre line of the PPT. Figure 3.9 gives an example

of the calibration line of a PPT of 130 kPa in the range of 0 to 40kPa. Table 3.3 gives the calibration constants for different transducers.

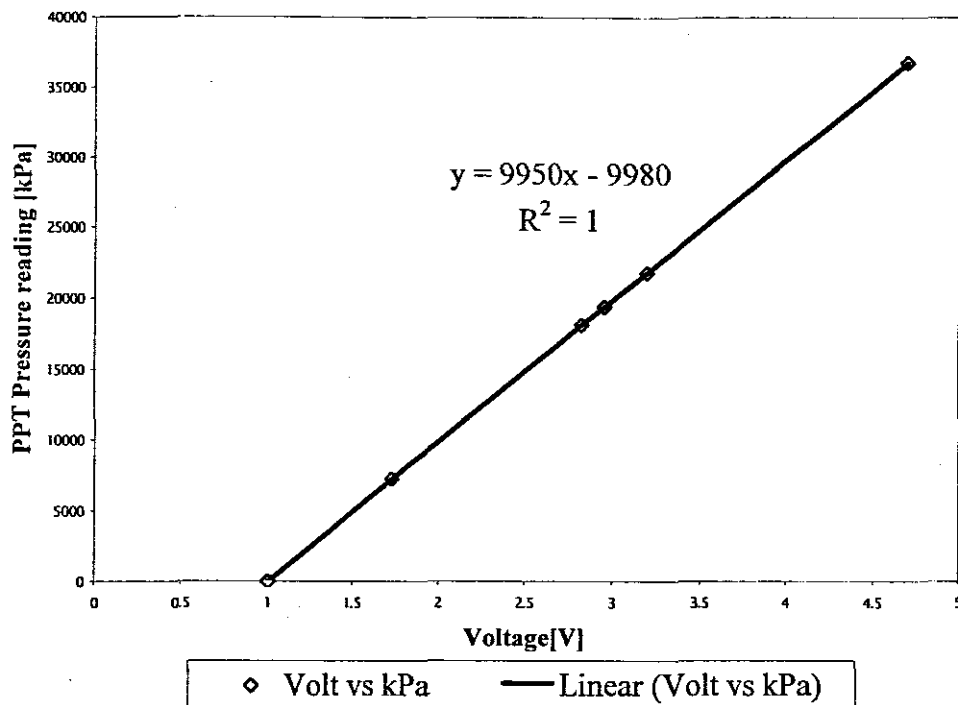


Figure 3. 9 Calibration regression line of a Point pressure transducer of 130 kPa

**Table 3.3 Calibration constants for different transducers**

PPT	RANGE	Ax	B	R <sup>2</sup>
1	0-40	10010.35x	-10046	1
	0-130	32476.02x	-32544	1
2	0-40	9950.038x	-9980	1
	0-130	32382x	-32498	1
3	0-40	9986.15x	-9996.4	1
	0-130	32783.99x	-32303	1
4	0-40	9990.15x	-9994.7	1
	0-130	32419x	-32478	1
5	0-40	9962.22x	-10046	1
	0-130	32413.23x	-32484	1
6	0-40	9975.65x	-9985.6	1
	0-130	32435x	-32475	1
7	0-40	9973.85x	-9987.4	1
	0-130	32542.59x	-32542	1
8	0-40	9971.99x	-10002	1
	0-130	32422.77x	-32516	1
9	0-40	9987.98x	-9992.4	1
	0-130	32457.46x	-32422	1

### 3.4.1.3 Load Cell

The load cell that supports the header or weigh tank is depicted in Appendix 1. It is used to weigh the fluid diverted from the mainstream flow. To calibrate it, the fluid is weighed in a container using an electronic scale. The fluid is then poured in the weigh tank, and the container is weighed again to take the difference in masses. Once the difference in mass between the container with fluid and the empty container is taken, the voltage output is recorded. For every increase in load, the increase in voltage is recorded.

The recorded values of the increase in load are plotted against the recorded values of the corresponding voltage as shown in Figure 3.10. A linear regression of the plot will give

the relationship between the load and the corresponding voltage. This is then entered in the program to be used to calculate the flow rate.

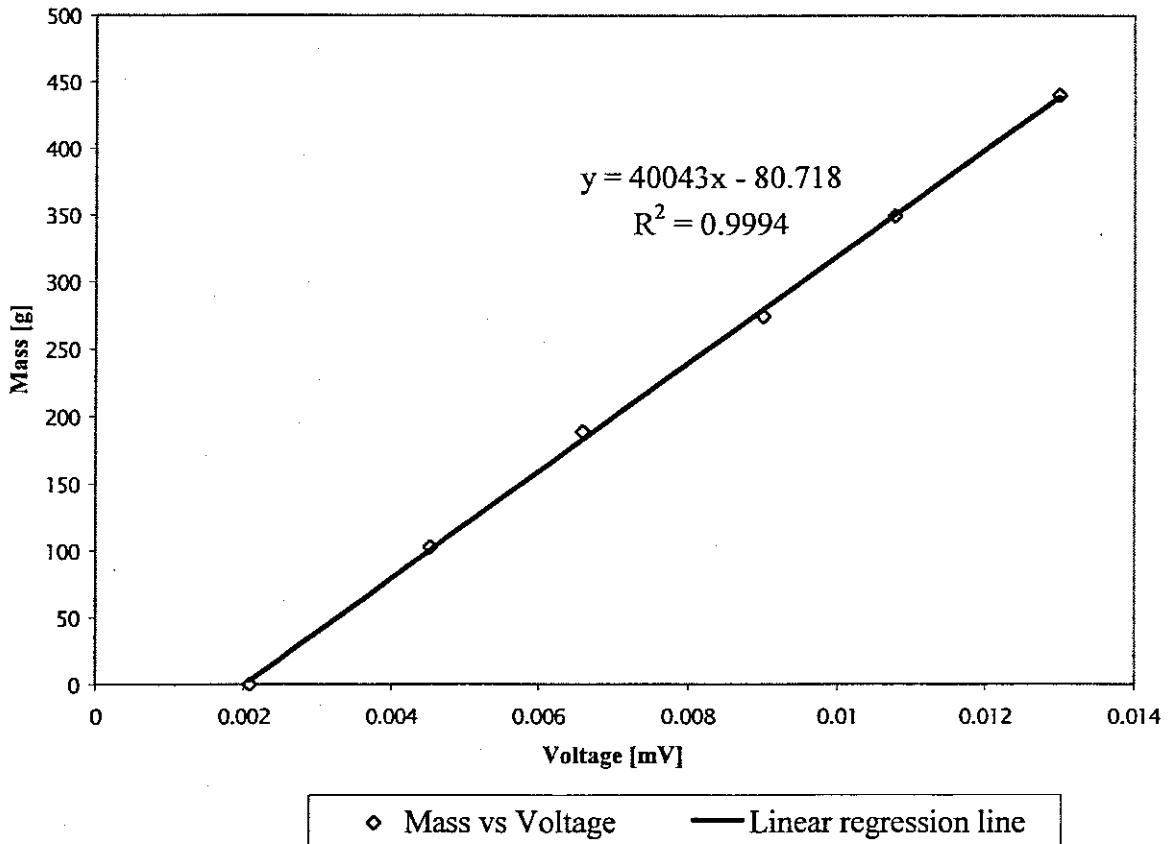


**Figure 3. 10 Calibration regression line of Load Cell**

#### 3.4.1.4 Flow meter

The materials tested vary in chemical composition and concentration, so each material is tested over the flow rates used by diverting the flow into the weigh tank. The flow meters that measure the flow rates are, according to the manufacturers, accurate for slurries. To confirm this, each flow meter is calibrated with each slurry concentration that will be tested.

The calibration procedure is as follows:

For each flow meter the flow rate range is divided into 12 different flow rates over the whole range that the flow meter can measure. Each flow rate is then weighed with time in the weigh tank. The data logger continuously samples the change in weight with time, and from these readings the average flow rate is calculated. The sampling period varies from 120 s for low flow rates to 12 s for the high flow rates. This is repeated for all the flow rates.

The flow rates versus voltages are then plotted and the straight-line regression gives the relationship between flow rate and volts as well as the error fit. Figure 3.11 gives a typical calibration regression line for a flow meter.

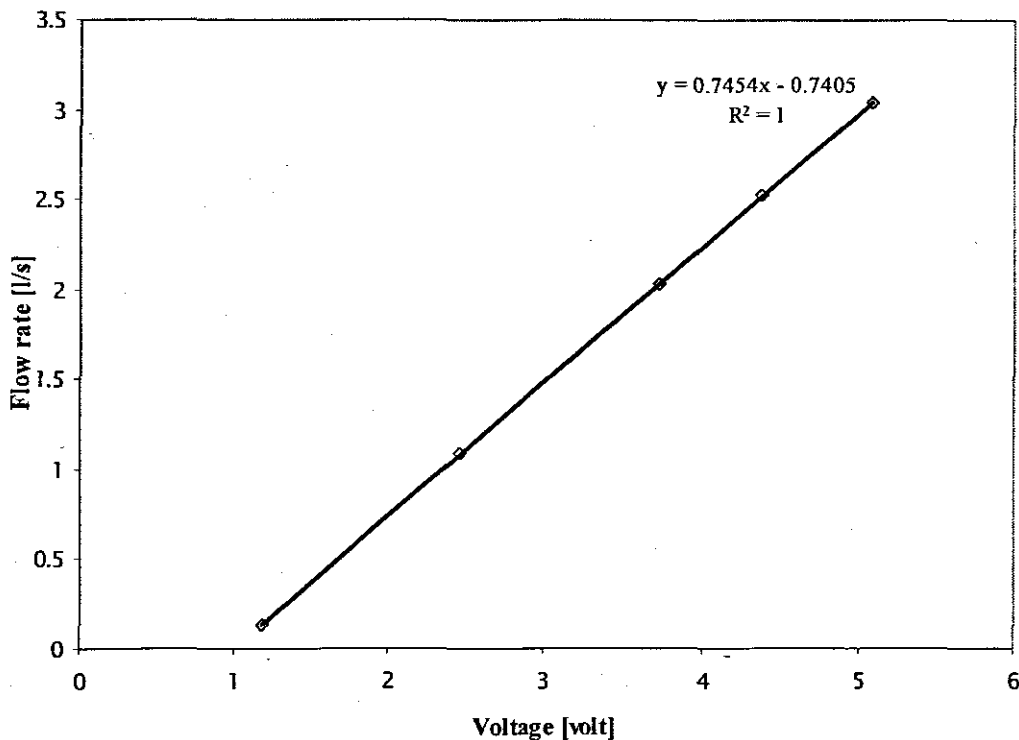


Figure 3. 11 Calibration regression line for the Krohne flow meter

### 3.4.2 Experimental Test Method (Valve Pressure Drop Test and Straight Pipe Test or Tube Viscometry)

The valve test rig is a versatile instrument and is a miniature pipeline. Two principal types of tests may be conducted on the valve test rig: the viscometry test or straight pipe test and the valve pressure drop test. These tests may be conducted simultaneously or separately.

The rheology or straight pipe test consists of measuring the pressure drop in the straight pipe sections at different flow rates whereas the valve pressure drop test consists of measuring the pressure drop incurred by the test valve at different flow rates.

Generally, there are two approaches to measure the valve pressure drop: The hydraulic grade line (HGL) approach and the total pressure drop approach. In the context of this investigation, as said earlier, the hydraulic grade line approach was used. Because the valve test rig was specially designed for that approach. This approach can be applied in an automatic mode or a manual mode depending on flow conditions as follows:

In automatic mode, all the pressure readings are taken simultaneously using all the nine transducers and every transducer reads a pressure on one tapping.

The HGL automatic mode is selected when the static pressure in the test section is high enough so that different PPT's can measure accurately the pressure gradient along the test section. This condition is likely to happen when testing small diameters (50, 63 and 75 millimetres OD) or bigger diameters at higher flow rates (90, 110 millimetres OD) or testing very dense materials.

The HGL manual mode is the technique in which, one transducer is used to read the static pressure drop at each tapping at a time and this technique is facilitated by the PLB. This technique is selected when the pressure drops between different pressure tapings on the test section are small and can be measured accurately by one Point Pressure Transducer (PPT) at a time. This condition is likely to occur when testing bigger pipes (90 and 110 millimetres OD) or very light materials.

DP Cell mode: this mode is also manual and consists of measuring the HGL but using a DP Cell this mode is also applicable on bigger pipes. Using the PLB, the high side of the DP Cell is connected to the first pod and the low side to the other pods, one by one. The DP Cell mode is also used for the straight pipe test or rheology test.

The American standard method (ASM): this method uses two DP cells at the same time to measure pressure gradients between 10 diameters and 20 diameters upstream and downstream of the valve.

The HGL automatic and ASM may be conducted by one operator whereas the HGL manual and the DP Cell mode require at least two operators.

The operating procedures of the modes cited above are explained in the sections below.

### 3.4.2.1 Main stream flow

The core of any technique selected is the same, as it requires having a flow of the slurry tested on the test section. This flow is called the mainstream flow. The mainstream flow is set by following this procedure (Figure 3.12)

- Make sure the pump by-pass valve is open to direct the flow back to the tank.
- Switch on the pump, this allows the slurry to mix
- Choose the test line (pipe diameter) to be tested
- Choose the correct route leading to the test line by using control valves 1A or 1B on Figure 3.12. If 1A is chosen then 2A or 2B can be selected.

If 1B is chosen then either 2C, 2D, 2E or 2F can be selected.

Start closing the by-pass valve so that the mainstream flow is established in the selected pipe at the required flow rate.

The flow rate can be regulated by throttling the by-pass valve of the pump or by using the variable speed control.

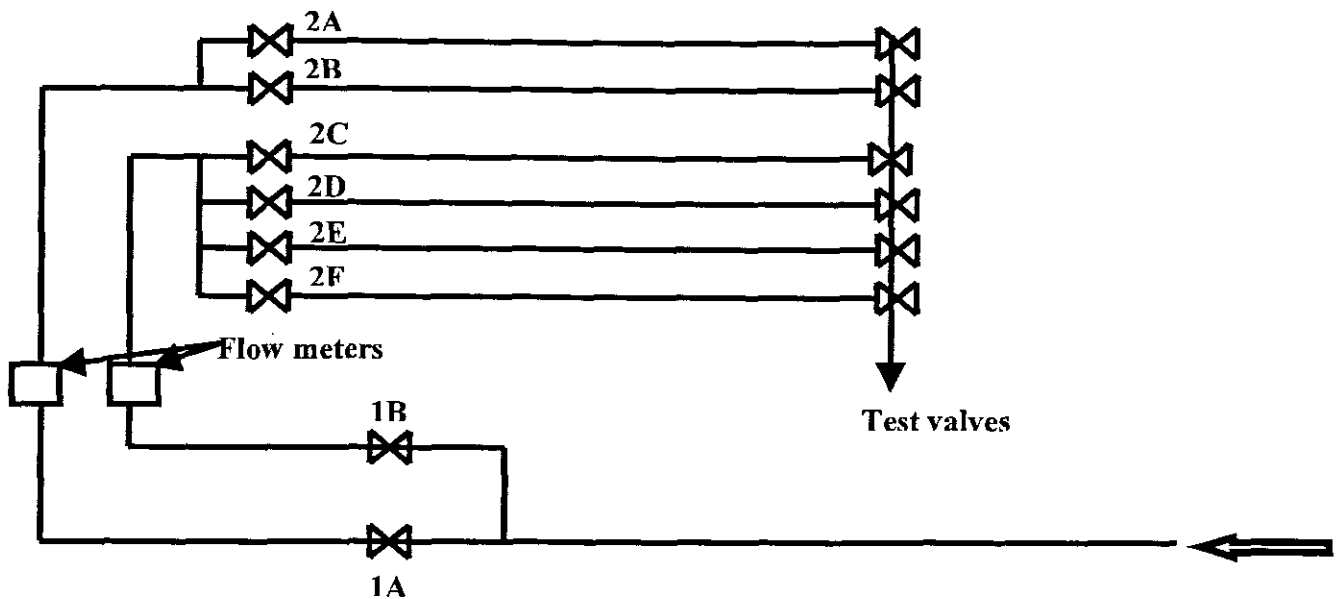


**Figure 3. 12 Over view of the Valve test- rig direction valves. Valves (1&2) are on-off valves to direct the mainstream flow**

#### 3.4.2.2 HGL automatic mode

The automatic mode on the Valve test rig is achieved by setting the ball valves on the Pressure Lines Board (Figure 3.6) as follows:

The exit valves: E1, E2, E3, E4, E5, E6, E7, E8 and E9 are closed. The deviation valves: D1, D2, D3, D4, D5, D6, D7, D8 and D9 are opened. The pressures coming from all nine tappings and pods are directed straight to the PPT.

In this mode the static pressures are read for all the tapping points simultaneously to obtain the pressure gradient upstream and downstream the test valve.

#### 3.4.2.3 HGL manual mode

The manual mode on the Valve test rig can be conducted by using only one PPT:

- On the PLB (Figure 3.6), the exit valves: E1 is open to read the pressure on tapping 1
- E2 to E9 are closed.



- The deviation valves: D1 to D9 are closed. The isolation valves (I1, I2, I3 and I4) are also open
- The by-pass ball valves (B1, B2, B3, B4, B5 and B6) are closed, also closed are all the connecting ball valves C except C1.
- C1 is connected to a pressure transducer.
- Take the reading.
- Close valve E1 and open E2
- Read the pressure, close E2 and open E3
- Continue this procedure until valve E9 is open.

#### 3.4.2.4 DP Cell mode

This procedure is used in three ways:

- The straight pipe test
- The hydraulic grade line and
- The American standard method

##### 3.4.2.4.1 Straight pipe test

The straight pipe test can be done simultaneously downstream and upstream of the test-valve and the procedure is as follows.

1. Choose the straight pipe sections in which the pressure drop will be measured, upstream and downstream of the test valve and record the tapping distance respectively.
2. On the pressure lines board (Figure 3.6) close the isolating valve I1 (or I2), I3 and I4 (or I5)
3. Open the valves E according to the test sections chosen, deviation valves D and other E must be closed
4. Close the bypass valve B2, B4, B5 and B6
5. Use the pressure lines PL-1 and PL-2 to measure the pressure drop upstream of the test valve by opening the connecting valves C1 and C2

6. Ensure that the pressure line PL-1 is connected to the high side of the DP Cell and PL-2 to the low side of the DP-Cell
7. Use the pressure lines PL-3 and PL-4 to measure the pressure drop downstream of the test valve by opening the connecting valves C3 and C4.
8. Ensure that the pressure line PL-3 is connected to the High side of the DP Cell and PL-4 to the Low side of the DP Cell.

#### 3.4.2.4.2 The hydraulic grade line

The HGL in this case is done using a DP Cell by isolating the first pod from the others and by opening the pods (pressure tappings) one after another and recording the pressure gradient. The procedure is the same as the straight pipe test described above up to step 8 then proceeds:

9. Open the isolating valve I3
10. Open the respectively E2, take the reading, close E2 and open E3 and continue up to E9
11. Change the flow rate and repeat step 10.

#### 3.4.2.5 The American standard method

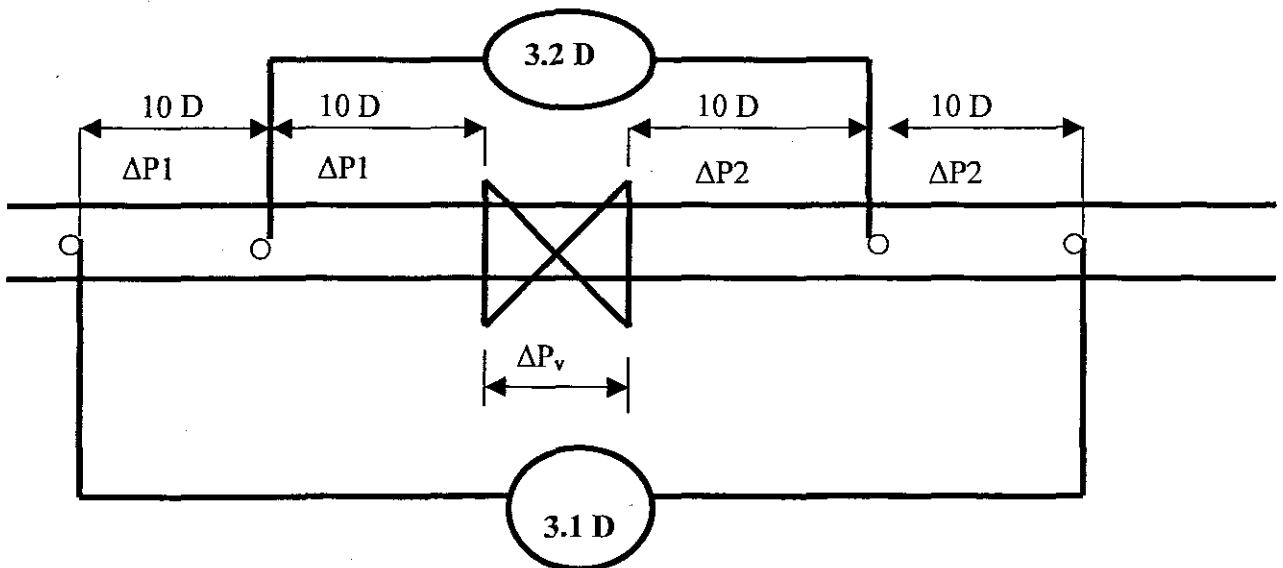


**Figure 3. 13 DP Cells position in the American Standard Method**

In this procedure two DP Cells are used. The DP Cells are connected as shown in Figure 3.13. The tapping points for the first DP Cell are placed respectively at 10D upstream and downstream of the test valve and the tapping points for the second DP Cell are placed respectively 20D upstream and downstream from the test valve.

The procedure is the same as the straight pipe test described earlier.

### **3.5 EXPERIMENTAL ERRORS**

Absolute accuracy in measuring or counting does not always happen, unless the data are discrete numbers. It is important to be able to determine the margins of error which may be found in a set of data and to know how they are affected by various arithmetic processes such as addition, multiplication, root extraction, etc.

#### **3.5.1 Error Theory**

There are three types of error: Gross errors, systematic errors and random errors.

#### **3.5.2 Gross Errors**

Gross errors are due to blunders, equipment failure, and power failure. A gross error is immediate cause for rejection of a measurement (Benzinger & Aksay, 1999)

#### **3.5.3 Systematic or Cumulative Errors**

Systematic errors result in a constant bias in an experimental measurement. Systematic errors are those that are due to known conditions. These conditions might be:

- Natural (temperature, pressure, humidity, etc.)
- Instrumental (calibration, graduation, range, etc.)
- Personal (poor sight of the experimenter, inability of the experimenter to take correct reading, etc.) size (Barry, 1991).

In this work, systematic errors are not taken into account. Precautions were taken to prevent these errors from occurring: e.g. checking the calibration of instruments by another instrument not related to the instrument in use or independent calibration and also by checking the reproducibility of results.

### 3.5.4 Random Errors

Random errors are those that are due to chance variation. Most experiments proceed with minor variations that change from event to event and follow no systematic trend. The same quantity may be measured many times, giving close but not identical results. The fluctuations in the measurement are assumed to be random and lead to a distribution of values.

### 3.5.5 Precision and Accuracy

Precision and accuracy are terms that refer to the quality of data.

Accuracy distinguishes systematic errors, highly accurate measurements have minimal systematic error (Benziger & Aksay, 1999).

Precision distinguishes random errors. Precision is a gauge of the variation of repeated measurements. Precise measurements have minimal random error.

### 3.5.6 Evaluation of Errors

#### 3.5.6.1 Single error: absolute and relative error

The absolute error is the difference between the true value of any number or quantity and the value obtained or used for that number or quantity in a given circumstance. If the true value of a number or quantity is  $X$ , the value obtained or used for that number or quantity is  $A$ , and the absolute error is  $\Delta A$  then:

$$X = A \pm \Delta A \quad (3.1)$$

This means that  $X$  is comprised between  $A - \Delta A$  and  $A + \Delta A$ .  $\Delta A$  is called the maximum error or absolute error. If  $X$  is a quantity,  $\Delta A$  is expressed in the same unit.  $\Delta A$  is here the smallest division of the instrument, the smallest value detected by the instrument (Barry, 1991).  $\Delta A$  is calculated from the standard deviation of a set of repeated measurements as well. The absolute error for  $A$  at 99,9% confidence interval is given by the equation:

$$\Delta A = 3,29\sigma \quad (3.2)$$

If a 95% confidence level is considered, then the absolute error may be approximated by:

$$\Delta A = 2\sigma \quad (3.3)$$

The relative or percentage error of a number or quantity is calculated by:

$$\delta A = \frac{\Delta A}{A} \quad (3.4)$$

### 3.5.6.2 Combined errors

When a variable is a result of a computation of other variables with their subsequent errors, the resulting error is the combination of the independent variable errors (mean quadratic value of the independents errors). If a variable X is a function of n other variables i.e.,  $X=F(a, b, c, \dots, n)$ , the expected highest error (Brinckworth, 1968) can be calculated from:

$$\left(\frac{\Delta X}{X}\right)^2 = \sum \left(\frac{\partial X}{\partial n}\right)^2 \left(\frac{n}{X}\right)^2 \left(\frac{\Delta n}{n}\right)^2 \quad (3.5)$$

Where X is the computed result

$\Delta X$  is the computed result absolute error

n are the independent variables involved

$\Delta n$  are the independent variables absolute errors.

### 3.5.7 Error in Measurable Variables

#### 3.5.8 Axial Distance

The axial distances or tapping point distances are measured using a measuring tape graduated in millimetres. The absolute error of the measurement is 0,001 m.

#### 3.5.9 Weight

The weights of all the samples were measured using the balance in gramme. The absolute error on measurements is 0,001 kg.

### 3.5.10 Flow Rate

The flow meters used are accurate to 0,001 l/s, which can be assumed as absolute error.

### 3.5.11 Pressure

The pressure transducers used are accurate at 0,25%. Care should be taken in calibration so that a correlation coefficient must be 0,999. Such calibration can rise to an average error of 0,35% (Baudouin, 2003).

### 3.5.12 Error in derived variables

In this section the different equations used in the determination of all derived variables are given. The application of the equation (3.5) to all the equations is also given.

#### 3.5.12.1 Pipe internal diameter

The pipe internal diameter was determined weighing a mass of water ( $M_{H_2O}$ ) in to a known length of pipe (L). The pipe diameter is then calculated using the formula:

$$D = \sqrt{\frac{4M_{H_2O}}{\pi\rho_{H_2O}L}} \quad (3.6)$$

The highest expected error in calculating the pipe diameter is obtained by applying the equation (3.5) to equation (3.6) and that yields:

$$\frac{\Delta D}{D} = \pm \frac{1}{2} \sqrt{\left(\frac{\Delta M_{H_2O}}{M_{H_2O}}\right)^2 + \left(\frac{\Delta L}{L}\right)^2} \quad (3.7)$$

The highest expected error and experimental errors on the measurements of the five diameters of the valve test rig is given in the Table 3.4:

**Table 3. 4 Expected Highest errors and experimental errors in the measurements of the Valve test- rig pipe diameters**

Pipe position	Nominal Diameter OD [mm]	Mass-average [kg]	Length [mm]	Highest Expected Error [%]	Experimental Error [%]
Top	50	0.0421	1000	2.38	0.63
2nd Top	63	0.0528	1000	1.90	0.32
3rd Top	75	0.0631	1000	1.59	0.45
4th Top	90	0.0804	1000	1.25	0.22
2 <sup>nd</sup> Bottom	110	0.0991	1000	1.01	0.36
Bottom	110	0.0972	1000	1.03	0.37

### 3.5.12.2 Velocity

The velocity in a pipe is determined from the continuity equation (2.11):

$$V = \frac{Q}{A}$$

Q and A are respectively, the flow rate and the cross section area of the pipe.

The application of equation (3.6) to equation (3.11) yields the highest expected error on the velocity given by:

$$\frac{\Delta V}{V} = \pm \sqrt{\left(\frac{\Delta Q}{Q}\right)^2 + 4\left(\frac{\Delta D}{D}\right)^2} \quad (3.8)$$

### 3.5.12.3 Pseudo shear rate

The pseudo shear rate is determined using the relation (2.43):

$$\dot{\gamma}_o = \frac{8V}{D}$$

The application of equation (3.5) to (2.43) gives the expected highest error of the pseudo shear rate and it yields:

$$\frac{\Delta \dot{\gamma}_o}{\dot{\gamma}_o} = \pm \sqrt{\left(\frac{\Delta Q}{Q}\right)^2 + 5\left(\frac{\Delta D}{D}\right)^2} \quad (3.9)$$

### 3.5.12.4 Wall shear stress

The shear stress is determined from the relation (2.8):

$$\tau_o = \frac{\Delta PD}{4L}$$

The application of equation (3.5) to (2.8) gives the expected highest error of the shear stress and that yields:

$$\frac{\Delta\tau_o}{\tau_o} = \pm \sqrt{\left(\frac{\Delta(\Delta P)}{\Delta P}\right)^2 + \left(\frac{\Delta D}{D}\right)^2 + \left(\frac{\Delta L}{L}\right)^2} \quad (3.10)$$

### 3.5.12.5 Viscosity

The rheological characterisation was done most of the time with a correlation coefficient of at least 99%. Thus the error in viscosity or other rheological parameters did not exceed 1%.

### 3.5.12.6 Reynolds number

The Reynolds numbers errors in this work are evaluated on the Newtonian Reynolds number  $Re$  equation (2.12):

$$Re = \frac{\rho VD}{\mu}$$

Application of equation (3.6) to (2.12) yield:

$$\frac{\Delta Re}{Re} = \sqrt{\left(\frac{\Delta\rho}{\rho}\right)^2 + \left(\frac{\Delta Q}{Q}\right)^2 + \left(\frac{\Delta D}{D}\right)^2 + \left(\frac{\Delta\mu}{\mu}\right)^2} \quad (3.11)$$

### 3.5.12.7 The valve loss coefficient

The valve loss coefficient is obtained from the equation (2.51):

$$H_v = k_v \frac{V^2}{2g}$$



or the pressure loss due to a valve is related to the head loss by:

$$\Delta P_v = \rho g H_v$$

then:

$$k_v = \frac{\Delta P_v}{\frac{1}{2} \rho V^2}$$

$$\left( \frac{\Delta k_v}{k_v} \right)^2 = \left( \frac{\Delta(\Delta P_v)}{\Delta P_v} \right)^2 + \left( \frac{\Delta \rho}{\rho} \right)^2 + 4 \left( \frac{\Delta Q}{Q} \right)^2 + 16 \left( \frac{\Delta D}{D} \right)^2 \quad (3.12)$$

In order to determine different quantities entering in the determination of experimental errors, valve pressure drop tests for clear water were run in the Valve test rig, for all the five pipe diameters. The technique consisted of keeping the output of the pump constant and taking 100 runs reading. The data was analysed statistically by determining the following quantities: mean value, average deviation, spread, median value. Equations (3.2) and (3.3) were used to calculate the absolute error and Equation (3.4) to calculate the relative error. For the variables: velocity, pseudo shear rate, shear stress, Reynolds number, valve loss coefficient and valve pressure drop ( $\Delta P_v$ ).

From the data above mentioned can then be calculated the highest expected errors of each of the above variables mentioned using equations (3.8) to (3.12) and the actual errors of the valve test rig. The highest expected errors and actual errors of the valve test rig are given in tables 3.5, 3.6, 3.7 and 3.8.

Figure 3.14 illustrates the variation of normalised principal tests parameters for the line of 42.12 mm diameter.

On the x-axis is the name of the test and on the y-axis every parameter divided by its average value for the test described above. It can be seen that the wall shear stress and the valve loss coefficient present bigger variations than other parameters and eventually bigger errors.

In Tables 3.5, 3.6, 3.7, and 3.8, all the errors are calculated at 99% confidence level. These errors give the degree of confidence of a variable, the smaller the error, the more precise is the variable and the bigger the error, the less precise is the variable.

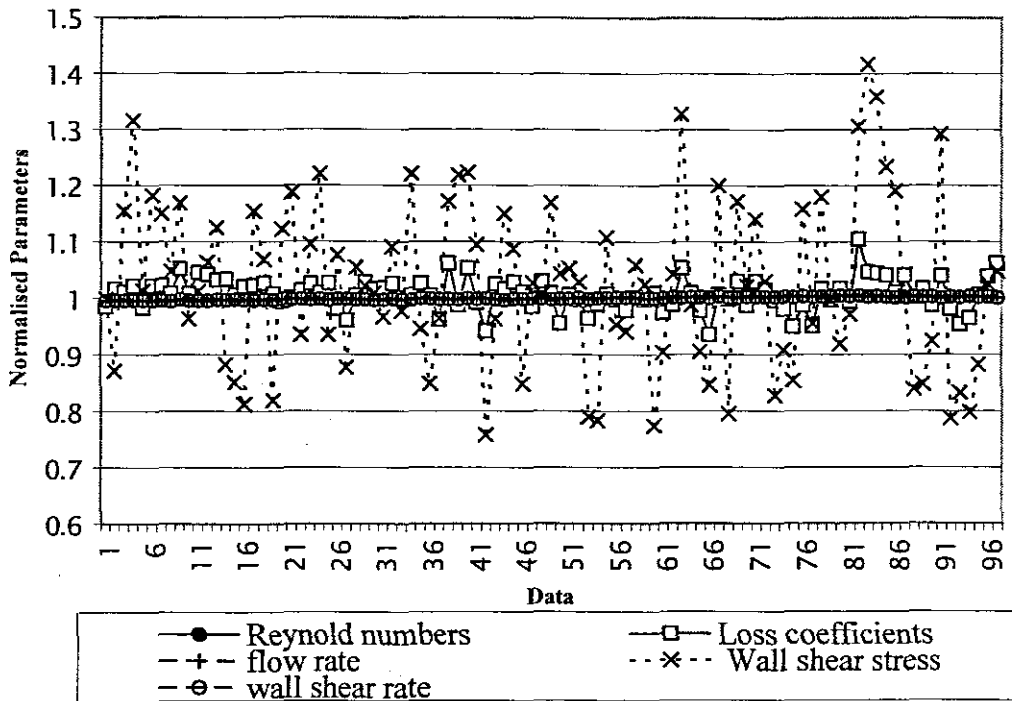


Figure 3.14 Comparison of variation of principal parameters of the Valve test rig

Table 3. 5 Highest expected error in measurable variables of the Valve test rig:

OD	ID	Average Velocity (V)	Pseudo shear rate, $8V/D$	Wall Shear Stree( $\tau_w$ )	Reynolds number (Re)
[mm]	[mm]	[l/s]	[ $s^{-1}$ ]	[Pa]	-
50	42	1.895	1.997	11.802	1.549
63	53	0.668	0.740	0.372	0.372
75	63	17.557	17.562	17.539	17.539
90	80	1.788	2.026	21.910	1.747
110	97	1.298	1.350	16.679	1.129

**Table 3. 6 Highest Expected errors of the Valve loss coefficient**

Valve Dimension	Loss Coefficient ( $k_v$ )
[mm]	
40	12.38
50	11.16
65	40.80
80	22.20
100	16.88

In Table 3.6 the diaphragm valve of 65 mm nominal bore diameter has the highest expected error on the valve loss coefficient ( $k_v$ ) compared to the other valves. The standard deviation, the spread and the average deviation of the variables studied (average velocity ( $V$ ), pseudoshear rate ( $8V/D$ ), wall shear stress ( $\tau_o$ ) and Reynolds number ( $Re$ ) are higher than in any other line).

Table 3. 7 Errors of the Valve test rig

OD	ID	Reynolds number (Re)	PseudoShear Rate (8V/D)	Average Velocity (V)	Wall Shear Stress( $\tau_w$ )
[mm]	[m]	-	[1/s]	[m/s]	[Pa]
50	42	0.532	0.532	0.532	45.786
63	53	0.169	0.169	0.169	7.259
75	63	3.016	2.894	2.871	6.443
90	80	1.469	1.469	1.469	28.810
110	97	0.766	0.791	0.791	6.900

**Table 3. 8 Errors of the Valve loss coefficient**

Valve Dimension [mm]	Loss Coefficient ( $k_v$ ) Error [%]
40	8.841
50	9.594
60	18.316
80	20.389
100	13.252

### 3.5.12.8 Slurry Relative Density

The Relative Density Test was done on the tested fluid by collecting a sample of the fluid under test.

The test was performed as followed:

- Three clean, dry volumetric flasks were weighed respectively ( $M_1$ )
- The fluid was poured in those flasks to approximately half the volume and weighed respectively ( $M_2$ )
- Water was added up to the graduated mark of the flasks, and weighed respectively ( $M_3$ ). The flasks had to be shaken gently to remove any air bulbs.
- The flasks were emptied and rinsed with water and alcohol to dry. Afterwards they were filled completely with water and weighed respectively ( $M_4$ ).

#### Calculations

Mass of fluid:  $M_2 - M_1$

Mass of water filling the flask  $M_4 - M_1$

Mass of water filling the space left by the fluid:  $M_3 - M_2$

Mass of water having a volume equal to that of the fluid  $(M_4 - M_1) - (M_3 - M_2)$

therefore:

$$RD = \frac{M_2 - M_1}{(M_4 - M_1) - (M_3 - M_2)} \quad (3.13)$$

The arithmetic mean of the values obtained from the three flasks was taken as the actual RD.

The mass was measured with an electronic balance accurate to  $\pm 0,001$  g, which is an absolute error of  $\pm 10^{-6}$  kg.

### 3.6 MATERIALS TESTED

#### 3.6.1 Introduction

The different materials tested were: water, glycerine, CMC and kaolin. The materials tested were selected in a way to represent different characteristics needed in this investigation. Water and glycerine being Newtonian fluids and CMC and kaolin non-Newtonian fluids, with CMC presenting pseudoplastic behaviour and kaolin yield pseudoplastic behaviour.

Fluids were selected that exhibit Newtonian, pseudoplastic and yield pseudoplastic behaviour to demonstrate that dynamic similarity can be obtained at the same Reynolds number provided that the Reynolds number correctly accounts for the viscous properties of the fluid.

#### 3.6.2 Water

Water was used as a standard liquid, to commission the experimental test loop, to establish its credibility, accuracy and precision, because of its well-known properties and availability.

Tap water was used in both straight pipe tests and the valve pressure drop test (hydraulic grade line).

The water straight pipe results were correlated to the Colebrook & White equation (2.19). Graphs for different pipe sizes are presented in Appendix 2. Figure 3.15 gives a typical graph in linear coordinates and Figure 3.16 in logarithmic coordinates for the pipe of 42.12 mm ID (50 mm OD).

The valve pressure drop tests were also conducted and results were compared to the results found in the literature. These results are presented in Appendix 6. Figure 3.17 gives a typical valve pressure drop test for water.

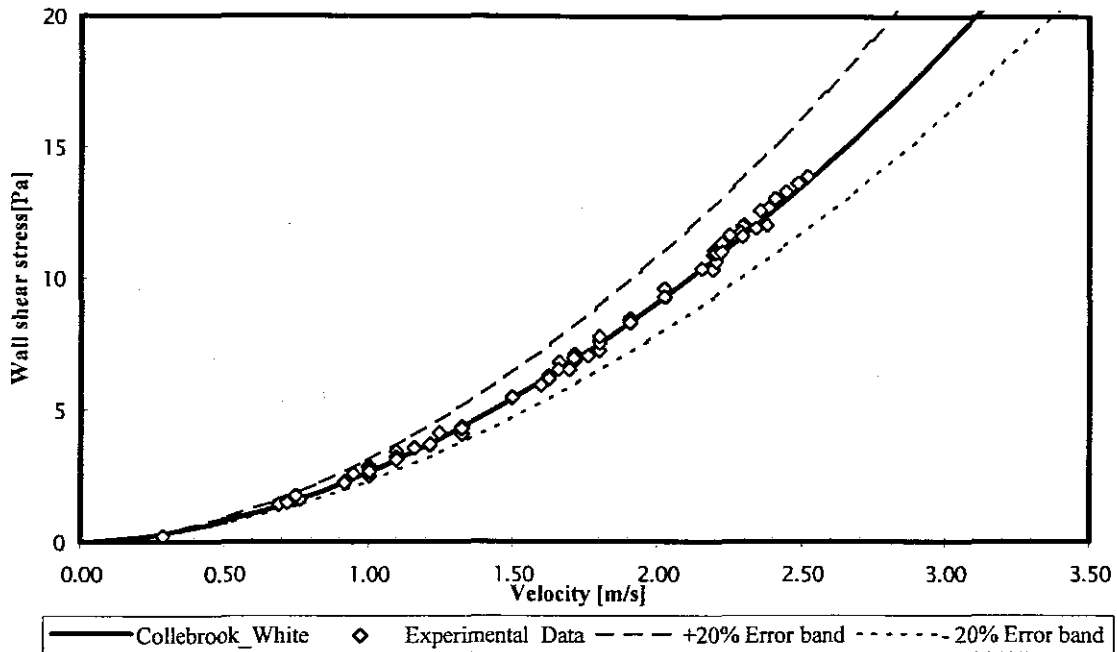
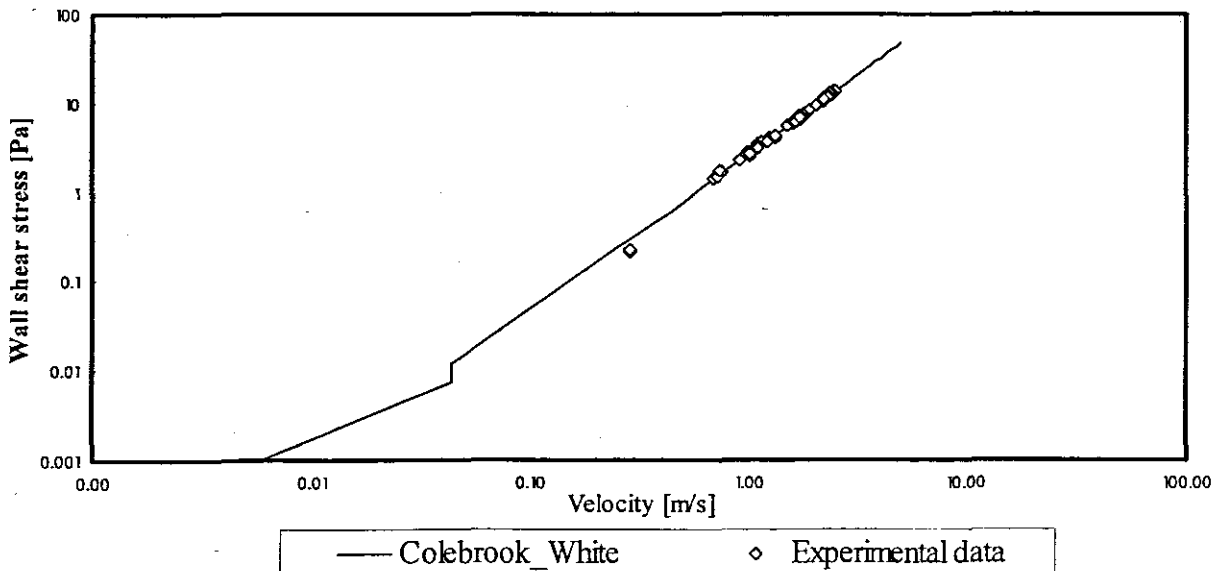
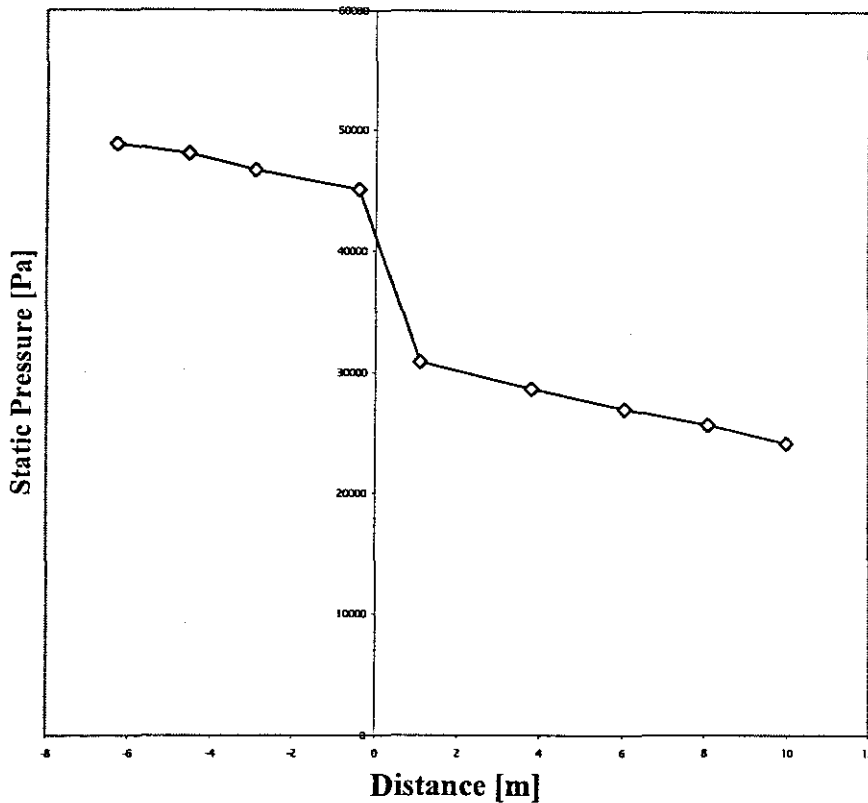


Figure 3.15 Comparison of water test results with Colebrook & White equation





**Figure 3. 16 Comparison of water test results with Colebrook & White equation  
in double logarithmic scale**



**Figure 3. 17 Typical valve pressure drop curve of water in a 40 mm Diaphragm valve ( $V=1.79$  m/s and  $Re_3=75753.99$ )**

### 3.6.3 Carboxyl Methyl Cellulose Solution (CMC)

The CMC used in the test work is supplied in a powder form by Protea Chemicals and is dissolved in tap water to make a solution. CMC is widely used in industries as paper glue, protective colloid and resin emulsion (Pienaar, 1999). The powder was slowly dissolved in water and mechanically mixed using an agitator and care was taken to avoid the formation of large lumps. Mass concentration of 5 and 8% were tested.

Figure 3.18 gives a typical straight pipe test for CMC and Figure 3.19 gives typical valve pressure drop curve for CMC.

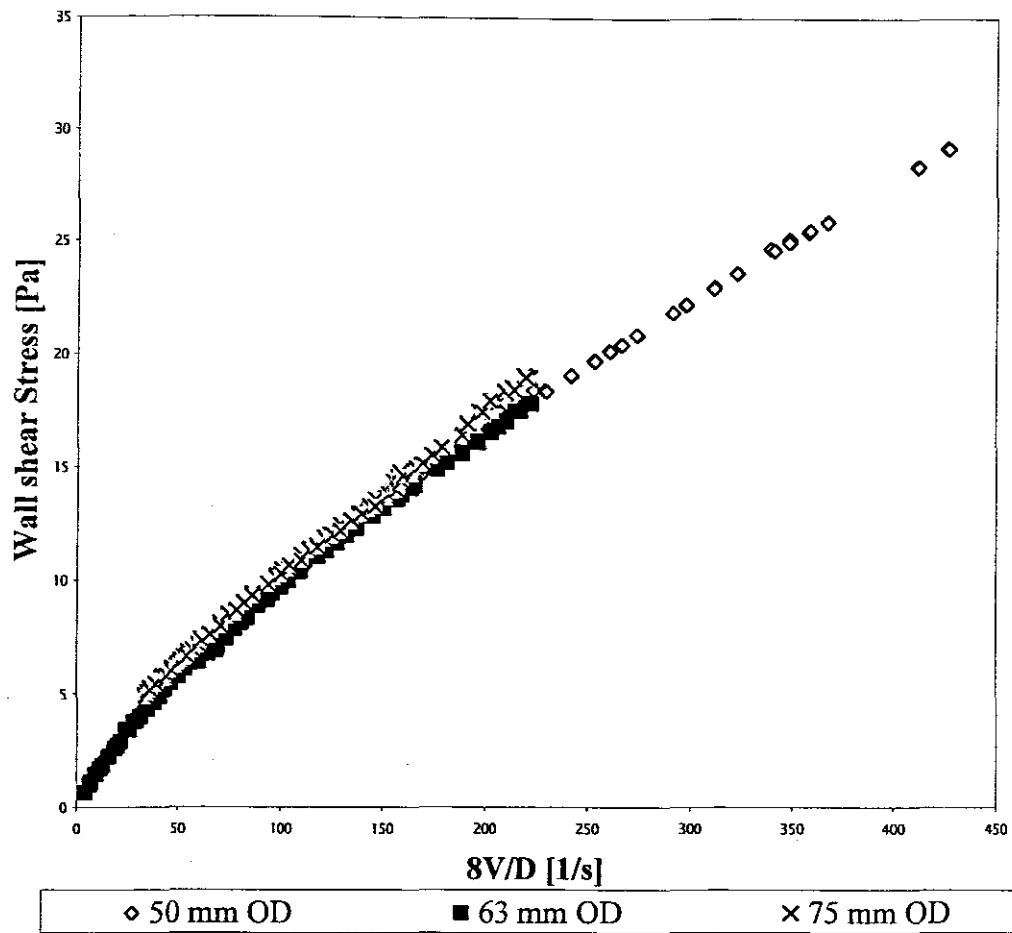
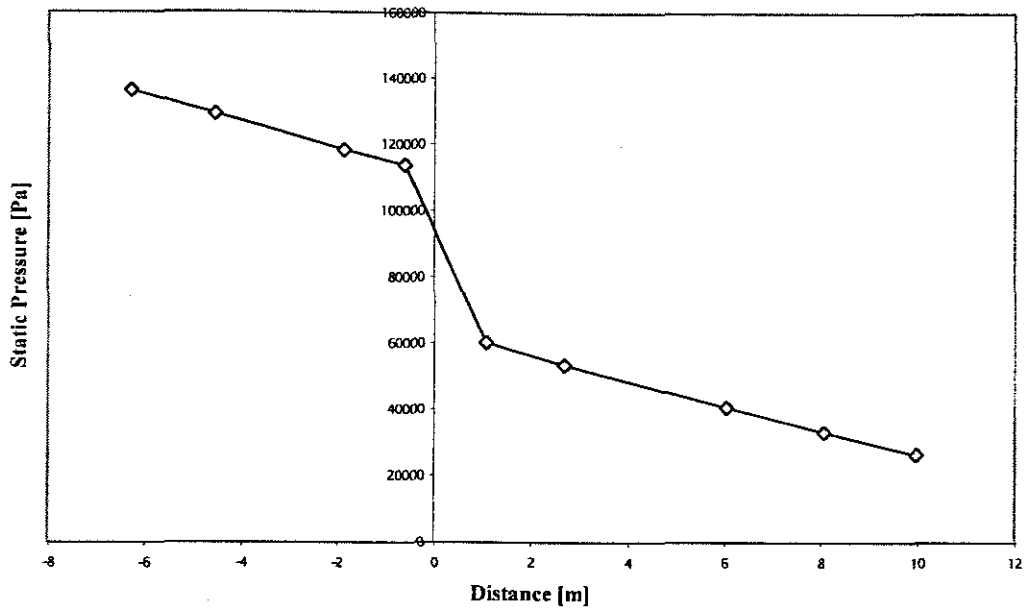


Figure 3. 18 Straight pipe test of CMC 5% in three pipe diameters



**Figure 3. 19 Typical valve pressure drop curve of CMC 5% in a 40 mm nominal bore Diaphragm valve ( $V=3.04$  m/s and  $Re_3=0.042$ )**

### 3.6.4 Kaolin Slurry

The kaolin used in the preparation of kaolin suspensions is also supplied in powder form by Serina Kaolin (Pty) Ltd, and is mined in the Fish Hoek area near Cape Town. It is dissolved in tap water to obtain kaolin slurries. Volumetric concentrations of 10% and 13% were tested. Table 3.9 and 3.10 give the physical and chemical properties of dry kaolin and Figure 3.20 gives the particle size distribution (PSD) graph for kaolin powder. Figure 3.21 gives typical straight pipe tests curve for kaolin and Figure 3.22 gives typical valve pressure drop curve for kaolin.

**Table 3. 9 Physical properties of dry kaolin**

Physical Properties		Typical	
1	Abrasiveness (Einlehner tester)	35 g/m <sup>2</sup>	
2	Particle Size Distribution:		
		below 20 micron	100%
		12 micron	94%
		10 micron	90%
		6 micron	80%
		4 micron	70%
		3 micron	60%
	2 micron	48%	
3	Reflectance Minimum (Elrepho)	83%	
4	pH Value	5	
5	Residue (Screen 45 um)	Max 0,20%	
6	Specific gravity of kaolin mineral	2,60	
7	Moisture:		
		Powder	0 - 1%
		Pellets	8 - 12%
8	Oil absorption of powder	45 - 50%	
9	Bulk density of powder in bags	0,7g/cc	

**Table 3. 10 Chemical properties of dry kaolin.**

Chemical Analysis	Typical %
SiO <sub>2</sub>	46,00%
Al <sub>2</sub> O <sub>3</sub>	38,00%
Fe <sub>2</sub> O <sub>3</sub>	0,85%
TiO <sub>2</sub>	0,58%
CaO	0,10%
MgO	0,18%
K <sub>2</sub> O	1,00%
Na <sub>2</sub> O	0,20%
L.O.I.	13,10%

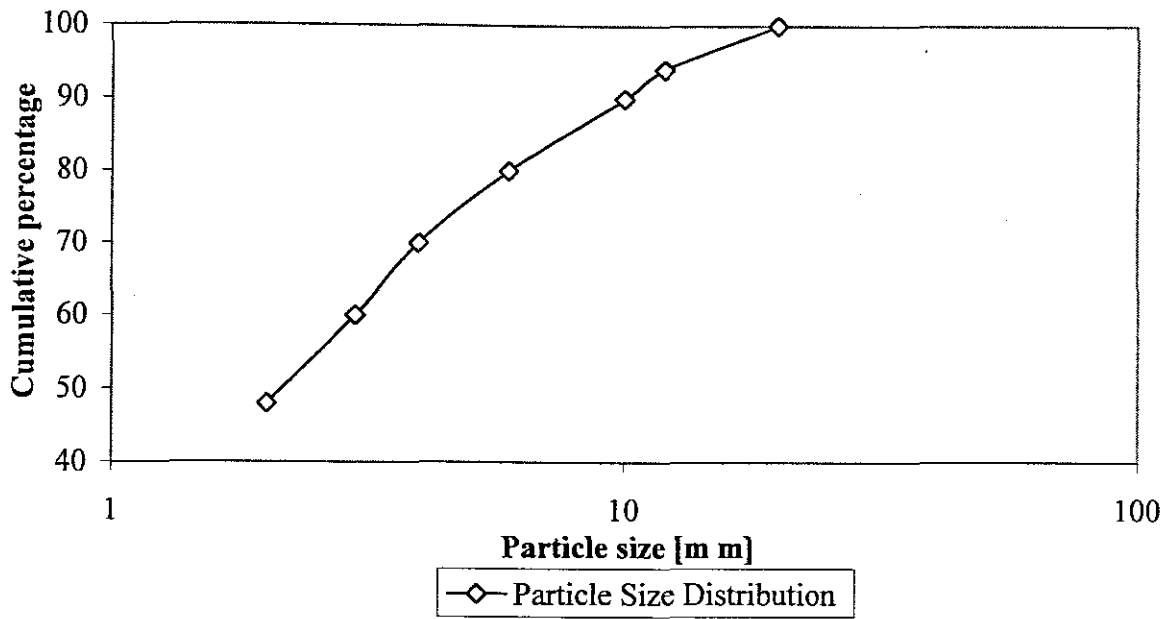


**Figure 3. 20 Particle Size Distribution (PSD) Graph for kaolin powder**

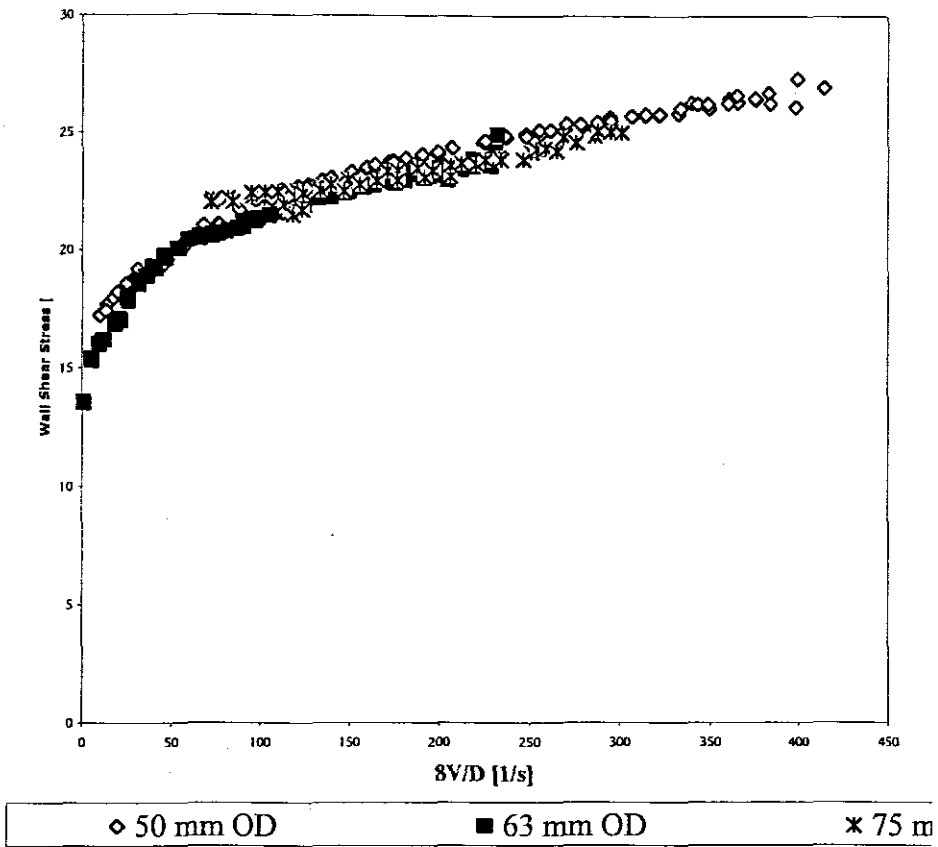
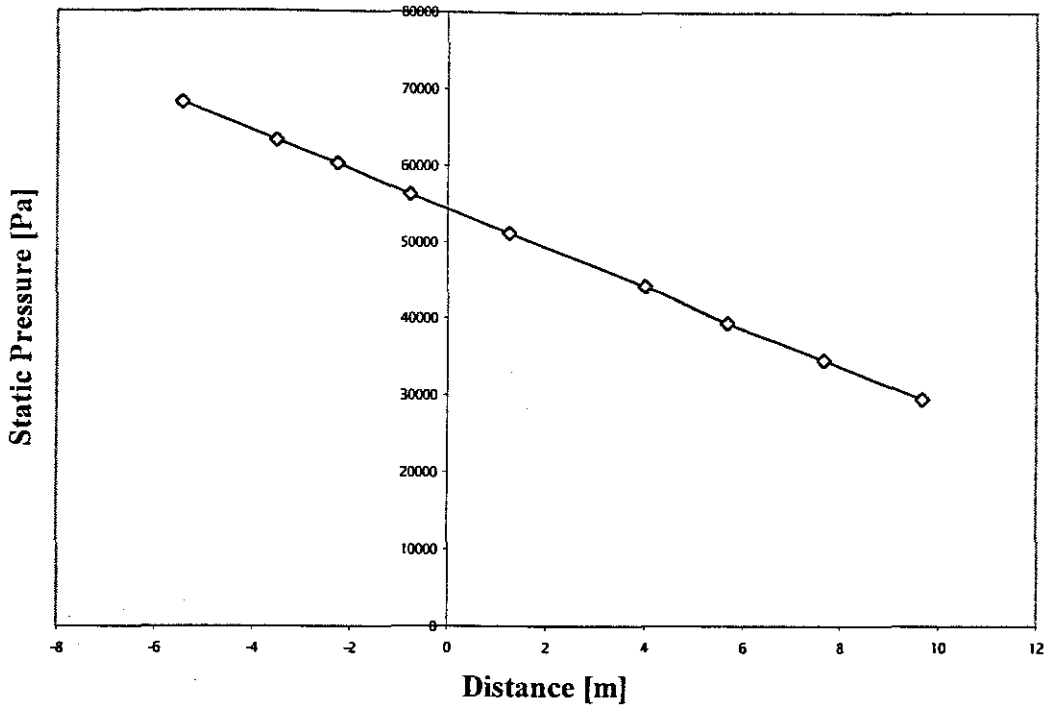


Figure 3. 21 Straight pipe test for kaolin 10% in three pipes diameters.



**Figure 3. 22 Typical valve pressure drop curve of kaolin 13% in a 65 mm Diaphragm valve ( $V=0.029\text{m/s}$  and  $Re_3=4.30$ )**

### 3.7 CONCLUSION

In this chapter the experimental test loop, the valve test rig, has been described.

The diaphragm valve used has also been analysed and it has been established that there are no geometric similarities among the 5 sizes of the diaphragm valve tested.

Experimental procedures (calibration and experimental tests procedures) have been explained.

Experimental errors have been quantified.

The materials tested have been described and raw experimental tests results of these materials have been presented and will be analysed in the next chapter.

Water test results in straight pipes have been correlated to the Colebrook & White equation and are within 20% error limits.

In conclusion, the valve test rig has been shown to be a reliable tool for valve pressure drop tests and for tube viscometry.

# **CHAPTER 4**



## CHAPTER 4 ANALYSIS OF RESULTS

### 4.1 INTRODUCTION

In this chapter, the analysis of experimental results is explained and presented: This includes the rheological characterisation of materials tested and the presentation of loss coefficients in laminar, transitional and turbulent flow regimes. The study of the effect of the choice of the Reynolds number on the loss coefficient is also done.

### 4.2 RHEOLOGICAL CHARACTERISATION

Two types of materials were tested: Newtonian fluids and non-Newtonian fluids. In this section, the determination of rheological parameters of these materials is presented.

In this investigation, rheological characterisation was done using tube viscometry. The effect of entrance and exit losses during tube viscometry was avoided by doing the straight pipe test in the region of fully developed flow (50 diameters after the entrance and 50 diameters after the test valve). The wall slip was evaluated by doing straight pipe test in pipes of three different diameters and the no-slip condition was confirmed.

#### 4.2.1 Newtonian fluids

Newtonian materials tested were: water, 100% and 75% volume concentrations of glycerine.

The Newtonian model fitting was done to determine the viscosity of the two concentrations of glycerine.

The flow curve of a Newtonian fluid is a straight line and the slope of the straight line gives the viscosity of the fluid: Considering the laminar flow data ( $\tau_0$ ,  $8V/D$ ) of the fluid through a straight pipe, using excel, a straight line trend passing through the origin is fitted and the slope of the straight line gives the Newtonian viscosity of the fluid  $\mu_N$ .

An example of such a fit ( Figure 4.1) gives the flow curve of glycerine 100%. Table 4.1 and Table 4.2 gives the properties of glycerine 100% and 75% tested.

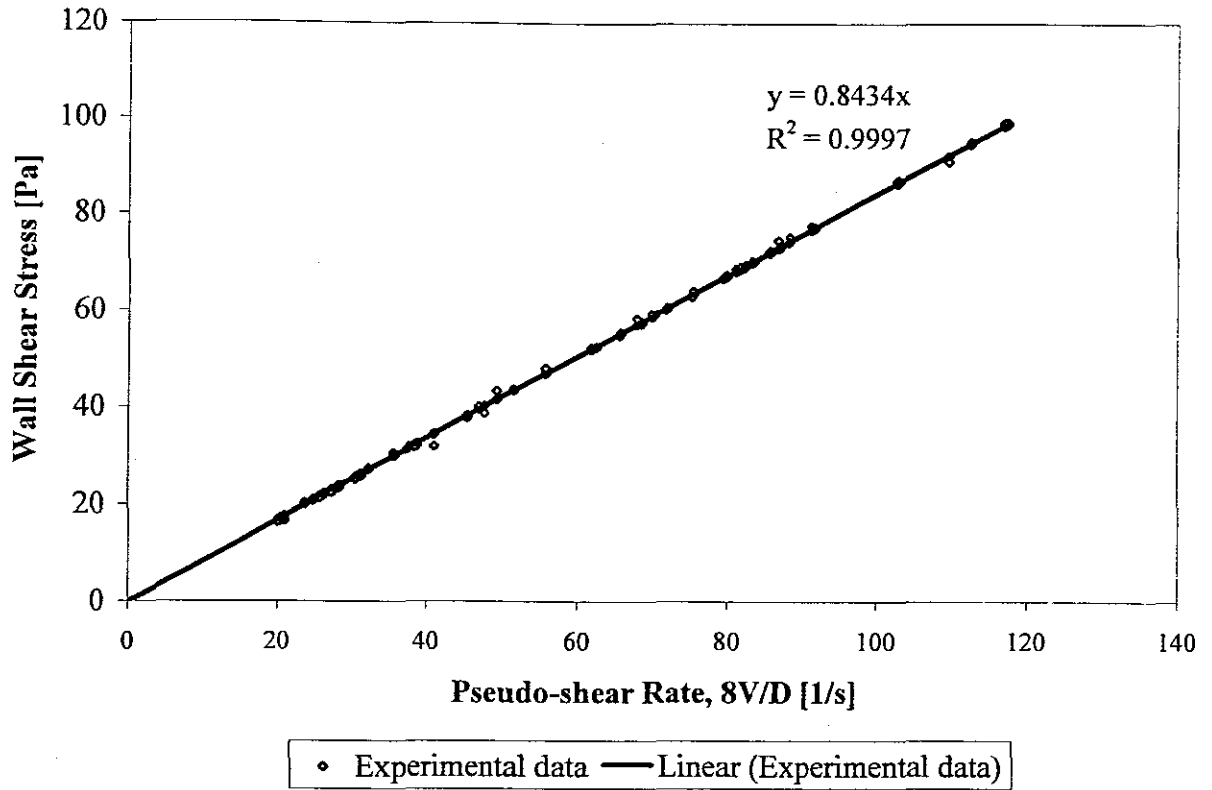


Figure 4. 1 Flow curve of Glycerine 100% at an average temperature of 21 °C

Table 4. 1 Properties of glycerine 100% tested

Date	$\mu$ [Pa.s]	$R^2$	Density [kg/m <sup>3</sup> ]	Temperature [°C]
23/11/2004	0.842	1	1270	21
24/11/2004	0.843	0.9997	1270	20
25/11/2004	0.844	0.9977	1270	20

**Table 4. 2 Properties of glycerine 75% tested**

Date	$\mu$ [Pa.s]	$R^2$	Density [kg/m <sup>3</sup> ]	Temperature [°C]
01/12/2004	0.0196	0.7639	1197.2	21
30/11/2004	0.0184	0.9041	1197.2	22

### 4.2.2 Non-Newtonian fluids

Non-Newtonian materials tested were: 10% and 13% volumetric concentrations of kaolin, 5% and 8% mass concentration of CMC.

All concentration of CMC were characterised as pseudoplastic fluids and those of kaolin as yield pseudoplastic fluids. The Rabinowitsch-Mooney method was not used for rheological characterisation for non-Newtonian fluids in this work. In this work, an in-depth investigation on the calculation of  $n'$  and  $K'$  was done. It was observed that when using the classical method of calculating  $n'$  by fitting a polynomial equation to the double logarithmic plot of  $\tau_o$  vs.  $8V/D$ , if the multiple regression correlation coefficient ( $R^2$ ) of the fit is between 1 and 0.98 the percentage error was acceptable. Below 0.98, the error increased, resulting in higher errors for the calculation of the true shear rate using the Rabinowitch-Mooney relation. An equation was derived for calculating  $K'$  and  $n'$  for yield pseudoplastic fluids. The derivation is given in Appendix 5.

#### 4.2.2.1 Fitting the pseudoplastic model

All concentrations of CMC were characterised as pseudoplastic fluids: The laminar data from a straight pipe test were plotted on linear scale and using excel, a power law trend curve was fitted to the data to give the constant  $n'$  (apparent flow behaviour index) and  $K'$  (apparent fluid consistency index) because for non-Newtonian fluids:

$$\tau_o = K' \left( \frac{8V}{D} \right)^{n'} \quad (2.23)$$

To obtain  $n$ , for a Pseudoplastic fluid:  $n = n'$  and

$$K' = K \left( \frac{3n+1}{4n} \right)^n \quad (2.27)$$

Figure 4.2 gives an example of a fit of the pseudoplastic model for a CMC 5% solution based on three pipes tested on the same day confirming that no slip existed at the pipe wall. Table 4.3 and Table 4.4 gives the properties of CMC 5% and CMC 8% tested. It is clear that the fluid behaviour changed daily and the rheology was tested each day and used for calculations. Using the rheology of the previous day could lead to errors on the  $f$ - $Re$  graph of up to 6 % in the calculation of the friction factor ( $f$ ). The reason for changes in the rheology did not form part of this investigation. An effort was however made to accurately account for the changes.

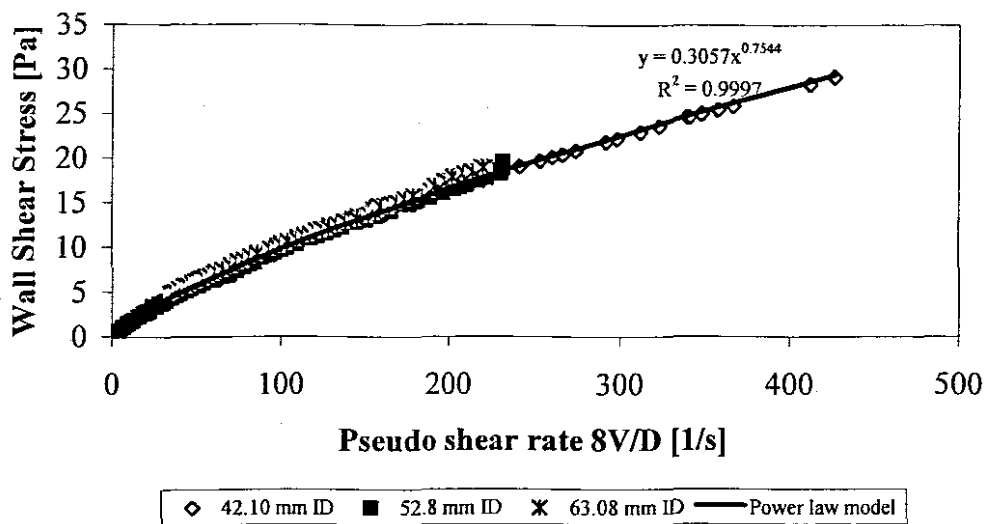


Figure 4. 2 Flow curve of CMC 5%

Table 4. 3 Fluid properties of CMC 5% tested

Date	Density [ $\text{kg}/\text{m}^3$ ]	K	n	$R^2$
22/10/2004	1029	0.304	0.723	0.9993
2/11/2004	1028.2	0.148	1.036	0.9914
3/11/2004	1024	0.442	0.67	0.9937

Table 4. 4 Fluid properties of CMC 8% tested

Date	Density [kg/m <sup>3</sup> ]	K	n	R <sup>2</sup>
5/11/2004	1040	5.252	0.799	0.9976
9/11/2004	1037.5	5.252	0.790	0.9667
11/11/2004	1040	6.434	0.503	0.9948
12/11/2004	1040	5.908	0.799	0.9984

#### 4.2.2.2 Fitting the Yield Pseudoplastic model

All kaolin suspension concentrations were characterised as yield pseudoplastic fluids. The method of characterisation was explained in chapter 2 (2.4).

Figure 4.3 gives an example of a flow curve of a kaolin suspension of 10%. Table 4.5 and Table 4.6 gives the properties of kaolin 10% and kaolin 13% tested. E in Tables 4.5 and Table 4.6 is the root mean square error of the fit function and is given by equation 2.47.

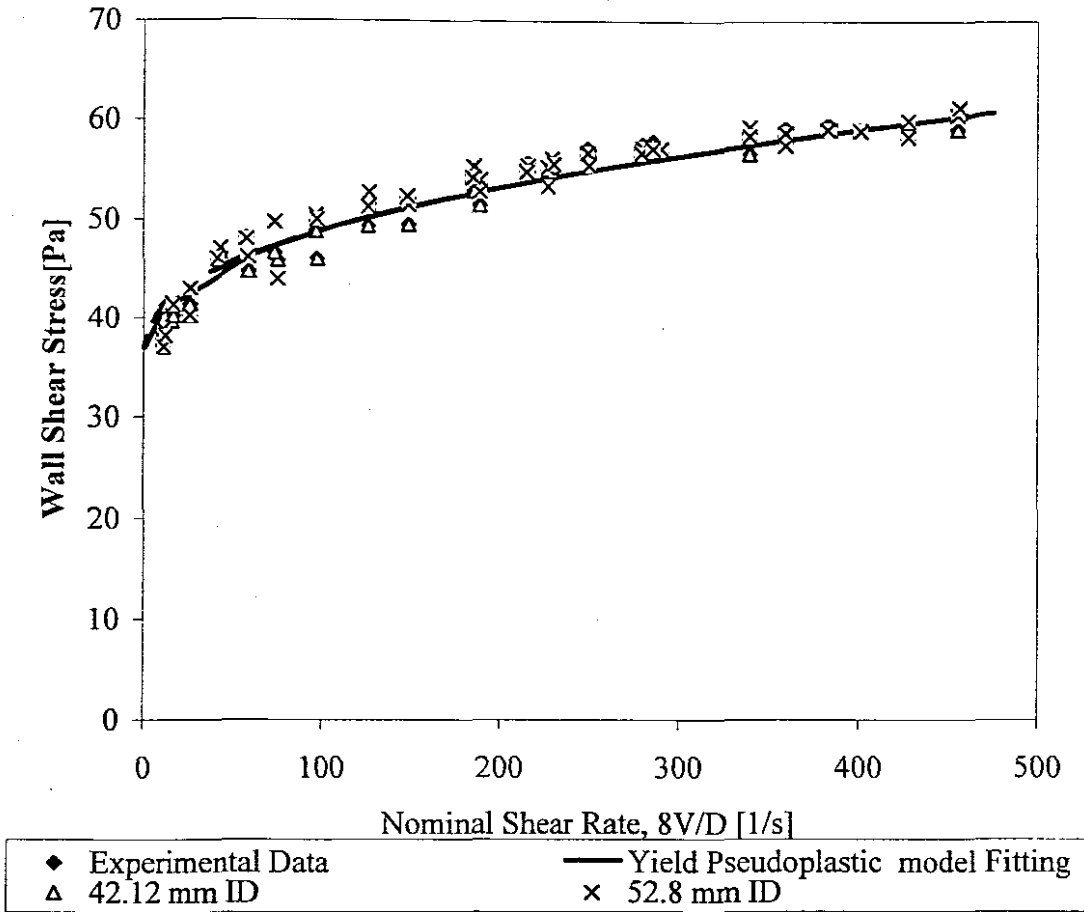


Figure 4. 3 Flow curve of kaolin 13 %

Table 4. 5 Fluids properties of Kaolin 10% tested

Density [kg/m <sup>3</sup> ]	$\tau_y$ [Pa]	K [Pa.s <sup>n</sup> ]	n	E
1172.4	10.7	2.2	0.32	11.30
1163.4	9.4	2.2	0.32	8.46

Table 4. 6 Fluids properties of Kaolin 13% tested

Density [kg/m <sup>3</sup> ]	$\tau_y$ [Pa]	K [Pa.s <sup>n</sup> ]	n	E
1214	35	0.8	0.5	2.48
1214	30	1.37	0.5	9.25

### 4.3 FLOW IN STRAIGHT PIPES

In the laminar flow regime, in straight pipes, the well-known  $f$  -  $Re$  relation relates the friction factor  $f$  and the Reynolds number:

For Newtonian fluids:

$$f = \frac{16}{Re} \quad (2.18)$$

For non-Newtonian fluids:

$$f = \frac{16}{Re_{MR}} \quad (2.45)$$

$$\text{and } f = \frac{2\tau_0}{\rho V^2} = \frac{D \Delta p}{2 \rho V^2 L} \quad (2.10)$$

In this investigation, experimental results for straight pipe sections for both Newtonian and non-Newtonian fluids were obtained from the same experiments from which the data for the valve loss coefficient was obtained.

Because the Slatter Reynolds number takes into account the yield stress and can accommodate any rheological model, this Reynolds number was used in the relation  $f$ - $Re$  (2.18) and (2.45)

A plot of the Fanning friction factor ( $f$ ) against the Slatter Reynolds number ( $Re_3$ ) for both the Newtonian and non-Newtonian fluids tested is shown in Figure 4.4. In Figure 4.4 it can be observed that the experimental results of this work, fall within  $\pm 20\%$  of the calculated theoretical line.

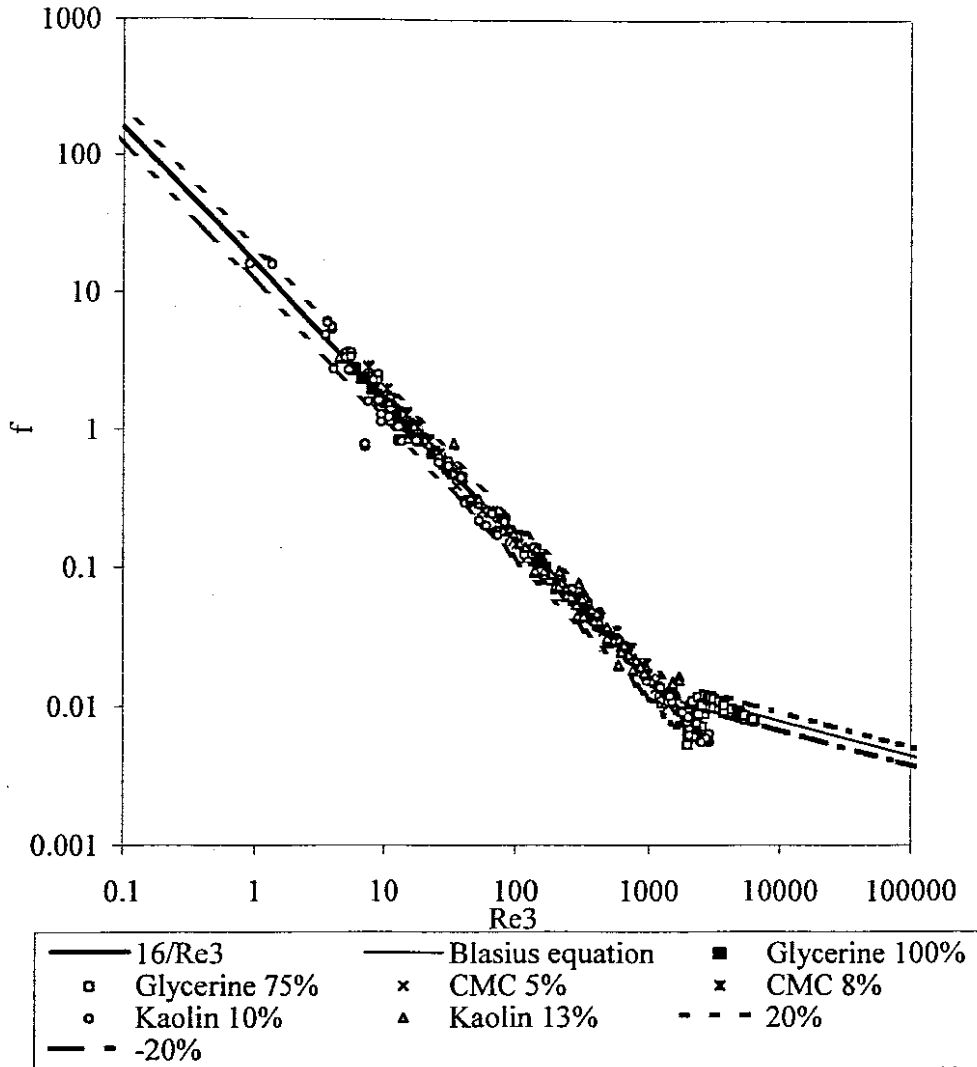


**Figure 4. 4 Comparison of experimental values of the friction factor in laminar flow for different fluids in straight pipe of diameter 42.12 mm ID pipe.**

Such an agreement indicates the validity and degree of accuracy of the experimental technique and equipment used in this investigation and was used as the first criteria in the validation of experimental results.

In the turbulent flow regime, in straight pipes, the well-known Blasius equation relates the friction factor  $f$  and the Reynolds number:

$$f = \frac{0.079}{(\text{Re})^{0.25}} \quad (2.20)$$



In this case also the Slatter Reynolds number was used. This also gives a first good degree of validity of experimental results in turbulent flow. For water in turbulent flow in straight pipes, as said in chapter 3, the experimental data were compared with the Colebrook & White equation:

$$\frac{1}{\sqrt{f}} = -4 \log \left[ \frac{k}{3,7D} + \frac{1,26}{Re\sqrt{f}} \right] \quad (2.19)$$

It must be noted that for Newtonian fluids the Slatter Reynolds number reverts to the Newtonian Reynolds number and that was observed during calculations made on the experimental results on Newtonian fluids.

## 4.4 LOSS COEFFICIENTS

### 4.4.1 Procedure for calculating the valve loss coefficient

The following steps were followed in the calculation of the valve loss coefficient as illustrated on Figure 2.8 (After the establishment of the appropriate f-Re relationship as defined above):

- Measurement of static pressures at different points upstream and down stream of the test valve (In total 9 points were used, 4 points upstream and 5 points downstream of the test valve)
- Calculation of the shear stress in the two pipes upstream and downstream of the test valve in regions of fully developed flow (50 diameters of the entrance length of the pipe upstream the test valve and 50 diameters of the exit length of the pipe downstream the test valve), 6 points were used to calculate the shear stress, 3 points upstream and 3 points downstream respectively of the test valve, all in regions of fully developed flow as defined above. The 3 points close to the test valve, 1 point upstream and 2 points downstream were discarded because they are in the region of influence of the fitting (valve). The shear stress in the two pipes upstream and downstream is calculated using the following equation:

$$\tau_o = \frac{\Delta p D}{4L} \quad (2.8)$$

- The friction factor was calculated using the relation:

$$f = \frac{2\tau_o}{\rho V^2} \quad (2.10)$$

In laminar flow, the above friction factor was compared to:

$$f = \frac{16}{Re} \quad (2.18)$$

and in turbulent flow to the Blasius equation:

$$f = \frac{0.079}{(Re)^{0.25}} \quad (2.20)$$

- The valve pressure loss is obtained as an extrapolation to the test valve plane of the pressure gradients measured in the fully developed flow regions upstream and downstream of the test valve. The slope and intercept upstream and downstream of the test valve (in the regions of fully developed flow) are calculated (in this case using Excel). Six points were used to calculate the slopes and intercepts, 3 points upstream and 3 points downstream respectively of the test valve, all in the region of fully developed flow as explained above. It must be established that the slopes upstream (SUS or  $m_1$ ) and downstream (SDS or  $m_2$ ) are parallel, thus the difference of the intercepts upstream (IUS or  $I_1$ ) and downstream (IDS or  $I_2$ ) yields the pressure drop due to the valve ( $\Delta p_v$ ):

$$\Delta p_v = I_1 - I_2 \quad (2.58)$$

The slopes  $m_1$  and  $m_2$  can be visually parallel but there is always a percentage error difference involved ( $\%Error = \frac{m_1 - m_2}{m_1} * 100$ ) and it was observed that for a percentage

error of up to 20 %, the slopes  $m_1$  and  $m_2$  were still parallel and that was retained as a cut-off value. For errors greater than 20% negative pressure drop were observed in extreme cases. The percentage error in this case varies from materials to materials for fluids like CMC and glycerine the percentage error was always less than 10%. For water and kaolin this was not always the case and one had to be careful when observing the data because many points deviated from 20% and had to be discarded.

- Calculation of the valve loss coefficient from the relation:

$$k_v = \frac{\Delta p_v}{\frac{1}{2}\rho V^2} \quad (2.59)$$

which yields:

$$k_v = \frac{(I_1 - I_2)}{\frac{1}{2}\rho V^2} \quad (2.60)$$

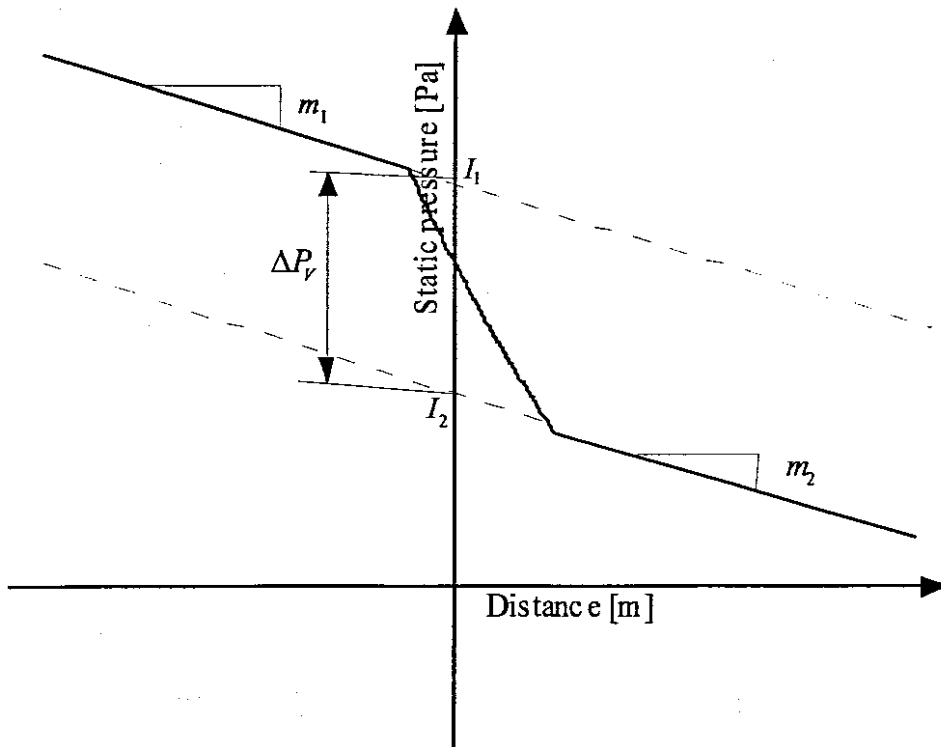


Figure 2. 10 Diagram illustrating the calculation of valve loss coefficient

#### 4.4.2 Graphical presentation of the valve loss coefficient $k_v$ versus Reynolds number

It is customary in fluid mechanics to represent experimental data of loss coefficient on a graph  $k_v$  versus Reynolds number (Edwards *et al.*, 1985; Turian *et al.*, 1997; Pienaar, 1998).

In this investigation, the Slatter Reynolds number ( $Re_3$ ) is used to make such representation. It was very difficult to identify the transition by deviation for the diaphragm valves. The intersection method was therefore used to obtain the point of transition.

##### 4.4.2.1 Diaphragm Valve of 40 millimetres nominal bore diameter

For the 40 millimetres diaphragm valve the loss coefficient in laminar flow  $C_v = 1200$ . In turbulent flow the loss coefficient is constant and an average of  $k_v = 7.96$  (0.226 standard deviation) was calculated. The range of Reynolds numbers is between 1 and 100000.

The transition by intersection of the laminar and turbulent loci is calculated at  $Re_3 = 150.75$ . The loss coefficient data are presented in Figure 4.5.

##### 4.4.2.2 Diaphragm valve of 50 millimetres nominal bore diameter

For the 50 millimetres diaphragm valve the loss coefficient in laminar flow  $C_v = 946$ . In turbulent flow the loss coefficient is constant and an average of  $k_v = 2.53$  (0.209 standard deviation) was calculated. The range of Reynolds numbers is between 1 and 100000.

The transition by intersection of the laminar and turbulent loci is calculated at  $Re_3 = 373.9$ . The loss coefficient data are presented in Figure 4.6.

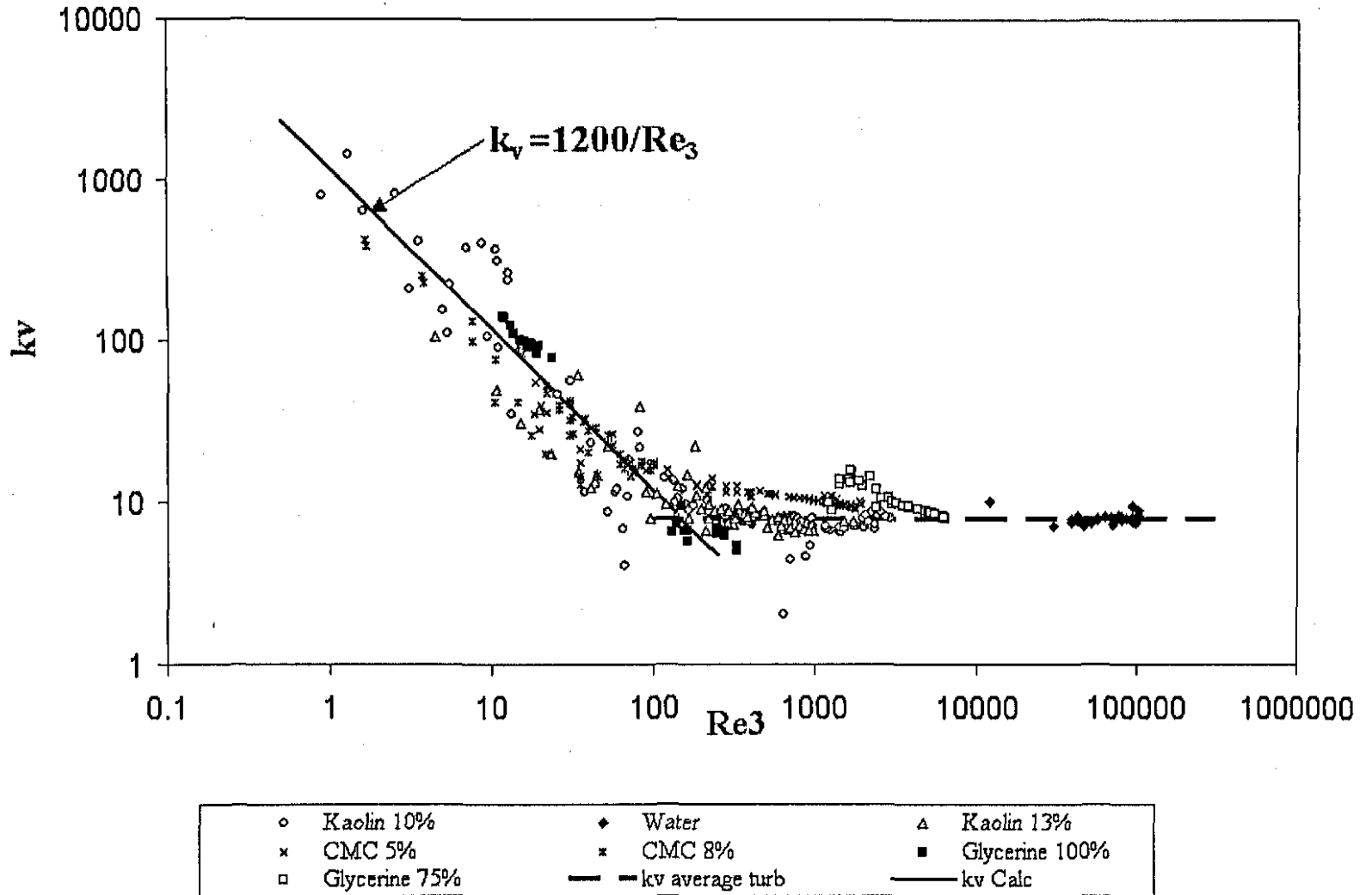


Figure 4. 5 Loss coefficient  $k_v$  vs Reynolds number for 40 millimetres bore diameter diaphragm valve

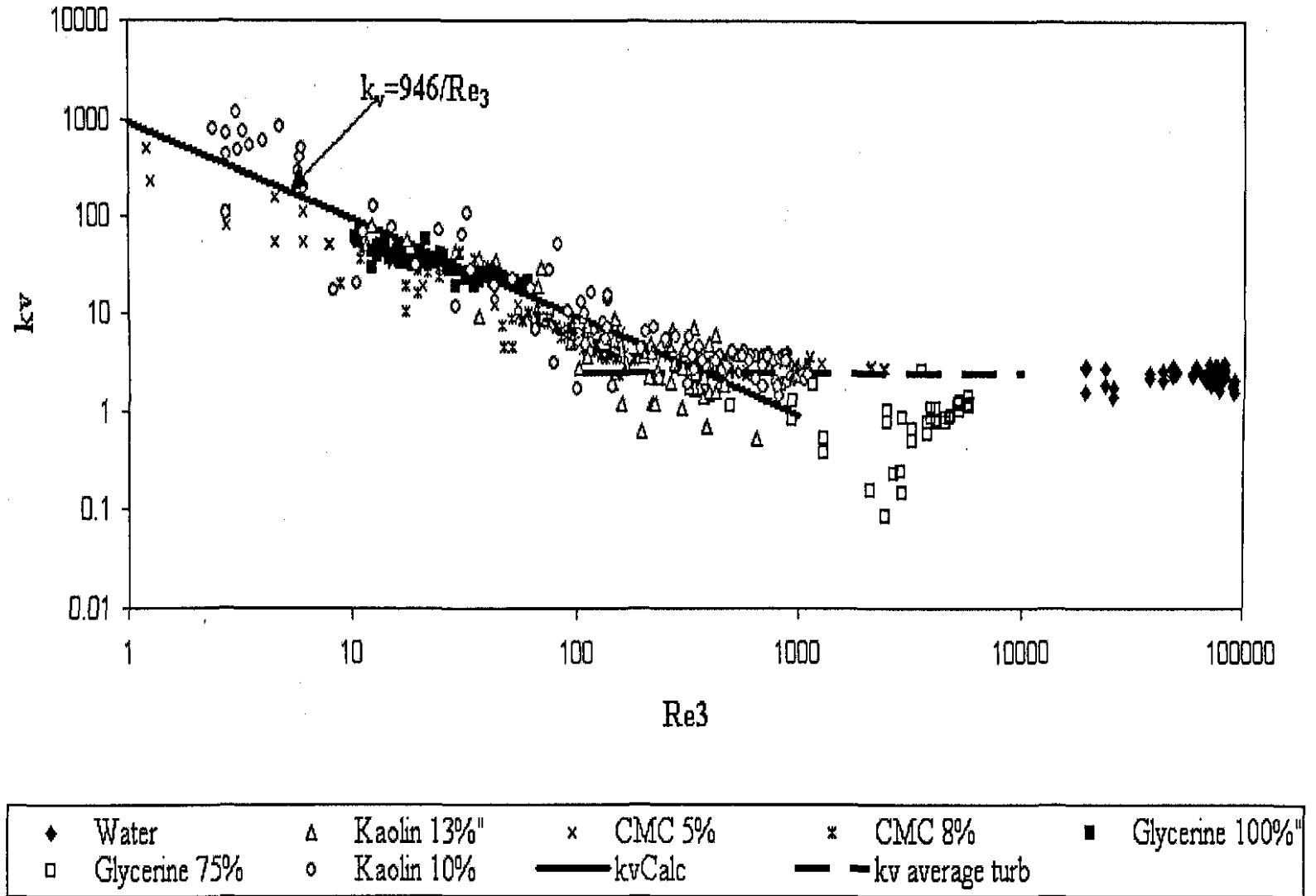


Figure 4. 6 Loss coefficient  $k_v$  vs. Reynolds number for 50 millimetres bore diameter diaphragm valve

#### 4.4.2.3 Diaphragm valve of 65 millimetres nominal bore diameter

For the 65 millimetres diaphragm valve the loss coefficient in laminar flow  $C_v = 555$ . In turbulent flow the loss coefficient is constant and an average of  $k_v = 1.21$  (0.121 standard deviation) was calculated. The range of Reynolds numbers is between 1 and 100000.

The intersection of the laminar and turbulent loci is calculated at  $Re_3 = 633$ . The loss coefficient data are presented in Figure 4.7.

#### 4.4.2.4 Diaphragm valve of 80 millimetres nominal bore diameter

For the 80 millimetres diaphragm valve the loss coefficient in laminar flow  $C_v = 515.14$ . In turbulent flow the loss coefficient is constant and an average of  $k_v = 2.54$  (0.116 standard deviation) was calculated. The range of Reynolds numbers is between 0.1 and 100000.

The intersection of the laminar and turbulent loci is calculated at  $Re_3 = 202.76$ . The loss coefficient data are presented in Figure 4.8.

#### 4.4.2.5 Diaphragm valve of 100 millimetres nominal bore diameter

For the 100 millimetres diaphragm valve the loss coefficient in laminar flow  $C_v = 69$ . In turbulent flow the loss coefficient is constant and an average of  $k_v = 1.3$  (0.155 standard deviation) was calculated. The range of Reynolds numbers is between 0.05 and 100000.

The intersection of the laminar and turbulent loci is calculated at  $Re_3 = 53$ . The loss coefficient data are presented in Figure 4.9.

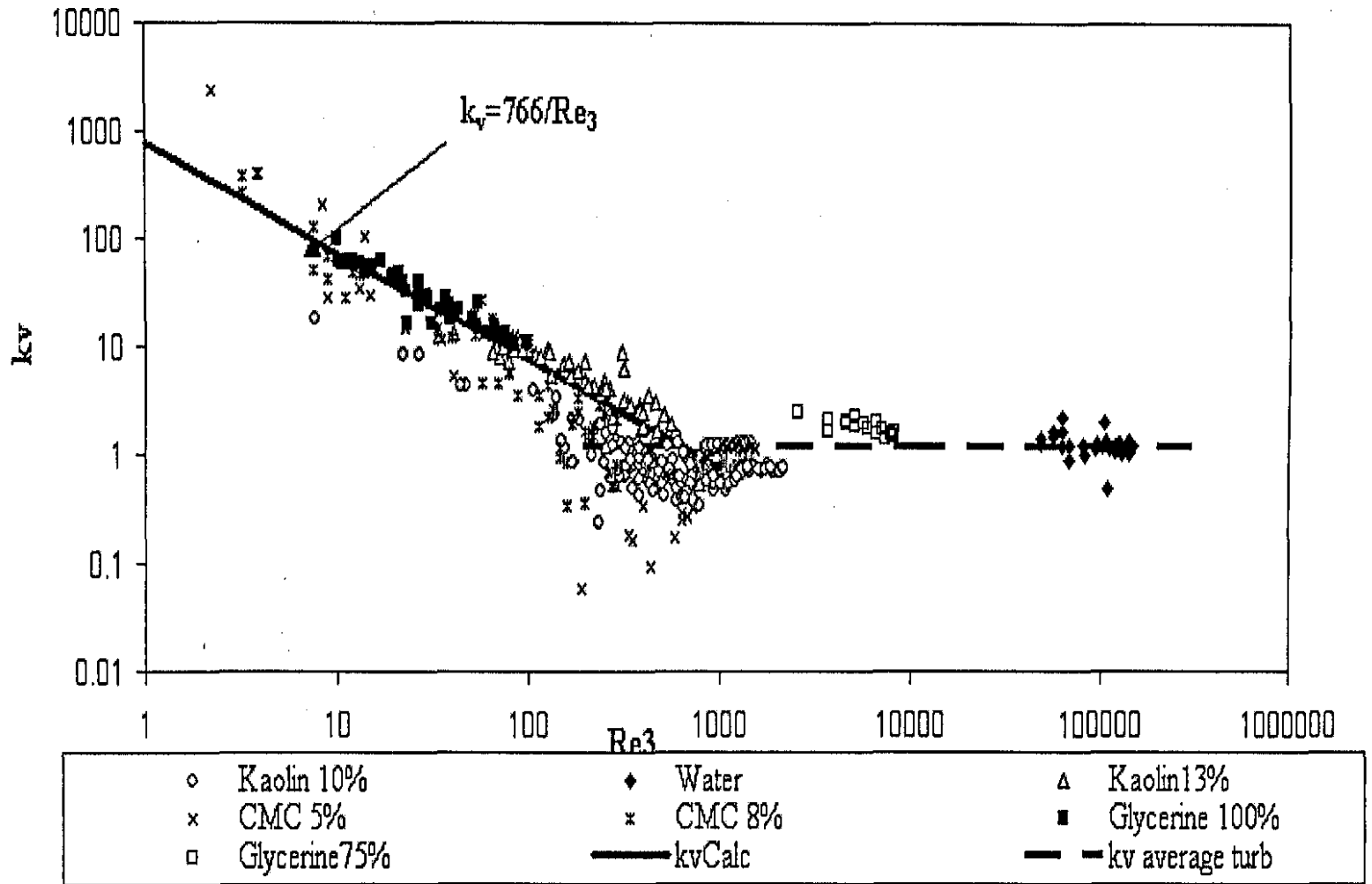


Figure 4. 7 Loss coefficient  $k_v$  vs. Reynolds number for 65 millimetres bore diameter diaphragm valve



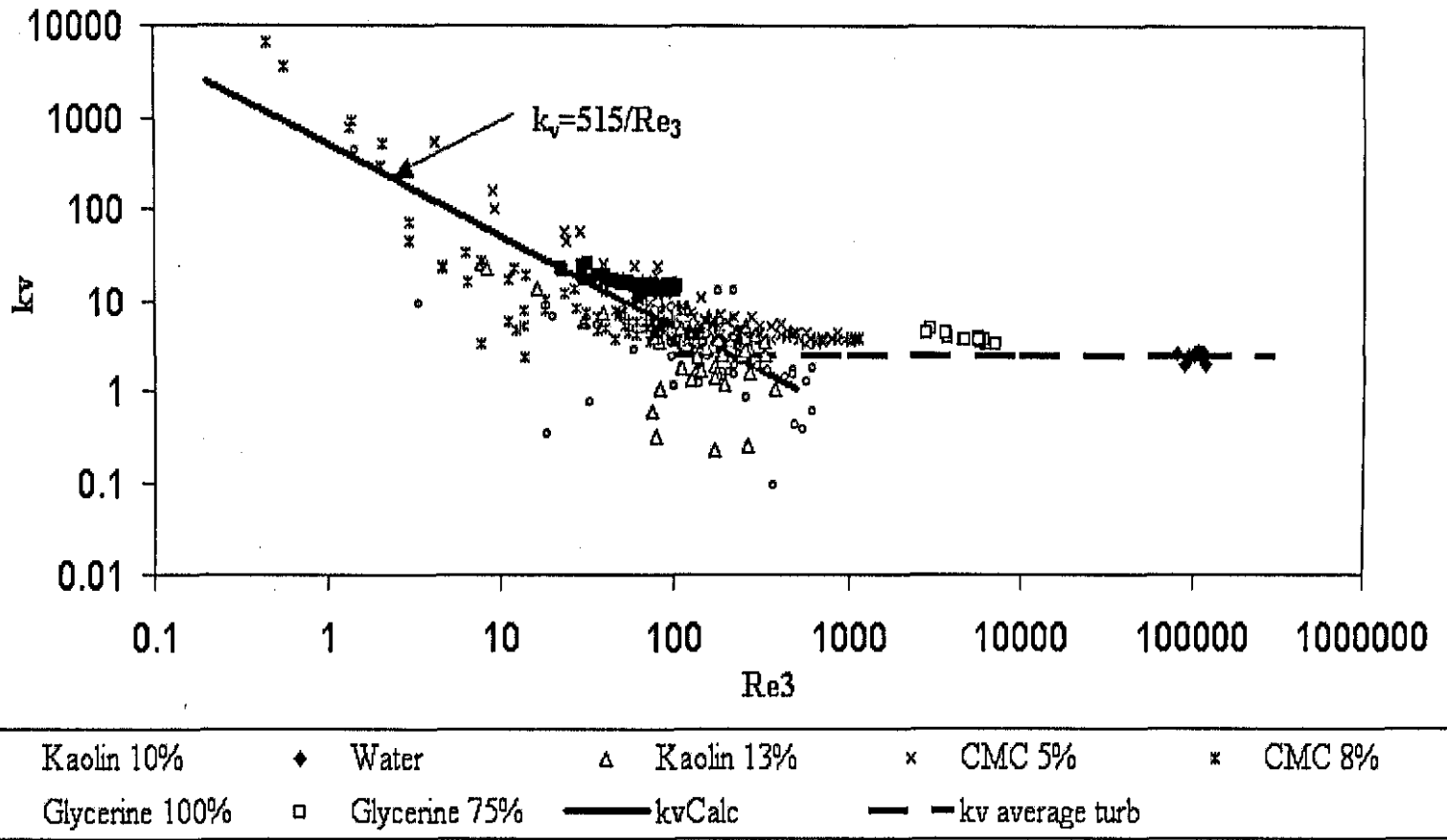


Figure 4. 8 Loss coefficient  $k_v$  vs. Reynolds number for 80 millimetres bore diameter diaphragm valve

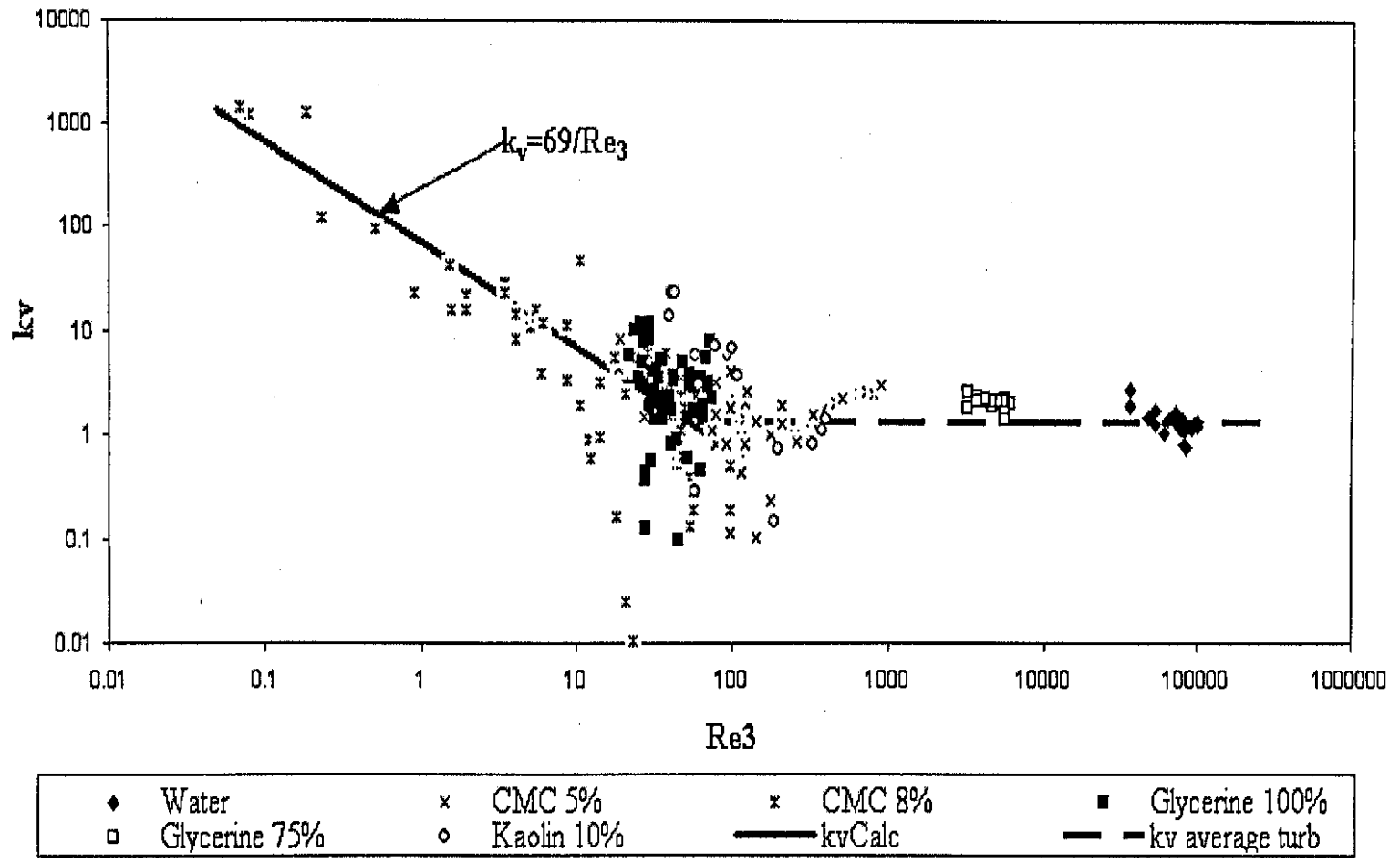


Figure 4. 9 Loss coefficient  $k_v$  vs Reynolds number for 100 millimetres bore diameters diaphragm valve

**Table 4. 7 Summary of  $C_v$  and  $k_v$  values obtained in this work**

Valve dimension [mm]	$C_v$	$k_v$
40	1200	7.96
50	946	2.53
65	555	1.21
80	515	2.54
100	69	1.30

#### 4.5 EFFECT OF REYNOLDS NUMBER ON THE VALVE LOSS COEFFICIENT

In this analysis, other Reynolds numbers are used to predict the laminar loss coefficient and to predict the laminar-turbulent transition in valves for individual fluids of given characteristics. The Reynolds numbers used are the Newtonian Reynolds number and the Metzner and Reed generalised Reynolds number. The results are then compared to the results obtained using the Slatter Reynolds number.

The Newtonian Reynolds number is generally used when the fluid has Newtonian behaviour and the Metzner and Reed generalised Reynolds number is used for fluids exhibiting non-Newtonian behaviour especially pseudoplastic fluids.

In comparison with the Slatter Reynolds number ( $Re_3$ ), the Newtonian Reynolds number gives the same result as  $Re_3$  and the prediction of the laminar loss coefficient and the transition region, using the two Reynolds numbers is the same and that was experienced with water, 75 and 100% Glycerine. In this case the Slatter Reynolds number reverts to the Newtonian Reynolds number.

In the case of the Metzner and Reed generalised Reynolds number, this Reynolds number was used for pseudoplastic fluids and yield pseudoplastic fluids using relations (2.27) and (2.31) and (2.32) in section 2.3.7.2. For pseudoplastic fluids, the Metzner and Reed generalised Reynolds number predicts a lower loss coefficient than the Slatter Reynolds number and even the transition using the Metzner and Reed generalised Reynolds number is earlier than the transition predicted using the Slatter Reynolds number. This is illustrated on the Fig.4.10 for the loss coefficient of a 5% CMC solution in a diaphragm valve of 50 millimetres nominal bore diameter.

From Figure 4.10 the difference between the prediction of the laminar valve loss coefficient ( $C_v$ ) and the transition from laminar to turbulent flow values, is 10.89% greater when the Slatter Reynolds number is used than when the Metzner and Reed generalised Reynolds number is used for this pseudoplastic material.

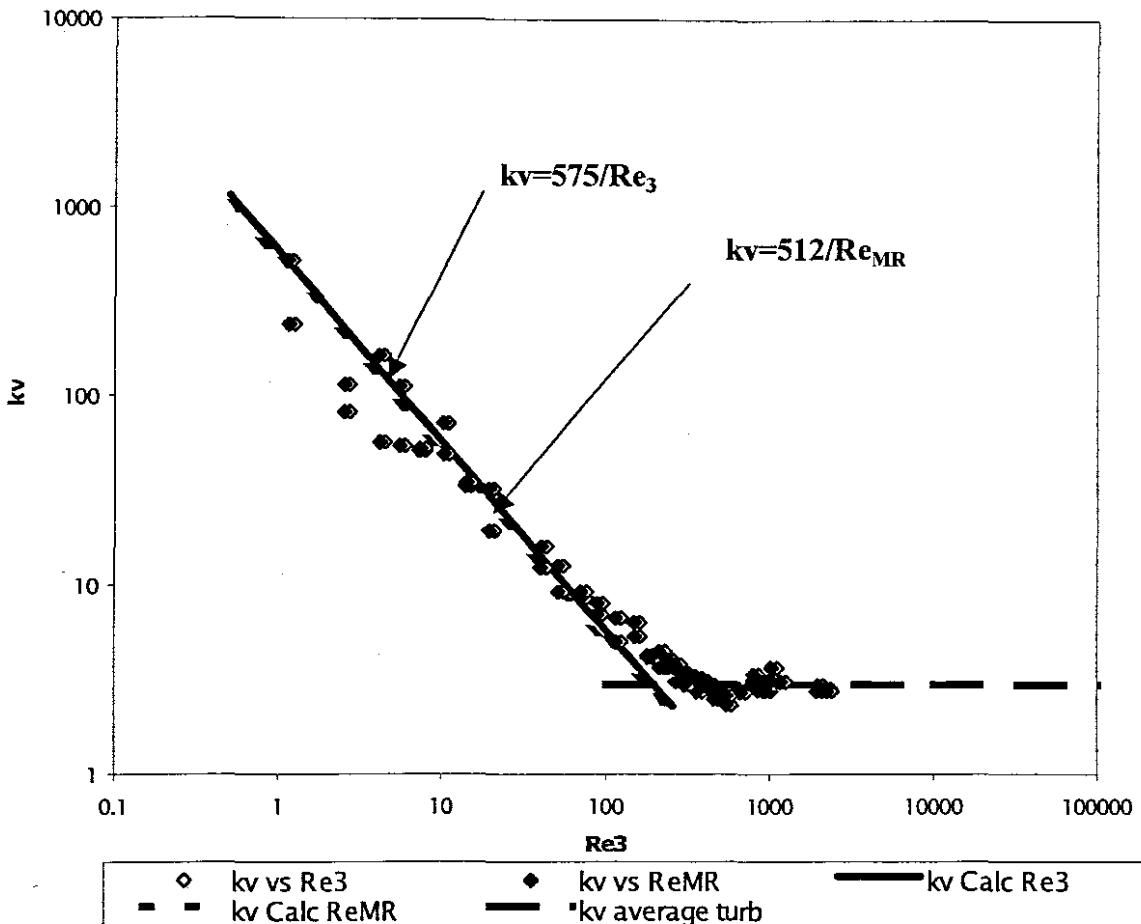


**Figure 4.10 Comparison of loss coefficient using  $Re_3$  and  $Re_{MR}$  for a pseudoplastic fluid.**

In the case of yield pseudoplastic fluids, the Slatter Reynolds number gives also a higher loss coefficient than the Metzner and Reed generalised Reynolds number. The prediction of the transition is earlier with the Metzner and Reed Reynolds number, which is illustrated on Figure 4.11.

Figure 4.11 shows the difference in the prediction of the laminar loss coefficient. In this case it is about 6 % greater using Slatter Reynolds number than when using the Metzner and Reed generalised Reynolds number.

The essence of this analysis is not to determine which Reynolds number better predicts the laminar loss coefficient or the transition, and is beyond the scope of this investigation and could be a subject of future investigations. This analysis showed that the Slatter Reynolds number can be used for design purposes for Newtonian, pseudoplastic and yield pseudoplastic fluids.

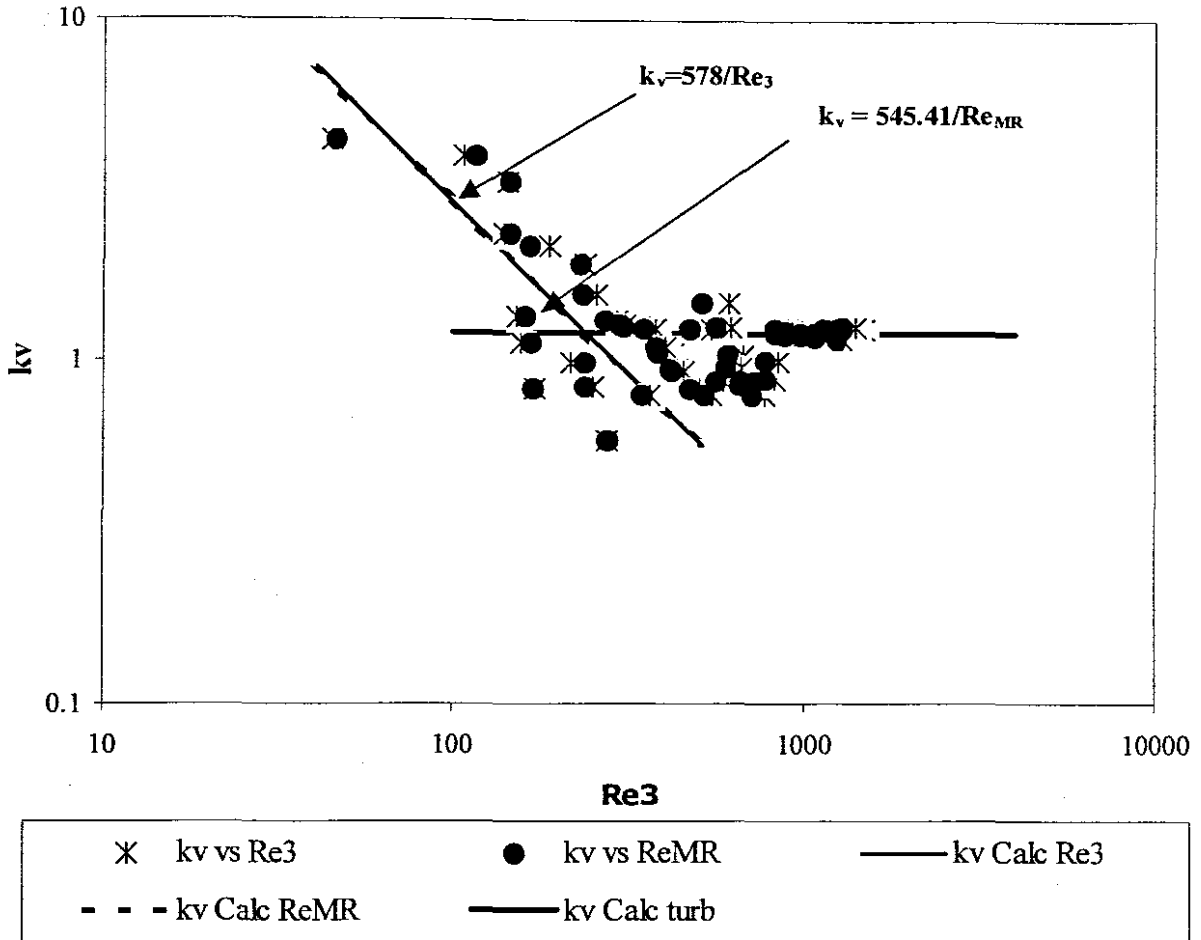


**Figure 4.11 Comparison of loss coefficient using  $Re_3$  and  $Re_{MR}$  for a yield pseudoplastic fluid.**

#### 4.6 CONCLUSION

The rheological characterisation of all materials tested has been presented.

Flow in straight pipes has been analysed and compared to theoretical models for friction factors.

Loss coefficient values in laminar flow, transition and turbulent regimes have been calculated in diaphragm valves of 40, 50, 65, 80 and 100 millimetres nominal bore diameters.

The effect of the choice of the Reynolds number has been established and it has been shown that the Slatter Reynolds number is a very useful tool and can be used for design purpose when dealing with non-Newtonian material.

# CHAPTER 5



## **CHAPTER 5 DISCUSSION AND EVALUATION OF RESULTS**

### **5.1 INTRODUCTION**

In order to evaluate, the objectives of this investigation, the subject of discussion are:

- The literature review
- The experimental test loop
- The experimental method
- Materials tested
- Rheological characterisation
- Loss coefficients
- Comparison with literature and originality of this work

### **5.2 THE LITERATURE REVIEW**

An in-depth literature review has been done in this investigation from both a theoretical and practical engineering point of view to establish the need for the investigation. Thus giving to the reader a comprehensive overview of valves in general and diaphragm valves in particular.

It has been established after review of the open literature that data on non-Newtonian loss coefficients through diaphragm valves are scarce. Most of the data on non-Newtonian loss coefficients through valves are on gate and globe valves and were only relevant to this investigation by their methodology.

Some work on fluid flow through diaphragm valves was found in the literature, on qualitative and quantitative analysis of Newtonian loss coefficients in diaphragm valves (Hooper, 1981). The work of Hooper, (1981) using the two-K method defined a dimensionless factor  $K$ , as the excess head loss in a pipe fitting, expressed in velocity heads.

The drawback of Hooper's work is the fact that there is no valve dimension specification, assuming geometric similarity. This work investigated the assumption of geometric similarity by testing several sizes of valves from the same manufacturer.

### 5.3 EXPERIMENTAL TEST LOOP

The experimental test loop used is the new state-of-the-art valve test rig. The valve test rig was designed and built at the Cape Peninsula University of Technology. The valve test rig has 5 diaphragm valves ranging from 40 to 100 mm nominal bore diameter. It is fitted with multiple transducers. It can accommodate other types of valves as well as contraction and expansions with minor modifications. From a practical point of view, viscometry tests as well as tests for the determination of loss coefficients for many types and dimension of valves can be performed on the valve test rig.

The Valve test rig is a plant in miniature and experimental values obtained for loss coefficients on this test loop are reliable because it simulates what happens in industry when a fluid is being pumped from one point to another. For that reason values obtained for valve loss coefficients from this test loop can be used for design purposes for 100% open NATCO diaphragm valves.

The Valve test rig as it is presently built can perform beyond its present capabilities, but is limited by instrumentation capabilities.

### 5.4 PUMP AND INSTRUMENTATION

The main components of the valve test rig when running tests are the pump, the flow meters and the pressure transducers.

The pump used is a progressive cavity positive displacement (PD) pump and the main drawback was that the flow rate was pulsating and it could not deliver very high flow rates due to power limitations.

The difficulties experienced on the Valve test rig were most of the time due to the limitation of the instrumentation mentioned above: materials with low viscosities could not be tested within a very large range of Reynolds number in bigger pipes, due to very low pressure drops between tapping points even in small pipe diameters and could be tested only at very high flow rates, because of the limitation of the PPT and DP Cells ranges.

Materials with very high viscosity could not be tested in smaller pipe diameters due to the limitation of the pump power. In bigger pipe diameters where pressure drops between tapping points were very small, the PPT and DP Cells limitation was a problem but also the pump power not allowing to reach very high flow rates.

### 5.5 THE EXPERIMENTAL METHOD

The experimental method used is the hydraulic grade line approach. This method is expensive compared to the total pressure method because of the number of pressure transducers (in this case nine) is needed, compared to 1 differential pressure transducer in the case of the total pressure method. The approach was used because the Valve test rig was especially built to accommodate this method. The positive fact about this method is the fact that the frictional losses are actually measured in the straight pipes and need not to be estimated. In the calculation of the valve loss coefficient; it does use only the definition of loss coefficient given by Miller (1978)(Figure 2.4).

The difficulties observed at this point were the fact that with low viscosity materials like water, the two slopes of pressure gradients upstream and downstream the test valve in regions of fully developed flow were not always parallel.

In some cases with very viscous materials, especially in bigger pipes, the slope of the two pressure gradient upstream and downstream of the test valve were not always parallel and in some cases, the intercept of the pressure gradient downstream was bigger than that of the pressure drop gradient line upstream of the test valve. The difference in the upstream and downstream slopes may be due to the slight differences obtained in the actual internal diameter of the pipes during the manufacturing process.

### 5.6 MATERIALS TESTED

The materials tested were selected to represent different characteristics needed in this investigation. Water and glycerine were selected as Newtonian fluids and CMC and kaolin

as non-Newtonian fluids. CMC presents pseudoplastic behaviour and kaolin yield pseudoplastic behaviour.

Water was used to obtain very high flow rates thus very high Slatter Reynolds numbers, Glycerine 100% was used to obtain valve loss coefficients in laminar flow for Newtonian fluid and Glycerine 75% to obtain data for loss coefficients in the transition region and the early turbulent flow for Newtonian fluids.

CMC and kaolin were used because of their well-known non-Newtonian rheological behaviour, being pseudoplastic and yield pseudoplastic materials respectively. High concentrations ensured that sufficient data could be obtained in laminar flow.

### 5.7 RHEOLOGICAL CHARACTERISATION

Rheological characterisation was done by tube viscometry test. Glycerine 75% and 100% were characterised as Newtonian fluids, CMC 5% and 8% were characterised as pseudoplastic fluids and kaolin 10 and 13% were characterised as yield pseudoplastic fluids.

Rheological characterisation is not easy and is beyond the scope of this work and is used in this investigation as a stepping-stone. Rheological characterisation is said to be a stepping-stone because, it is used in this case to determine rheological parameters which are used to verify some correlations in straight pipes (2.20) and (2.45) and not used for an in-depth study of rheological behaviour based on the physical or chemical basis of the slurries.

### 5.8 LOSS COEFFICIENTS

Loss coefficients obtained in this investigation confirmed the general qualitative trend given in the literature that in laminar flow the loss coefficient increases significantly with decreasing Reynolds number and in turbulent flow, the loss coefficient is constant. This is true for any type of fluid, both Newtonian or non-Newtonian.

The transition from laminar to turbulent flow by deviation, for all the valves sizes starts at Reynolds number between 10 and 100 and confirms the general theory that in fittings in general and valves in particular the transition occurs earlier than in straight pipes.

For all the diaphragm valves diameter, the transition region where there is transition by intersection, goes from 10 to 1000 Slatter Reynolds number and in that region the flow is very unstable and the value of the valve loss coefficient is fluctuating.

The transition by intersection for the different valves sizes is given in Table 5.1 below.

**Table 5. 1 Transition by intersection for the different valves.**

Valve nominal bore diameter [mm]	Transition Reynolds number
40	150.75
50	373.9
65	633
80	202.75
100	53

## 5.9 COMPARISON WITH LITERATURE AND ORIGINALITY OF THIS WORK

Values found in the literature on diaphragm valves in fully open position are as follows:

Hooper (1981):  $C_v=1000$  and  $k_v=2$

Miller (1978):  $k_v=0.8$

Perry & Chilton (1973):  $k_v=2.3$

From the literature, it can be seen that little data on non-Newtonian and Newtonian losses are found in the literature and these data are scattered.

The work of Hooper, Miller and Perry & Chilton do not specify the dimensions of the diaphragm valves tested. This work investigated and addressed this issue. Table 5.2 compares values of diaphragm valve loss coefficients from the literature to this work.

A comparison of values of the valve loss coefficients of this work to that from the literature in the turbulent region is given in Figure 5.1.

**Table 5. 2 Comparison of loss coefficients of this work with literature.**

Valve dimension [mm]	This work		Hooper		Miller		Perry & Chilton	
	$C_v$	$k_v$	$C_v$	$k_v$	$C_v$	$k_v$	$C_v$	$k_v$
40	1200	7.96	1000	2	-	0.8	-	2.3
50	946	2.53						
65	555	1.21						
80	515	2.54						
100	69	1.3						

It can be seen that the value of the valve loss coefficient given by Hooper in laminar flow is more or less equal to that found in this work for the valve dimension of 50 mm in laminar flow. And Perry & Chilton's value for turbulent flow coincides with the value found in this work for the valves of 50 and 80 mm nominal bore diameters in turbulent flow.

The value of the valve loss coefficient given by Miller in turbulent flow does not coincide with any loss coefficient value in this work and is under predicting the loss coefficient. This confirms the need that studies should be carried out with a range of diaphragm valves of different sizes and that the details of the valve should be supplied together with the loss coefficient details.

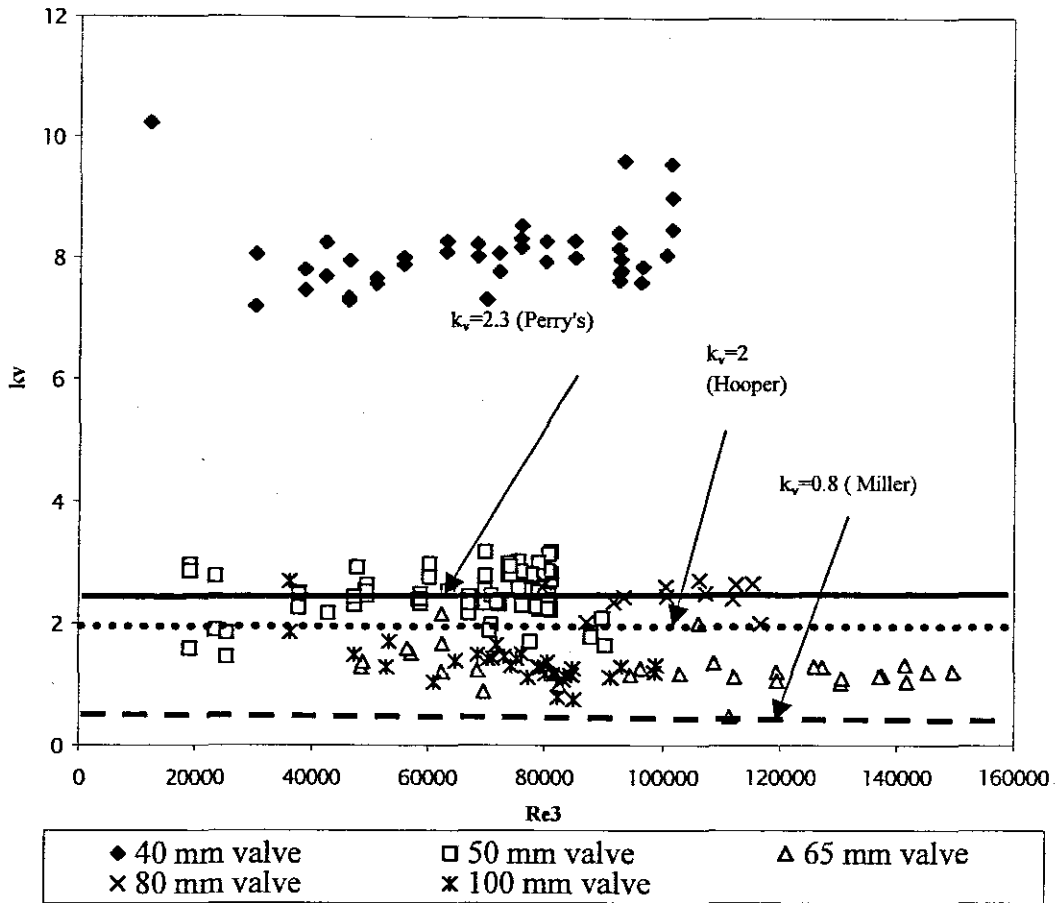


**Figure 5. 1 Comparison of this work turbulent flow valve loss coefficients to valve loss coefficients found in the literature**

### 5.10 SIMILARITIES ANALYSIS

Although geometric similarity was not achieved for the type of valves tested, a dynamic similarity analysis was done on experimental data obtained for the 5 valves sizes, to establish if any analytical relationship could be established between the size of the valve and the loss coefficients in laminar and turbulent flow regimes.

According to 2.7.4 two systems geometrically similar are dynamically similar if their Reynolds numbers are the same. Also Turian *et al.*, (1997) suggested that because it has been found using dimensional analysis that  $k_v$  for incompressible Newtonian fluids is a dimensionless function of Reynolds number (Re) and of dimensionless geometric ratios characteristics of the valve:

$$k_v = \text{fn}(\text{Re}, \text{geometric ratios}) \quad (2.62)$$

Thus the valve loss coefficient  $k_v$  is the same for all sizes of a given type of valve provided dynamic similarity is enforced for instance equality of Reynolds number and geometric similarity are maintained. Around these two assumptions above mentioned will gravitate the similarity analysis.

As shown on Figure 5.2, for the laminar loss coefficient ( $C_v$ ), there is a big variation of the laminar valve loss coefficient as a function of the valve dimension. This variation is almost linear, the laminar valve loss coefficient is a function of the valve size, and the laminar valve loss coefficient increases with the decrease of size and vice versa. Figure 5.3 gives diaphragm valve loss coefficients for CMC 8% in laminar flow. But for turbulent flow there is no big variation of valve loss coefficient with size, and the values of valve loss coefficients are random but close beside the 40 mm valve and follow the trend given on Figure 5.2. Figure 5.4 gives the values of different valve loss coefficient obtained in turbulent flow

Both in turbulent and laminar flows, dynamic similarity is not achieved because of lack of geometric similarities.

In conclusion, it has been established that dynamic similarity is not achieved with the diaphragm valves studied as opposed to other type of valves in the literature. In general, valves of different sizes and from different manufacturers, although apparently similar, are not always geometrically similar. For instance, in small sizes, one valve body may be



offered with a variety of end connection sizes and in some cases a valve of one nominal size may be available with several seat sizes. Also in this specific case of diaphragm valves studied, dynamic similarity is not achieved as in other types of valves. This could be due to the fact that the internal lining of the valve is in rubber and is inserted manually compared to globe valves for example where the internal part of the valve is machined from metal to exact repeatable dimensions.

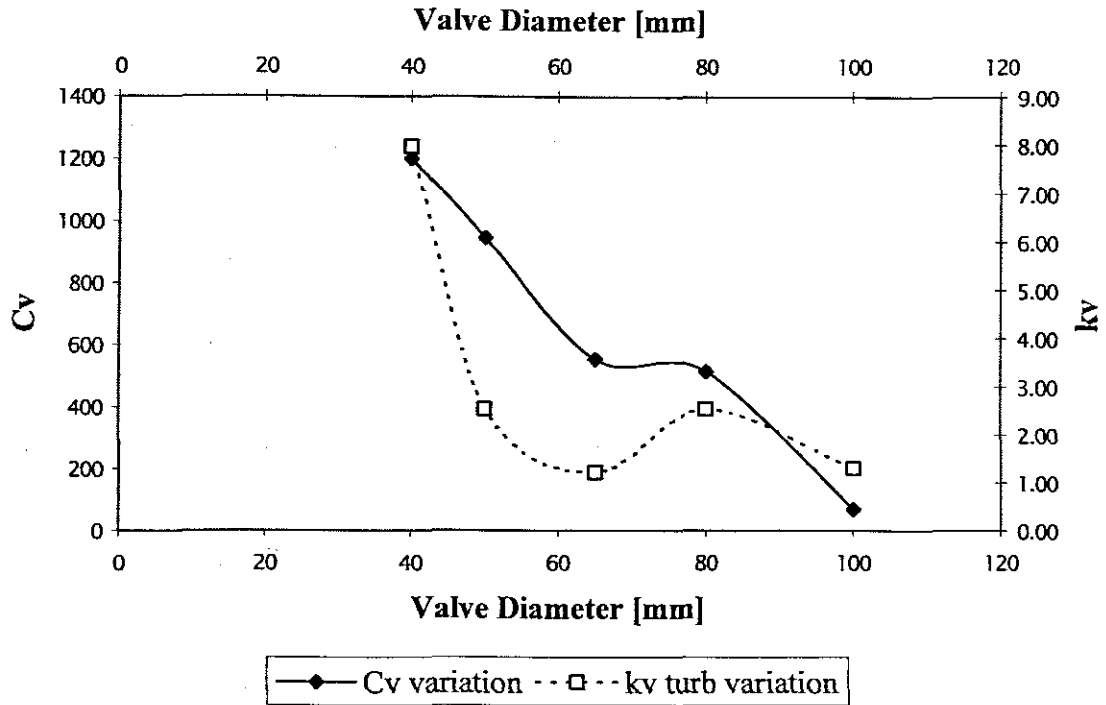


Figure 5. 2 Variation of loss coefficient in laminar and turbulent flow

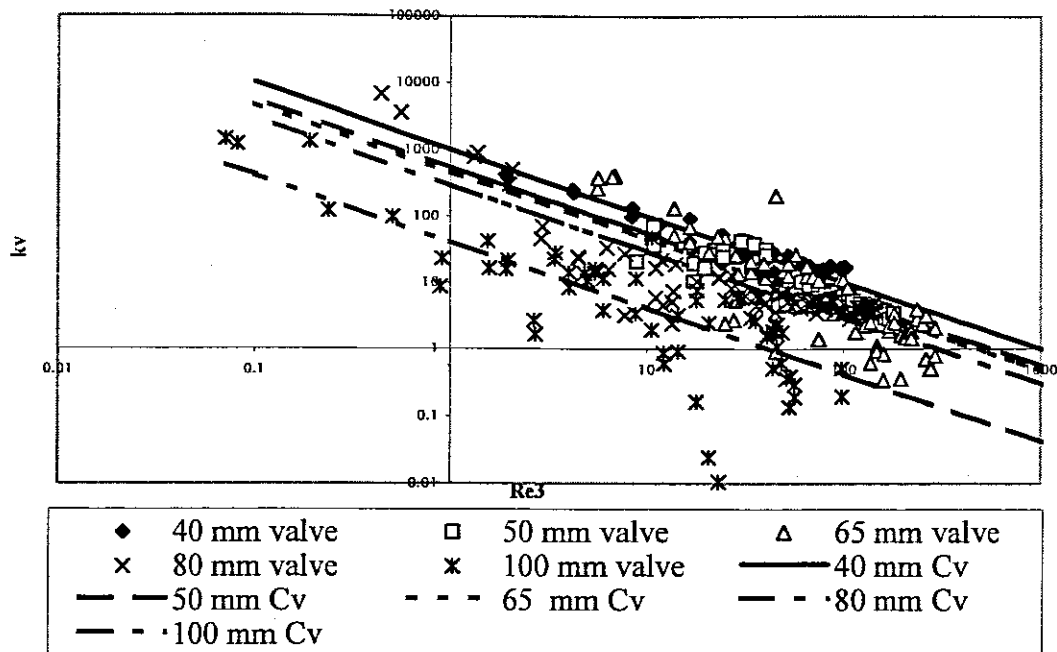


Figure 5.3 Diaphragm valve loss coefficients for CMC 8% in laminar flow

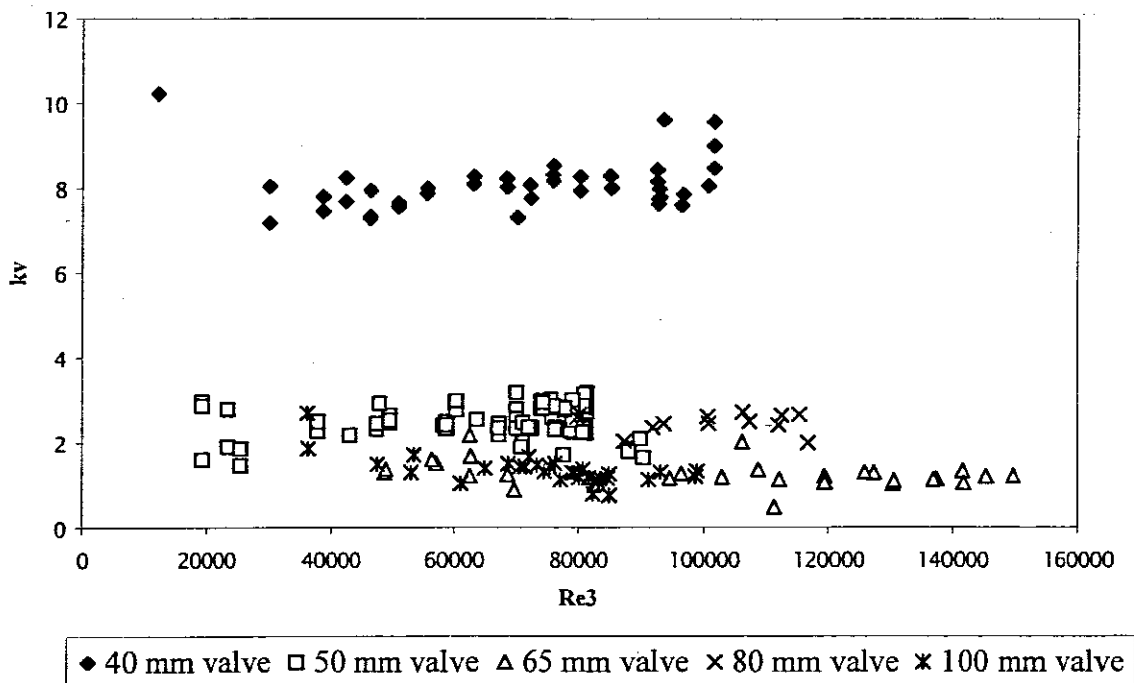


Figure 5.4 Diaphragm valves loss coefficients for water in turbulent flow

## 5.11 CONCLUSION

It has been shown that there is lack of data on diaphragm valves in the literature and the available data in the literature are scattered.

The experimental test loop has also been discussed and proved to be reliable and accurate.

The experimental method has been discussed and evaluated.

The instrumentation has been described and evaluated.

Materials tested have been discussed and their use justified.

The diaphragm valve loss coefficients and the rheological characterisation has been discussed and evaluated.

A similarity analysis has been done and it has been established that dynamic similarity is not achieved with the diaphragm valves studied and possible reasons for this were given.

# **CHAPTER 6**

## CHAPTER 6

### SUMMARY, CONTRIBUTIONS AND RECOMMENDATIONS

#### 6.1 INTRODUCTION

The literature review, the experimental method, as well as the analysis of results and discussion and evaluation of results have been presented.

In this chapter the contributions of this work will be summarised and some recommendations proposed.

#### 6.2 SUMMARY

This investigation was concerned with the evaluation of valve loss coefficients in diaphragm valves when non-Newtonian materials flow through the valve in laminar, transitional and turbulent flow. Qualitative and quantitative data on non-Newtonian losses in diaphragm valves is scarce.

An experimental test loop referred to as the Valve test rig was designed, built, commissioned and optimised. The Valve test rig was fitted with five diaphragm valves of 40, 50, 65, 80, and 100 millimetre nominal bore diameters. Various Newtonian (water and glycerine) and non-Newtonian fluids (CMC and kaolin slurries of various concentrations) were rheologically characterised and the valve loss coefficients were determined using the HGL approach.

The results were presented as plots of valve loss coefficient versus Reynolds number. Loss coefficients for laminar, transitional and turbulent flow were determined for all five valves.

### 6.3 CONTRIBUTIONS

The present investigation has confirmed the general theory on valve loss coefficients in laminar, transitional and turbulent flow and in particular:

- It has confirmed that the loss coefficient in laminar flow increases significantly with decreasing Reynolds number and is a hyperbolic function of the Reynolds number:

$$k_v = \frac{C_v}{Re} \quad (2.56)$$

- This investigation has also confirmed that in turbulent flow, the valve loss coefficient is essentially constant and is independent of the Reynolds number.

Further more this investigation has:

- Confirmed that the transition from turbulent flow to laminar flow occurs earlier in valves than in straight pipes.
- Highlighted the usefulness of the Slatter Reynolds number for both Newtonian and non-Newtonian fluids for the first time.
- Produced quantitative data on loss coefficients through diaphragm valves (Table 4.7) for use by slurries pipeline design engineers.
- Highlighted the need that studies should be carried out with a range of diaphragm valves to establish if geometric similarity is achieved and subsequently to establish dynamic similarity.
- Highlighted the need to investigate the internal details of the valve with the corresponding loss coefficient details and not to conclude at first sight that geometric and dynamic similarities are achieved.

**Table 4.7 Summary of  $C_v$  and  $k_v$  values obtained**

Valve dimension [mm]	$C_v$	$k_v$
40	1200	7.96
50	946	2.53
65	555	1.21
80	515	2.54
100	69	1.30

## 6.4 RECOMMENDATIONS

The following recommendations are suggested:

- Further experimental test work must be done on the determination of valve loss coefficients in general and diaphragm valve loss coefficients in particular.
- The determination of valve loss coefficients should be done for different valve openings (fully open,  $\frac{3}{4}$  open,  $\frac{1}{2}$  open and  $\frac{1}{4}$  open) for different types of materials. But for a refinement in the research, fluids of the same characteristics (Newtonian, pseudoplastic, yield pseudoplastic and Bingham plastic) should be tested and evaluated separately.
- Further study on geometrically similar valves in general and diaphragm valves in particular from other manufacturers should be done.
- The two experimental methods: the Hydraulic grade line approach and the Total pressure method should be done on the Valve test-rig, evaluated and then discussed.
- Further market research on the available fluid flow instrumentation should be done so that instruments with very large capabilities can be identified.

# **REFERENCES**



**REFERENCES**

AEA Technology plc. 1996. *Valves for slurry pipeline service*, Report for wet solids handling projects, Industrial consortium of companies.

Banerjee, TK. 1992. Studies on non-Newtonian flow through globe and gate valves. Unpublished MTech thesis, Calcutta, University of Calcutta.

Banerjee, TK, Das, M & Das, SK. 1994. Non-Newtonian liquid flow through globe and gate valves. *Can. J. Chem. Eng.*, 72:207-211, April.

Baudouin, MM. 2003. Contraction and expansion losses for non-Newtonian fluids. Unpublished MTech thesis, Cape Technikon, Cape Town.

Barry, BA. 1991. *Error in practical measurement in surveying, engineering and technology*. Rancho Cordova, Calif.: Landmark Entreprises.

Benziger JB & Aksay IA. 1999. Unpublished notes on data analysis. Princeton, Department of Chemical engineering, Princeton University.

Brinkworth, BJ. 1968. *Introduction to experimentation*. London:English Universities Press.

Brown, NP & Heywood, NI. 1991. *Slurry handling: Design of solid liquid systems*. London: Elsevier applied science.

Chhabra, RP & Richardson, JF. 1985. Hydraulic transport of coarse particles in viscous Newtonian and non-Newtonian media in a horizontal pipe. *Chem. Eng. Res. Des.*, 63: 390-397.

Chhabra, RP & Richardson, JF. 1999. *Non-Newtonian flow in the process industries*. Oxford: Butterworth-Heinemann.

Chhabra, RP & Slatter, PT. 2002. The flow of non-Newtonian slurries and sludges in pipes, short course. Unpublished course notes, Cape Technikon, Cape Town.

Crane Co. 1981. *Flow through valves, fittings, and pipe: SI units*. Technical Paper No.410M. London: Crane Co.

Edwards, MF, Jadallah, MSM & Smith, R. 1985. Head losses in pipe fittings at low Reynolds numbers. *Chem. Eng. Res. Des.*, 63: 43-50, January.

Giles, RV. 1977. *Fluid mechanics and hydraulics*. 2<sup>nd</sup> edition. New York: Schaum publishing co.

Govier, GW & Aziz, K. 1972. *The flow of complex mixtures in pipes*. New York: Van Nostrand Reinhold.

Hanks, RW & Ricks, L. 1975. Transitional and turbulent pipe flow of pseudoplastic fluids. *J. Hydraulics*,

Heywood, NI & Richardson, JF. 1978. Head loss reduction by gas injection for highly shear-thinning suspensions in horizontal pipe flow. Proceedings of the Hydrotransport 5<sup>th</sup> international conference, Cranfield, UK, May 1978:1-22 [Paper C1]

Hooper, WB. 1981. The two-K method predicts head losses in pipe fittings. *Chem. Eng.*: 96-100, August.

Jadallah, MSM. 1980. Flow in pipe fittings at low Reynolds numbers. Unpublished PhD thesis, University of Bradford, UK.

Johnson, M. 1982. Non-Newtonian fluid system design-some problems and their solutions, 8<sup>th</sup> *Int.Conf.on the hydraulic transport of solids in pipes*, Hydrotransport 8 Paper F3.

Kittredge, CP & Rowley, DS. 1957. Resistance coefficients for laminar and turbulent flow through one-half-inch valves and fittings. *Trans. ASME*, 79:1759-1766.

Lahlou, ZM. 2002. Valves. Tech. brief. *National Drinking Water Clearinghouse fact sheet*. NDWC West Virginia University, Morgantown.

Malkin, AY. 1994. *Rheology Fundamentals*. Toronto: ChemTec.

Massey, BS. 1970. *Mechanics of fluids*. 2nd edition. Van Nostrand Reinhold.

McNeil, DA & Morris, SD. 1995. A mechanistic investigation of laminar flows through an abrupt enlargement and a nozzle and its application to other pipe fittings. *Report EUR 16348 EN*. Edinburgh: Department of Mechanical and Chemical Engineering, Heriott Watt University

Metzner, AB. 1954. Pipeline design for non-Newtonian fluids. *Chemical Engineering Progress*. 50(1).

Metzner, AB. 1957. Relationships between recent pressure-drop correlations. *Non-Newtonian Fluid Flow*. 49(9).

Metzner, AB & Reed, JC. 1955. Flow of non-Newtonian fluids-correlation of the laminar ,transitio and turbulent flow regions. *AIChEJ*.1(9)

Metzner, A.B., 1956 "Non-Newtonian Technology: Fluid Mechanics, Mixing and Heat Transfer", Chap.II in "*Advances in Chemical Engineering*", vol.I, Academic Press, New York.

Miller, DS. 1978. *Internal flow systems*. Cranfield: BHRA Fluid Engineering.

Paterson, A & Cooke, R. 1999. The design of slurry pipelines systems. Unpublished course notes presented at The Breakwater Lodge Victoria & Alfred Waterfront, Cape Town, 24-26 March.

Perry, RH & Chilton, CH. 1973. *Chemical engineers' handbook*. 5<sup>th</sup> edition. New York: Mc Graw-Hill.

Pienaar, VG, Slatter, PT, Alderman, NJ & Heywood, NI. 2004. Review of frictional pressure losses for flow of Newtonian and non-Newtonian slurries through valves.

Pienaar, VG, Alderman, NJ & Heywood, NI. 2001. Slurry handling: A review of frictional pressure losses for flow of non-Newtonian fluids through pipe fittings. 2(6): 85-98. Culham, Oxfordshire: AEA Technology plc.

Pienaar, VG. 1998. Non-Newtonian fittings losses, Unpublished MTech thesis, Cape Technikon, Cape Town.

Piggot, RJS. 1950. Pressure losses in tubing, pipe and fittings. *Trans. ASME* 72:629.

Shook CA & Roco MC. 1991. *Slurryflow: principles and practice*. Oxford: Butterworth-Heinemann.

Shook CA, Gillies RG & Sanders RS. 2002. *Pipeline hydrotransport with application in the oil sand industry*. Saskatoon: SRC Pipe Flow Technology Centre.

Skelland, AHP. 1967. *Non-Newtonian Flow and Heat Transfer*. New York: Wiley.

Slatter, PT. 1994. Transitional and turbulent flow of non-Newtonian slurries in pipes. Unpublished PhD thesis, University of Cape Town.

Slatter, PT. 1999. A new friction factor for yield stress fluids. *14<sup>th</sup> International conference on slurry handling and pipeline hydrotransport 14*, Maastricht, September 1999: 255-2654.

Slatter, PT & Pienaar, VG. 1999. Establishing dynamic similarity for non-Newtonian fittings loss, *14<sup>th</sup> Int.Conf. On slurry handling and pipeline transport*, Hydro transport, BHR Group, 245-254.

Slatter, PT & Chhabra, RP. 2002. The flow of non-Newtonian slurries and sludges in pipes, Unpublished short course notes. Cape Town: Cape Technikon

Steffe, JF, Mohamed, IO & Ford, EW. 1984. Pressure drop across valves and fittings for pseudoplastic fluids in laminar flow. *ASAE*, Paper No.83-6004.

Thomas, AD & Wilson, KC. 1987. New analysis of non-Newtonian –yield-power – law fluids. *Can.J.Chem.Eng.*, 65:335-338.

Turian, RM, Ma, FLG, Sung, MDJ & Plackmann, GW. 1997. Flow of concentrated non-Newtonian slurries: 2. Friction losses in bends, fittings, valves and venturi meters. *Int. J. Multiphas.Fllow*, 24(2), 243-269.

# **APPENDICES**

## CONTENTS

- APPENDIX 1: photographs of the experimental test loop and instrumentation
- APPENDIX 2: comparison of water test results with Colebrook & White equation
- APPENDIX 3: rheograms of fluids tested
- APPENDIX 4: comparison of experimental values of the friction factor to the theoretical values for different fluids in straight pipe ( $f - Re$  graphs)
- APPENDIX 5: Calculation of the apparent fluid consistency index ( $K'$ ) and the apparent fluid behaviour index ( $n'$ ) for a yield pseudoplastic fluid
- APPENDIX 6: diaphragm valve loss coefficients data

## LIST OF PHOTOGRAPHS

Photograph 1. Overview of the Valve test rig.....	6
Photograph 2. Diaphragm valves connected to pipes .....	6
Photograph 3. Diaphragm valves, pipes, PPT and DP Cell.....	7
Photograph 4. PPT .....	8
Photograph 5. DP Cells.....	8
Photograph 6. PLB.....	9
Photograph 7. Hand Held Communicator.....	9
Photograph 8. Data Acquisition Unit.....	10
Photograph 9. PC and Data Acquisition Unit.....	10
Photograph 10. Krohne magnetic flow meter.....	11
Photograph 11. Safmag magnetic flow meter.....	11
Photograph 12. Mixing tank .....	12
Photograph 13. Weight tank wit Load cell .....	12
Photograph 14. Orbit PD pump .....	13

## LIST OF FIGURES

Figure 1 Comparison with Colebrook and White for water test, pipe of 52.08 mm.....	14
Figure 2 Comparison with Colebrook and White for water test, pipe of 63.08 mm.....	15

Figure 3 Comparison with Colebrook and White for water test, pipe of 80.43 mm.....	16
Figure 4 Comparison with Colebrook and White for water test, pipe of 97.17 mm.....	17
Figure 5 Rheogram Glycerine 100% .....	20
Figure 6 Rheogram Glycerine 100% .....	21
Figure 7 Rheogram Glycerine 100% .....	22
Figure 8 Rheogram Glycerine 75% .....	23
Figure 9 Rheogram Glycerine 75% .....	24
Figure 10 Rheogram CMC 5% .....	25
Figure 11 Rheogram CMC 5% .....	26
Figure 12 Rheogram CMC 5% .....	27
Figure 13 Rheogram CMC 8% .....	28
Figure 14 Rheogram CMC 8% .....	29
Figure 15 Rheogram CMC 8% .....	30
Figure 16 Rheogram kaolin 10% .....	31
Figure 17 Rheogram kaolin 10% .....	32
Figure 18 Rheogram kaolin 13% .....	33
Figure 19 Rheogram kaolin 13% .....	34
Figure 20 Comparison of experimental values of the friction factor with the theoretical line for different fluids in straight pipe of Diameter 52.8 mm ID pipe .....	36
Figure 21 Comparison of experimental values of the friction factor with the theoretical line for different fluids in straight pipe of Diameter 63.08 mm ID pipe .....	37
Figure 22 Comparison of experimental values of the friction factor with the theoretical line for different fluids in straight pipe of Diameter 80.43 mm ID pipe .....	37
Figure 23 Comparison of experimental values of the friction factor with the theoretical line for different fluids in straight pipe of Diameter 97.17 mm ID pipe .....	38

### LIST OF TABLES

Table 1 HGL Test for water.....	43
Table 2 HGL Test for water.....	43
Table 3 HGL Test for water.....	44
Table 4 HGL Test for water.....	45
Table 5 HGL Test for water.....	46
Table 6 HGL Test for water.....	46
Table 7 HGL Test for water.....	47
Table 8 HGL Test for water.....	47
Table 9 HGL Test for water.....	48
Table 10 HGL Test for water.....	48

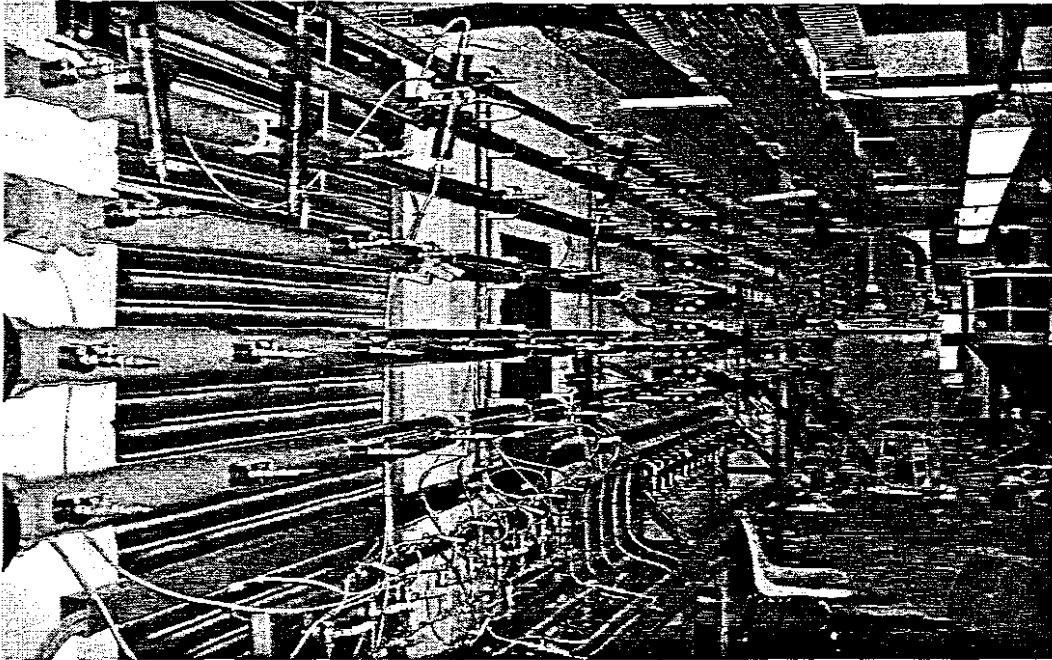


Table 11 HGL Test for Glycerine 100%.....	49
Table 12 HGL Test for Glycerine 100%.....	50
Table 13 HGL Test for Glycerine 100%.....	51
Table 14 HGL Test for Glycerine 100%.....	52
Table 15 HGL Test for Glycerine 100%.....	53
Table 16 HGL Test for Glycerine 75%.....	54
Table 17 HGL Test for Glycerine 75%.....	55
Table 18 HGL Test for Glycerine 75%.....	55
Table 19 HGL Test for Glycerine 75%.....	56
Table 20 HGL Test for Glycerine 75%.....	56
Table 21 HGL Test for CMC 5% .....	57
Table 22 HGL Test for CMC 5% .....	58
Table 23 HGL Test for CMC 5% .....	58
Table 24 HGL Test for CMC 5% .....	59
Table 25 HGL Test for CMC 5% .....	60
Table 26 HGL Test for CMC 5% .....	61
Table 27 HGL Test for CMC 5% .....	62
Table 28 HGL Test for CMC 5% .....	63
Table 29 HGL Test for CMC 5% .....	64
Table 30 HGL Test for CMC 8% .....	65
Table 31 HGL Test for CMC 8% .....	65
Table 32 HGL Test for CMC 8% .....	66
Table 33 HGL Test for CMC 8% .....	67
Table 34 HGL Test for CMC 8% .....	68
Table 35 HGL Test for CMC 8% .....	69
Table 36 HGL Test for kaolin 10% .....	70
Table 37 HGL Test for kaolin 10% .....	70
Table 38 HGL Test for kaolin 10% .....	70
Table 39 HGL Test for kaolin 10% .....	71
Table 40 HGL Test for kaolin 10% .....	71
Table 41 HGL Test for kaolin 10% .....	72
Table 42 HGL Test for kaolin 10% .....	72
Table 43 HGL Test for kaolin 10% .....	72
Table 44 HGL Test for kaolin 10% .....	73
Table 45 HGL Test for kaolin 10% .....	73
Table 46 HGL Test for kaolin 10% .....	74
Table 47 HGL Test for kaolin 10% .....	74
Table 48 HGL Test for kaolin 10% .....	75
Table 49 HGL Test for kaolin 13% .....	75
Table 50 HGL Test for kaolin 13% .....	76
Table 51 HGL Test for kaolin 13% .....	77
Table 52 HGL Test for kaolin 13% .....	77
Table 53 HGL Test for kaolin 13% .....	78
Table 54 HGL Test for kaolin 13% .....	78
Table 55 HGL Test for kaolin 13% .....	79
Table 56 HGL Test for kaolin 13% .....	79

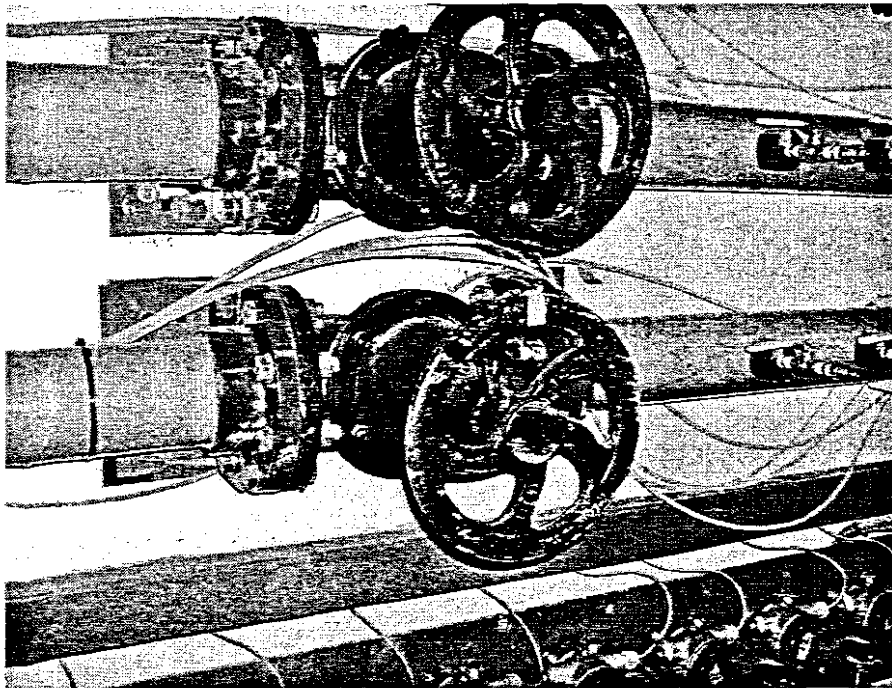
---

Table 57 HGL Test for kaolin 13% .....	80
--	----

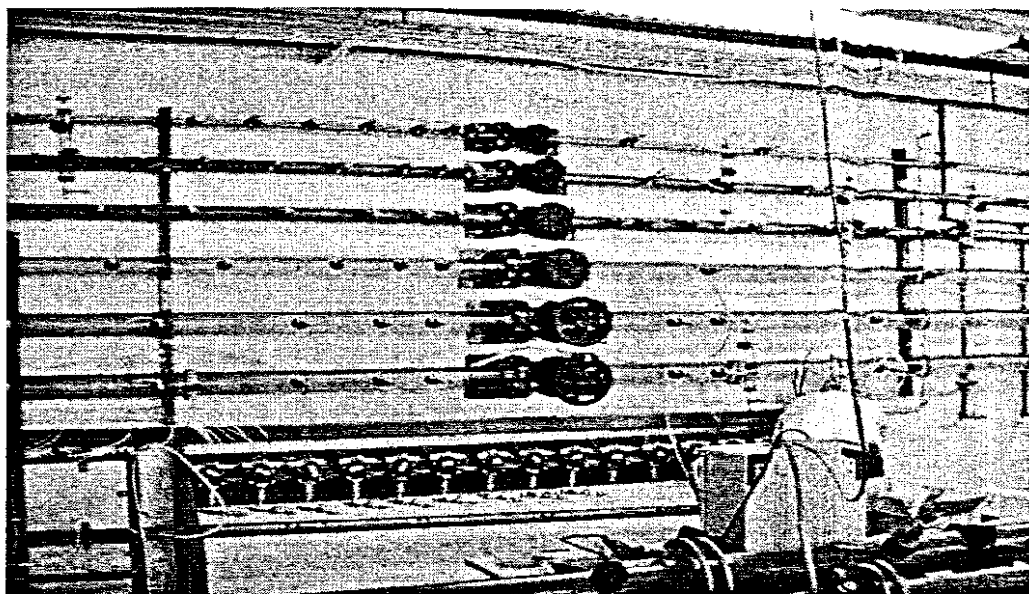
**APPENDIX 1**  
**PHOTOGRAPHS OF THE EXPERIMENTAL**  
**TEST LOOP AND INSTRUMENTATION**



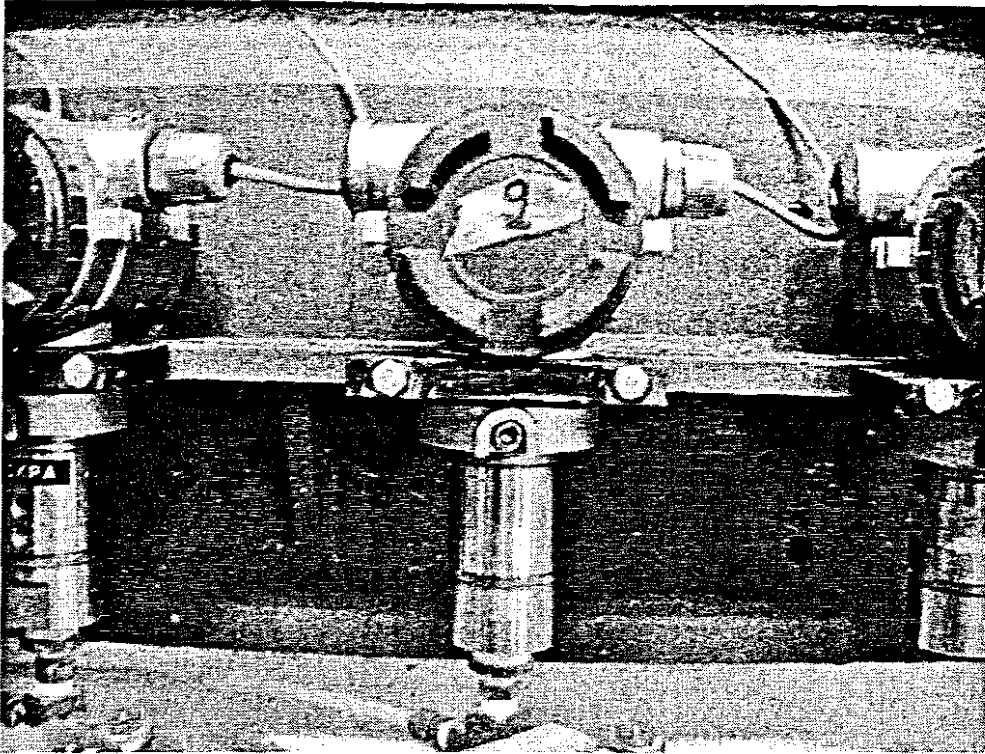
**Photograph 1. Overview of the Valve test rig**



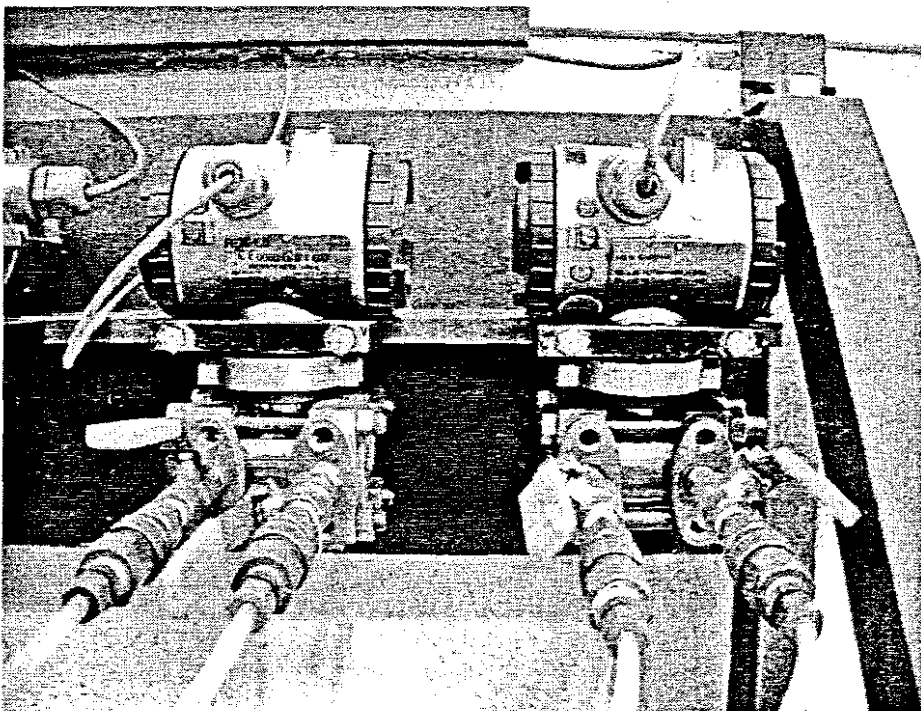
**Photograph 2. Diaphragm valves connected to pipes**



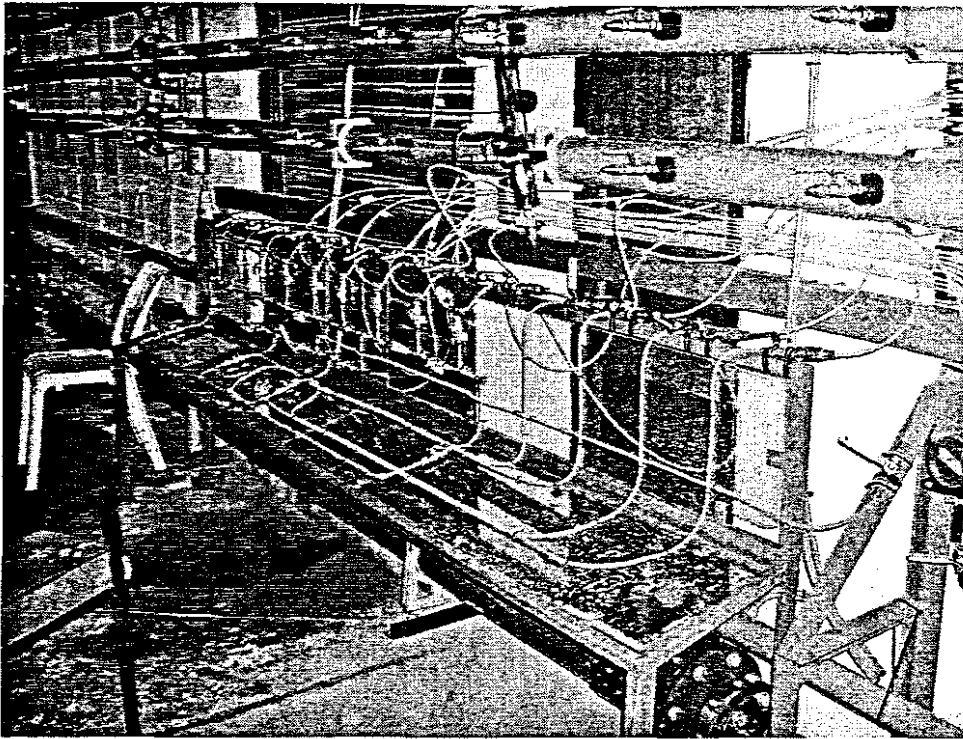
**Photograph 3. Diaphragm valves, pipes, Point Pressure Transducers and Differential Pressure Cell**



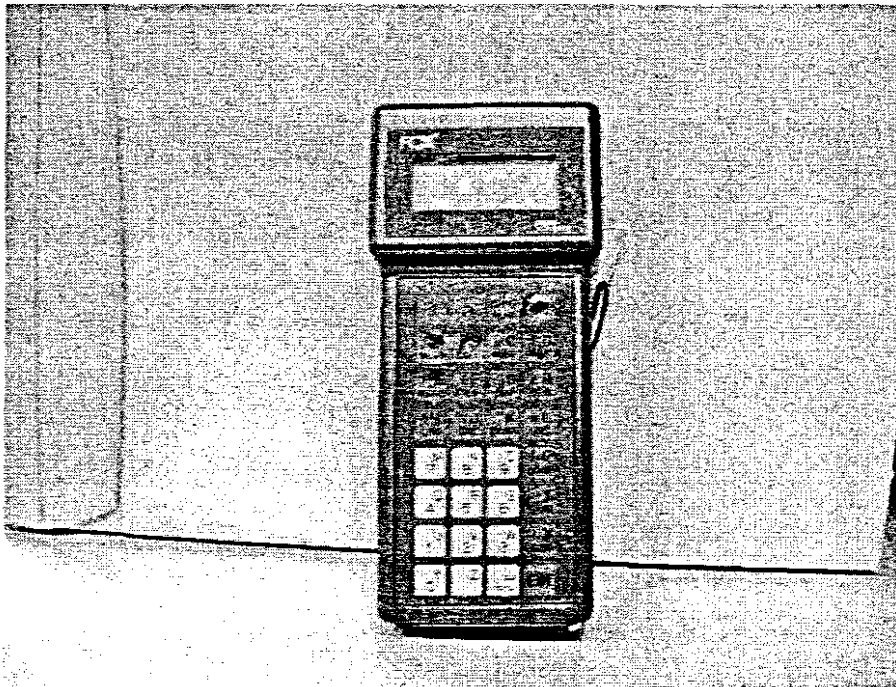
**Photograph 4. Point Pressure Transducer**



**Photograph 5. Differential Pressure Cells**



**Photograph 6. Pressure Lines Board**



**Photograph 7. Hand Held Communicator**

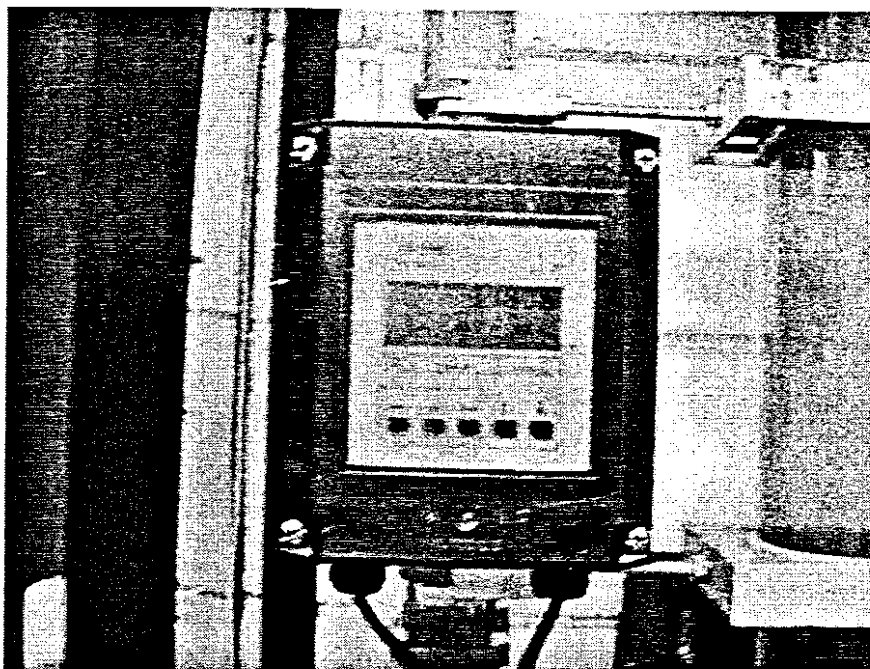


**Photograph 8. Data Acquisition Unit**

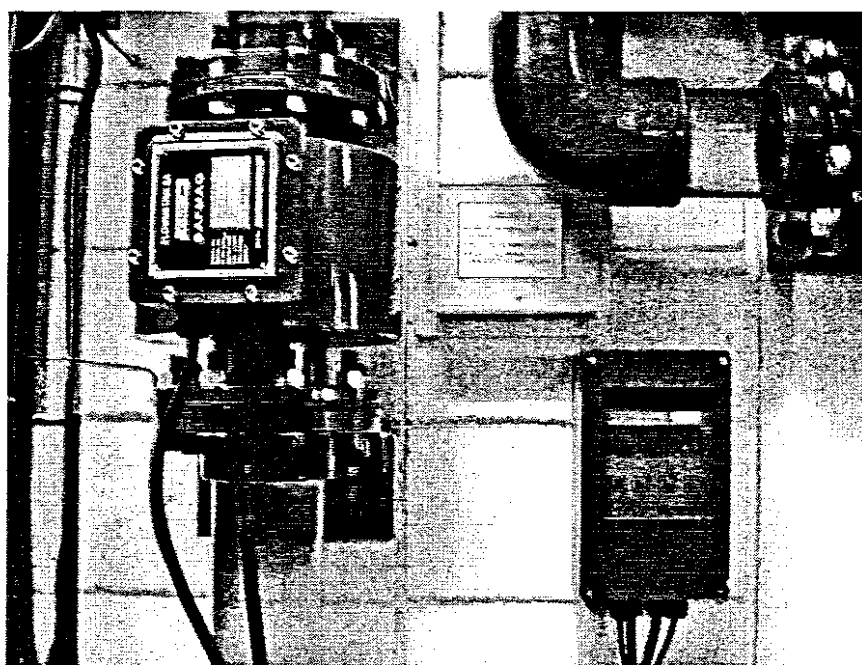


**Photograph 9. PC and Data Acquisition Unit**

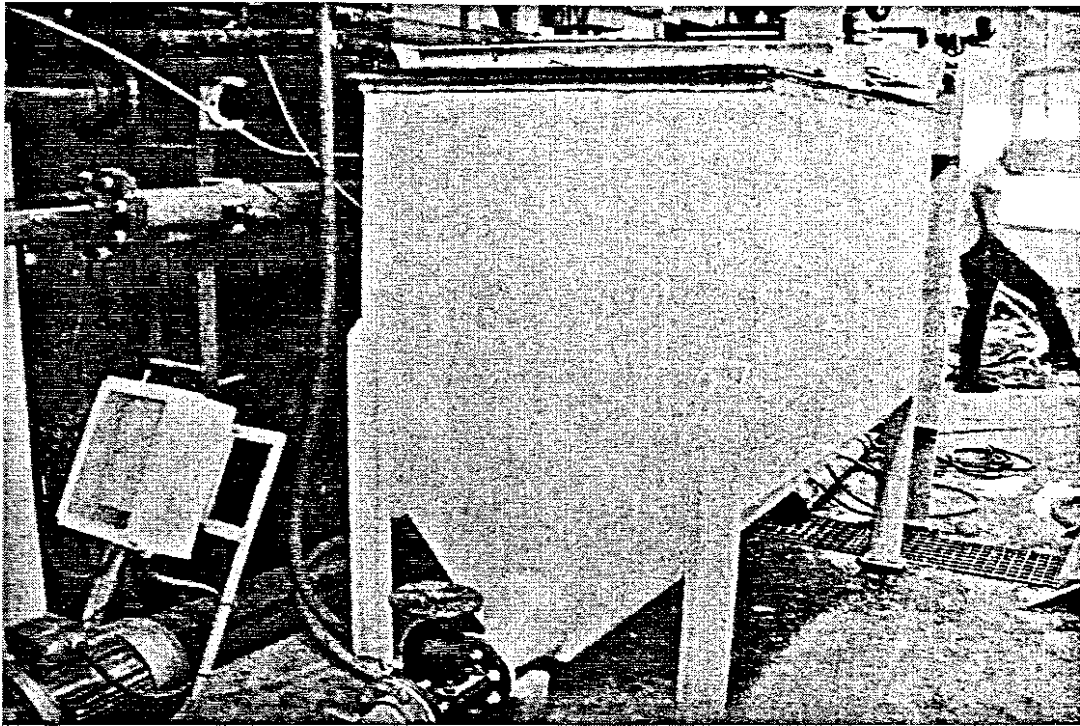




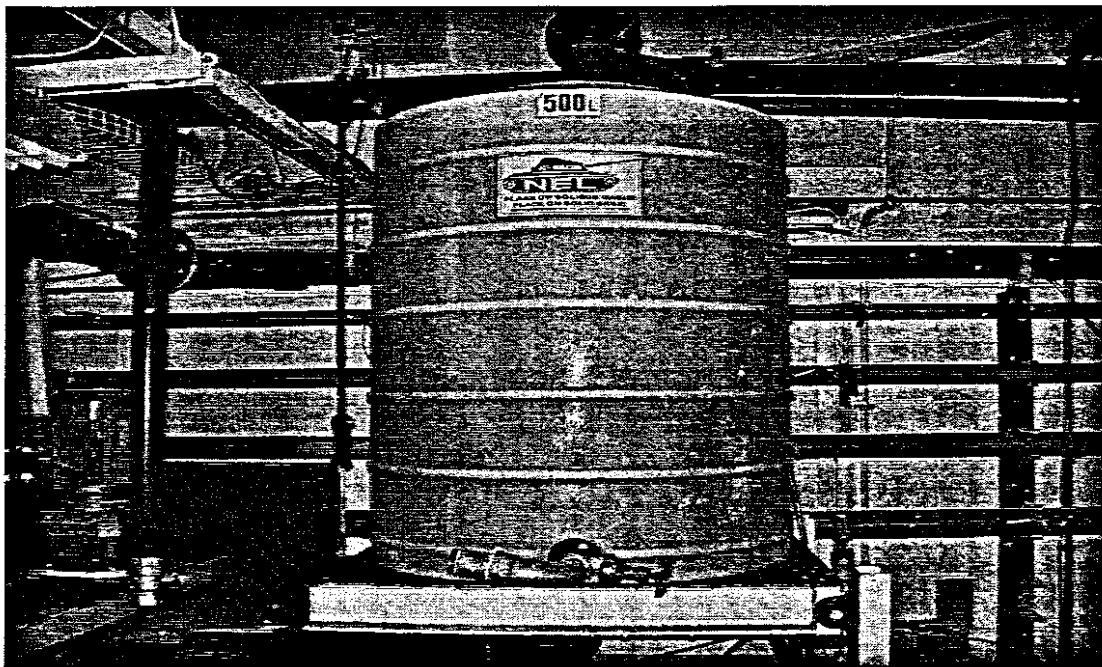
**Photograph 10. Krohne magnetic flow meter**



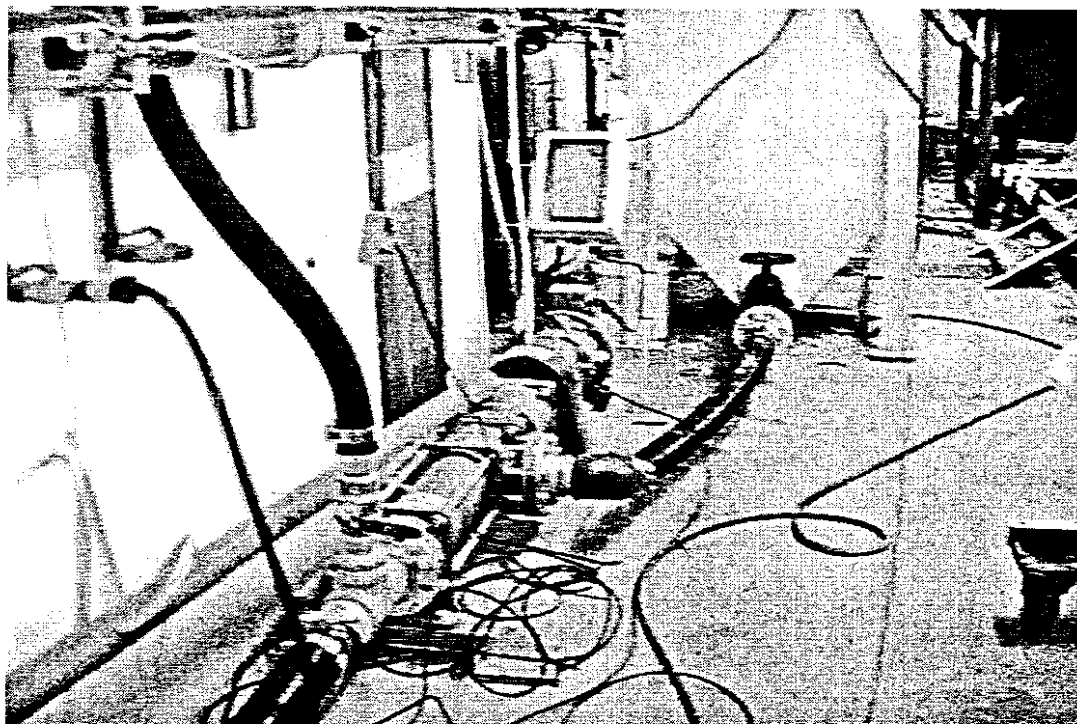
**Photograph 11. Safmag magnetic flow meter**



**Photograph 12. Mixing tank**



**Photograph 13. Weigh tank with Load cell**



**Photograph 14. Orbit PD pump**

**APPENDIX 2**  
**COMPARISON OF WATER TEST RESULTS**  
**WITH COLEBROOK & WHITE EQUATION**

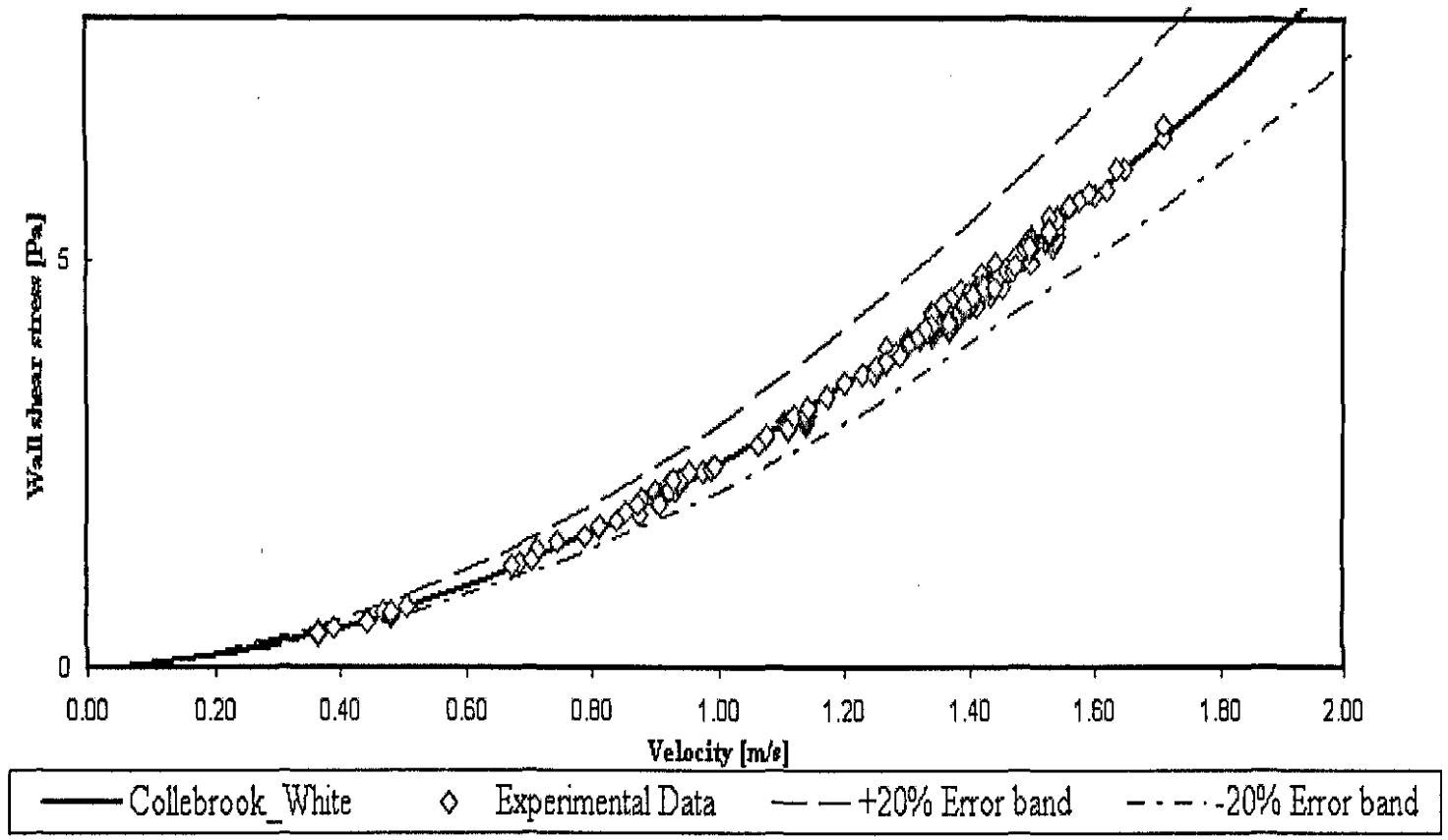


Figure 1 Comparison with Colebrook and White for water test, pipe of 52.08 mm

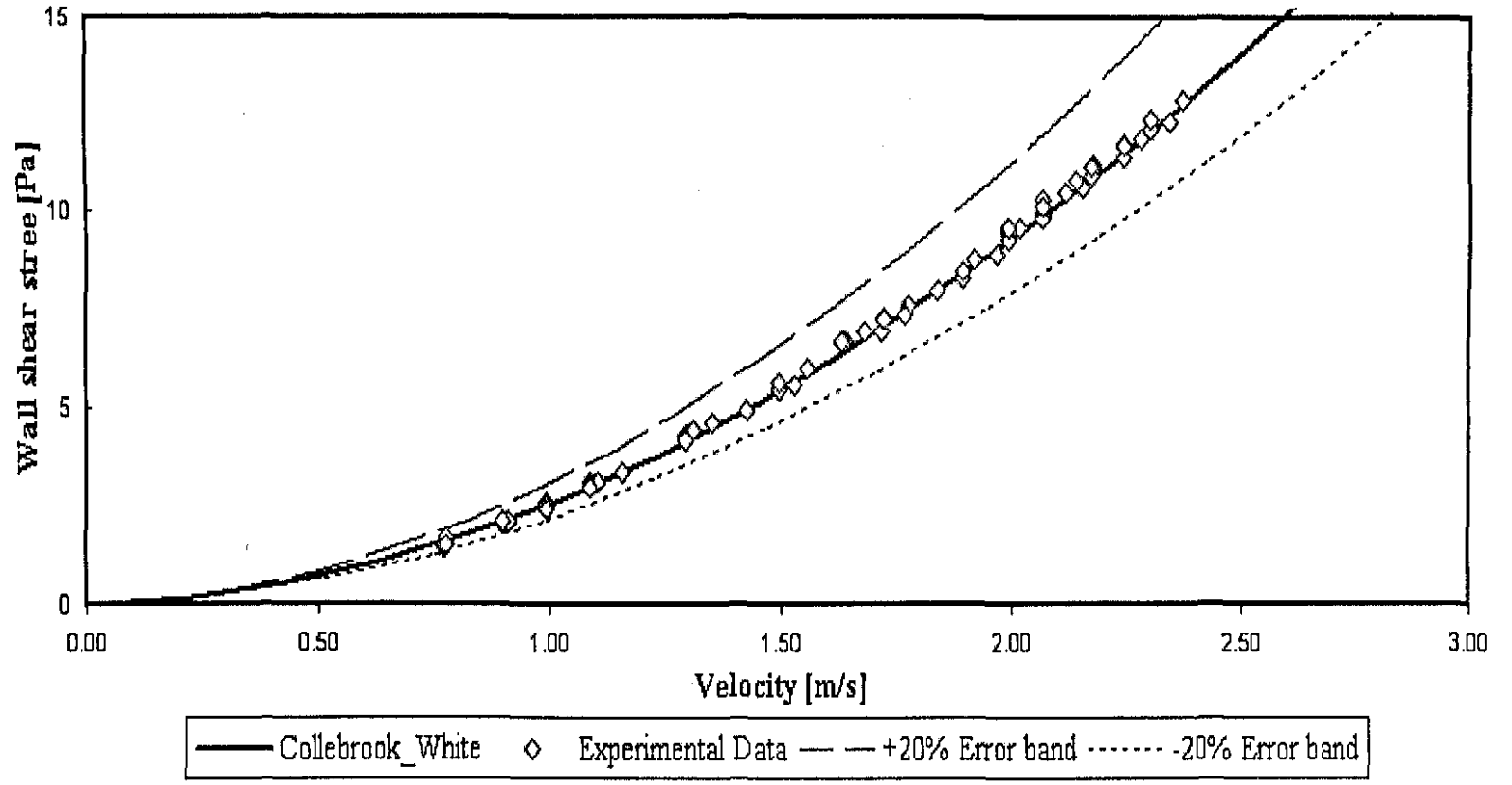


Figure 2 Comparison with Colebrook and White for water test, pipe of 63.08 mm

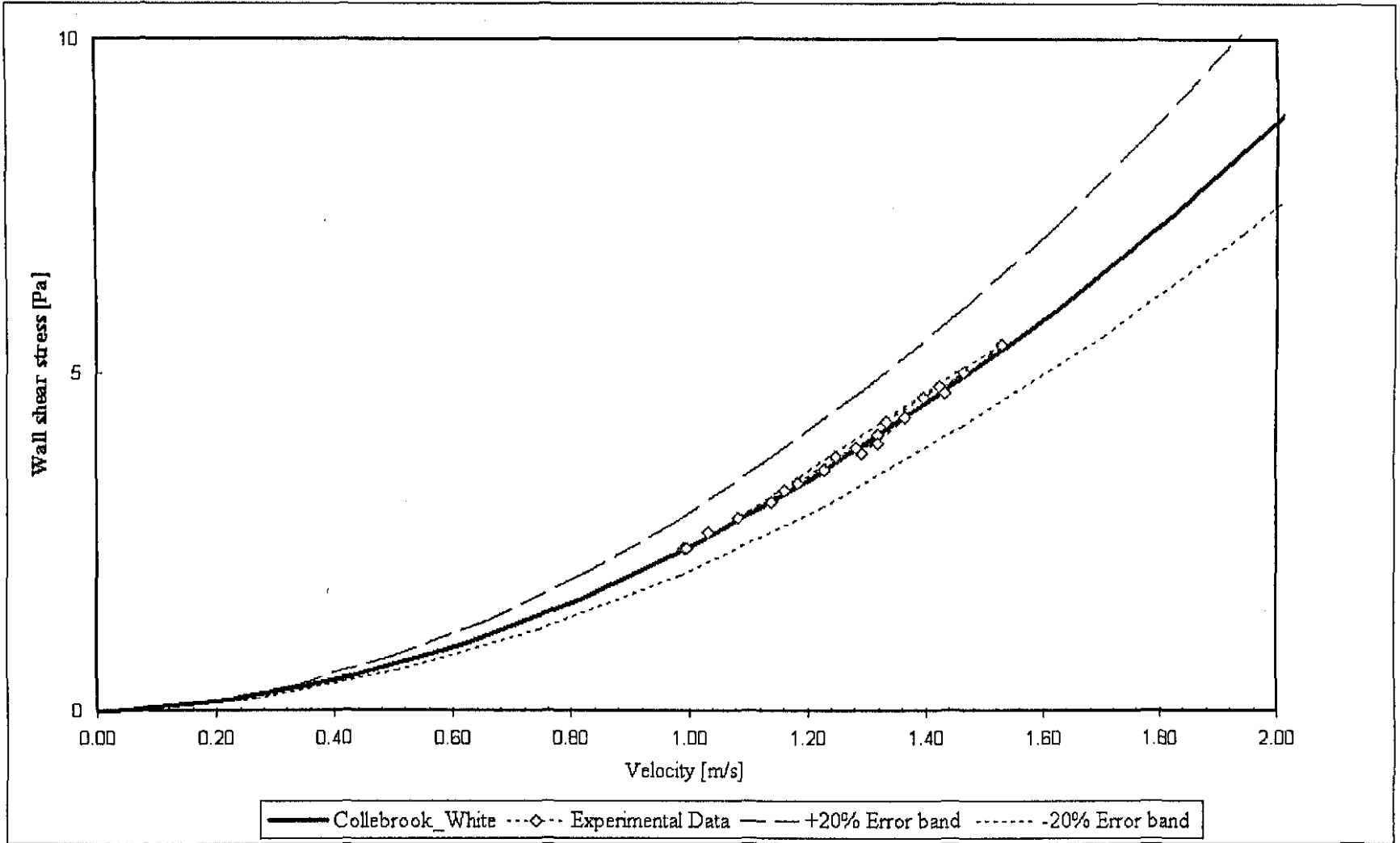


Figure 3 Comparison with Colebrook and White for water test, pipe of 80.43 mm

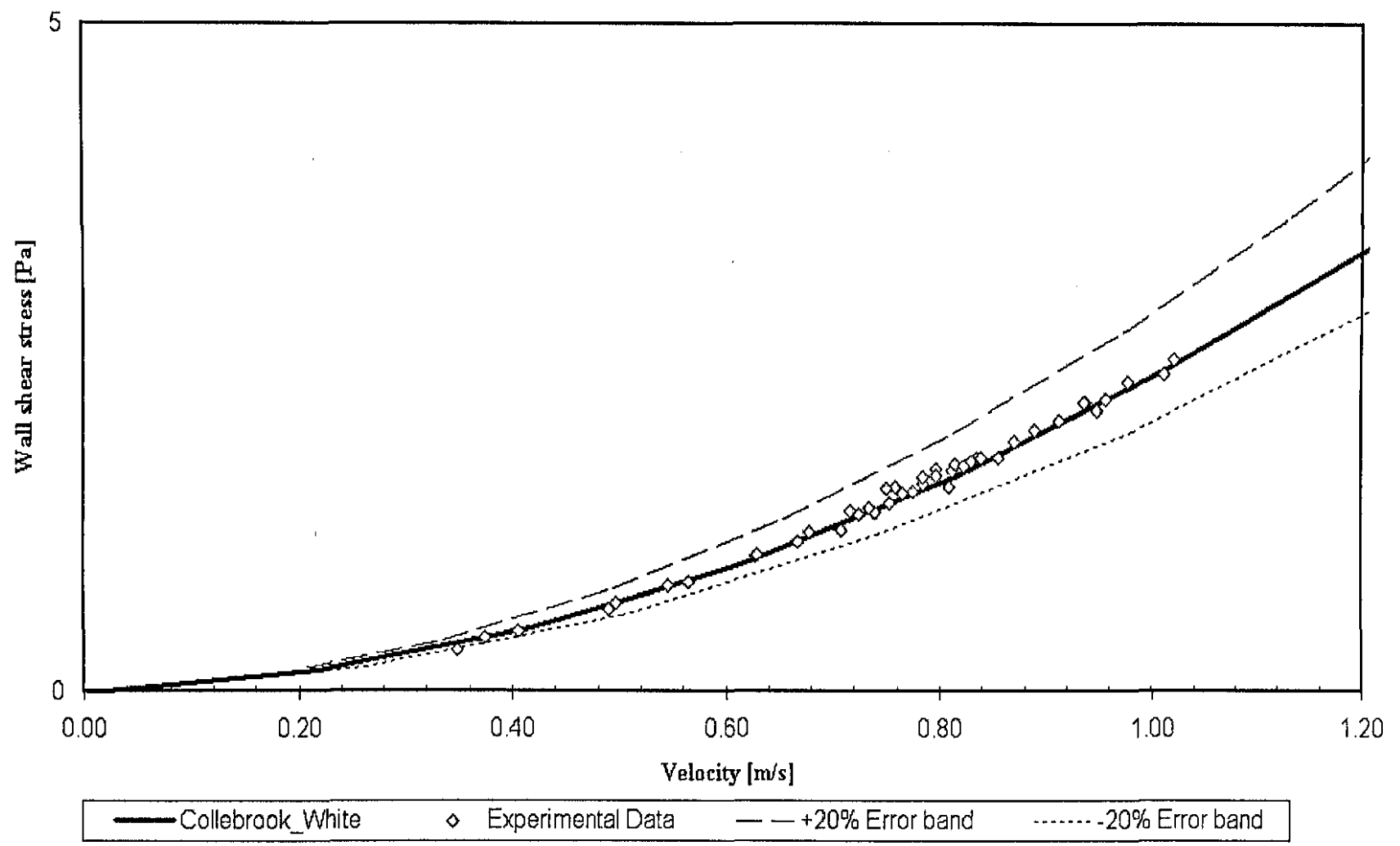


Figure 4 Comparison with Colebrook and White for water test, pipe of 97.17 mm



**APPENDIX 3**  
**RHEOGRAMS OF FLUIDS TESTED**

GLYCERINE 100%

SLURRY PROPERTIES	
Date	22/11/2004
Slurry Relative Density	1270 kg/m <sup>3</sup>
Volume Concentration	100%
Viscosity	0.842 Pa.s
Temperature	25.5°C

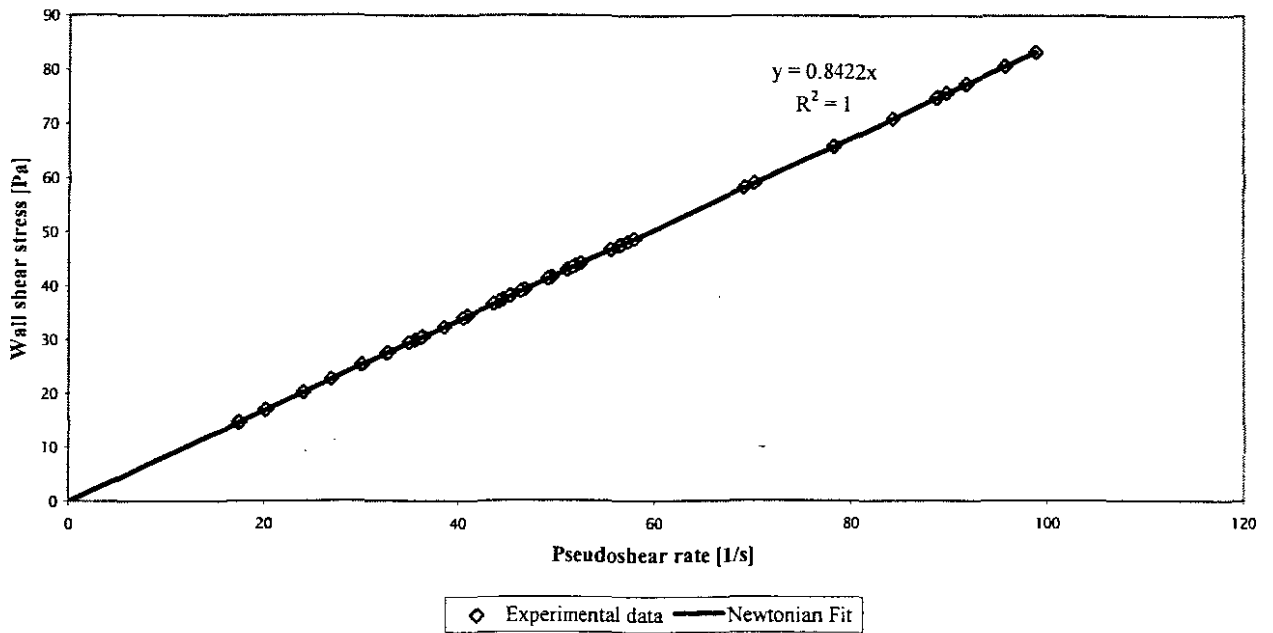


Figure 5 Rheogram Glycerine 100%

## GLYCERINE 100%

SLURRY PROPERTIES	
Date	19/11/2004
Slurry Relative Density	1252.61 kg/m <sup>3</sup>
Volume Concentration	100%
Viscosity	0.175 Pa.s
Temperature	27°C

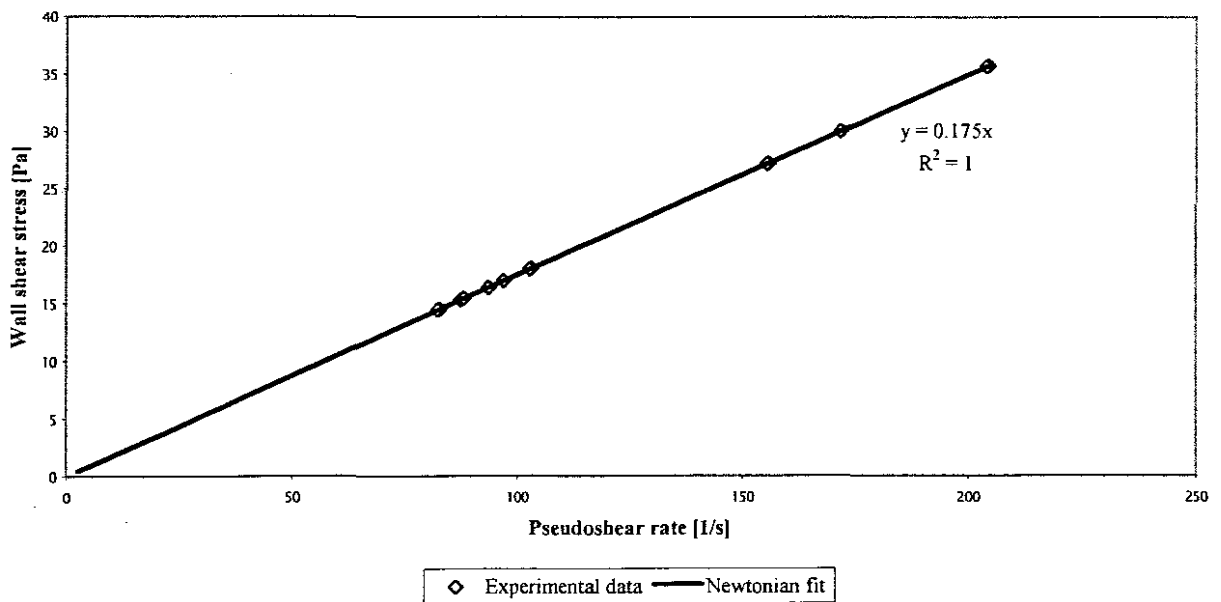


Figure 6 Rheogram Glycerine 100%

GLYCERINE 100%

SLURRY PROPERTIES	
Date	25/11/2004
Slurry Relative Density	1256 kg/m <sup>3</sup>
Volume Concentration	100%
Viscosity	0.693 Pa.s
Temperature	22°C

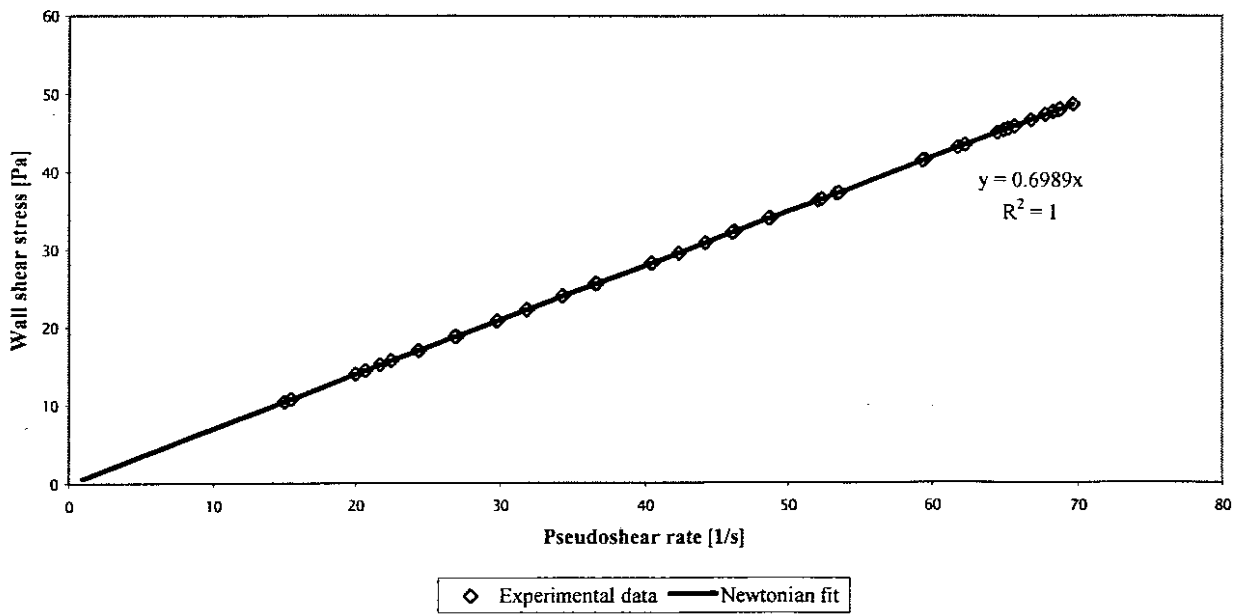


Figure 7 Rheogram Glycerine 100%

## GLYCERINE 75%

SLURRY PROPERTIES	
Date	1/12/2004
Slurry Relative Density	1197.2 kg/m <sup>3</sup>
Volume Concentration	75%
Viscosity	0.0196 Pa.s
Temperature	21°C

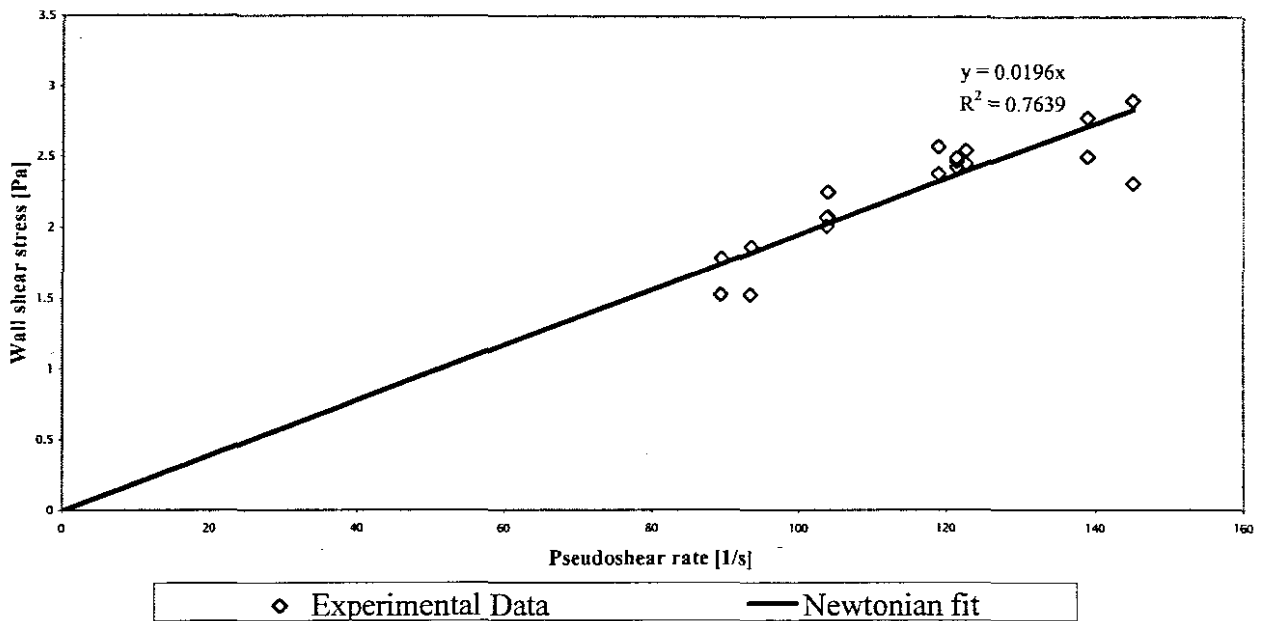


Figure 8 Rheogram Glycerine 75%

## GLYCERINE 75%

SLURRY PROPERTIES	
Date	30/11/2004
Slurry Relative Density	1197.2 kg/m <sup>3</sup>
Volume Concentration	75%
Viscosity	0.0184 Pa.s
Temperature	21°C

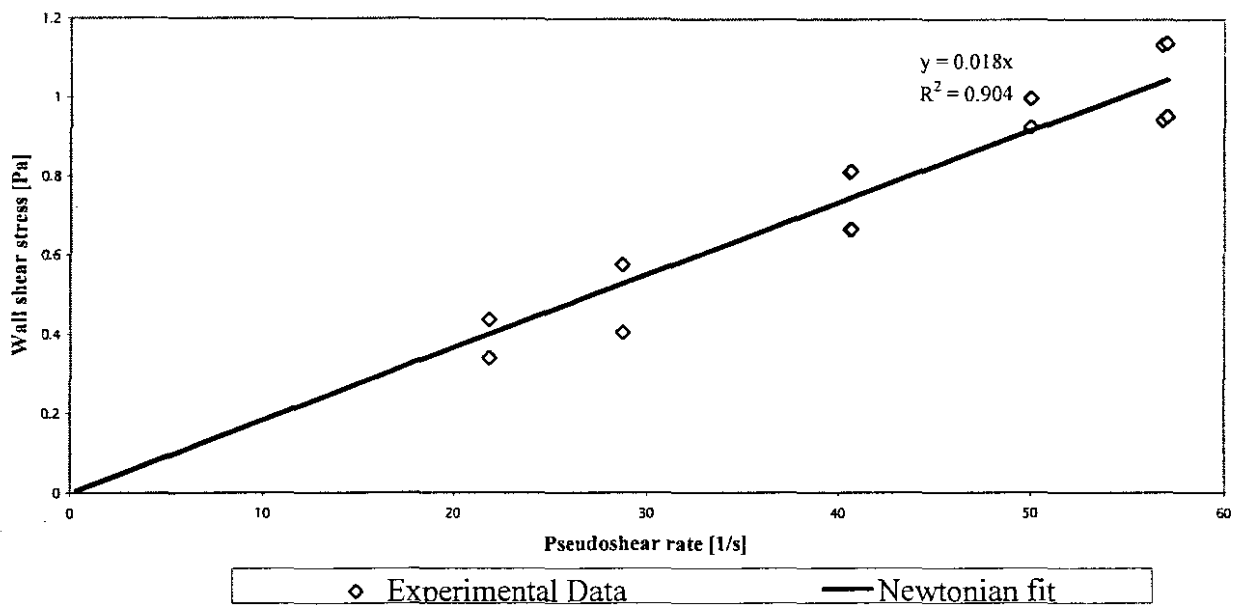


Figure 9 Rheogram Glycerine 75%

## CMC 5%

SLURRY PROPERTIES	
Date	22/10/2004
Slurry Relative Density	1029 kg/m <sup>3</sup>
Mass Concentration	5%
Fluid Consistency Index	0.304 Pa.s <sup>n</sup>
Flow Behaviour Index	0.723

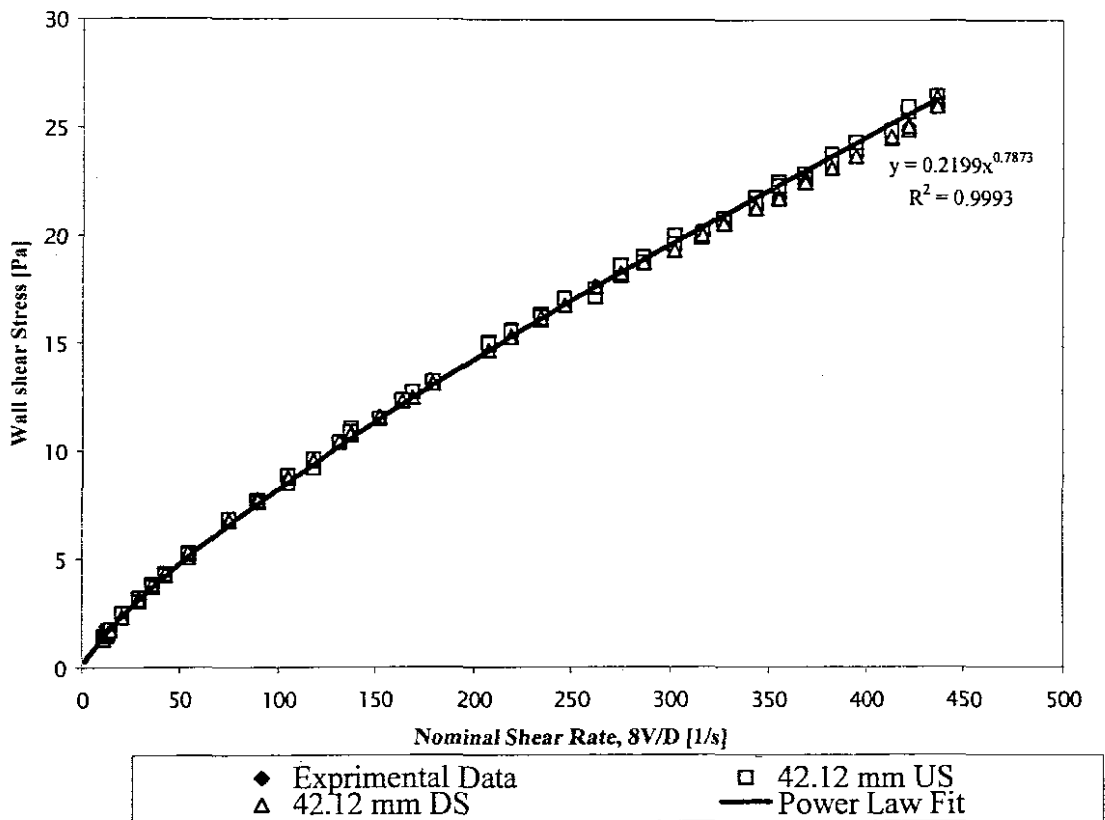


Figure 10 Rheogram CMC 5%

CMC 5%

SLURRY PROPERTIES	
Date	26/10/2004
Slurry Relative Density	1026.5 kg/m <sup>3</sup>
Mass Concentration	5%
Fluid Consistency Index	0.472 Pa.s <sup>n</sup>
Flow Behaviour Index	0.742

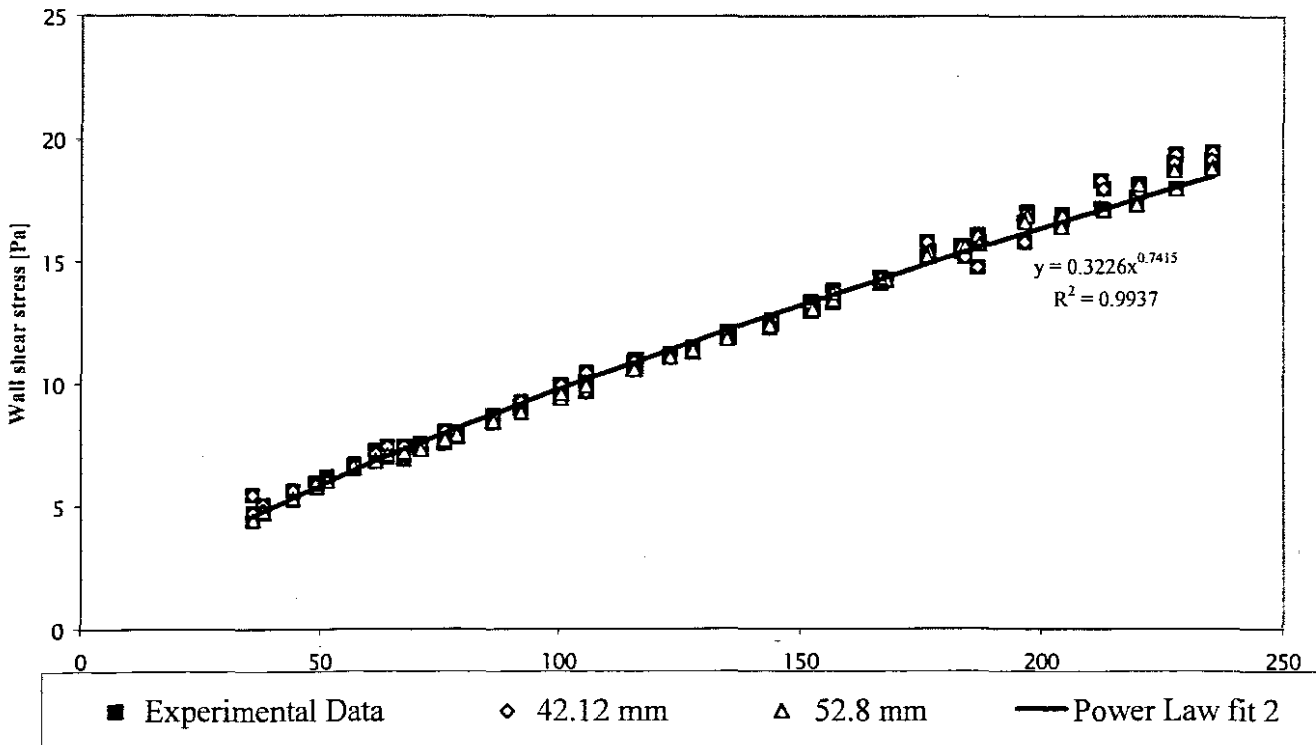


Figure 11 Rheogram CMC 5%



CMC 5%

SLURRY PROPERTIES	
Date	2/11/2004
Slurry Relative Density	1028.2 kg/m <sup>3</sup>
Mass Concentration	5%
Fluid Consistency Index	1.095 Pa.s <sup>n</sup>
Flow Behaviour Index	0.798

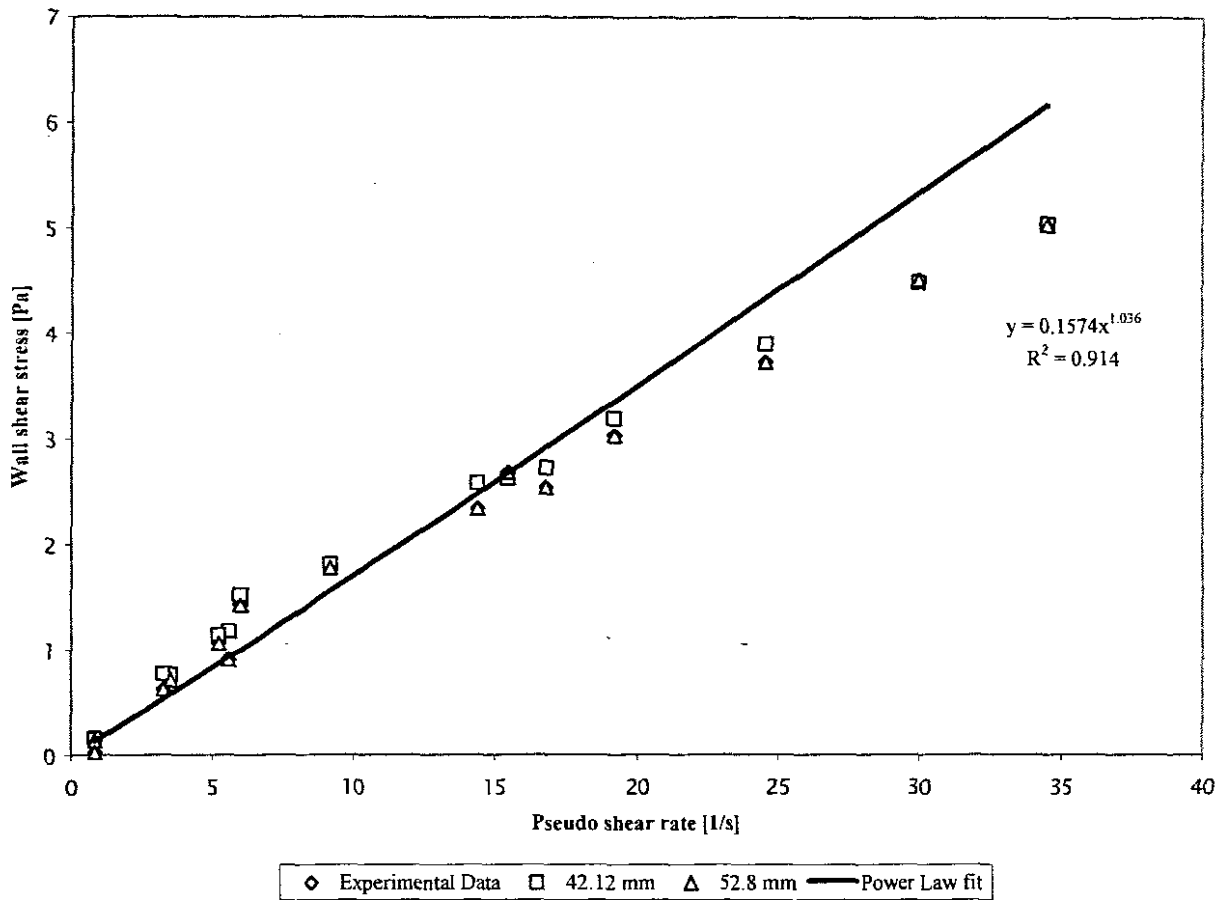


Figure 12 Rheogram CMC 5%

CMC 8%

SLURRY PROPERTIES	
Date	12/11/2004
Slurry Relative Density	1040 kg/m <sup>3</sup>
Mass Concentration	8%
Fluid Consistency Index	5.908 Pa.s <sup>n</sup>
Flow Behaviour Index	0.6147

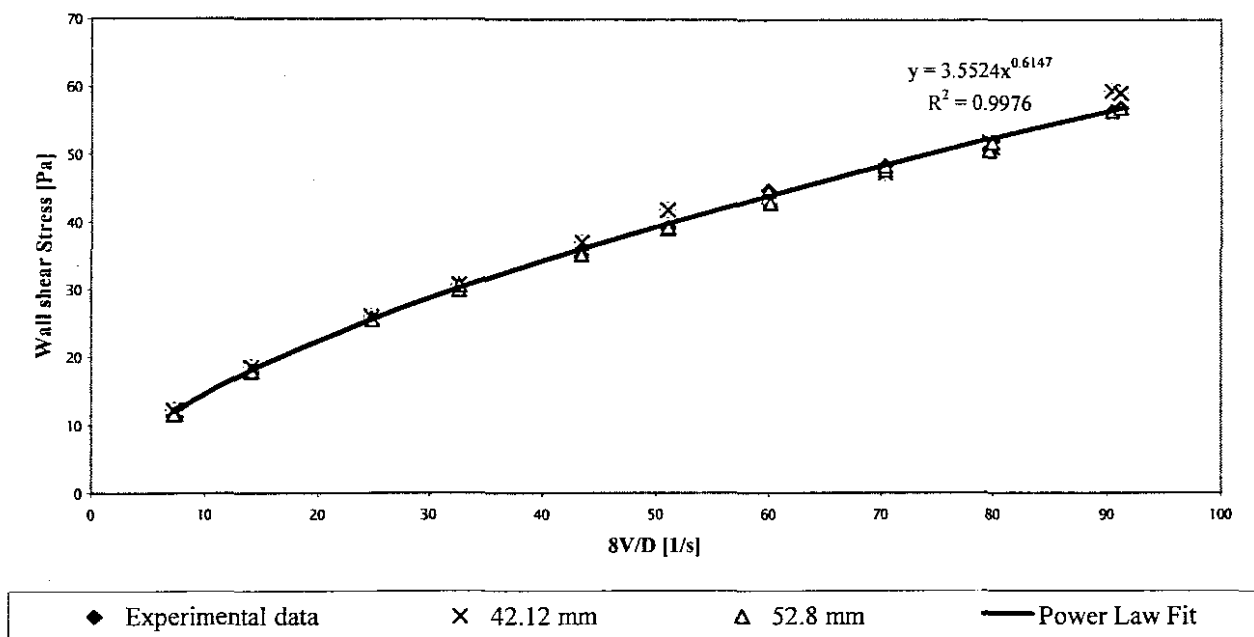


Figure 13 Rheogram CMC 8%

## CMC 8%

SLURRY PROPERTIES	
Date	08/11/2004
Slurry Relative Density	1037.5 kg/m <sup>3</sup>
Mass Concentration	8%
Fluid Consistency Index	8.68 Pa.s <sup>n</sup>
Flow Behaviour Index	0.54

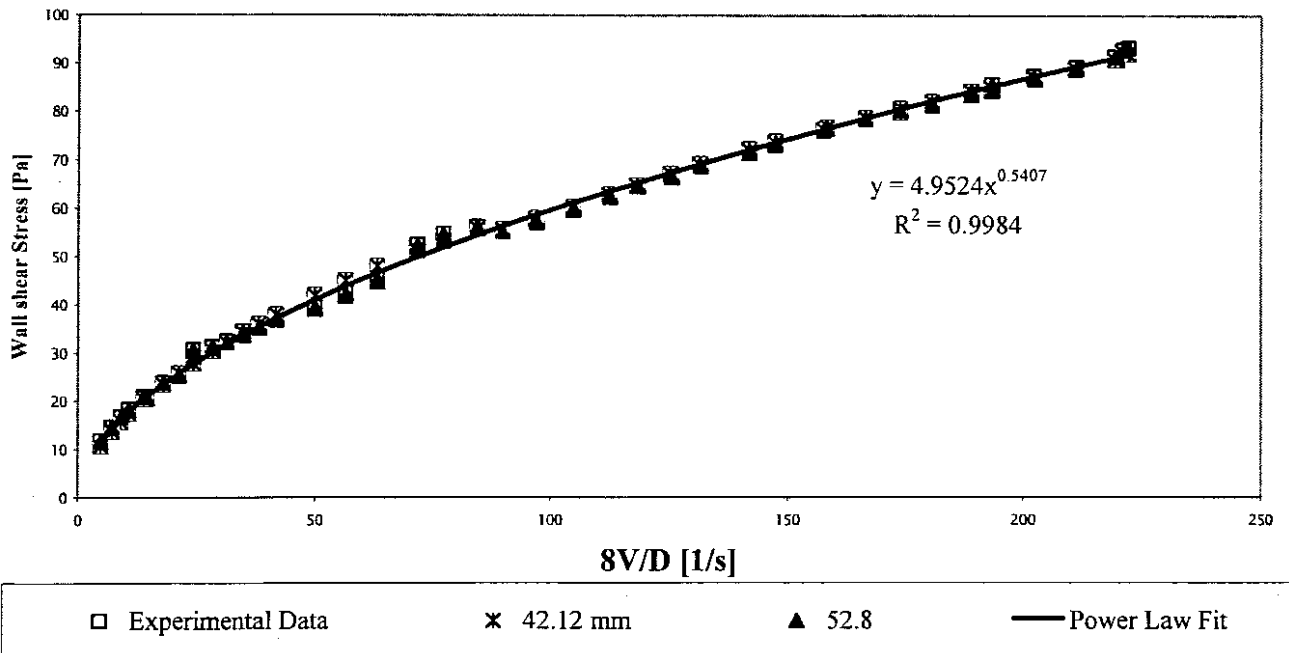


Figure 14 Rheogram CMC 8%

CMC 8%

SLURRY PROPERTIES	
Date	10/11/2004
Slurry Relative Density	1044 kg/m <sup>3</sup>
Mass Concentration	8%
Fluid Consistency Index	10.29 Pa.s <sup>n</sup>
Flow Behaviour Index	0.53

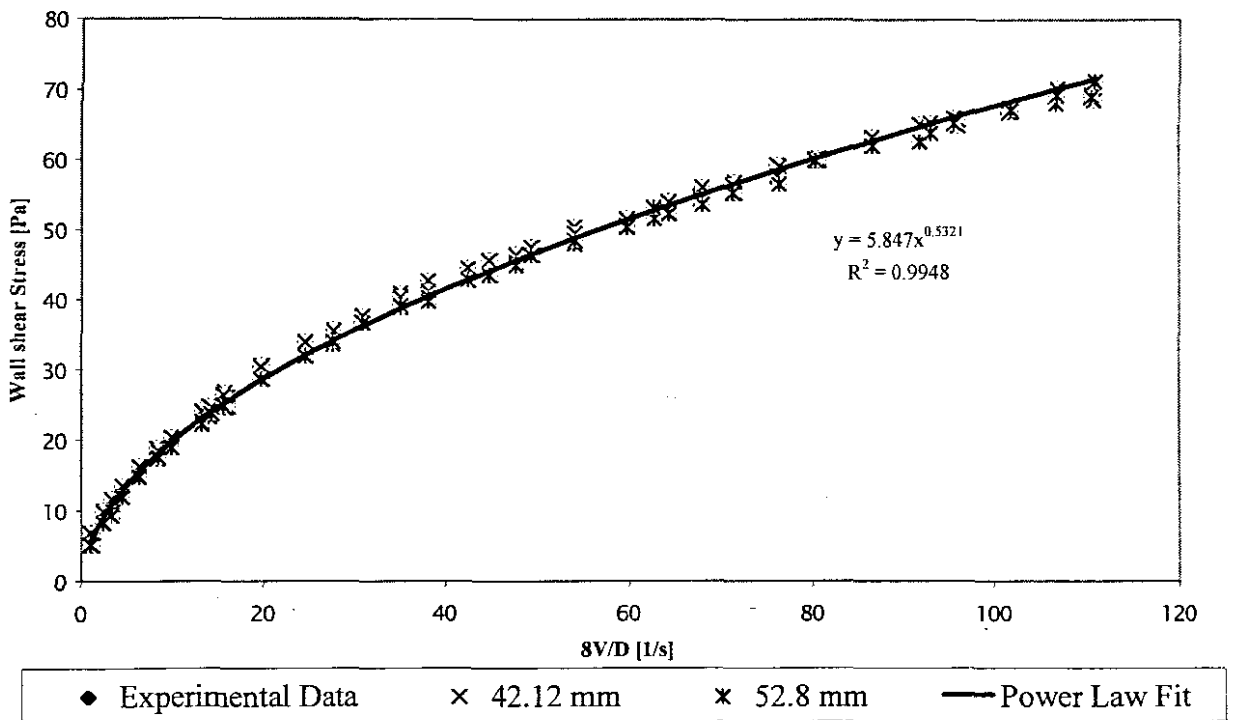


Figure 15 Rheogram CMC 8%

## KAOLIN 10%

SLURRY PROPERTIES	
Date	20/08/2004
Slurry Relative Density	1163.4kg/m <sup>3</sup>
Mass Concentration	10%
Yield stress	10 Pa
Fluid Consistency Index	3.15 Pa.s <sup>n</sup>
Flow Behaviour Index	0.240

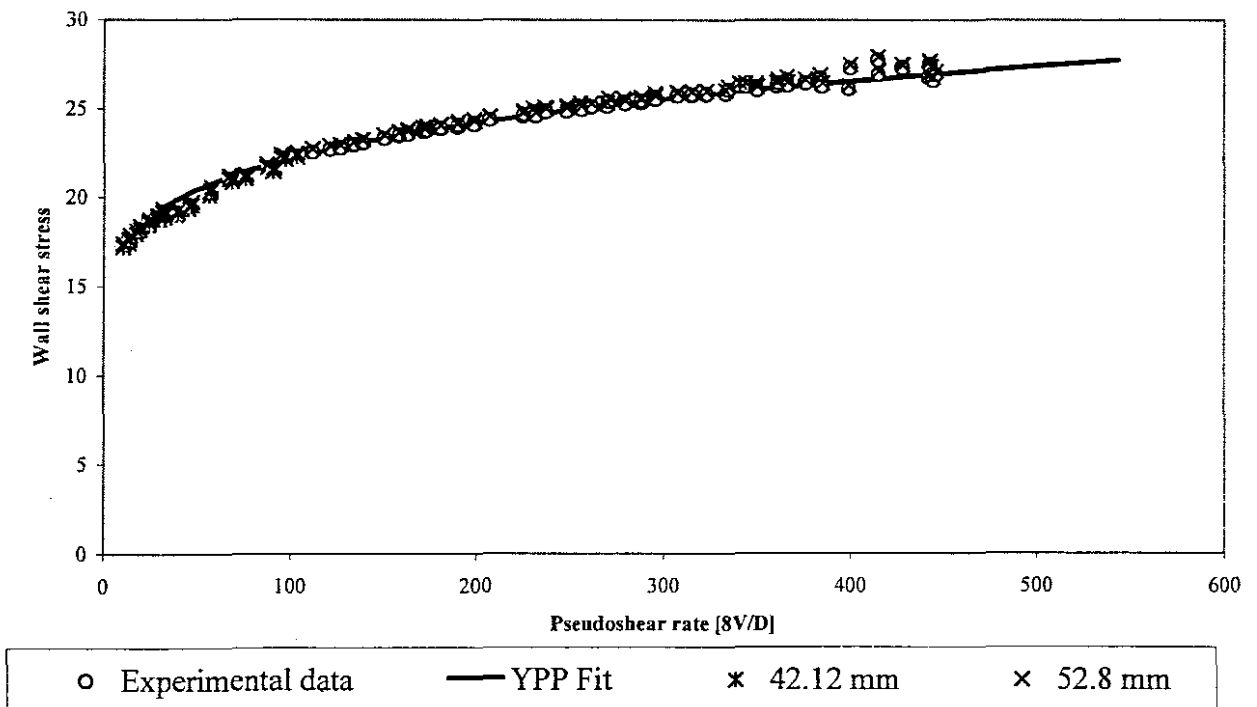


Figure 16 Rheogram kaolin 10%

## KAOLIN 10%

SLURRY PROPERTIES	
Date	11/08/2004
Slurry Relative Density	1172.4kg/m <sup>3</sup>
Mass Concentration	10%
Yield stress	10.7 Pa
Fluid Consistency Index	2.2 Pa.s <sup>n</sup>
Flow Behaviour Index	0.32

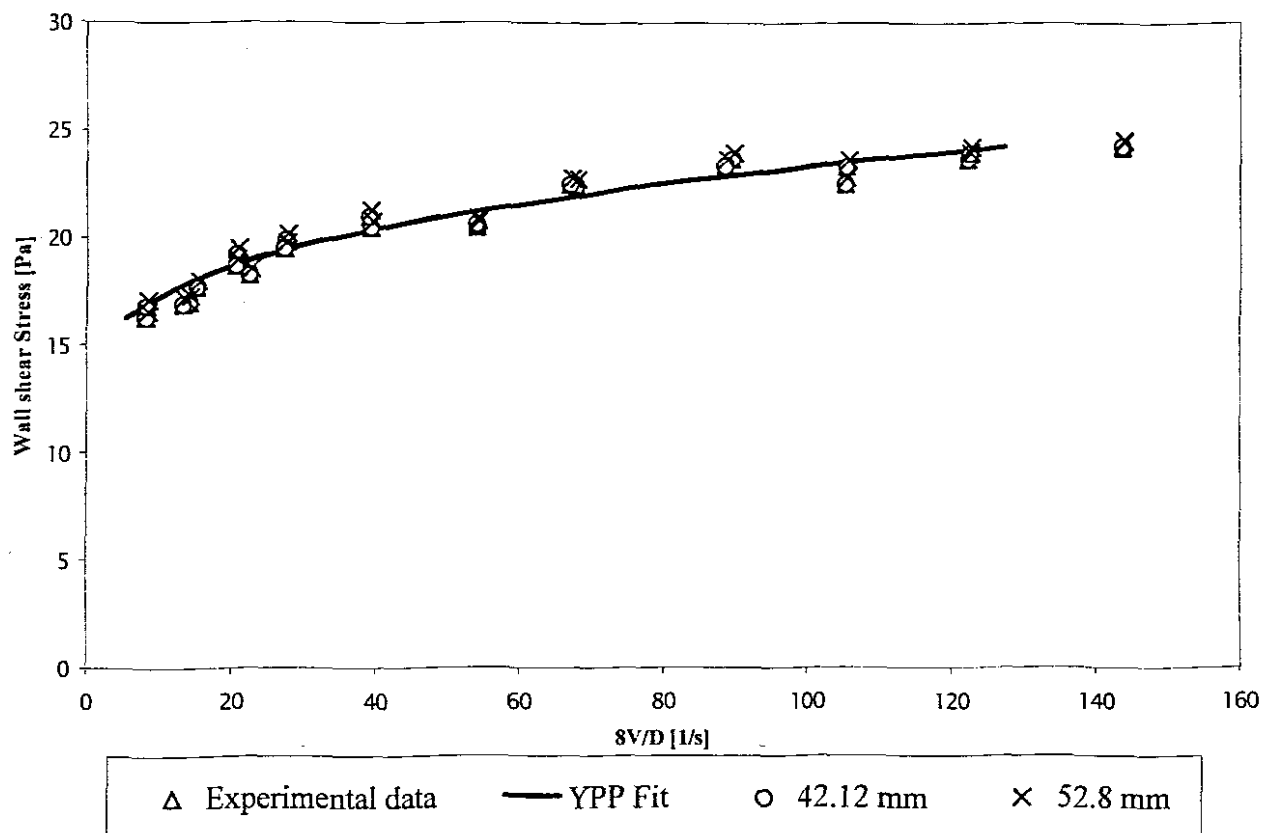


Figure 17 Rheogram kaolin 10%

## KAOLIN 13%

SLURRY PROPERTIES	
Date	30/09/2004
Slurry Relative Density	1214 kg/m <sup>3</sup>
Mass Concentration	13 %
Yield stress	35 Pa
Fluid Consistency Index	0.8 Pa.s <sup>n</sup>
Flow Behaviour Index	0.5

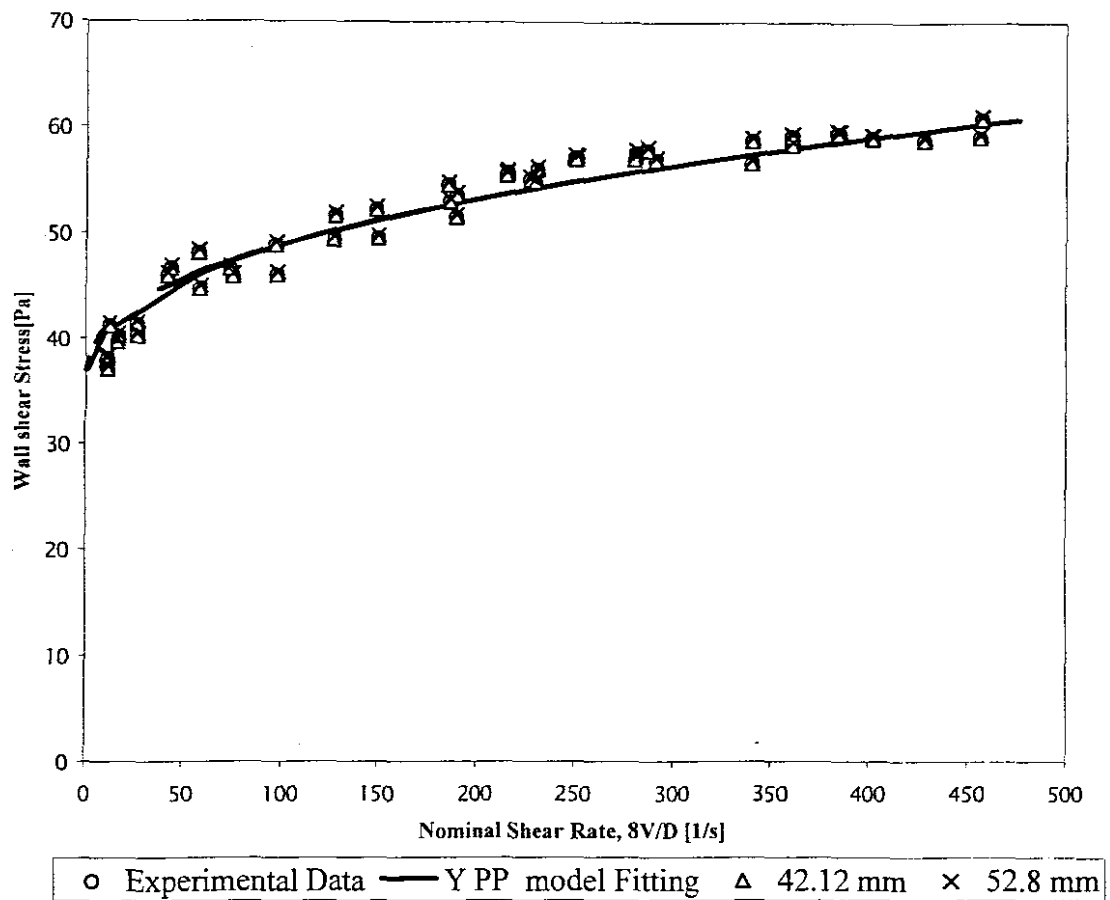


Figure 18 Rheogram kaolin 13%

## KAOLIN 13%

SLURRY PROPERTIES	
Date	07/10/2004
Slurry Relative Density	1210.2 kg/m <sup>3</sup>
Mass Concentration	13 %
Yield stress	35 Pa
Fluid Consistency Index	0.55 Pa.s <sup>n</sup>
Flow Behaviour Index	0.5

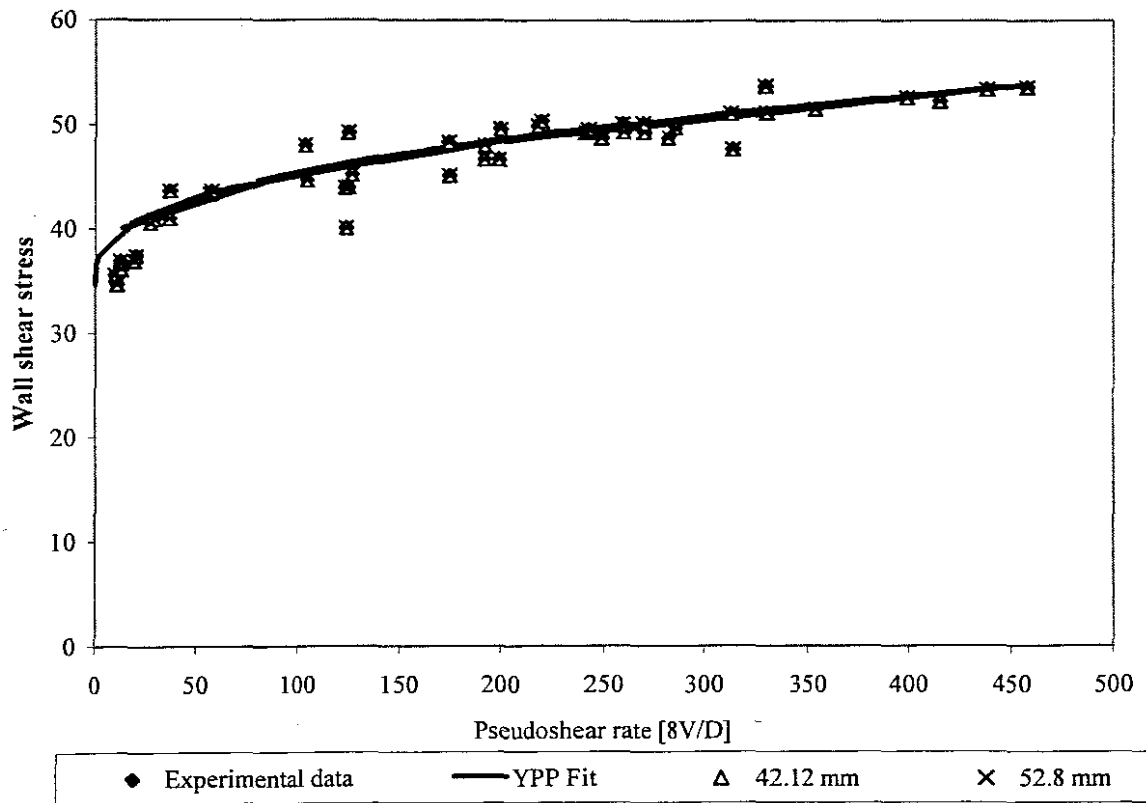
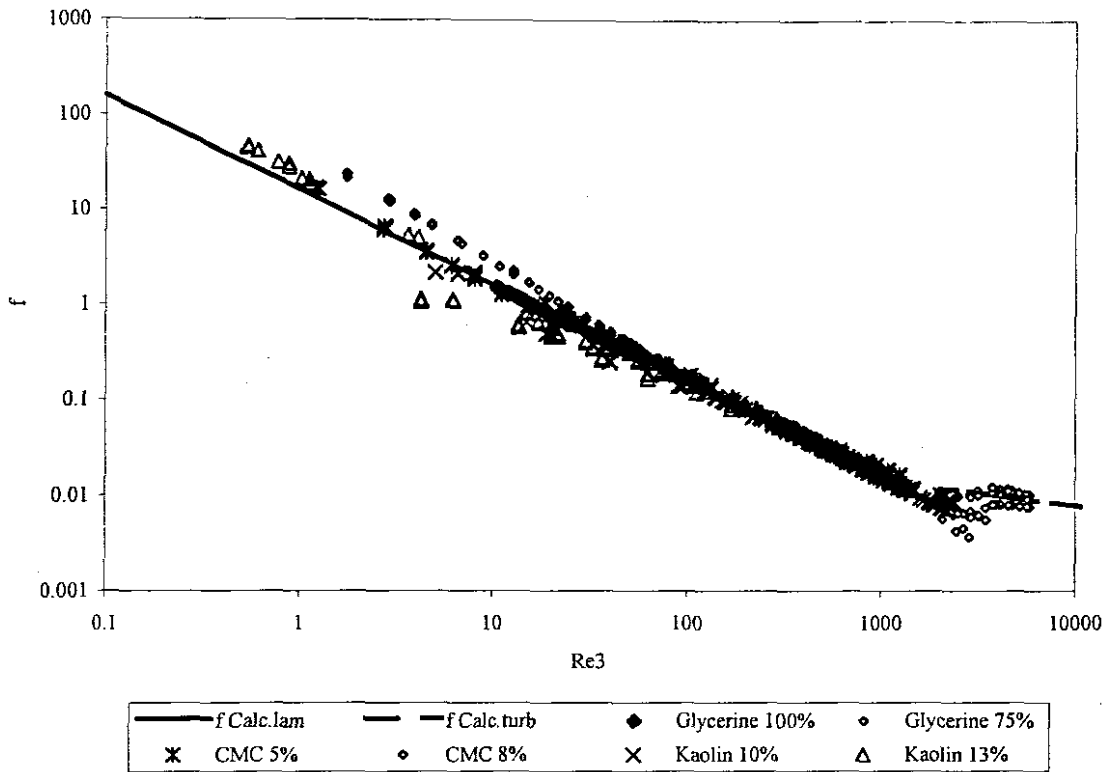


Figure 19 Rheogram kaolin 13%



**APPENDIX 4**  
**COMPARISON OF EXPERIMENTAL VALUES**  
**OF THE FRICTION FACTOR TO THE**  
**THEORETICAL VALUES FOR DIFFERENT**  
**FLUIDS IN STRAIGHT PIPE (f – Re GRAPHS)**



**Figure 20 Comparison of experimental values of the friction factor with the theoretical line for different fluids in straight pipe of Diameter 52.8 mm ID pipe**

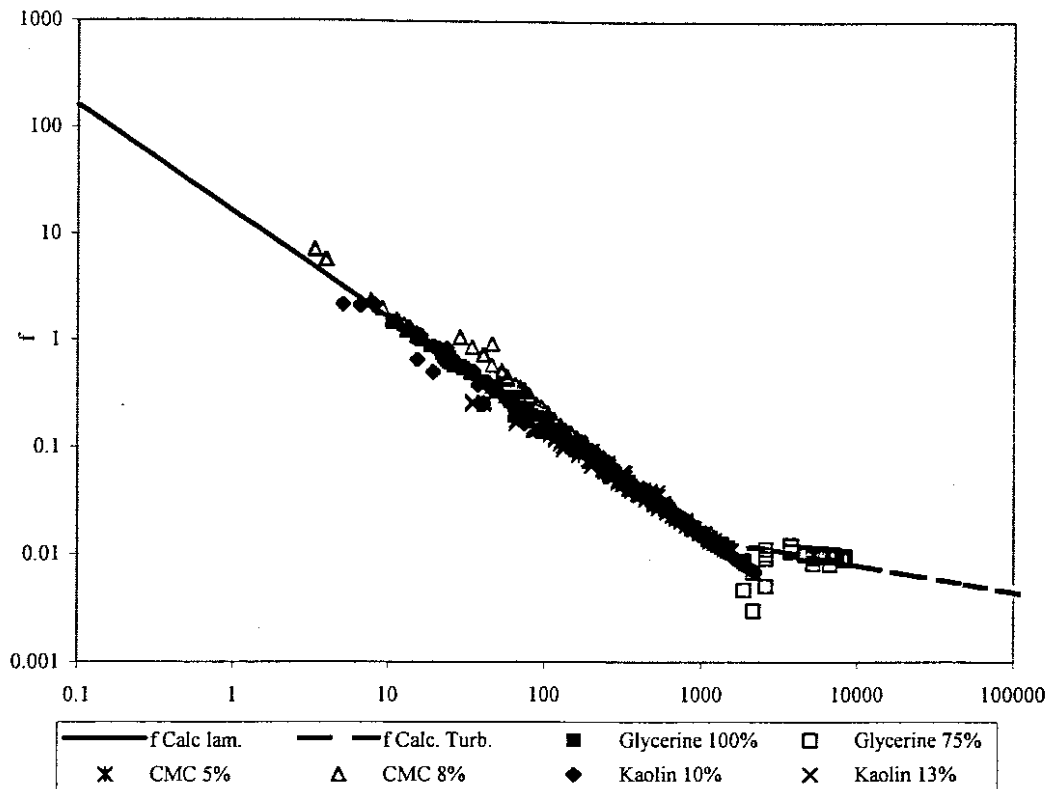


**Figure 21 Comparison of experimental values of the friction factor with the theoretical line for different fluids in straight pipe of Diameter 63.08 mm ID pipe**

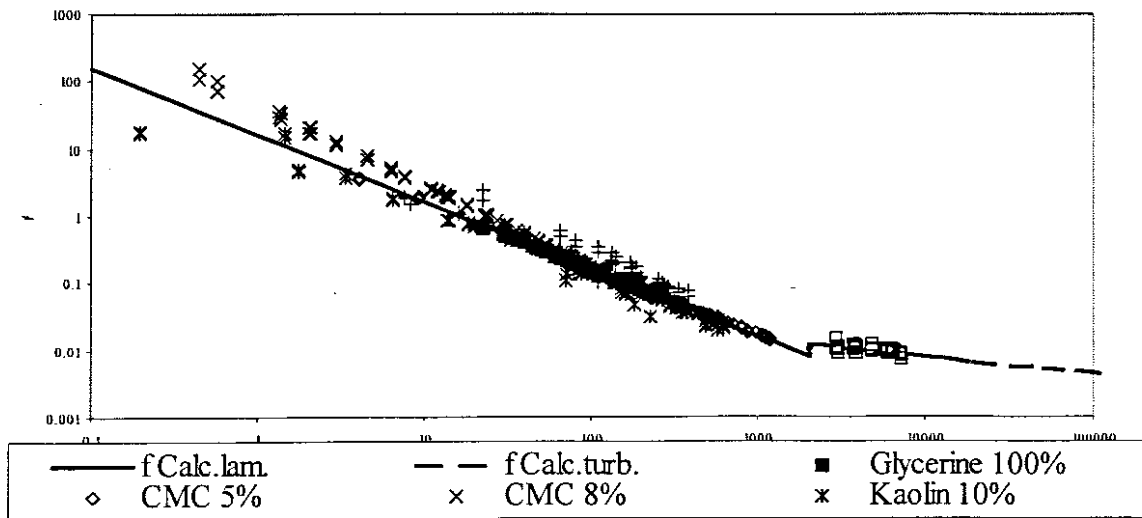


**Figure 22 Comparison of experimental values of the friction factor with the theoretical line for different fluids in straight pipe of Diameter 80.43 mm ID pipe**

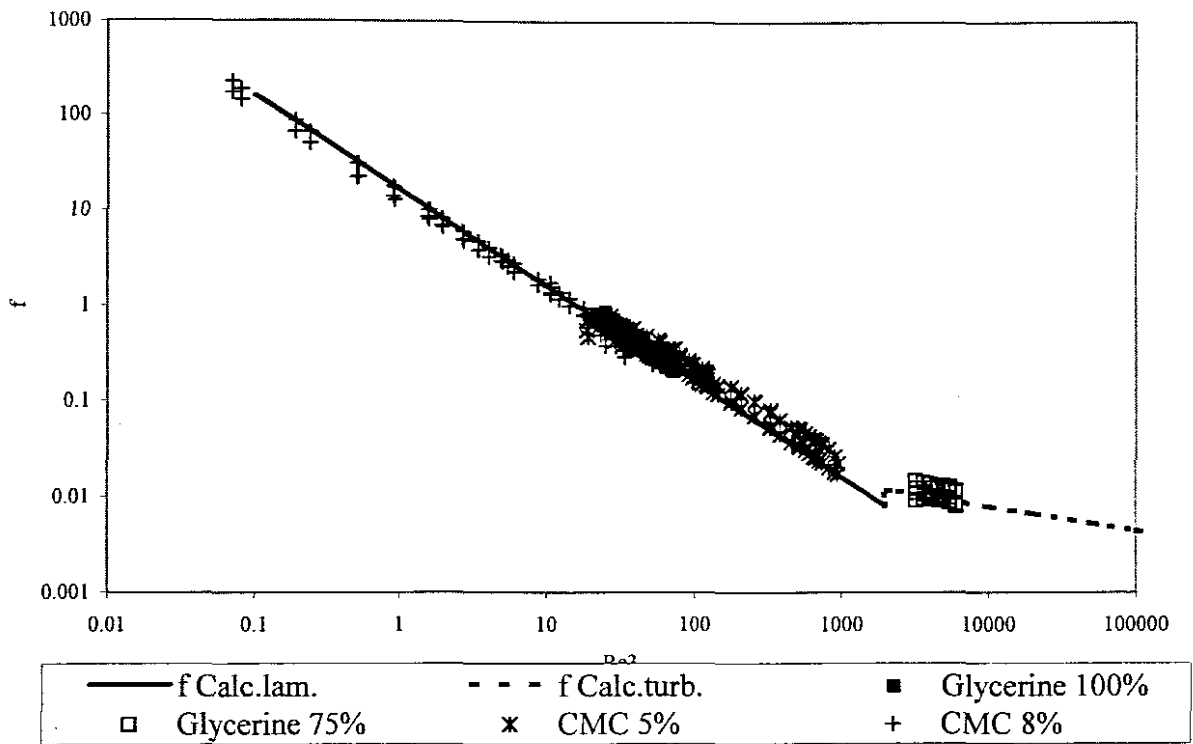


**Figure 23 Comparison of experimental values of the friction factor with the theoretical line for different fluids in straight pipe of Diameter 97.17 mm ID pipe**

## **APPENDIX 5**

**Calculation of the apparent fluid consistency index ( $K'$ ) and the apparent flow behaviour index ( $n'$ ) for a yield pseudoplastic fluid**

It has been demonstrated that for the laminar flow of any given time independent fluid,  $8V/D$  is some function of  $\tau_o$  only. This may be expressed as (Metzner & Reed, 1955):

$$\tau_o = K' \left( \frac{8V}{D} \right)^{n'} \quad (2.23)$$

To derive the relationship between  $K'$  and  $n'$  and the parameters characterising the Herschel – Bulkley model ( $\tau_y$ ,  $K$  and  $n$ ). It must be proceeded as follows:

For a yield Pseudoplastic fluid:

$$\frac{32Q}{\pi D^3} = \frac{8V}{D} = \frac{4n}{K^n \tau_o^3} (\tau_o - \tau_y)^{1+n} \left[ \frac{(\tau_o - \tau_y)^2}{1+3n} + \frac{2\tau_y(\tau_o - \tau_y)}{1+2n} + \frac{\tau_y^2}{1+n} \right] \quad (2.42)$$

(2.42) In logarithmic form:

$$\text{Log} \left( \frac{8V}{D} \right) = \text{Log} 4n - \frac{1}{n} \text{Log} K - 3 \text{Log} \tau_o + \frac{1+n}{n} \text{Log} (\tau_o - \tau_y) + \text{Log} \left[ \frac{(\tau_o - \tau_y)^2}{1+3n} + \frac{2\tau_y(\tau_o - \tau_y)}{1+2n} + \frac{\tau_y^2}{1+n} \right] \quad (1)$$

Differentiating (1) with respect to  $d(\text{Log} \tau_o)$ :

$$\frac{d(\text{Log} 8V/D)}{d(\text{Log} \tau_o)} = \frac{-3d(\text{Log} \tau_o)}{d(\text{Log} \tau_o)} + \frac{1+n}{n} \frac{d[\text{Log}(\tau_o - \tau_y)]}{d(\text{Log} \tau_o)} + \frac{d \left\{ \text{Log} \left[ \frac{(\tau_o - \tau_y)^2}{1+3n} + \frac{2\tau_y(\tau_o - \tau_y)}{1+2n} + \frac{\tau_y^2}{1+n} \right] \right\}}{d(\text{Log} \tau_o)} \quad (2)$$

By definition:

$$n' = \frac{d(\text{Log} \tau_o)}{d(\text{Log} 8V/D)} \quad (2.26)$$

$$\frac{1}{n'} = -3 + \left( \frac{1+n}{n} \right) \frac{(\tau_o - \tau_y)}{\tau_o} + \frac{d \left[ \frac{(\tau_o - \tau_y)^2}{1+3n} + \frac{2\tau_y(\tau_o - \tau_y)}{1+2n} + \frac{\tau_y^2}{1+n} \right]}{\frac{(\tau_o - \tau_y)^2}{1+3n} + \frac{2\tau_y(\tau_o - \tau_y)}{1+2n} + \frac{\tau_y^2}{1+n}} \tau_o d\tau_o$$

$$\frac{1}{n'} = -3 + \frac{1+n}{n} \frac{\tau_o}{\tau_o - \tau_y} + \frac{d \left[ \frac{(\tau_o - \tau_y)^2}{1+3n} \right] + d \left[ \frac{2\tau_y(\tau_o - \tau_y)}{1+2n} \right]}{\left[ \frac{(\tau_o - \tau_y)^2}{1+3n} + \frac{2\tau_y(\tau_o - \tau_y)}{1+2n} + \frac{\tau_y^2}{1+n} \right]} \tau_o d\tau_o$$

$$\frac{1}{n'} = -3 + \frac{1+n}{n} \frac{\tau_o}{\tau_o - \tau_y} + \frac{2\tau_o(1+n)(\tau_o + 2n\tau_o + n\tau_y)}{(1+n)(1+2n)(\tau_o - \tau_y)^2 + 2\tau_y(\tau_o - \tau_y)(1+n)(1+3n) + \tau_y^2(1+2n)(1+3n)}$$

$$n' = \frac{1}{-3 + \frac{1+n}{n} \frac{\tau_o}{\tau_o - \tau_y} + \frac{2\tau_o(1+n)(\tau_o + 2n\tau_o + n\tau_y)}{(1+n)(1+2n)(\tau_o - \tau_y)^2 + 2\tau_y(\tau_o - \tau_y)(1+n)(1+3n) + \tau_y^2(1+2n)(1+3n)}}$$

Knowing that (2.23):

$$\tau_o = K' \left( \frac{8V}{D} \right)^{n'}$$

$$K' = \frac{\tau_o}{\left( \frac{8V}{D} \right)^{n'}} \quad (3)$$

8V/D is obtained from (2.42) thus:

$$K' = \frac{\tau_o}{\left\{ \frac{4n}{K^n \tau_o^3} (\tau_o - \tau_y)^{1+n} \left[ \frac{(\tau_o - \tau_y)^2}{1+3n} + \frac{2\tau_y(\tau_o - \tau_y)}{1+2n} + \frac{\tau_y^2}{1+n} \right] \right\}^{n'}} \quad (4)$$

**APPENDIX 6**  
**DIAPHRAGM VALVE LOSS COEFFICIENTS**  
**DATA**



**Table 1 HGL Test for water**

		Actual distances	-2.928	-1.982	-1.08	-0.621	1.076	3.805	4.922	8.075	9.975	
		Valve plane	0									
			Post 1	Post 2	Post 3	Post 4	Post 5	Post 6	Post 7	Post 8	Post 9	Average flow rate
			Pa	Pa	Pa	Pa	Pa	Pa	Pa	Pa	Pa	(l/s)
8/26/2004												
Valve Type:	Diaphragm		25422.420	25370.820	25333.680	25325.035	24925.551	24846.567	24783.211	24730.654	24671.428	0.399
Valve diameter(mm):	40		29210.373	28652.701	28435.676	28430.006	26118.221	25732.986	25577.629	25110.270	24849.956	0.998
Valve position:	Open		31951.068	30924.297	30864.956	30541.863	26803.221	26524.543	25986.916	25305.529	24889.330	1.278
Pipe Diameter (mm):	42.12		33121.191	32330.000	32065.957	31819.010	27247.459	26928.650	26194.914	25386.479	24881.301	1.399
Material Type:	Water		32998.688	32141.656	31787.354	31513.516	27131.906	26404.985	26196.203	25287.555	24911.791	1.399
Density(kg/m <sup>3</sup> ):	998.168		30311.313	37240.516	36669.783	35778.594	28746.055	27466.680	27029.223	25701.256	24921.076	1.845
μ(Pa.s)	0.001		38735.848	36885.469	36935.902	36343.070	28711.830	27326.137	26971.115	25715.506	24903.078	1.843
			36659.160	35265.965	34925.863	34263.754	28106.793	27155.322	26687.824	25407.006	24925.410	1.689
			37895.117	35134.340	35114.160	34398.305	28081.170	27154.179	26708.029	25612.963	24929.164	1.690
			41795.206	40712.781	39999.180	39237.910	39597.057	28114.811	27555.818	25894.055	24923.552	2.088
			45225.105	43027.360	42869.086	41852.645	30217.894	28691.713	27834.230	25925.625	24923.764	2.262
			44769.449	43122.332	42179.859	41947.262	30277.929	28620.064	2784.045	25967.811	24920.666	2.263
			47383.648	45080.803	44148.457	43966.445	30794.482	28912.621	28119.379	26134.648	24818.777	2.390
			46923.475	44795.039	44453.102	43350.453	30741.254	28940.259	28188.730	26126.941	24824.646	2.365
			52360.129	50253.145	48877.172	47970.352	31985.020	29961.178	28975.201	26361.934	24770.211	2.654
			51918.176	49618.617	48367.438	47975.195	32031.621	28849.234	28808.674	26342.473	24811.520	2.655
			55729.840	52634.516	51701.715	50179.496	32893.940	30364.527	29255.449	26320.000	24754.729	2.821
			61368.316	57257.277	56084.102	54659.246	34125.266	31270.990	29994.441	26278.881	24628.789	3.066
			60953.195	57396.203	56491.238	55275.703	33802.891	31325.462	29979.996	26247.529	24709.889	3.071
			64498.652	59518.105	58428.677	57296.496	34913.445	31717.910	30326.510	26709.295	24984.534	3.189
			64333.145	59783.797	58895.639	57532.366	34742.504	31396.764	30368.424	26826.143	24693.738	3.158
			67896.047	63543.531	63131.363	59688.008	35333.965	32212.441	30877.365	26875.984	24602.736	3.095

**Table 2 HGL Test for water**

		Actual distances	-6.298	-4.568	-2.932	-0.421	1.076	3.805	6.046	8.075	9.975	
		Valve plane	0									
			Post 1	Post 2	Post 3	Post 4	Post 5	Post 6	Post 7	Post 8	Post 9	Average flow rate
			Pa	Pa	Pa	Pa	Pa	Pa	Pa	Pa	Pa	(l/s)
9/6/2004												
Valve Type:	Diaphragm		48818.879	48029.887	46661.641	43876.102	30910.443	28692.355	27011.764	25694.109	24170.645	2.506
Valve diameter(mm):	40		34063.238	33249.430	32865.410	32158.502	27196.666	26310.428	25627.730	25018.281	24423.135	1.531
Valve position:	Open		33968.191	33079.547	32828.633	32381.080	23144.697	26317.518	25598.857	25012.148	24433.264	1.531
Pipe Diameter (mm):	42.12		49139.802	48055.477	46800.926	44174.340	30742.078	28693.281	27113.613	25597.291	24228.469	2.508
Material Type:	Water		40425.188	38722.496	36575.906	33984.008	33172.316	30516.070	28101.879	25877.477	23990.336	3.066
Density(kg/m <sup>3</sup> ):	998.168		61345.613	58289.824	56928.938	54127.025	33406.348	30460.123	28777.633	25962.796	23949.918	3.059
μ(Pa.s)	0.001		60164.125	59055.547	56456.980	53964.434	33070.824	30481.990	27891.803	25937.291	24022.473	3.055
			71175.773	68906.813	66917.617	63522.059	35714.203	32180.941	28955.652	26226.887	23638.166	3.2945
			71477.359	68975.070	66304.738	63780.168	35990.270	32101.771	28925.916	26326.426	23700.271	3.3547
			66249.234	63758.023	62228.956	58991.887	34594.098	31331.447	28506.979	26124.986	23759.164	3.3239
			45422.516	44046.652	43021.746	41487.438	29831.701	28325.964	26681.223	25582.987	24394.379	2.5147
			45916.496	43945.051	43366.520	41468.195	29807.389	28344.027	26525.979	25499.396	24402.602	2.5108

**Table 3 HGL Test for water**

		Axial distance	-6.574	-5.47	-3.526	-1.531	0.510	2.509	4.108	7.666	9.669	
		Valve plane	0									
			Pod 1	Pod 2	Pod 3	Pod 4	Pod 5	Pod 6	Pod 7	Pod 8	Pod 9	Average Flow rate
			Pa	Pa	Pa	Pa	Pa	Pa	Pa	Pa	Pa	[m <sup>3</sup> /s]
1022/2004												
Valve Type:	Diaphragm		27027.016	26554.324	25816.590	24955.076	21959.906	21104.988	20095.535	18824.057	17947.473	3.364
Valve dimension (mm):	SU		27020.516	26554.691	25764.768	24934.822	21952.357	21099.781	20107.975	18775.346	17983.203	3.366
Valve position:	Open		26981.307	26557.549	25789.709	24923.801	21915.744	21086.330	20062.646	18806.959	17949.723	3.362
Pipe Diameter (mm):	52.8		26506.496	26117.826	25334.639	24572.426	21734.582	20914.971	19923.252	18760.678	17956.504	3.261
Material Type:	Water		26521.672	26101.045	25340.967	24556.648	21765.219	20925.686	19950.834	18733.744	17951.438	3.263
Density (kg/m <sup>3</sup> ):	1000		26567.320	26082.611	25366.219	24534.541	21741.629	20937.760	19942.316	18751.393	17922.045	3.262
$\mu$ (Pa.s)	0.001		25304.740	24828.469	24332.531	23600.506	21217.691	20500.797	19703.016	18659.057	17959.084	3.001
			25317.482	24970.197	24357.303	23609.375	21178.895	20539.805	19741.775	18636.688	17958.053	2.958
			25316.420	24899.113	24352.377	23647.768	21239.559	20517.795	19727.799	18715.518	17937.951	2.996
			24485.859	24065.131	23574.258	22994.271	20833.078	20222.117	19514.537	18392.275	18000.740	2.782
			24439.379	24114.223	23507.195	22972.504	20845.736	20240.672	19537.439	18626.559	18008.959	2.780
			27846.451	27595.910	27312.287	26991.985	25904.426	25566.473	25159.928	24676.113	24356.564	1.970
			27830.469	27612.133	27325.272	26986.084	25978.635	25550.133	25153.826	24645.221	24345.722	1.969
			27345.834	27109.344	26883.025	26585.656	25719.340	25451.123	25110.818	24729.537	24421.635	1.782



Table 5 HGL Test for water

		Axial distances									Average Flow rate
		-6.574	-5.47	-3.526	-1.531	0.510	2.509	4.108	7.666	9.669	
Valve plane		0									
		Pod 1	Pod 2	Pod 3	Pod 4	Pod 5	Pod 6	Pod 7	Pod 8	Pod 9	
		Pa	Pa	Pa	Pa	Pa	Pa	Pa	Pa	Pa	
7/26/2004	Diaphragm	22971.986	22398.451	21400.523	20673.412	17215.684	16438.914	15334.930	13990.175	12870.327	3.745
	SD	22706.262	22340.500	21617.924	21141.996	17422.764	16400.949	15419.493	13887.534	13093.213	3.370
	Open	23291.186	22847.582	21169.932	21184.250	17293.152	16390.524	15254.767	13883.954	12931.680	3.370
	52.8	23324.244	22783.232	22074.127	21078.736	17365.361	16478.965	15298.732	13998.975	12743.926	3.370
	Water	22537.080	22101.307	21305.047	20791.676	16965.803	15989.448	14753.324	13783.982	12839.436	3.351
	1.000	22444.977	21898.033	21251.283	20278.891	16976.381	16124.182	15055.616	13804.682	13033.058	3.330
	0.001	22429.033	21992.670	21089.145	20439.637	16998.756	16102.568	15145.691	13711.912	12988.233	3.346
		22296.422	21863.727	21266.447	20134.771	16990.615	16106.790	15029.941	13736.907	12911.374	3.346
		22162.143	21597.865	20966.408	19970.467	16843.166	15930.409	14972.507	13743.753	13028.585	3.280
		21903.293	21619.308	20789.643	20197.023	16823.576	15868.709	15041.447	13919.804	12863.631	3.277
		21992.926	21665.340	20943.539	20072.473	16606.285	15942.404	14944.707	13588.503	13003.673	3.276
		21291.215	20739.537	20243.250	19357.830	16578.037	15552.183	14865.177	13655.730	13051.879	3.136
		21251.691	20893.557	20019.098	19530.186	16484.084	15811.451	14864.969	13707.096	13086.545	3.133
		21320.574	21015.986	20136.191	19253.279	16108.084	15856.821	14773.875	13700.261	12968.193	3.139
		21068.630	20741.480	20164.473	19724.609	16386.059	15713.844	14833.628	13866.763	13075.282	3.066
		21017.766	20718.230	20068.494	19142.056	16728.429	15632.257	14889.778	13805.004	13083.026	3.063
		20481.008	20104.688	19363.949	18853.811	16049.584	15431.947	14700.102	13794.312	13136.705	2.940
		20495.887	21138.855	19488.236	18809.236	16378.427	15493.828	15211.053	14110.018	13435.672	2.940
		20718.053	20310.732	20640.742	20499.433	21636.320	20852.293	19888.521	18741.174	17937.352	3.221
		20808.30273	20341.94141	20647.40623	20884.16797	21647.73438	20833.36443	19882.28966	18649.79047	17939.99803	3.225
		20741.37109	20300.43672	20654.13672	20871.44727	21629.27794	20871.21875	19946.16797	18731.13281	17936.69141	3.223
		20355.55469	20021.88086	20341.30469	20573.10547	21533.73863	20747.39297	19823.98673	18697.74023	17913.39648	3.148
		20369.13281	20583.13477	20333.45117	20599.20703	21526.43751	20760.6875	19828.23977	18750.77734	17961.75586	3.147
		20444.09766	20030.4375	20377.55664	20421.35742	21528.59961	20784.72077	19803.64648	18714.35136	17933.93399	3.130
		20384.16902	20697.66406	20642.23242	20415.64648	21401.00781	20844.50977	19746.75195	18661.30078	17965.52344	3.078
		20117.69336	20715.13672	20381.52734	20396.67188	21338.99219	20639.03125	19758.11133	18694.1875	17955.41797	3.081
		20092.64063	20745.56914	20123.01758	20444.56289	21333.76172	20617.64684	19758.06836	18685.5293	17962.22617	3.078
		20364.36719	20293.83203	20879.93753	20390.21094	20333.77794	19839.72442	19261.10742	18536.72852	17953.38867	2.777
		20361.37695	20315.17773	20365.55664	20292.7832	20363.59844	19836.3437	19243.98438	18518.17188	18025.24414	2.500
		20369.86469	20372.37891	20260.82303	20423.07617	20368.21484	19830.09375	19278.98438	18543.30078	17993.83008	2.499
		20376.95703	20329.33352	20071.86139	20299.89063	20380.89648	19833.29102	19257.26492	18543.04102	18019.91622	2.501
		20193.04297	21743.15625	21447.86664	21232.86133	19703.08594	22164.23828	23140.78316	24653.92984	24318.15039	2.033
		20910.4707	20798.7591	20493.98242	20178.32031	20668.09961	23388.85347	23167.89453	24660.60347	24310.15625	1.989

Table 6 HGL Test for water

		Axial distances									Average Flow rate
		-6.574	-5.47	-3.526	-1.531	0.510	2.509	4.108	7.666	9.669	
Valve plane		0									
		Pod 1	Pod 2	Pod 3	Pod 4	Pod 5	Pod 6	Pod 7	Pod 8	Pod 9	
		Pa	Pa	Pa	Pa	Pa	Pa	Pa	Pa	Pa	
7/21/2004	Diaphragm	20226.084	20074.990	19559.703	19051.146	17129.870	16603.969	16020.906	15119.037	14564.332	2.929
	SD	20235.271	20090.053	19581.205	19085.551	17242.803	16602.684	15967.844	15152.481	14600.640	2.626
	Open	20728.547	20304.441	19700.678	18966.889	16560.080	15876.600	15030.644	14006.127	13330.940	2.978
	52.8	20151.748	20684.809	20047.904	20237.826	21630.098	20830.285	19909.504	18785.623	18027.244	3.162
	Water	20136.199	20700.160	20054.948	20304.467	21579.270	20816.016	19965.566	18954.387	18047.365	3.161
	1.000	20362.307	20484.879	20736.867	20916.135	21989.830	21131.779	20103.127	18885.787	18052.492	3.347
	0.001	20971.789	20512.893	20736.166	20931.672	22093.234	21098.266	20117.100	18866.141	18008.234	3.344

Table 7 HGL Test for water

		Axial distances	-4.9735	-4.8855	-2.985	-0.937	0.987	1.968	2.938	3.916	4.898	
		Valve plane	0									
			Post 1	Post 2	Post 3	Post 4	Post 5	Post 6	Post 7	Post 8	Post 9	Average Flow rate
			Pa	Pa	Pa	Pa	Pa	Pa	Pa	Pa	Pa	[l/s]
8/31/2004			41743.625	40037.028	38688.945	36258.840	32203.672	31478.678	30592.266	29404.285	28541.893	7.409
Valve Type:	Diaphragm		41704.305	40197.570	38558.910	36925.316	32343.287	31522.492	30678.304	29785.744	28929.701	7.199
Valve dimension(mm):	65		40987.672	39529.586	38078.188	36529.176	31897.832	31377.508	30443.893	29536.664	28997.797	7.008
Valve position:	Open		41080.441	39524.426	37893.039	36367.953	32032.348	31700.935	30576.304	29748.855	28976.885	7.016
Pipe Diameter (mm):	63.08		39563.693	38386.121	36914.457	35444.125	31303.635	30802.850	30101.164	29227.527	28655.979	6.812
Material Type:	Water		39558.242	38188.152	36721.555	35364.613	31211.939	30738.867	30027.240	29224.670	28667.064	6.787
Density(kg/m <sup>3</sup> ):	1000		37923.344	36675.856	35619.215	34240.406	30648.289	30162.900	29493.036	28822.725	28279.357	6.304
μ (Pa.s):	0.001		38041.777	36804.984	35498.484	34246.598	30628.260	30063.072	29569.838	28757.279	28055.242	6.452
			36561.977	35401.859	34367.363	33155.020	30025.697	29579.458	29007.248	28378.848	27926.299	5.915
			36479.781	35479.707	34340.332	33072.316	30003.625	29587.076	29131.602	28419.928	27918.949	5.915
			35479.602	34139.922	33026.133	31999.111	29172.730	29030.529	28763.936	28057.697	27588.223	5.513
			35672.766	34432.129	33373.500	32523.559	29619.600	29029.994	28535.176	27790.987	27565.838	5.555
			33733.707	32927.967	32026.678	31276.553	28885.234	28465.203	28044.586	27569.033	27229.588	5.095
			35096.258	34261.836	33213.223	32535.182	29997.244	28932.900	28456.979	27919.238	27541.357	5.388
			36567.781	37216.410	35947.199	34592.790	30794.285	31035.174	29566.475	28888.584	28317.861	6.230
			38666.336	37300.941	35995.184	34738.254	30707.039	30314.645	29700.211	28830.471	28325.133	6.461
			32793.695	32030.721	31294.648	30633.000	28516.674	28230.781	27789.934	27341.633	27024.486	4.678
			32772.895	32026.834	31348.973	30621.859	28493.441	28208.994	27759.572	27362.300	27001.717	4.772
			30093.021	30373.441	29785.768	29247.875	27690.893	27398.500	27152.455	26742.232	26565.230	4.047
			30951.299	30406.459	29747.129	29271.129	27651.127	27458.299	27140.888	26803.664	26530.248	4.387
			30077.727	29174.379	28307.408	28496.010	26742.137	26976.152	26776.969	26574.789	26198.531	3.575
			28400.461	28297.152	28318.787	27432.230	26534.969	26244.025	26397.459	26226.047	25904.549	3.054

Table 8 HGL Test for water

		Axial distances	-4.9735	-4.8855	-2.985	-0.937	0.987	2.938	6.427	8.432	10.433	
		Valve plane	0									
			Post 1	Post 2	Post 3	Post 4	Post 5	Post 6	Post 7	Post 8	Post 9	Average Flow rate
			Pa	Pa	Pa	Pa	Pa	Pa	Pa	Pa	Pa	[l/s]
9/1/2004			30167.082	29716.779	29233.262	28791.922	28043.443	27438.828	26782.660	26159.498	25962.713	3.448
Valve Type:	Diaphragm		30129.354	29659.977	29262.818	28868.684	27811.785	27413.387	26653.832	26131.473	25882.473	3.400
Valve dimension(mm):	65		29276.469	29071.492	28591.520	28346.387	27423.410	27072.646	26497.652	26185.646	25936.875	3.099
Valve position:	Open		29405.838	29131.105	28735.424	28316.303	27230.699	27076.668	26479.938	26125.877	25860.398	3.105
Pipe Diameter (mm):	63.08		26657.969	28446.625	28118.432	27818.496	26966.361	26699.445	26260.439	25984.320	25713.879	2.840
Material Type:	Water		28704.150	28468.609	28156.422	27829.914	26990.305	26729.574	26272.996	25986.520	25728.561	2.806
Density(kg/m <sup>3</sup> ):	1000		27827.508	27922.379	27310.988	27108.141	26519.752	26245.023	25931.418	25742.039	25552.451	2.419
μ (Pa.s):	0.001		27757.119	27511.926	27315.123	27088.592	26444.875	26236.230	25938.730	25748.168	25540.598	2.432

Table 9 HGL Test for water

		Axial distances	-4.413	-4.809	-3.61	-1.629	0.707	3.907	5.273	8.461	9.956	
		Valve plane	0									
			Pod 1	Pod 2	Pod 3	Pod 4	Pod 5	Pod 6	Pod 7	Pod 8	Pod 9	Average Flow rate
			$P_a$	$P_a$	$P_a$	$P_a$	$P_a$	$P_a$	$P_a$	$P_a$	$P_a$	[l/s]
9/2/2004												
Valve Type:	Diaphragm		30067.029	29782.479	29574.584	29302.188	27260.092	26637.363	26427.219	25911.689	25660.918	5.205
Valve dimension[mm]:	80		30134.840	29864.680	29555.357	29304.630	27236.953	26632.123	26410.533	25897.572	25610.858	5.794
Valve position:	Open		30865.742	30397.066	30365.758	29921.531	27678.547	26910.557	26639.168	26024.574	25703.859	6.348
Pipe Diameter [mm]:	80.43		30862.248	30560.795	30272.602	29958.734	27595.387	26956.611	26393.119	26036.449	25686.193	6.358
Material Type:	Water		31424.305	31117.543	30854.982	30406.789	27819.452	27047.965	26717.838	26119.143	25792.777	6.710
Density[kg/m <sup>3</sup> ]:	1000		31477.918	31156.646	30946.145	30436.697	27821.839	27043.674	26793.594	26091.391	25690.730	6.777
$\mu$ [Pas]	0.001		32205.871	31774.084	31485.051	31053.615	28121.430	27253.633	26953.383	26217.555	25834.980	7.071
			32217.982	31812.924	31622.941	31023.150	28156.673	27321.471	26964.361	26246.068	25832.391	7.106
			32475.205	32069.475	31815.406	31313.121	28236.713	27424.928	26976.665	26232.621	25880.000	7.287
			32638.033	32165.227	31784.451	31275.158	28203.762	27424.002	27157.240	26312.449	25887.314	7.374
			29623.381	29363.873	29025.773	28819.727	27172.277	26500.990	26267.943	25764.461	25531.248	5.509
			28846.039	28947.678	28925.668	28481.496	26527.369	26346.061	26204.568	25783.225	25548.630	5.034
			28465.943	28259.752	28125.084	28622.572	26929.625	26151.252	26367.354	25716.533	25492.707	5.060

Table 10 HGL Test for water

		Axial distances	-5.030	-3.042	-2.542	-0.659	0.700	2.502	4.499	5.010	9.511	
		Valve plane	0									
			Pod 1	Pod 2	Pod 3	Pod 4	Pod 5	Pod 6	Pod 7	Pod 8	Pod 9	Average Flow rate
			$\Delta P_1$	$\Delta P_2$	$\Delta P_3$	$\Delta P_4$	$\Delta P_5$	$\Delta P_6$	$\Delta P_7$	$\Delta P_8$	$\Delta P_9$	[l/s]
9/3/2004												
Valve Type:	Diaphragm		0.000	166.251	225.988	322.437	906.748	1082.156	1150.776	1288.432	1746.347	5.887
Valve dimension[mm]:	100		0.000	151.729	171.305	287.916	764.557	929.632	1005.829	1184.832	1516.251	5.435
Valve position:	Open		0.000	166.251	225.988	322.437	906.748	1082.156	1150.776	1288.432	1746.347	5.887
Pipe Diameter [mm]:	97.17		0.000	151.729	171.305	287.916	764.557	929.632	1005.829	1184.832	1516.251	5.435
Material Type:	Water		0.000	155.790	193.248	310.004	884.501	1042.963	1133.930	1299.233	1703.375	6.049
Density[kg/m <sup>3</sup> ]:	1000		0.000	154.829	190.267	315.252	872.469	1027.777	1109.162	1271.838	1666.576	6.231
$\mu$ [Pas]	0.001		0.000	191.250	244.539	438.661	1192.445	1460.317	1541.839	1795.408	2256.754	7.544
			0.000	200.328	255.964	416.423	1154.997	1419.388	1580.606	1761.222	2312.275	7.523
			0.000	161.388	228.687	336.323	1017.977	1161.300	1280.000	1406.000	1824.076	6.479
			0.000	168.149	238.525	334.903	1007.371	1166.319	1175.138	1256.300	1816.875	6.486
			0.000	133.181	167.850	278.615	771.873	989.247	1043.216	1184.969	1538.266	5.752
			0.000	130.200	165.772	284.277	809.628	966.235	1027.589	1228.711	1513.042	5.818
			0.000	113.453	138.128	247.796	695.706	830.520	956.820	1107.127	1384.777	5.487
			0.000	104.023	139.499	228.872	667.718	788.595	880.196	953.998	1258.127	5.235
			0.000	108.441	115.722	206.235	612.323	726.633	756.515	862.635	1117.548	4.930
			0.000	98.866	122.704	160.344	540.755	708.006	664.801	775.754	1045.117	4.654
			0.000	79.230	85.201	153.542	424.956	568.547	580.530	645.900	824.930	4.089
			0.000	67.545	91.088	152.964	452.389	518.834	504.992	623.558	785.434	4.052
			0.000	60.544	76.691	133.617	390.316	412.564	459.862	527.185	669.285	3.630
			0.000	56.954	52.685	79.169	226.871	234.558	340.440	308.430	436.598	2.771
			0.000	38.983	47.496	70.477	229.835	296.293	343.907	375.368	452.490	2.760

Table 11 HGL Test for Glycerine 100%

		Axial distances	-6.298	-4.568	-2.932	-0.832	1.076	2.685	6.046	8.075	9.975	
		Valve place	0									
			Pod 1	Pod 2	Pod 3	Pod 4	Pod 5	Pod 6	Pod 7	Pod 8	Pod 9	Average flow rate
Temperature	25.5°C		$\Delta P_1$	$\Delta P_2$	$\Delta P_3$	$\Delta P_4$	$\Delta P_5$	$\Delta P_6$	$\Delta P_7$	$\Delta P_8$	$\Delta P_9$	
22/11/2004			$P_a$	$P_a$	$P_a$	$P_a$	$P_a$	$P_a$	$P_a$	$P_a$	$P_a$	[ $\mu$ ]
Valve Type:	Diaphragm		0.000	3566.989	9385.270	15690.515	23742.049	28501.135	38159.688	43800.371	49239.543	0.261
Valve dimension(mm):	40		0.000	4983.221	9419.583	15602.231	23642.261	28448.000	37998.905	43590.023	49172.621	0.257
Valve position:	Open		0.000	5515.025	10347.409	16923.379	25809.309	30951.914	41369.375	47604.586	53510.551	0.282
Pipe Diameter (mm):	42.12		0.000	5491.529	10344.870	17047.236	25820.014	30912.056	41304.227	47422.051	53390.117	0.282
Material Type:	Glycerine 100%		0.000	5828.247	11000.604	18036.154	27402.451	32863.512	43817.535	50258.023	56723.956	0.300
Density(kg/m <sup>3</sup> ):	1270		0.000	5982.000	11007.419	18059.191	27399.125	32822.184	43786.066	50248.770	56599.543	0.300
$\mu$ (Pa.s)	0.842		0.000	6673.835	11966.745	19469.695	29645.465	35474.223	47422.441	54393.303	61246.707	0.326
			0.000	6710.753	11863.936	19427.084	29640.412	35406.996	47223.574	54220.051	61057.480	0.323
			0.000	6774.523	12571.463	20449.879	31283.898	37350.426	49795.711	57142.480	64262.912	0.343
			0.000	7099.193	12463.105	20439.814	31208.539	37174.871	49327.965	56777.559	63906.957	0.340
			0.000	7190.658	12007.282	21631.725	33156.527	39615.176	52640.094	60378.613	67918.984	0.363
			0.000	7394.890	12005.260	21576.014	33000.770	39498.543	52569.395	60214.898	67776.984	0.360
			0.000	7650.565	13769.910	22444.498	34504.277	41249.148	54811.594	62865.793	70736.086	0.375
			0.000	8018.901	13725.224	22407.020	34395.828	41132.813	54555.891	62641.145	70381.875	0.374
			0.000	7697.799	14127.473	22957.148	35631.859	42414.891	56301.480	64577.105	72649.313	0.385
			0.000	8454.119	13997.710	23000.783	35447.520	42255.848	56221.844	64290.457	72408.047	0.381
			0.000	8219.145	13901.546	22749.313	35298.715	42070.578	55768.410	63860.148	71806.109	0.379
			0.000	8996.306	15164.017	24796.031	38606.984	46018.344	61144.184	70039.084	78797.016	0.413
			0.000	9473.310	15233.040	24857.230	38624.480	46054.227	61248.965	70216.859	79009.133	0.415
			0.000	8233.594	15422.583	25197.344	39054.863	46567.496	61929.238	70950.523	79807.992	0.420
			0.000	10634.353	18878.932	30747.998	48318.723	57480.684	76185.594	87238.867	98025.789	0.514
			0.000	8093.587	21051.492	34437.020	55386.746	65696.914	86796.414	99310.345	109195.539	0.574
			0.000	9487.057	23948.965	39205.816	63860.395	75443.719	99481.094	113765.445	125736.227	0.653
			0.000	13009.630	23901.480	39108.238	63717.313	75328.695	99771.688	113596.047	125082.000	0.651
			0.000	13462.658	25782.133	42385.000	69532.336	82165.641	108066.305	123478.672	136385.625	0.703
			0.000	-1099.775	4637.779	7829.043	11799.213	14298.604	19090.686	21860.347	22853.180	0.126
			0.000	-1099.750	4694.583	7852.646	11847.295	14395.796	19202.467	22012.713	23068.119	0.128
			0.000	-682.824	5416.985	9066.894	13636.618	16512.363	22030.691	25236.949	26678.525	0.148
			0.000	-608.189	5436.595	9077.637	13649.655	16540.662	22039.459	25249.984	26680.934	0.148
			0.000	3976.250	6448.511	10539.313	15769.153	19020.277	25005.852	28570.807	30327.303	0.176
			0.000	4013.628	6465.009	10552.603	15785.689	19059.777	25033.691	28596.877	30343.480	0.176
			0.000	4420.224	7233.161	11827.548	17749.289	21387.998	28163.527	32169.482	34385.684	0.197
			0.000	4356.388	7237.753	11827.337	17735.723	21388.523	28153.357	32131.301	34340.602	0.197
			0.000	4890.979	8075.520	13264.645	19962.768	24027.502	31709.748	36178.250	38611.098	0.220
			0.000	4934.398	8121.035	13294.069	20004.313	24048.416	31726.159	36240.820	39059.129	0.221
			0.000	5308.175	8789.071	14371.594	21752.809	26296.920	34502.449	39294.852	42319.188	0.239
			0.000	5478.600	8831.463	14398.267	21755.592	26114.082	34479.445	39335.191	42424.465	0.241
			0.000	5974.331	9779.966	15930.815	24158.256	28967.086	38349.938	43743.848	47294.508	0.266
			0.000	5390.845	9752.901	15932.161	24116.953	28944.080	38276.664	43705.336	47170.160	0.266
			0.000	6701.529	11720.472	19134.992	29321.816	35050.215	46279.902	52973.199	57268.250	0.319
			0.000	6666.170	11697.716	19112.732	29250.912	35000.930	46202.676	52746.070	57245.461	0.319
			0.000	7293.640	12184.369	19950.303	30681.930	36677.520	48393.055	55287.328	60195.574	0.332
			0.000	7540.765	12162.216	19915.396	30656.918	36543.832	48367.234	55155.090	59858.402	0.331
			0.000	14195.943	24194.750	39615.805	64716.520	76415.617	100420.734	114390.406	125608.914	0.659
			0.000	12279.644	22687.021	37055.285	60168.758	71257.430	93520.938	106681.484	117192.656	0.618
			0.000	12716.377	21030.049	34288.520	55268.956	65350.625	85975.281	98206.500	107854.281	0.573
			0.000	10737.938	18608.912	30346.734	48328.473	57333.883	75614.730	86307.086	94376.992	0.507
			0.000	9009.627	15582.549	25413.275	39897.375	47542.064	62742.781	71563.117	78219.008	0.425
			0.000	9011.606	14933.459	24423.033	38179.824	45543.484	60027.281	68694.555	75018.266	0.407
			0.000	6136.698	10881.945	17785.006	27313.488	32721.531	43224.582	49313.477	55459.500	0.297
			0.000	14585.301	24719.867	40311.500	66804.891	78696.914	103217.555	117787.586	129944.484	0.674
			0.000	13381.576	24738.664	40309.387	66714.484	78668.656	103048.859	117485.055	129493.148	0.674
			0.000	15401.742	26609.889	43353.367	72674.344	85542.805	111682.242	127276.500	140762.234	0.725

Table 12 HGL Test for Glycerine 100%

		Axial distances	-6.298	-4.568	-2.932	-0.832	1.076	2.685	6.046	8.075	9.975	
		Valve plane	0									
		Pod 1	Pod 2	Pod 3	Pod 4	Pod 5	Pod 6	Pod 7	Pod 8	Pod 9	Average Flow rate	
Temperature	27°C	DP <sub>1</sub>	DP <sub>2</sub>	DP <sub>3</sub>	DP <sub>4</sub>	DP <sub>5</sub>	DP <sub>6</sub>	DP <sub>7</sub>	DP <sub>8</sub>	DP <sub>9</sub>		
11/19/2004		P <sub>a</sub>	P <sub>a</sub>	P <sub>a</sub>	P <sub>a</sub>	P <sub>a</sub>	P <sub>a</sub>	P <sub>a</sub>	P <sub>a</sub>	P <sub>a</sub>	[Q]	
Valve Type:	Diaphragm	0.000	2701.912	4639.613	7562.665	11258.888	13494.032	17824.922	26629.561	23181.803	0.608	
Valve dimension(mm):	40	0.000	2689.120	4615.703	7558.782	11228.120	13474.991	17799.309	26594.480	23174.670	0.605	
Valve position:	Open	0.000	2837.890	4898.820	8093.548	12056.617	14492.524	19155.373	22150.705	24907.111	0.642	
Pipe Diameter (mm):	42.12	0.000	2865.699	4938.461	8121.496	12365.771	14496.234	19165.799	22138.164	24899.484	0.648	
Material Type:	Glycerine 100%	0.000	3136.670	5426.389	8941.302	13279.903	16012.077	21159.145	24445.010	27517.412	0.712	
Density(kg/m <sup>3</sup> ):	1252.61	0.000	3129.670	5241.307	8911.486	13329.260	15989.339	21154.861	24459.854	27485.264	0.687	
$\mu$ (Pa.s)	0.175	0.000	3323.059	5775.890	9521.111	14276.807	17084.330	22526.881	26127.506	29370.926	0.757	
		0.000	3323.769	5753.882	9486.066	14249.255	17054.199	22585.678	26096.953	29374.561	0.755	
		0.000	4737.972	8701.943	14282.565	21939.021	26146.053	34904.375	40224.195	45179.805	1.141	
		0.000	4709.354	8683.627	14276.526	21877.088	26168.637	34948.395	40256.242	45150.633	1.139	
		0.000	5207.805	9597.317	15717.863	24248.941	28940.885	38677.512	44484.090	49856.867	1.259	
		0.000	5222.186	9591.481	15740.182	24285.615	28912.393	38668.004	44514.859	49954.090	1.258	
		0.000	6110.700	11430.271	18467.387	28940.484	34532.438	45756.316	52642.055	59154.473	1.499	
		0.000	6118.117	11403.418	18615.623	29142.240	34585.785	45788.977	52764.977	59100.527	1.495	









**Table 16 HGL Test for Glycerine 75%**

		3.824	4.72	5.726	6.731	7.237	8.012	8.666	9.669		
		Valve position									
Temperature	21°C	Pod 1	Pod 2	Pod 3	Pod 4	Pod 5	Pod 6	Pod 7	Pod 8	Pod 9	Average flow rate
Valve Type	Diaphragm	Pa	Pa	Pa	Pa	Pa	Pa	Pa	Pa	Pa	(m)
Valve diameter(mm)	40	26574.872	26564.950	26598.711	26502.600	26497.145	26490.412	26522.354	26346.963	26149.012	0.315
Valve position(mm)	90	26715.311	26556.412	26916.145	26492.908	26511.822	26479.541	26570.302	26353.912	26147.658	0.146
Pipe Diameter (mm)	Open	27130.000	27050.000	26988.670	26866.680	26707.471	26628.879	26442.467	26302.002	26242.021	0.387
Material Type	Glycerine 75%	27529.000	27447.482	27341.330	27174.891	26905.990	26677.316	26437.965	26275.941	26236.286	0.588
Density(kg/m <sup>3</sup> )	1197.2	27569.439	27476.486	27370.920	27172.145	26946.127	26658.911	26394.730	26254.599	26233.246	0.824
$\mu(Pa.s)$	0.020	27592.160	27454.578	27349.162	27175.107	27020.279	26798.722	26568.206	26342.981	26287.258	0.722
		28185.258	28020.353	27865.463	27614.959	27370.422	27062.742	26743.222	26505.201	26359.314	1.227
		43027.215	41132.309	39630.715	37614.516	35443.742	33130.428	30429.223	28224.012	26432.321	3.309
		45489.609	44229.188	42824.247	40828.508	38547.660	35919.016	32999.402	29617.494	26386.316	3.691
		45535.724	44266.301	42493.565	40034.113	36979.609	33911.711	30316.654	26624.050	24381.973	3.691
		44580.402	43268.184	41691.344	39232.730	36336.922	32977.855	29148.662	25548.656	24434.477	3.378
		44279.219	43437.273	41699.180	39286.668	36349.793	33227.082	30141.842	26352.136	24382.828	3.285
		41940.348	40785.172	39416.176	37362.230	35341.438	33272.822	29371.645	26235.204	24428.281	3.264
		41909.586	40734.766	39408.777	37362.098	35340.398	33262.664	29395.854	26298.479	24440.152	3.285
		39783.262	38723.172	37498.283	35772.051	34211.125	31300.445	29179.836	26122.023	24439.471	3.022
		29677.980	28742.641	27521.199	25823.287	24233.988	21268.277	19193.616	18107.756	16456.119	3.011
		28681.926	27690.848	26729.738	25240.023	23928.441	20928.275	18941.926	18010.160	16481.226	2.874
		28618.236	27714.275	26601.516	25224.224	23877.178	20911.273	18923.206	18024.420	16458.268	2.877
		26663.684	25862.813	24927.486	23193.277	21028.281	18220.242	16263.553	14800.190	13478.252	2.613
		26614.294	25800.250	24910.802	23193.583	21026.439	18222.217	16251.228	14800.961	13475.971	2.615
		26472.224	25855.473	24936.145	23166.684	20970.729	18146.282	16279.205	14844.424	13473.191	2.628
		25394.227	24789.148	24099.914	22829.348	20483.294	18445.281	16242.219	14732.246	13483.603	2.445
		25394.660	24823.029	24036.492	22792.344	20482.225	18443.226	16241.220	14722.609	13483.176	2.449
		24730.287	24011.461	23407.281	22296.512	20093.434	18074.742	16215.296	14661.092	13468.679	2.375
		25138.022	24269.254	23613.715	22112.934	20340.613	18415.602	16245.154	14672.824	13489.224	2.400
		23813.580	22800.750	22418.254	21282.200	19221.725	16741.280	14942.208	13236.715	12456.243	2.259
		23113.267	21674.715	21123.287	20270.262	18416.086	16078.257	14967.136	12730.172	12473.204	2.267
		21897.162	21283.926	20887.225	19938.928	18282.930	16231.578	14681.205	12766.028	12492.268	2.056
		21286.102	21227.025	20777.545	20136.028	18292.262	16230.443	14669.448	12709.708	12430.298	2.029
		20229.736	20286.777	20022.984	19474.271	18272.863	16045.245	14521.222	12422.222	12343.240	1.945
		20788.103	20262.186	20041.460	19492.617	18422.113	16078.246	14543.298	12229.228	12456.271	1.832
		20834.200	20492.543	20203.291	19877.295	18073.228	17145.111	14681.150	12121.431	12454.923	1.587
		20948.600	20506.563	20208.129	19889.660	18058.066	17158.536	14693.949	12130.438	12451.969	1.589
		20868.490	20560.021	20422.986	20108.186	19553.719	17377.088	14972.209	12456.576	12410.281	1.811
		20850.627	20525.016	20441.298	20269.545	19570.010	17366.820	14999.275	12466.984	12456.869	1.696
		20420.713	20150.400	20022.082	19736.451	19341.861	17222.220	14668.609	12475.658	12467.641	1.613
		20426.670	20127.826	20030.200	19758.969	19324.982	17193.222	14654.242	12466.972	12461.012	1.596



**Table 19 HGL Test for Glycerine 75%**

		Axial distances									
		-4.413	-4.909	-2.428	-1.259	0.707	3.907	5.977	8.461	9.956	
		Valve plane									
		Pod 1	Pod 2	Pod 3	Pod 4	Pod 5	Pod 6	Pod 7	Pod 8	Pod 9	Average Flow rate
Temperature	21°C	Pa	Pa	Pa	Pa	Pa	Pa	Pa	Pa	Pa	[m]
3/12/2004		41904.029	41272.824	39656.621	39061.203	34253.738	32368.111	31229.143	29987.174	29126.158	7.223
Valve Type:	Diaphragm	41678.867	41154.820	39780.730	39078.914	34413.816	32446.383	31303.549	29990.227	29139.018	7.461
Valve diameter(mm)	80	40389.680	39386.059	38056.247	37453.553	32365.713	31698.379	30638.447	29468.102	28863.549	6.617
Valve position:	Open	40197.367	39304.824	38231.602	37678.961	32518.480	31820.266	30754.143	29613.636	28994.314	6.460
Pipe Diameter (mm)	80.43	38714.121	38024.285	36691.254	36447.523	32714.457	31293.264	30454.082	29287.928	28822.654	6.139
Material Type:	Glycerine 75%	38680.539	38089.762	37024.539	36492.113	32860.602	31338.074	30428.922	29401.955	28822.854	5.952
Density(kg/m <sup>3</sup> )	1192.5	38641.121	38040.027	37030.801	36374.406	32824.898	31343.994	30474.088	29400.027	28793.328	5.988
μ(Pa.s)	0.020	35391.125	34927.230	34093.766	33818.267	31264.266	30154.377	29394.209	28852.643	28468.123	4.869
		35337.961	34913.191	34116.820	33762.043	31266.803	30193.727	29389.959	28834.883	28482.000	4.935
		32356.639	32216.168	31745.205	31587.018	29956.633	29260.363	28640.404	28316.638	28170.203	3.948
		32376.805	32274.402	31830.908	31531.652	29950.637	29218.879	28648.117	28373.066	28163.646	3.797
		30870.553	30680.592	30372.492	30201.003	29158.994	28646.527	28387.646	28144.195	27989.174	3.110
		30943.590	30742.211	30338.449	30236.916	29211.770	28628.525	28447.545	28108.494	28013.203	2.974

**Table 20 HGL Test for Glycerine 75%**

		Axial distances									
		-4.532	-3.042	-2.542	-1.040	0.700	2.502	3.501	5.010	9.511	
		Valve plane									
		Pod 1	Pod 2	Pod 3	Pod 4	Pod 5	Pod 6	Pod 7	Pod 8	Pod 9	Average Flow rate
Temperature	22°C	ΔP <sub>1</sub>	ΔP <sub>2</sub>	ΔP <sub>3</sub>	ΔP <sub>4</sub>	ΔP <sub>5</sub>	ΔP <sub>6</sub>	ΔP <sub>7</sub>	ΔP <sub>8</sub>	ΔP <sub>9</sub>	[m]
3/12/2004		0.000	276.453	432.411	771.364	2498.214	2897.197	3130.774	3609.340	4853.760	7.540
Valve Type:	Diaphragm	0.000	255.290	409.174	753.661	2438.135	2873.807	3056.486	3612.883	4881.292	7.540
Valve diameter(mm)	100	0.000	233.882	389.896	696.774	2246.870	2652.334	2872.708	3298.330	4428.136	6.937
Valve position:	Open	0.000	236.959	409.113	693.378	2281.342	2696.066	2867.916	3310.240	4494.563	6.858
Pipe Diameter (mm)	97.17	0.000	220.947	374.752	658.789	2081.830	2504.758	2678.078	3085.014	4162.104	6.827
Material Type:	Glycerine 75%	0.000	209.477	369.720	651.164	2126.677	2530.482	2698.339	3103.326	4178.189	6.869
Density(kg/m <sup>3</sup> )	1192.5	0.000	191.478	336.859	581.269	1885.795	2234.476	2391.745	2723.004	3733.051	6.192
μ(Pa.s)	0.020	0.000	183.485	349.505	597.689	1917.093	2252.606	2409.153	2751.355	3749.029	6.305
		0.000	140.930	281.181	485.602	1564.886	1836.698	1967.843	2230.314	3139.907	5.842
		0.000	124.637	290.971	485.647	1565.122	1865.300	1988.191	2268.057	3098.029	5.833
		0.000	96.463	243.553	407.650	1314.905	1578.328	1707.234	1885.060	2648.394	5.316
		0.000	68.533	239.347	404.121	1327.027	1551.186	1669.582	1891.262	2631.722	5.128
		0.000	58.566	205.681	318.235	1053.036	1248.175	1354.297	1450.780	2006.882	4.655
		0.000	46.550	180.646	319.898	1064.380	1272.623	1299.388	1497.072	2102.426	4.619
		0.000	34.879	136.742	243.611	817.403	987.023	1018.585	1093.063	1689.821	4.088



**Table 22 HGL Test for CMC 5%**

		Axial distances	-6.258	-4.568	-1.880	-0.621	1.076	2.685	6.046	8.075	9.975	
		Valve plane	0									
			Pod 1	Pod 2	Pod 3	Pod 4	Pod 5	Pod 6	Pod 7	Pod 8	Pod 9	Average Flow rate
			Pa	Pa	Pa	Pa	Pa	Pa	Pa	Pa	Pa	(%)
3/11/2004			94431.290	89592.133	82189.953	78953.734	58847.978	46126.570	36708.602	31168.785	25928.309	2.824
Valve Type:	Diaphragm		94980.516	90108.367	82874.984	79447.734	51640.359	47011.277	37706.436	32180.232	25850.531	2.829
Valve dimension(mm):	40		100674.727	95525.567	87849.516	84161.609	52343.051	47386.297	37392.762	31495.744	25975.053	3.088
Valve position:	Open		100630.664	95574.883	87794.375	83886.758	52525.246	47482.332	37587.680	31766.748	26323.258	3.056
Pipe Diameter (mm):	42.12		105011.438	99823.914	91660.219	87889.156	53983.324	48736.348	38344.129	32319.408	26798.307	3.375
Material Type:	CMC 5%		104756.359	99571.977	91519.828	87932.291	53911.504	48590.090	38370.855	32386.852	26756.240	3.257
Density(kg/m <sup>3</sup> ):	1024		135605.266	128944.813	118201.734	113941.211	60882.371	54026.313	41154.128	32785.105	26989.836	4.293
T <sub>p</sub> :	0.000		136168.984	128020.922	118125.727	113663.398	60306.371	53306.766	40590.324	33137.783	26367.896	4.237
K:	0.304											
n:	0.770											

**Table 23 HGL Test for CMC 5%**

		Axial distances	-5.574	-3.526	-2.281	-1.021	1.257	3.012	5.666	7.666	9.669	
		Valve plane	0									
			Pod 1	Pod 2	Pod 3	Pod 4	Pod 5	Pod 6	Pod 7	Pod 8	Pod 9	Average Flow rate
			Pa	Pa	Pa	Pa	Pa	Pa	Pa	Pa	Pa	(%)
3/11/2004			49898.728	45832.191	44061.473	42076.629	37496.988	33020.086	31020.949	28355.338	25677.211	2.680
Valve Type:	Diaphragm		50721.063	46868.793	45121.691	43045.219	38427.789	33989.758	31984.834	29163.408	26600.000	2.707
Valve dimension(mm):	50		51816.456	47488.504	45784.352	43443.590	38391.043	33791.633	31494.070	28600.451	25464.605	2.917
Valve position:	Open		51769.969	47465.547	45504.504	43373.965	38343.625	33774.793	31441.914	28578.883	25711.717	2.931
Pipe Diameter (mm):	52.8		54384.313	50078.590	47747.121	45400.742	39443.523	36665.938	31994.877	28954.084	25795.102	3.242
Material Type:	CMC 5%		54390.816	49933.023	47822.027	45472.754	39626.039	36705.426	32044.082	28915.432	26344.865	3.177
Density(kg/m <sup>3</sup> ):	1024		57771.035	52700.602	50223.922	47678.029	41081.230	37480.199	32549.225	29267.031	25834.775	3.611
T <sub>p</sub> :	0.000		70943.359	63877.953	61098.965	57774.672	46801.313	42016.453	35150.531	30691.564	26273.561	5.247
K:	0.442		70589.688	64059.105	61504.676	57929.777	46711.762	42208.902	35227.277	30869.020	26420.436	5.306
n:	0.670		75184.406	67847.602	64810.598	61115.641	48573.840	43370.832	35890.980	31100.307	26491.123	5.863
			74849.148	67780.273	64864.297	61453.160	48585.137	43437.605	36009.434	31244.781	26527.492	5.779







Table 26 HGL Test for CMC 5%

		Axial distand	-6.413	-4.809	-3.610	-1.209	0.707	3.907	5.977	8.461	9.956	
		Valve plane				0						
			Pod 1	Pod 2	Pod 3	Pod 4	Pod 5	Pod 6	Pod 7	Pod 8	Pod 9	Average Flow rate
			$\Delta P_1$	$\Delta P_2$	$\Delta P_3$	$\Delta P_4$	$\Delta P_5$	$\Delta P_6$	$\Delta P_7$	$\Delta P_8$	$\Delta P_9$	
			Pa	Pa	Pa	Pa	Pa	Pa	Pa	Pa	Pa	[l/s]
2/11/2004			0.000	210.676	383.828	741.644	1134.375	1594.970	1913.038	2295.481	2521.203	0.854
Valve Type:	Diaphragm		0.000	200.252	374.021	708.487	1108.861	1543.748	1839.723	2189.153	2382.088	0.844
Valve dimension[mm]:	80		0.000	188.313	351.214	685.276	1066.989	1470.111	1764.034	2120.873	2262.915	0.752
Valve position:	Open		0.000	194.937	350.583	674.793	1040.676	1503.520	1805.494	2082.978	2285.143	0.769
Pipe Diameter [mm]:	80.43		0.000	174.903	312.362	621.418	918.824	1303.283	1564.121	1860.006	2028.218	0.680
Material Type:	CMC 5%		0.000	172.258	311.387	614.596	921.271	1315.270	1577.196	1880.051	2053.565	0.685
Density[kg/m <sup>3</sup> ]:	1028.2		0.000	155.171	279.143	554.955	823.111	1191.315	1431.425	1694.611	1841.401	0.604
$\tau_c$ :	0.000		0.000	178.803	302.976	581.941	866.817	1211.120	1447.390	1695.554	1890.029	0.594
K:	1.095		0.000	151.048	267.302	511.618	778.533	1044.587	1276.399	1511.427	1660.033	0.502
n:	0.798		0.000	152.213	271.994	512.334	762.613	1065.879	1272.719	1513.934	1655.210	0.500
			0.000	130.875	223.847	434.867	633.268	911.096	1100.849	1285.684	1432.643	0.421
			0.000	135.684	225.076	425.234	629.429	904.475	1057.996	1258.648	1437.430	0.430
			0.000	111.631	185.738	367.986	529.640	773.068	889.509	1073.243	1160.642	0.335
			0.000	112.685	189.276	358.218	527.664	756.672	920.863	1058.853	1163.624	0.326
			0.000	88.894	162.800	316.433	459.039	633.914	772.390	921.628	992.023	0.284
			0.000	91.085	161.453	320.541	453.055	652.307	767.846	960.420	975.801	0.278
			0.000	52.376	83.095	172.050	245.031	348.930	416.477	488.840	543.224	0.129
			0.000	60.847	82.149	162.680	232.375	346.115	416.723	497.318	532.530	0.124
			0.000	31.598	42.599	98.721	120.502	192.633	235.180	280.299	293.508	0.065



**Table 28 HGL Test for CMC 5%**

		Axial distances	-5.050	-3.544	-2.542	-1.040	0.700	2.502	4.499	5.010	9.511	
		Valve plane				0						
			Pod 1	Pod 2	Pod 3	Pod 4	Pod 5	Pod 6	Pod 7	Pod 8	Pod 9	Average Flow rate
			$\Delta P_1$	$\Delta P_2$	$\Delta P_3$	$\Delta P_4$	$\Delta P_5$	$\Delta P_6$	$\Delta P_7$	$\Delta P_8$	$\Delta P_9$	
			Pa	Pa	Pa	Pa	Pa	Pa	Pa	Pa	Pa	[m]
28/10/2004			0.000	102.535	165.250	275.906	419.955	548.394	681.907	765.099	1084.386	0.894
Valve Type:	Diaphragm		0.000	102.477	167.267	275.362	420.517	557.267	676.241	755.895	1084.208	0.893
Valve dimension [mm]:	100		0.000	118.339	191.556	310.531	485.369	619.811	787.789	853.818	1251.013	1.066
Valve position:	Open		0.000	128.741	213.650	352.760	546.521	696.819	886.457	963.285	1396.475	1.210
Pipe Diameter [mm]:	97.17		0.000	128.971	210.842	342.402	546.846	698.908	864.265	951.949	1377.450	1.208
Material Type:	CMC 5%		0.000	121.589	207.133	334.262	520.702	663.932	834.340	924.633	1312.828	1.150
Density [kg/m <sup>3</sup> ]:	1027		0.000	142.086	229.381	375.404	584.728	749.985	954.723	1031.219	1497.783	1.296
$\tau_w$ :	0.000		0.000	143.414	228.647	367.114	572.258	745.131	944.152	1041.763	1485.917	1.295
K:	1.130		0.000	142.261	234.860	391.406	616.330	797.442	992.111	1096.014	1587.266	1.407
n:	0.784		0.000	160.311	255.322	410.354	660.320	836.236	1047.745	1166.888	1663.756	1.489
			0.000	165.853	252.828	408.578	656.605	840.371	1037.124	1147.681	1661.142	1.488









Table 33 HGL Test for CMC 8%

		Axial distance	-6.974	-3.865	-2.895	-0.937	0.987	2.938	6.427	8.432	10.433	
		Valve plane	0									
			Pod 1	Pod 2	Pod 3	Pod 4	Pod 5	Pod 6	Pod 7	Pod 8	Pod 9	Average Flow rate
			$\Delta P_1$	$\Delta P_2$	$\Delta P_3$	$\Delta P_4$	$\Delta P_5$	$\Delta P_6$	$\Delta P_7$	$\Delta P_8$	$\Delta P_9$	
			$P_a$	$P_a$	$P_a$	$P_a$	$P_a$	$P_a$	$P_a$	$P_a$	$P_a$	[l/s]
9/11/2004			0.000	7652.967	9658.114	14524.323	18977.877	23460.123	30436.504	34720.316	39494.379	0.800
Valve Type:	Diaphragm		0.000	7394.447	9537.080	14470.827	18975.234	23254.727	30302.996	34636.758	39512.758	0.800
Valve dimension [mm]:	65		0.000	7999.683	9989.782	15385.593	20141.250	25158.373	32355.600	37535.641	42167.617	0.926
Valve position:	Open		0.000	7554.899	10191.791	14674.006	20296.627	24941.949	32178.883	37374.191	42128.699	0.928
Pipe Diameter (mm):	63.08		0.000	8554.097	10965.667	16258.208	23240.588	27751.104	35245.375	40354.023	46114.117	1.053
Material Type:	CMC 8%		0.000	8480.470	11530.149	16882.217	23588.758	28637.742	36716.625	42253.332	47907.508	1.071
Density [kg/m <sup>3</sup> ]:	1037.5		0.000	8716.008	11308.776	16326.356	22568.010	28542.291	30742.838	42151.871	48046.617	1.183
T <sub>v</sub> :	0.000		0.000	9069.192	10996.116	16304.350	22875.473	28383.910	36725.102	42230.520	47592.648	1.183
K:	5.252		0.000	10302.869	12800.000	18500.000	25844.422	31172.434	39910.863	45800.637	51691.586	1.334
n:	0.790		0.000	9649.424	12118.228	18930.609	25005.656	30451.832	39203.660	45256.434	51676.246	1.333
			0.000	9923.541	13543.530	18922.203	24654.790	31296.611	40032.152	46261.109	52568.906	1.433
			0.000	10377.018	11643.161	17445.184	24966.225	30924.043	40450.090	46472.453	52343.121	1.431
			0.000	10482.264	14050.884	20950.098	28331.029	33834.449	42969.891	49677.223	55993.480	1.587
			0.000	10882.395	14562.153	20852.029	28153.041	33702.203	43219.363	49578.090	56206.727	1.587
			0.000	10633.630	13799.799	20641.217	27731.215	34735.012	44294.945	50769.398	57566.020	1.681
			0.000	10709.887	14044.871	21023.691	28205.152	34126.305	44091.012	51244.250	57840.707	1.682
			0.000	10612.736	13703.315	19656.645	28510.420	33836.949	43004.480	52289.805	59528.141	1.770
			0.000	10873.777	13670.957	21276.215	28588.816	35635.574	45654.559	53134.266	59619.902	1.773
			0.000	11293.798	14404.271	21935.100	28764.152	36464.449	46891.402	54244.254	61324.148	1.873
			0.000	11073.453	14400.070	22000.520	30023.205	36546.320	47563.445	54503.602	61203.977	1.876
			0.000	10704.304	13366.499	22839.012	29361.385	36008.113	46577.137	53781.086	60720.176	2.037
			0.000	12009.379	15177.537	21999.330	30750.297	37469.418	47990.563	54998.559	63198.977	2.172
			0.000	13121.910	15509.029	22780.293	30678.184	36928.672	48631.801	56122.863	63616.348	2.258
			0.000	11611.120	16653.146	21985.963	29962.012	38368.137	48707.277	56183.008	63726.781	2.258
			0.000	11947.200	15696.167	22514.449	31341.197	38083.137	49452.813	57102.594	65079.789	2.350
			0.000	12206.868	16612.311	21145.607	30649.428	38218.660	49839.938	57036.672	64885.590	2.349
			0.000	12320.313	16411.256	25053.162	33506.109	40497.426	52216.676	60043.555	68117.633	2.537
			0.000	12226.973	15848.758	24459.595	32970.344	40503.043	52243.840	60202.750	68253.336	2.540
			0.000	12991.690	17284.611	24799.008	34709.711	42650.820	54642.125	63047.594	71004.898	2.764
			0.000	13506.683	16960.684	24746.088	34422.031	42745.602	54137.414	63442.879	70874.109	2.766
			0.000	14306.660	17510.041	25866.930	35948.406	43040.133	56491.230	65047.754	73402.738	2.936
			0.000	14117.474	17292.063	26581.164	35754.305	44391.598	56864.200	64534.074	73223.859	2.930
			0.000	14241.090	17512.412	27360.086	36945.164	45468.277	58917.844	67699.453	76938.906	3.129
			0.000	13531.299	18515.959	26911.309	37908.328	46677.965	59521.680	67898.148	77360.773	3.120
			0.000	14406.320	19065.137	27335.285	37630.191	45536.055	59138.082	67842.781	77430.414	3.118
			0.000	14253.241	18893.799	27957.029	39255.379	48424.215	62660.918	71502.602	81268.789	3.356
			0.000	14148.417	19377.164	27990.107	38458.656	48308.438	62475.871	71600.828	81149.797	3.350
			0.000	16027.370	19977.006	29092.256	40267.867	49269.953	63806.082	74124.703	82914.594	3.541
			0.000	15724.432	20183.754	27218.848	40896.633	49700.426	64009.406	73770.773	83226.633	3.533
			0.000	17096.170	20500.973	31060.021	41427.418	51652.328	65594.561	75572.688	85595.141	3.725
			0.000	15448.370	20086.525	31409.664	41455.480	50783.074	65696.742	75561.906	86274.492	3.733
			0.000	16426.090	21716.408	32095.434	42264.281	53019.691	69373.180	78495.422	89550.344	3.980
			0.000	16597.477	20479.061	30532.143	43398.082	53270.180	69400.000	78505.445	89411.789	3.985
			0.000	17092.883	22422.133	32379.092	44124.164	54663.105	70746.031	80095.633	91709.414	4.164
			0.000	17023.037	20837.117	31769.021	43995.656	54800.438	69480.711	80623.414	91054.844	4.162
			0.000	17605.258	21855.779	33847.348	45999.613	55766.285	72148.531	82637.844	94481.180	4.387
			0.000	17421.623	22343.391	33166.203	45887.340	56353.016	72337.070	82800.953	94309.789	4.400
			0.000	18189.590	23368.307	34217.840	46385.895	58210.840	73972.477	85392.352	97060.586	4.648
			0.000	17711.205	23274.260	34046.738	46480.973	57400.520	73280.180	85678.273	97133.484	4.641
			0.000	17957.908	23876.223	36049.344	47673.027	59284.500	75782.398	88017.414	99651.109	4.892
			0.000	18273.143	23986.270	35377.320	47969.539	58398.277	75807.977	87789.602	99463.445	4.895
			0.000	18506.135	24279.254	36306.750	49157.426	61472.008	78067.258	89426.000	101419.531	5.043
			0.000	18585.344	24593.635	35691.215	48054.117	60926.770	77002.109	90320.789	101743.781	5.042
			0.000	18893.369	25474.457	36322.184	49450.938	62285.492	80218.719	91573.664	102871.063	5.261
			0.000	19407.264	24765.383	37001.273	49993.332	62375.609	79264.523	91902.977	102737.609	5.272
			0.000	19244.113	24530.236	37074.371	51096.965	63546.219	81788.125	93474.195	105603.219	5.485
			0.000	19583.662	25633.750	37689.930	52136.297	62617.363	80133.117	93479.328	105025.414	5.483

Table 34 HGL Test for CMC 8%

		Axial distance	-6.413	-4.809	-3.610	-1.209	0.707	3.907	5.977	8.461	9.956	
		Valve plane	0									
			Pos 1	Pos 2	Pos 3	Pos 4	Pos 5	Pos 6	Pos 7	Pos 8	Pos 9	Average flow rate
			Pa	Pa	Pa	Pa	Pa	Pa	Pa	Pa	Pa	(m)
10/11/2004	Valve Type: Diaphragm	0.000	1047.862	1626.475	2769.068	3860.231	5286.199	6426.680	7585.735	8785.050	0.169	
	Valve diameter: 80	0.000	1068.229	1617.539	2942.654	4034.258	5585.365	6682.142	7832.274	8509.299	0.164	
	Valve position: Open	0.000	1178.998	1886.480	3313.521	4711.050	6642.854	7865.220	9365.738	10243.511	0.227	
	Pipe Diameter: 80.43	0.000	1249.372	1876.040	3320.519	4695.085	6623.960	7876.385	9380.537	10235.101	0.224	
	Material Type: CM 8%	0.000	1374.822	2368.823	4005.717	5729.082	8070.482	9562.445	11388.370	12479.892	0.322	
	Density (kg/m <sup>3</sup> ): 1044	0.000	1420.652	2362.746	4015.040	5726.396	8065.076	9580.535	11371.902	12504.339	0.322	
	Tp: 0.000	0.000	1538.789	2635.387	4600.217	6593.786	9403.078	11065.926	13244.828	14489.451	0.422	
	K: 7.400	0.000	1710.031	2568.654	4586.021	6673.590	9327.552	11140.186	13248.942	14603.061	0.430	
	R: 0.790	0.000	1721.615	2811.370	5080.268	7303.604	10303.747	12245.769	14566.113	15984.414	0.302	
		0.000	1740.837	2837.649	5062.040	7266.897	10278.455	12194.437	14513.051	15940.393	0.303	
		0.000	2101.959	3359.980	6024.638	8514.528	12237.746	14444.657	17251.121	18920.154	0.676	
		0.000	2038.833	3349.483	5959.985	8607.232	12234.040	14484.682	17194.736	18881.932	0.676	
		0.000	2116.412	3449.081	6188.705	8965.819	12756.475	15108.545	17945.783	19711.936	0.715	
		0.000	2070.344	3430.463	6135.747	8878.275	12641.909	14970.629	17908.936	19656.963	0.727	
		0.000	2251.861	3643.278	6726.898	9598.975	13511.379	16025.325	19084.746	20914.279	0.818	
		0.000	2274.609	3729.160	6633.811	9456.010	13375.826	16014.229	19047.227	20883.289	0.801	
		0.000	1012.481	1599.838	2372.615	3329.808	4654.527	5496.475	6508.606	7130.171	0.120	
		0.000	1016.489	1374.577	2379.011	3316.487	4630.989	5497.500	6510.014	7129.680	0.116	
		0.000	716.512	956.394	1379.912	2156.936	2996.410	3531.429	4164.516	4531.938	0.058	
		0.000	794.237	953.815	1378.254	2160.504	2996.943	3525.701	4164.692	4544.086	0.067	
		0.000	2271.613	3624.700	6544.608	9255.809	12303.013	15811.449	18954.656	20706.652	0.792	
		0.000	2237.128	3675.465	6568.594	9431.239	12361.691	15882.207	18954.814	20792.182	0.792	
		0.000	2623.485	4265.940	7659.608	11025.333	15606.785	18539.221	23070.402	24215.166	1.007	
		0.000	2550.495	4255.101	7623.039	10989.900	15562.379	18475.886	23024.791	24139.105	1.004	
		0.000	2917.204	4733.974	8576.500	12325.009	17498.027	20837.082	24805.504	27171.230	1.252	
		0.000	2950.234	4724.720	8583.421	12348.433	17365.445	20799.426	24806.498	27106.000	1.250	
		0.000	2972.706	4972.938	8948.403	12965.056	18424.318	21930.389	26037.309	28592.018	1.404	
		0.000	3074.100	4929.417	8991.191	12967.669	18373.510	21864.934	26036.506	28591.260	1.407	
		0.000	3184.357	5228.754	9581.311	13923.415	19658.486	23322.063	27861.111	30584.561	1.567	
		0.000	3098.371	5248.790	9591.523	13776.099	19610.082	23240.484	27674.131	30490.875	1.571	
		0.000	3419.327	5707.703	10169.749	14830.864	21085.305	24994.303	29775.754	32693.406	1.789	
		0.000	3417.071	5625.180	10282.230	14784.650	21006.238	25009.402	29774.648	32748.564	1.788	
		0.000	3573.749	5946.844	10708.682	15414.990	21904.080	26036.781	31089.127	34012.391	1.929	
		0.000	3673.696	5735.543	10671.446	15378.813	21850.020	26113.916	30863.979	33975.902	1.940	
		0.000	3639.523	6084.007	11293.195	16348.937	23161.418	27474.268	32777.738	35966.309	2.160	
		0.000	3759.225	6202.629	11237.766	16337.311	23094.830	27378.215	32704.150	35858.633	2.159	
		0.000	3686.591	6363.262	11570.282	16816.648	23952.004	28228.293	33702.703	36879.246	2.261	
		0.000	3728.983	6364.993	11510.363	16779.059	23788.434	28303.594	33628.867	36920.020	2.275	
		0.000	3943.182	6492.917	11737.525	17327.748	24451.375	29076.064	34381.074	38051.516	2.430	
		0.000	4012.182	6468.346	11851.251	17427.619	24526.199	29217.437	34659.480	38102.496	2.427	
		0.000	3929.893	6619.219	12073.894	17706.713	24889.068	29763.072	35277.273	38948.625	2.520	
		0.000	3985.565	6628.973	12130.806	17663.158	25014.930	29605.033	35419.965	38777.090	2.513	
		0.000	4563.304	7030.408	12671.867	18664.266	26373.363	31235.561	37181.793	40723.082	2.758	
		0.000	4238.918	6901.144	12708.362	18399.059	26156.236	31245.740	37086.578	40852.516	2.762	
		0.000	4342.327	7194.368	13200.452	19343.320	27355.389	32536.691	38794.172	42558.184	3.045	
		0.000	4351.051	7187.335	13193.914	19340.902	27475.152	32591.342	38862.504	42553.352	3.045	
		0.000	4283.712	7412.732	13548.545	19949.527	28102.295	33514.164	39941.883	43723.359	3.198	
		0.000	4219.972	7417.132	13589.030	19920.410	28036.137	33489.853	39891.473	44002.309	3.195	
		0.000	4482.613	7545.146	13717.842	20184.355	28436.297	33930.082	40568.477	44351.496	3.276	
		0.000	4444.676	7523.841	13743.379	20314.285	28493.463	33993.339	40478.176	44337.441	3.278	
		0.000	4517.164	7639.715	14317.530	20819.637	29130.229	34895.832	41611.941	45661.625	3.455	
		0.000	4628.625	7819.689	14174.167	20880.887	29489.275	34928.746	41686.803	45587.762	3.465	
		0.000	4639.333	7927.540	14557.664	21457.627	30345.814	36064.563	42855.578	47010.820	3.645	
		0.000	4682.452	7870.311	14457.690	21589.977	30236.510	36129.254	42937.777	47076.957	3.634	
		0.000	4869.002	8267.971	14902.830	22207.330	31515.502	37344.730	44486.283	48774.949	3.884	
		0.000	4981.142	8233.355	15043.961	22623.324	31460.861	37604.508	44510.793	48798.805	3.894	
		0.000	5133.618	8402.855	15403.714	23000.818	32385.928	38416.949	45799.125	50273.852	4.113	
		0.000	5274.757	8380.250	15533.089	23068.824	32450.525	38469.105	45844.316	50200.914	4.094	
		0.000	5308.002	8778.892	16080.226	24122.746	33745.949	40092.332	47837.469	52371.988	4.414	
		0.000	5872.593	8824.753	15946.150	24080.738	33895.500	40149.302	47772.574	52424.551	4.416	
		0.000	6139.952	9385.050	16485.861	25052.629	35219.047	41846.734	49692.555	54250.969	4.690	
		0.000	6191.660	9109.919	16455.625	25051.854	35064.273	41657.770	49451.469	54296.043	4.752	
		0.000	5423.738	9049.582	16810.961	25418.463	35348.664	42341.086	50275.227	55350.074	4.905	
		0.000	5317.287	9200.467	16852.967	25579.633	35822.707	42194.047	50289.781	55106.555	4.883	
		0.000	5497.994	9412.302	17455.428	26381.311	36539.801	43782.047	52213.324	57012.707	5.188	
		0.000	5596.741	9331.749	17327.891	26216.043	36846.070	43888.441	51985.527	57177.164	5.201	
		0.000	5702.578	9634.096	17841.992	27539.426	37950.055	45171.973	53439.754	58643.164	5.451	
		0.000	5561.869	9786.507	17959.109	27270.535	38008.266	44994.891	53382.570	58697.746	5.450	
		0.000	5528.170	9563.588	18226.998	27811.590	38716.398	45777.602	54478.086	59873.809	5.661	
		0.000	5676.476	9674.475	18039.646	27969.441	38710.301	45979.645	54470.773	59636.676	5.643	

Table 35 HGL Test for CMC 8%

		Axial distances										Average Flow rate [l/s]
		-5.050	-3.544	-2.542	-1.040	0.700	2.502	3.501	5.010	9.511		
Valve plane		0										
		Pod 1	Pod 2	Pod 3	Pod 4	Pod 5	Pod 6	Pod 7	Pod 8	Pod 9		
		P <sub>a</sub>	P <sub>a</sub>	P <sub>a</sub>	P <sub>a</sub>	P <sub>a</sub>	P <sub>a</sub>	P <sub>a</sub>	P <sub>a</sub>	P <sub>a</sub>		
11/11/2004		69481.531	66460.930	64388.535	61284.051	56806.621	53075.520	51034.994	46640.152	36419.172	5.788	
Valve Type:	Diaphragm	69420.781	66297.664	64194.289	61138.926	56549.098	52891.461	50860.023	46684.281	36334.047	5.807	
Valve dimension [mm]:	100	29026.340	28800.000	28659.557	28415.795	28084.693	27795.838	27625.549	27290.426	26490.412	0.051	
Valve position:	Open	29029.117	28783.010	28669.715	28428.803	28092.932	27802.188	27630.512	27289.826	26489.803	0.046	
Pipe Diameter [mm]:	97.17	30638.344	30330.000	30127.967	29784.500	29294.193	28864.998	28617.238	28143.156	27007.697	0.089	
Material Type:	CM 8%	30657.197	30292.623	30135.668	29784.184	29311.135	28878.254	28666.656	28155.461	27014.326	0.104	
Density [kg/m <sup>3</sup> ]:	1040	32210.004	31765.779	31530.861	31125.219	30488.301	29955.506	29651.254	29004.352	27509.414	0.174	
T <sub>v</sub> :	0.000	33835.301	33230.992	33014.609	32492.958	31727.070	31049.648	30674.131	29905.742	28081.023	0.256	
K:	6.434	33867.316	33265.363	33010.582	32460.498	31679.977	31001.887	30630.678	29865.031	28006.662	0.252	
n:	0.303	35615.133	35006.480	34561.344	33889.617	32965.387	32159.521	31721.262	30802.855	28557.277	0.368	
		35605.719	34884.848	34506.602	33845.074	32925.953	32119.443	31673.984	30763.189	28548.902	0.364	
		36562.625	35788.172	35371.305	34636.234	33625.727	32750.563	32263.795	31250.951	28826.037	0.428	
		36630.426	35849.977	35443.488	34683.039	33672.320	32787.820	32290.852	31268.637	28831.773	0.422	
		38049.645	37196.727	36709.738	35870.734	34716.906	33716.906	33156.918	32019.273	29267.791	0.527	
		38011.105	37286.977	36693.438	35873.188	34749.914	33765.105	33221.871	32069.992	29301.721	0.532	
		39229.883	38413.395	37785.598	36841.359	35605.758	34496.715	33887.094	32626.514	29627.797	0.621	
		39137.559	38304.020	37728.516	36817.219	35566.434	34505.516	33872.770	32634.002	29640.596	0.618	
		40118.457	39120.633	38599.305	37597.086	36268.883	35092.430	34451.473	33165.977	29947.631	0.693	
		40197.938	39213.242	38676.863	37684.859	36327.551	35176.020	34501.203	33165.906	29944.994	0.693	
		41497.953	40430.055	39724.289	38683.531	37227.387	35974.820	35282.152	33825.715	30363.533	0.784	
		41514.133	40430.262	39743.965	38705.746	37251.234	35983.063	35277.477	33831.633	30362.607	0.800	
		41934.176	40853.906	40145.152	39117.773	37631.055	36319.930	35603.828	34110.895	30523.906	0.847	
		42013.574	40799.613	40206.570	39144.332	37648.531	36319.914	35589.461	34073.605	30478.039	0.850	
		42472.066	41347.949	40686.391	39508.969	37935.461	36620.508	35910.480	34339.395	30642.869	0.902	
		42417.070	41218.363	40640.828	39388.293	38034.273	36693.625	35939.645	34415.887	30696.654	0.903	
		45031.996	43687.352	42847.344	41808.070	39821.859	38269.029	37433.402	35669.457	31431.973	1.162	
		45010.395	43681.723	42851.832	41575.852	39817.691	38282.379	37367.262	35655.801	31422.740	1.157	
		46196.578	44780.816	43983.160	42607.824	40717.941	39108.723	38863.505	36316.359	31792.729	1.316	
		46206.422	44816.859	43913.461	42579.168	40704.313	39046.688	38112.309	36162.008	31805.311	1.315	
		47497.051	46017.262	45105.320	43632.547	41680.297	39932.551	38922.195	36968.465	32189.285	1.445	
		47490.609	46034.559	45112.621	43638.121	41651.523	39908.414	38953.934	36953.824	32191.248	1.448	
		48842.832	47342.230	46334.535	44782.953	42663.402	40816.973	39780.543	37686.109	32803.336	1.611	
		48805.621	47211.051	46286.273	44762.668	42618.152	40815.508	39787.961	37668.461	32605.693	1.611	
		46974.879	45420.727	44324.887	42578.090	40136.273	38299.500	37185.398	35071.965	29585.873	1.860	
		47064.648	45485.691	44721.602	42663.465	40425.695	38318.168	37286.520	35048.395	29577.777	1.864	
		47989.566	46340.313	45218.328	43474.285	41084.730	38965.230	37856.031	35467.797	29793.525	2.056	
		47915.918	46272.121	45136.230	43437.313	41017.953	38922.203	37834.004	35445.914	29723.045	2.057	
		48513.445	46671.621	45727.809	43851.516	41389.227	39383.703	38189.953	35814.477	29919.963	2.223	
		49028.313	47402.875	46265.234	44458.984	41961.129	39750.313	38542.043	36075.672	30155.637	2.339	
		50705.594	48967.145	47818.984	45959.406	43208.949	40859.852	39590.508	36972.074	30714.234	2.572	
		52180.914	50456.340	49043.895	47052.426	44351.645	41937.707	40513.605	37794.656	31170.000	2.863	
		52679.711	50836.711	49592.840	47538.367	44702.961	42214.051	40938.707	38019.484	31275.439	2.965	
		53311.777	51502.398	50127.027	47938.164	44948.219	42627.965	41165.789	38220.754	31573.211	3.082	
		53525.551	51356.598	49878.668	48062.500	45083.500	42552.742	41213.633	38367.480	31354.439	3.082	
		54273.031	51906.723	50685.957	48670.051	45793.895	43174.199	41772.375	38778.500	31679.084	3.249	
		54374.246	51929.633	50728.836	48571.949	45729.164	43183.145	41704.324	38614.520	31846.422	3.249	
		54958.402	52776.820	51527.246	49281.234	45773.332	43585.324	42240.066	39221.250	31832.156	3.410	
		54933.066	52784.977	51317.891	49364.016	46185.641	43466.191	42148.027	39286.352	31983.348	3.402	
		55232.895	53012.059	51592.418	49346.270	46115.371	43763.456	42382.383	39281.008	32029.258	3.472	
		55289.184	52943.386	51689.551	49505.082	46195.789	43899.168	42059.410	39301.465	32110.680	3.469	
		55296.961	53490.816	51803.617	49699.012	46269.695	43950.035	42486.293	39257.844	32094.357	3.521	
		55502.781	53351.035	51892.809	49624.996	46630.344	43836.535	42489.227	39254.414	32133.393	3.523	
		55947.816	53897.133	52258.738	50051.242	46934.699	44269.414	42610.117	39714.094	32349.457	3.648	
		55907.246	53864.867	52246.977	50110.375	46800.672	44207.901	42664.434	39721.719	32220.689	3.637	
		56752.180	54508.016	53094.543	50722.711	47525.574	44789.691	43330.438	40007.191	32447.770	3.785	
		57444.184	55259.777	53694.320	51268.578	48040.254	45175.055	43712.445	40475.613	32750.322	3.874	
		57488.777	55164.270	53654.004	51396.453	48028.637	45190.066	43711.488	40480.598	32720.010	3.905	
		58210.148	55780.090	54228.766	51835.102	48446.539	45697.805	44080.195	40784.531	32982.887	4.033	
		58199.742	55790.500	54247.363	51844.836	48440.977	45608.461	44006.840	40866.055	32977.934	4.029	

Table 36 HGL Test for kaolin 10%

		Axial distances																	
		-4.208		-4.568		-2.932		-0.822		1.076		3.805		6.046		8.075		9.975	
Valve phase		Pos 1		Pos 2		Pos 3		Pos 4		Pos 5		Pos 6		Pos 7		Pos 8		Pos 9	
Pa		Pa		Pa		Pa		Pa		Pa		Pa		Pa		Pa		Pa	
1180004	Diaphragm	32930.070	51269.910	48722.129	45307.727	41754.621	37732.433	33769.602	30494.576	27805.361	0.038								
Valve diameter [mm]	40	54061.180	51072.031	48663.918	45097.340	41767.777	37777.219	33648.457	30446.734	27463.824	0.039								
Valve position	Open	34.559.443	51792.862	49157.930	45697.438	42312.610	38444.434	34244.236	30311.143	27872.170	0.039								
Pipe Diameter [mm]	42.12	55622.563	52701.164	49562.438	46401.230	42897.176	39579.213	36420.105	32947.775	29656.740	0.110								
Material Type	Kaolin 10%	57163.129	54307.938	51329.524	47689.979	43869.758	39664.380	36083.177	31362.400	27805.323	0.165								
Density [kg/m <sup>3</sup> ]	1172.4	57562.648	54436.484	51420.673	47623.974	43973.887	39199.105	34932.715	31265.857	27820.193	0.152								
f <sub>p</sub>	10.700	57562.215	54637.637	51407.707	47839.566	44036.633	37783.055	34932.469	31226.430	27971.799	0.151								
K	2.2	58729.586	55688.973	52380.238	48489.633	44692.836	39852.297	35297.452	31304.638	27921.072	0.202								
n	0.32	58823.082	55918.441	52604.172	48454.798	44700.570	38522.838	35229.213	31511.434	27904.771	0.201								
		60419.832	57277.426	53872.238	49759.678	45697.023	40446.445	35221.327	31418.377	28019.072	0.288								
		60428.375	57092.836	53876.313	49944.793	45730.312	39828.341	35940.405	31775.301	28223.303	0.286								
		61812.094	58412.734	55225.547	50929.063	46299.348	39729.730	36164.609	31937.104	28170.215	0.396								
		63107.429	59413.664	53924.443	47011.496	43097.113	36320.402	32867.178	28182.207	0.497									
		63182.325	59406.285	55993.503	51586.283	46966.789	39872.891	36247.844	32979.836	28248.742	0.491								
		64410.523	60431.707	56823.613	52344.879	47424.258	39693.159	36137.990	32134.933	28119.023	0.635								
		64432.488	60631.648	56974.232	52546.050	47411.145	38354.263	36254.813	32192.939	28294.223	0.648								
		65591.928	61632.895	58141.529	53437.918	47663.798	39893.434	36707.370	32221.581	28326.713	0.773								
		65590.527	61624.746	58222.880	53236.473	47711.660	39604.441	36694.617	32121.012	28322.254	0.772								
		66772.252	62893.164	59207.747	54373.922	48821.191	39562.297	36823.688	32211.217	28323.688	0.997								
		66802.086	62824.926	59157.236	54401.304	47962.684	40244.148	36787.039	32141.693	28181.884	0.898								
		68019.284	64228.391	60489.577	55648.805	48310.213	39329.570	36922.836	32148.590	28033.682	1.054								
		68128.648	64343.151	60375.941	55593.371	48214.785	39066.578	36924.617	32241.939	28029.498	1.053								
		69697.246	65863.029	61120.232	57494.695	49811.301	38910.465	36996.781	31618.918	28338.402	1.290								
		69973.777	65894.730	61126.941	57398.066	47798.066	47796.333	38651.133	31625.887	28454.006	1.292								
		57145.287	54107.527	51263.125	47537.695	43803.090	38471.211	34619.520	31376.967	28376.082	1.472								
		57087.207	54078.648	51190.195	47512.629	43882.070	38433.883	34669.715	31364.289	28356.746	1.436								

Table 37 HGL Test for kaolin 10%

		Axial distances																	
		-4.208		-4.568		-2.932		-0.822		1.076		3.805		6.046		8.075		9.975	
Valve phase		Pos 1		Pos 2		Pos 3		Pos 4		Pos 5		Pos 6		Pos 7		Pos 8		Pos 9	
Pa		Pa		Pa		Pa		Pa		Pa		Pa		Pa		Pa		Pa	
5820004	Diaphragm	64018.656	57048.937	54980.289	52634.031	45719.629	40170.211	37923.094	31545.375	27630.219	1.125								
Valve diameter [mm]	40	63963.039	57204.211	55772.477	51946.924	45733.004	40026.262	37921.809	31527.176	27645.373	1.121								
Valve position	Open	63742.813	58814.984	56480.622	53868.477	46127.398	40344.437	38119.832	31382.943	27621.561	1.280								
Pipe Diameter [mm]	42.12	66070.477	58846.391	56361.496	53831.750	46183.680	40283.832	38198.339	31615.990	27635.972	1.278								
Material Type	Kaolin 10%	63769.839	58843.004	56621.543	53938.082	46223.563	40247.887	38199.824	31620.184	27649.471	1.274								
Density [kg/m <sup>3</sup> ]	1172.4	70158.453	62763.617	60430.023	57336.301	46992.948	41092.277	36645.220	31729.102	27569.049	1.668								
f <sub>p</sub>	10.700	70052.156	62693.387	60388.074	57346.598	46991.766	40973.176	36648.832	31754.794	27539.463	1.671								
K	2.2	69899.727	62687.578	60407.500	57447.785	46974.263	40902.742	36629.309	31628.932	27537.609	1.672								
n	0.32	73938.219	66403.648	63923.194	61100.211	47542.285	41428.711	38746.430	31836.430	27499.426	2.090								
		74067.906	66333.734	63869.141	61085.570	47393.839	41282.339	38736.895	31824.014	27523.080	2.094								
		76336.438	70344.945	68016.136	65283.945	47713.836	41627.930	39130.216	31840.674	27501.887	2.587								
		76308.313	70668.742	68131.038	65418.051	47878.668	41663.996	39119.445	31869.266	27521.879	2.588								
		87126.133	79362.523	76492.828	74064.273	48317.168	41667.746	39168.715	31582.049	27328.740	3.123								
		87347.023	79156.586	76679.227	73736.211	48325.328	41993.141	39195.273	31592.576	27098.529	3.148								
		89664.969	81126.938	79828.570	76696.332	48381.234	41500.266	39144.386	31222.523	26757.273	3.303								
		89698.875	82274.445	79856.906	76379.195	48320.039	41772.433	38986.191	31301.145	26841.113	3.304								

Table 38 HGL Test for kaolin 10%

		Axial distances																	
		-4.208		-2.932		-1.88		-0.621		1.076		3.805		4.920		8.075		9.975	
Valve phase		Pos 1		Pos 2		Pos 3		Pos 4		Pos 5		Pos 6		Pos 7		Pos 8		Pos 9	
Pa		Pa		Pa		Pa		Pa		Pa		Pa		Pa		Pa		Pa	
1282004	Diaphragm	64018.656	57048.937	54980.289	52634.031	45719.629	40170.211	37923.094	31545.375	27630.219	1.125								
Valve diameter [mm]	40	63963.039	57204.211	55772.477	51946.924	45733.004	40026.262	37921.809	31527.176	27645.373	1.121								
Valve position	Open	63742.813	58814.984	56480.622	53868.477	46127.398	40344.437	38119.832	31382.943	27621.561	1.280								
Pipe Diameter [mm]	42.12	66070.477	58846.391	56361.496	53831.750	46183.680	40283.832	38198.339	31615.990	27635.972	1.278								
Material Type	Kaolin 10%	63769.839	58843.004	56621.543	53938.082	46223.563	40247.887	38199.824	31620.184	27649.471	1.274								
Density [kg/m <sup>3</sup> ]	1172.4	70158.453	62763.617	60430.023	57336.301	46992.948	41092.277	36645.220	31729.102	27569.049	1.668								
f <sub>p</sub>	10.700	70052.156	62693.387	60388.074	57346.598	46991.766	40973.176	36648.832	31754.794	27539.463	1.671								
K	2.2	69899.727	62687.578	60407.500	57447.785	46974.263	40902.742	36629.309	31628.932	27537.609	1.672								
n	0.32	73938.219	66403.648	63923.194	61100.211	47542.285	41428.711	38746.430	31836.430	27499.426	2.090								
		74067.906	66333.734	63869.141	61085.570	47393.839	41282.339	38736.895	31824.014	27523.080	2.094								
		76336.438	70344.945	68016.136	65283.945	47713.836	41627.930	39130.216	31840.674	27501.887	2.587								
		76308.313	70668.742	68131.038	65418.051	47878.668	41663.996	39119.445	31869.266	27521.879	2.588								
		87126.133	79362.523	76492.828	74064.273	48317.168	41667.746	39168.715	31582.049	27328.740	3.123								
		87347.023	79156.586	76679.227	73736.211	48325.328	41993.141	39195.273	31592.576	27098.529	3.148								
		89664.969	81126.938	79828.570	76696.332	48381.234	41500.266	39144.386	31222.523	26757.273	3.303								
		89698.875	82274.445	79856.906	76379.195	48320.039	41772.433	38986.191	31301.145	26841.113	3.304								



**Table 41 HGL Test for kaolin 10%**

		Axial distance									Average Flow rate
		-5.74	-1.526	-2.281	-2.280	1.257	3.012	5.666	7.666	9.669	
		Valve plane									
		Post 1	Post 2	Post 3	Post 4	Post 5	Post 6	Post 7	Post 8	Post 9	[m]
Valve Type:	Diaphragm	Pa	Pa	Pa	Pa	Pa	Pa	Pa	Pa	Pa	[s]
Valve dimension(mm):	50	4493.876	43436.777	42155.303	40400.300	37912.304	35768.303	32489.320	26002.240	27772.025	3.293
Valve position:	Open	47354.598	42944.236	42587.432	40207.745	36224.728	36117.990	32570.362	29940.082	28031.363	0.092
Pipe Diameter (mm):	52.8	44236.222	43798.664	41238.390	40145.103	37341.211	35424.437	32324.813	29514.360	27751.649	0.082
Material Type:	Kaolin 10%	47327.236	44084.367	43235.704	40729.775	38272.051	36279.720	32623.676	29783.715	27811.025	0.108
Density(kg/m <sup>3</sup> ):	1172.4	48011.316	44728.133	42811.430	41131.738	38479.266	36204.172	32836.236	29708.261	27873.873	0.123
T <sub>p</sub> :	10.700	47919.228	44251.035	42829.286	41101.220	38303.734	36246.922	32816.404	29777.728	28125.908	0.123
K:	2.2	48415.083	44629.453	43144.613	41316.533	38402.121	36374.434	32826.273	29742.225	27854.797	0.135
n:	0.52	48269.967	44603.012	43140.016	41223.832	38622.047	36306.301	32773.213	29794.553	28059.461	0.131
		49023.500	45264.627	43729.945	41808.323	38993.980	36736.138	32909.188	30045.193	28351.046	0.145
		49281.688	45303.664	43833.390	41797.620	39072.544	36747.228	32878.568	30081.074	28134.842	0.143
		49997.020	45976.953	44356.855	42791.512	39495.301	37228.456	33194.231	30105.894	28008.220	0.203
		49663.222	46041.012	44319.813	42438.695	39478.523	37222.290	33188.680	30045.343	28304.682	0.205
		51409.230	47134.723	45359.294	43593.680	40273.871	37939.137	33671.422	30414.330	28166.010	0.328
		51426.730	47141.748	45457.522	43262.785	42001.188	37825.676	33468.793	30318.732	28236.208	0.326
		52286.512	47826.262	46229.905	43942.200	42919.820	38228.943	33698.102	30598.522	28204.330	0.477
		52317.366	47941.763	46135.480	43987.535	42915.539	38246.590	33538.148	30346.475	28241.367	0.433
		52580.711	48296.348	46462.779	44234.016	41201.129	38150.926	33526.365	30282.132	28201.132	0.513
		52744.664	48263.135	46255.139	44280.336	41221.129	38411.113	33529.728	30647.047	28159.023	0.509
		52948.664	48262.135	46255.139	44280.336	41221.129	38411.113	33529.728	30647.047	28159.023	0.717
		53112.840	48722.098	46793.234	44644.656	41272.586	38228.477	34294.109	30943.783	28229.041	0.720
		52913.508	48599.070	46722.836	43626.926	40933.694	37662.924	34261.508	30940.818	28243.269	0.716
		52958.564	48841.734	46946.719	43944.426	41182.219	38040.535	34316.590	31321.326	28280.411	0.885
		52922.531	48866.410	47014.164	44021.016	41028.992	37668.027	34240.402	31163.469	28418.148	0.883
		52721.668	48966.432	47123.040	44130.623	41164.109	37711.125	34189.669	31087.356	28279.475	0.920
		54760.277	50134.668	48224.234	45329.129	42328.219	39372.339	34839.785	31690.205	28333.269	1.024
		54339.543	50043.268	48090.528	45134.309	42038.117	39429.301	34791.910	31628.053	28325.480	1.018
		54911.512	50178.550	48085.416	45479.016	42039.977	39448.914	34723.129	31572.213	28382.393	1.119

**Table 42 HGL Test for kaolin 10%**

		Axial distance									Average Flow rate
		-5.74	-1.47	-3.526	-1.531	1.257	4.013	5.666	7.666	9.669	
		Valve plane									
		Post 1	Post 2	Post 3	Post 4	Post 5	Post 6	Post 7	Post 8	Post 9	[m]
Valve Type:	Diaphragm	Pa	Pa	Pa	Pa	Pa	Pa	Pa	Pa	Pa	[s]
Valve dimension(mm):	50	51764.754	52184.254	50236.603	47726.335	42229.727	38665.720	32477.152	30367.916	29269.664	0.245
Valve position:	Open	51480.029	51530.632	52386.298	49241.178	44334.074	39617.723	34256.145	32888.098	29477.893	0.522
Pipe Diameter (mm):	52.8	51013.242	51720.000	52435.016	49478.434	44272.355	39630.508	36323.191	32905.262	29492.162	0.521
Material Type:	Kaolin 10%	51763.652	51770.078	52530.930	49498.309	44294.621	39612.258	36300.452	32905.074	29491.619	0.518
Density(kg/m <sup>3</sup> ):	1168.2	58623.578	56807.426	53414.730	50132.234	44872.051	40266.914	36616.492	32120.641	29347.365	0.725
T <sub>p</sub> :	10.700	58163.492	56789.648	53468.730	49936.938	44929.387	40172.738	36615.023	32110.537	29371.627	0.723
K:	2.2	58162.207	56864.289	53456.809	49911.516	44910.703	40218.855	36613.023	32110.937	29371.627	0.722
n:	0.31	59264.063	57713.379	54226.180	50616.289	45428.898	40379.332	36809.201	32277.878	29658.133	1.025
		59070.844	57713.699	54270.832	50693.156	45424.194	40474.785	36841.523	32283.938	29631.613	1.018
		59295.719	57723.981	54261.027	50594.621	45449.629	40323.910	36833.727	32239.620	29646.516	1.027

**Table 43 HGL Test for kaolin 10%**

		Axial distance									Average Flow rate
		-4.298	-4.568	-2.932	-1.980	1.076	3.203	6.046	8.015	9.975	
		Valve plane									
		Post 1	Post 2	Post 3	Post 4	Post 5	Post 6	Post 7	Post 8	Post 9	[m]
Valve Type:	Diaphragm	Pa	Pa	Pa	Pa	Pa	Pa	Pa	Pa	Pa	[s]
Valve dimension(mm):	40	67638.727	64809.829	60983.295	56476.880	49281.398	44625.586	38388.135	33669.000	29829.068	1.353
Valve position:	Open	67694.523	63437.648	61128.527	56992.148	48667.461	43140.477	38376.363	34320.938	29825.738	3.355
Pipe Diameter (mm):	42.12	67584.813	63602.452	61004.414	56981.203	48665.484	43030.215	38099.728	34319.922	29785.533	3.353
Material Type:	Kaolin 10%	61575.590	59491.555	55790.131	51981.922	46322.082	43447.378	37544.543	34102.484	29856.406	1.258
Density(kg/m <sup>3</sup> ):	1168.2	61316.344	59404.684	53813.746	52067.492	46393.727	43551.832	37562.561	34061.746	29809.028	1.268
T <sub>p</sub> :	10.700	61784.160	61045.309	56295.689	52441.304	46757.684	43734.219	37618.273	34030.382	29911.193	1.385
K:	2.2	62411.422	60818.926	56749.855	52381.754	46723.418	43653.839	37622.746	33930.934	29904.308	1.390
n:	0.32	62045.199	59853.426	56151.382	52219.727	46761.246	43301.125	37711.805	33713.516	29870.854	1.590
		62754.390	60410.523	56871.532	52640.648	46788.777	43813.469	37715.480	33728.637	29717.634	2.125
		62437.445	61140.723	56859.480	52427.582	46565.121	43084.160	37653.020	33536.020	29948.441	2.124
		62343.297	62045.539	56177.123	51935.330	46761.609	43103.848	37419.023	33334.613	29941.130	2.127
		62140.434	62469.473	56548.404	52884.086	46570.477	43029.281	37281.918	33219.895	30019.434	2.577
		62543.129	60037.820	56548.941	52235.840	46178.180	42775.910	37104.371	32749.582	29619.188	2.579
		63401.035	60782.742	57199.387	52752.270	46510.883	42974.660	37118.719	32896.121	29829.107	2.796
		62257.039	60530.699	57143.156	52563.293	46446.773	42801.802	36989.832	32698.662	29877.410	2.791
		63277.281	60529.691	57070.621	52600.117	46140.820	42615.152	36845.414	32731.447	29989.393	2.790
		64231.672	61497.598	57916.303	53223.301	46333.316	42754.859	36925.656	32653.934	29962.803	3.057
		64381.047	61416.348	57882.728	53142.339	46435.777	42728.473	36819.316	32596.420	29823.061	3.057

Table 44 HGL Test for kaolin 10%

138/2004	Valve Type	Diaphragm	Axial distance																		
			-6.574		-3.47		-3.526		-1.231		1.257		3.012		5.666		7.666		9.669		Average Flow rate [l/s]
			Post 1	Post 2	Post 3	Post 4	Post 5	Post 6	Post 7	Post 8	Post 9	Post 1	Post 2	Post 3	Post 4	Post 5	Post 6	Post 7	Post 8	Post 9	
Value dimension [mm]	30	30	30	30	30	30	30	30	30	30	30	30	30	30	30	30	30	30	30	30	
Pipe Diameter [mm]	52.8	52.8	52.8	52.8	52.8	52.8	52.8	52.8	52.8	52.8	52.8	52.8	52.8	52.8	52.8	52.8	52.8	52.8	52.8	52.8	52.8
Material Type	Kaolin 10%	Kaolin 10%	Kaolin 10%	Kaolin 10%	Kaolin 10%	Kaolin 10%	Kaolin 10%	Kaolin 10%	Kaolin 10%	Kaolin 10%	Kaolin 10%	Kaolin 10%	Kaolin 10%	Kaolin 10%	Kaolin 10%	Kaolin 10%	Kaolin 10%	Kaolin 10%	Kaolin 10%	Kaolin 10%	Kaolin 10%
Density [kg/m <sup>3</sup> ]	1167.4	1167.4	1167.4	1167.4	1167.4	1167.4	1167.4	1167.4	1167.4	1167.4	1167.4	1167.4	1167.4	1167.4	1167.4	1167.4	1167.4	1167.4	1167.4	1167.4	1167.4
T <sub>0</sub>	10.700	10.700	10.700	10.700	10.700	10.700	10.700	10.700	10.700	10.700	10.700	10.700	10.700	10.700	10.700	10.700	10.700	10.700	10.700	10.700	10.700
K	2.2	2.2	2.2	2.2	2.2	2.2	2.2	2.2	2.2	2.2	2.2	2.2	2.2	2.2	2.2	2.2	2.2	2.2	2.2	2.2	2.2
n	0.32	0.32	0.32	0.32	0.32	0.32	0.32	0.32	0.32	0.32	0.32	0.32	0.32	0.32	0.32	0.32	0.32	0.32	0.32	0.32	0.32

Table 45 HGL Test for kaolin 10%  
HGL Test for kaolin 10%

138/2004	Valve Type	Diaphragm	Axial distance																		
			-6.574		-3.526		-2.201		-0.780		1.257		3.012		5.666		7.666		9.669		Average Flow rate [l/s]
			Post 1	Post 2	Post 3	Post 4	Post 5	Post 6	Post 7	Post 8	Post 9	Post 1	Post 2	Post 3	Post 4	Post 5	Post 6	Post 7	Post 8	Post 9	
Value dimension [mm]	30	30	30	30	30	30	30	30	30	30	30	30	30	30	30	30	30	30	30	30	
Pipe Diameter [mm]	52.8	52.8	52.8	52.8	52.8	52.8	52.8	52.8	52.8	52.8	52.8	52.8	52.8	52.8	52.8	52.8	52.8	52.8	52.8	52.8	52.8
Material Type	Kaolin 10%	Kaolin 10%	Kaolin 10%	Kaolin 10%	Kaolin 10%	Kaolin 10%	Kaolin 10%	Kaolin 10%	Kaolin 10%	Kaolin 10%	Kaolin 10%	Kaolin 10%	Kaolin 10%	Kaolin 10%	Kaolin 10%	Kaolin 10%	Kaolin 10%	Kaolin 10%	Kaolin 10%	Kaolin 10%	Kaolin 10%
Density [kg/m <sup>3</sup> ]	1167.4	1167.4	1167.4	1167.4	1167.4	1167.4	1167.4	1167.4	1167.4	1167.4	1167.4	1167.4	1167.4	1167.4	1167.4	1167.4	1167.4	1167.4	1167.4	1167.4	1167.4
T <sub>0</sub>	10.700	10.700	10.700	10.700	10.700	10.700	10.700	10.700	10.700	10.700	10.700	10.700	10.700	10.700	10.700	10.700	10.700	10.700	10.700	10.700	10.700
K	2.2	2.2	2.2	2.2	2.2	2.2	2.2	2.2	2.2	2.2	2.2	2.2	2.2	2.2	2.2	2.2	2.2	2.2	2.2	2.2	2.2
n	0.32	0.32	0.32	0.32	0.32	0.32	0.32	0.32	0.32	0.32	0.32	0.32	0.32	0.32	0.32	0.32	0.32	0.32	0.32	0.32	0.32

Table 46 HGL Test for kaolin 10%

		Axial distances									Average flow rate Q <sub>av</sub>
Valve plane		-4.9735	-4.8955	-2.985	-0.937	0.967	1.968	2.928	3.916	4.858	
		Post 1	Post 2	Post 3	Post 4	Post 5	Post 6	Post 7	Post 8	Post 9	Q <sub>av</sub>
		P <sub>a</sub>	P <sub>a</sub>	P <sub>a</sub>	P <sub>a</sub>	P <sub>a</sub>	P <sub>a</sub>	P <sub>a</sub>	P <sub>a</sub>	P <sub>a</sub>	Q <sub>av</sub>
19/8/2004											
Valve Type:	Diaphragm										
Valve diameter(mm):	65										
Valve position:	Open										
Pipe Diameter (mm):	67.08										
Material Type:	Kaolin 10%										
Density(kg/m <sup>3</sup> ):	1163.4										
γ:	10.700										
K:	2.2										
n:	0.32										
		31719.674	30463.227	47626.824	64887.298	81684.324	40235.188	38546.512	37381.371	36134.815	2.398
		37669.875	36211.753	47815.257	44919.848	41837.879	4019.936	3878.238	37533.102	36239.819	2.392
		37669.841	36704.145	47216.579	44922.914	41838.380	40249.855	39028.223	37681.293	36259.274	2.376
		37844.789	36917.177	48024.795	45128.566	42007.309	42586.219	39121.193	37788.961	36344.809	2.142
		37868.078	37889.941	47927.375	45362.361	41937.323	36308.555	37653.766	36388.756	36287.523	2.173
		54143.281	51123.848	48213.270	45257.924	41978.629	40629.323	39191.285	37849.691	36457.527	2.044
		54215.987	51825.340	48216.457	45267.977	42009.145	40621.273	39201.219	37877.426	36462.199	2.040
		54286.236	51310.969	48358.555	45448.680	42108.422	40756.477	39294.945	37928.504	36483.805	2.108
		54413.242	51315.129	48421.569	45464.375	42125.320	40715.410	39288.023	37928.180	36472.955	2.071
		54520.473	51321.267	48547.102	45468.383	42256.691	40840.938	39399.785	37923.971	36458.805	2.247
		54588.477	51526.617	48568.794	45779.324	42340.688	40819.125	39387.520	37955.133	36511.930	2.238
		54629.004	51720.254	48824.477	45827.465	42358.691	41015.105	39328.154	38067.328	36462.684	2.469
		54902.613	51643.903	48959.156	45844.727	42327.200	40953.629	39471.012	38069.211	36469.133	2.474
		55138.277	52013.222	49300.200	46203.117	42445.590	40995.168	39526.473	38117.191	36466.254	3.631
		55180.617	52077.121	49026.253	46289.766	42476.496	41036.949	39578.492	38101.289	36469.527	3.652
		55460.402	52197.926	49277.207	46278.291	42595.627	41354.289	39595.320	38192.305	36760.824	3.803
		55430.309	52314.355	49244.164	46268.668	42455.605	40976.129	39188.313	38187.523	36782.523	3.796
		55496.262	52422.730	49379.544	46268.480	42591.207	41240.000	39786.933	38213.282	36944.152	3.970
		55530.516	52781.928	49417.329	46337.941	42585.430	41161.941	39730.000	38207.738	36817.021	3.954
		55469.469	52571.297	49245.898	46314.230	42705.803	41253.504	39728.223	38265.273	36813.012	4.154
		55720.512	52578.891	49480.116	46306.715	42617.623	41190.875	39754.199	38273.286	36825.984	4.147
		55825.263	52676.652	49638.528	46687.220	42710.370	41325.523	39842.928	38339.242	36885.109	4.313
		55898.204	52771.352	49627.437	46662.617	42728.828	41282.227	39794.192	38221.256	36892.199	4.237
		56662.316	52473.496	50299.852	47275.031	43016.594	41511.957	40248.012	38513.492	36929.441	4.537
		56389.766	53503.730	50310.770	47228.891	42952.219	41494.281	40233.520	38510.282	37021.410	4.710
		57148.203	53935.133	50810.541	47728.340	43173.598	41682.308	40128.262	38699.918	37128.496	4.152
		57160.848	53912.453	50733.569	47690.832	43147.465	41625.648	40116.195	38603.473	37159.021	4.722
		57513.738	54226.918	51091.305	48019.418	43323.259	41763.265	40243.289	38712.688	37216.828	4.863
		57541.289	54248.215	51082.688	47961.547	43338.070	41799.109	40214.977	38694.586	37221.684	4.873
		58049.445	54779.953	51243.967	48473.809	43576.923	41949.941	40218.570	38877.047	37283.984	5.176
		58128.730	54719.525	51321.281	48414.757	43495.492	41925.236	40201.308	38803.629	37408.945	5.175
		58281.445	55121.684	51969.433	48847.594	43663.020	42129.437	40313.531	39023.113	37512.330	5.425
		58384.039	55195.715	51991.129	48875.523	43689.012	42126.971	40336.922	39028.399	37504.672	5.424
		58727.640	55440.582	52182.422	49138.922	43806.433	42188.207	40406.223	39068.188	37541.121	5.579
		58685.918	55382.898	52122.355	49029.582	43713.720	42198.828	40433.024	39044.964	37523.941	5.589
		59227.914	55854.965	52661.676	49448.632	44071.332	42328.180	40743.074	39208.039	37665.738	5.872
		59355.801	55819.189	52667.623	49512.603	44021.301	42355.152	40763.141	39203.063	37669.027	5.882
		59663.996	55740.301	52681.369	49496.390	43930.898	42272.580	40725.799	39151.695	37617.879	6.004
		59190.952	55681.523	52646.168	49454.281	43949.628	42282.996	40670.522	39091.070	37611.301	5.999
		56669.980	53771.660	50814.692	47876.629	44907.258	42787.695	41286.738	40352.370	39159.340	2.278
		54172.004	51053.273	48143.213	45360.703	42246.102	40834.402	39274.266	37861.957	36451.289	2.408
		53631.371	50358.766	47803.366	44960.375	41936.887	40524.871	39107.184	37700.000	36008.277	2.981
		53345.793	50303.371	47564.785	44846.555	41911.715	40452.508	38997.063	37671.348	36291.840	1.941
		53153.086	50287.926	47474.923	44720.512	41746.637	40312.934	38945.480	37608.352	36255.477	1.839
		53282.168	50203.615	47157.289	44746.348	41743.944	40317.473	38881.262	37575.277	36210.277	1.844
		53125.629	50228.031	47272.430	44658.898	41674.629	40236.684	38679.285	37498.125	36173.257	1.636
		53156.720	50205.359	47478.675	44592.374	41771.723	40274.680	38608.871	37544.645	36213.211	1.629
		52626.957	49552.627	46859.229	44292.652	41382.313	39940.781	38496.348	37284.246	35823.523	1.631
		52930.883	50025.028	47807.123	44626.200	41616.984	40534.920	38926.766	37933.652	36027.387	2.002
		52898.484	49938.984	47767.156	44720.156	41628.688	40599.143	38921.104	37921.914	36021.402	1.976
		51982.029	49043.566	46292.139	43254.266	40885.023	39663.547	38241.496	36922.449	35701.730	1.191
		51900.277	49046.773	46229.220	43276.220	40887.301	39611.508	38236.293	36895.145	35706.945	1.183
		50786.188	48117.125	45449.531	42816.641	40389.271	39053.724	37742.627	36482.910	35285.273	0.833
		48898.054	46449.453	44069.465	41698.782	39315.786	38168.418	36998.631	35877.539	34662.699	0.282
		50874.242	48153.336	45646.109	43023.734	40628.236	39215.224	37861.707	36638.910	35371.945	0.988
		50154.012	47791.715	45204.022	42626.035	40068.191	38829.949	37320.996	36249.949	35094.457	0.736

Table 47 HGL Test for kaolin 10%

		Axial distances									Average flow rate Q <sub>av</sub>
Valve plane		-6.413	-4.809	-3.41	-1.609	0.707	2.907	5.273	8.461	9.956	
		Post 1	Post 2	Post 3	Post 4	Post 5	Post 6	Post 7	Post 8	Post 9	Q <sub>av</sub>
		P <sub>a</sub>	P <sub>a</sub>	P <sub>a</sub>	P <sub>a</sub>	P <sub>a</sub>	P <sub>a</sub>	P <sub>a</sub>	P <sub>a</sub>	P <sub>a</sub>	Q <sub>av</sub>
19/8/2004											
Valve Type:	Diaphragm										
Valve diameter(mm):	80										
Valve position:	Open										
Pipe Diameter (mm):	80.43										
Material Type:	Kaolin 10%										
Density(kg/m <sup>3</sup> ):	1167.6										
γ:	10.000										
K:	1.588										
n:	0.300										
		51083.430	49288.816	47573.480	45129.668	41751.281	37802.164	36213.008	32667.404	30313.838	2.262
		50744.781	48783.129	47316.555	44796.117	41542.621	37443.012	35723.008	32021.381	30176.058	2.809
		51011.816	49077.901	47454.340	45241.191	41686.668	37610.313	35995.063	32069.178	30159.055	3.271
		51032.948	49081.469	47540.730	45379.477	41534.668	37573.457	36017.176	32004.230	30172.066	3.274



Table 48 HGL Test for kaolin 10%

		Axial distance									Average flow rate
		-6.413	-4.809	-3.61	-1.609	0.707	3.907	5.272	8.461	9.956	
Valve plane		0									
		Pod 1	Pod 2	Pod 3	Pod 4	Pod 5	Pod 6	Pod 7	Pod 8	Pod 9	
		Pa	Pa	Pa	Pa	Pa	Pa	Pa	Pa	Pa	[Pa]
16/02/2004											
Valve Type:	Diaphragm										
Valve dimension(mm):	50	43660.926	42751.316	41702.738	40103.136	38188.134	35599.703	34453.613	31862.109	30344.732	0.306
Valve position:	Open	48447.293	43188.645	44023.477	42159.434	39989.574	36956.703	33703.469	32627.869	31076.933	0.430
Pipe Diameter (mm):	80.43	48824.703	47267.445	46102.463	43574.956	41579.168	38271.160	36773.160	32401.916	31803.566	1.100
Material Type:	Kaolin 10%	49623.981	47186.988	46020.763	43540.160	41536.991	38257.025	36764.141	32353.693	31786.461	1.098
Density(kg/m <sup>3</sup> ):	1166	49448.898	47848.113	46665.027	44055.348	41963.934	38382.578	37136.242	33540.105	33025.512	1.446
T <sub>p</sub> :	10.000	50072.309	48407.039	47192.840	44591.316	42392.898	38883.884	37417.777	33851.625	33232.889	1.880
K:	1.568	49927.262	48476.230	47221.281	44620.883	42347.684	38957.172	37590.367	33968.775	33249.996	1.850
n:	0.5	44722.348	43451.582	41981.023	39747.316	37586.730	33998.438	32515.713	29262.991	27878.048	6.432
		44911.828	43140.367	41977.668	40682.797	37525.336	34194.384	32625.664	28452.339	27545.566	6.037
		44475.625	42302.362	42353.133	40169.992	37668.438	34370.367	32736.207	29052.986	27628.154	6.309
		43586.383	44026.148	42975.532	40728.238	38408.184	35304.815	32813.836	30766.304	29020.365	3.353
		44069.387	43833.020	42826.879	41181.043	38388.136	35106.504	33771.277	30317.678	29063.307	2.871
		43698.143	43788.736	42703.434	40672.313	37911.680	34986.977	33597.160	30328.726	28064.433	3.195

Table 49 HGL Test for kaolin 13%

		Axial distance									Average flow rate
		-6.307	-2.937	-1.885	-0.625	1.076	3.805	6.046	8.075	9.975	
Valve plane		0									
		Pod 1	Pod 2	Pod 3	Pod 4	Pod 5	Pod 6	Pod 7	Pod 8	Pod 9	
		ΔP <sub>1</sub>	ΔP <sub>2</sub>	ΔP <sub>3</sub>	ΔP <sub>4</sub>	ΔP <sub>5</sub>	ΔP <sub>6</sub>	ΔP <sub>7</sub>	ΔP <sub>8</sub>	ΔP <sub>9</sub>	[Pa]
10/5/2004											
Valve Type:	Diaphragm										
Valve dimension(mm):	40	0.000	14020.323	19278.629	24218.346	33758.066	44624.875	53186.039	63453.160	72275.461	0.303
Valve position:	Open	0.000	13725.393	20191.059	26326.980	34106.418	47954.582	57102.695	66364.336	75021.781	0.423
Pipe Diameter (mm):	42.12	0.000	13619.612	18768.127	26196.924	34842.871	46722.189	57375.680	66284.781	74971.700	0.428
Material Type:	Kaolin 13%	0.000	14813.058	19260.689	26667.922	36487.031	48300.477	58665.172	67927.289	73070.375	0.549
Density(kg/m <sup>3</sup> ):	1214	0.000	12913.122	19556.307	27893.697	37894.933	48183.016	58655.426	68134.492	77214.578	0.530
T <sub>p</sub> :	35.000	0.000	13211.420	20489.803	26931.869	35805.238	50018.672	60294.473	69904.273	79121.273	0.706
K:	0.99	0.000	13362.381	19312.055	26646.383	36365.500	49560.523	60278.574	69363.734	78945.188	0.711
n:	0.5	0.000	13578.240	20715.270	28197.979	37978.285	50675.605	62024.656	71850.336	81172.305	0.927
		0.000	16570.094	21636.711	27159.457	38588.758	51253.297	61283.516	71803.008	80965.000	0.932
		0.000	16752.389	20775.469	27546.904	39660.316	51993.469	64528.906	74332.141	82817.148	1.095
		0.000	15874.967	21911.182	27546.908	41444.836	53544.039	64288.829	74893.273	82830.750	1.089
		0.000	17319.020	21608.531	30053.572	44643.875	58218.445	69572.641	79516.695	89298.273	1.384
		0.000	16358.048	22477.395	28775.670	44393.887	58205.867	69354.977	79744.039	89509.936	1.386
		0.000	17618.291	23158.934	30638.785	46145.762	59242.902	70974.666	80697.203	90923.266	1.666
		0.000	15148.819	23087.898	26513.900	45913.730	59648.402	69918.609	80304.836	90539.969	1.664
		0.000	16366.205	22210.725	29169.412	42592.613	56939.980	67983.539	78662.313	88644.414	1.361
		0.000	17299.063	22879.742	29226.883	42528.992	56856.983	68313.984	78877.579	88566.633	1.356
		0.000	17888.621	23366.219	29640.369	45606.590	60089.375	71476.172	82211.789	92153.602	1.581
		0.000	18161.996	23287.180	29705.135	45645.586	59643.809	71780.781	82171.148	92236.680	1.576
		0.000	18029.727	23029.467	30017.254	47646.055	61671.605	72278.258	84207.578	94223.016	1.683
		0.000	18093.146	23504.957	29787.313	47261.266	61540.335	73757.664	84316.984	94510.031	1.692
		0.000	18177.121	23972.465	30288.547	49327.730	64138.965	75754.102	86274.267	96920.570	1.831
		0.000	17750.205	23917.139	30460.672	49492.805	62676.973	75973.625	86549.039	96678.211	1.836
		0.000	18310.697	24163.676	30845.018	51137.488	63573.969	77828.727	88523.875	99208.844	2.054
		0.000	18415.131	23939.498	30644.729	50842.430	63625.406	77728.891	88428.719	98894.016	2.051
		0.000	18483.773	23882.258	30598.966	52157.113	66454.219	78998.000	89917.164	100338.930	2.128
		0.000	18665.754	24283.053	30755.660	50989.707	65979.469	7814.609	89497.641	99642.641	2.095
		0.000	19120.897	24668.822	32063.881	56191.074	71241.172	81119.148	94375.719	105247.492	2.491
		0.000	18939.928	23778.084	31282.449	56236.047	71001.781	85353.320	94644.234	105168.602	2.491
		0.000	19366.391	24496.199	32589.539	56898.219	72429.781	85616.836	96253.609	107080.272	2.637
		0.000	18961.668	24826.426	32088.363	58007.207	72794.329	85091.586	96336.664	107011.492	2.637
		0.000	19943.234	24930.293	31477.928	59578.664	75113.636	87136.766	98767.895	109177.102	2.815
		0.000	19777.713	24936.371	31359.326	58742.121	75514.383	87465.742	98859.602	109308.172	2.807
		0.000	19961.816	24782.268	32930.922	61869.758	76348.984	89042.148	100649.375	111106.734	2.938
		0.000	19850.428	24759.766	31354.102	61304.051	76234.219	89186.102	100883.844	111170.836	2.942
		0.000	20069.572	24681.469	30470.516	64712.375	78687.383	91811.805	103241.219	114198.414	3.136
		0.000	19891.307	24690.551	32296.365	64263.328	79193.500	92059.633	102993.636	113849.930	3.136
		0.000	20126.240	24801.133	32649.031	66825.391	82476.250	94411.528	106744.867	116997.172	3.342
		0.000	17736.432	25522.465	32273.980	66604.259	81756.986	94255.422	106646.938	117125.211	3.351

Table 50 HGL Test for kaolin 13%

		Axial distance	-4.298	-4.568	-1.880	-0.621	1.076	3.805	6.046	8.075	9.975	
Valve plane		Pod 1	Pod 2	Pod 3	Pod 4	Pod 5	Pod 6	Pod 7	Pod 8	Pod 9	Average flow rate	
		$\Delta P_1$	$\Delta P_2$	$\Delta P_3$	$\Delta P_4$	$\Delta P_5$	$\Delta P_6$	$\Delta P_7$	$\Delta P_8$	$\Delta P_9$	[s]	
		$P_a$	$P_a$	$P_a$	$P_a$	$P_a$	$P_a$	$P_a$	$P_a$	$P_a$		
7/10/2004	Valve Type:	Diaphragm	0.000	0.000	0.000	0.000	0.000	0.000	0.000	0.000	0.200	
	Valve diameter (mm)	40	5942.124	17030.213	20363.252	28232.160	39306.746	46902.676	53246.871	62484.598	0.273	
	Valve position:	Open	0.000	0.000	0.000	0.000	0.000	0.000	0.000	0.000	0.369	
	Pipe Diameter (mm):	42.12	6419.931	17225.117	22988.203	29317.193	40362.406	49386.129	57235.332	64629.293	0.414	
	Material Type:	Kaolin 13%	0.000	0.000	0.000	0.000	0.000	0.000	0.000	0.000	0.421	
	Density (kg/m <sup>3</sup> ):	1208.6	0.000	0.000	0.000	0.000	0.000	0.000	0.000	0.000	0.761	
	Ty:	35.000	0.000	0.000	0.000	0.000	0.000	0.000	0.000	0.000	0.767	
	K:	0.5999	0.000	0.000	0.000	0.000	0.000	0.000	0.000	0.000	0.932	
	n:	0.5	0.000	0.000	0.000	0.000	0.000	0.000	0.000	0.000	0.910	
			7424.554	16234.957	27250.547	33772.438	48271.016	56789.125	66914.805	74829.492	0.919	
			0.000	0.000	0.000	0.000	0.000	0.000	0.000	0.000	0.906	
			0.000	0.000	0.000	0.000	0.000	0.000	0.000	0.000	0.918	
			0.000	0.000	0.000	0.000	0.000	0.000	0.000	0.000	1.277	
			0.000	0.000	0.000	0.000	0.000	0.000	0.000	0.000	1.407	
			0.000	0.000	0.000	0.000	0.000	0.000	0.000	0.000	1.497	
			0.000	0.000	0.000	0.000	0.000	0.000	0.000	0.000	1.459	
			0.000	0.000	0.000	0.000	0.000	0.000	0.000	0.000	1.463	
			0.000	0.000	0.000	0.000	0.000	0.000	0.000	0.000	1.600	
			0.000	0.000	0.000	0.000	0.000	0.000	0.000	0.000	1.614	
			0.000	0.000	0.000	0.000	0.000	0.000	0.000	0.000	1.771	
			0.000	0.000	0.000	0.000	0.000	0.000	0.000	0.000	1.778	
			0.000	0.000	0.000	0.000	0.000	0.000	0.000	0.000	1.973	
			0.000	0.000	0.000	0.000	0.000	0.000	0.000	0.000	1.568	
			0.000	0.000	0.000	0.000	0.000	0.000	0.000	0.000	1.824	
			0.000	0.000	0.000	0.000	0.000	0.000	0.000	0.000	1.824	
			0.000	0.000	0.000	0.000	0.000	0.000	0.000	0.000	1.897	
			0.000	0.000	0.000	0.000	0.000	0.000	0.000	0.000	1.901	
			0.000	0.000	0.000	0.000	0.000	0.000	0.000	0.000	2.089	
			0.000	0.000	0.000	0.000	0.000	0.000	0.000	0.000	2.065	
			0.000	0.000	0.000	0.000	0.000	0.000	0.000	0.000	2.290	
			0.000	0.000	0.000	0.000	0.000	0.000	0.000	0.000	2.299	
			0.000	0.000	0.000	0.000	0.000	0.000	0.000	0.000	2.411	
			0.000	0.000	0.000	0.000	0.000	0.000	0.000	0.000	2.413	
			0.000	0.000	0.000	0.000	0.000	0.000	0.000	0.000	2.591	
			0.000	0.000	0.000	0.000	0.000	0.000	0.000	0.000	2.926	
			0.000	0.000	0.000	0.000	0.000	0.000	0.000	0.000	3.043	
			0.000	0.000	0.000	0.000	0.000	0.000	0.000	0.000	3.213	
			0.000	0.000	0.000	0.000	0.000	0.000	0.000	0.000	3.355	



**Table 53 HGL Test for kaolin 13%**

		Axial distance									
		-5.47	-3.526	-2.281	-0.798	1.257	4.013	5.566	7.666	9.669	
		Valve phase									
		Post 1	Post 2	Post 3	Post 4	Post 5	Post 6	Post 7	Post 8	Post 9	Average Flow rate
		Pa	Pa	Pa	Pa	Pa	Pa	Pa	Pa	Pa	(l/s)
810/2004											
Valve Type:	Diaphragm	88071.230	81505.391	77017.648	71449.469	63696.895	53817.527	46682.668	35418.422	31974.428	1.759
Valve diameter(mm):	50	89542.445	82899.430	78281.219	72630.841	64717.926	54627.102	47292.793	35794.797	32948.372	2.174
Valve position:	Open	89955.648	83171.070	78363.719	72138.975	64299.059	54024.074	46474.063	36910.258	31173.996	2.594
Pipe Diameter (mm):	52.8	91327.370	84594.344	79923.555	73972.266	64985.742	54413.387	46723.324	36974.711	30929.766	3.077
Material Type:	Kaolin 13%	92216.137	85795.641	80826.544	74705.664	64998.582	54366.898	46762.168	38876.396	30886.273	3.354
Density(kg/m <sup>3</sup> ):	1210.2	94628.805	87288.905	82642.258	76249.856	64156.198	54177.324	46451.835	38842.707	31224.021	2.848
γ <sub>f</sub> :	30.000	89402.195	82745.891	78115.563	71964.625	64001.867	53726.852	46312.004	36766.238	31349.701	2.644
K:	1.200	88491.609	81975.991	77441.544	71905.227	63556.656	53476.553	46193.977	36813.965	31456.957	2.327
n:	0.619	87699.750	81741.319	77147.539	71664.008	63980.375	54117.105	46672.227	35461.983	32273.426	2.937
		85975.625	80210.914	75785.000	69942.391	62815.918	52940.016	46207.660	39074.422	32070.539	1.525
		84916.352	78235.614	73931.545	68413.906	61422.328	52144.027	45424.469	38557.879	31700.543	1.059
		81808.555	75970.977	71798.547	66869.781	59863.586	50996.301	44475.641	37881.987	31241.549	0.691

**Table 54 HGL Test for kaolin 13%**

		Axial distance									
		-6.9755	-4.9855	-2.885	-0.937	0.987	2.938	3.916	8.432	10.156	
		Valve phase									
		Post 1	Post 2	Post 3	Post 4	Post 5	Post 6	Post 7	Post 8	Post 9	Average Flow rate
		Pa	Pa	Pa	Pa	Pa	Pa	Pa	Pa	Pa	(l/s)
256/2004											
Valve Type:	Diaphragm	96407.047	88689.016	81397.844	74975.180	67637.078	60712.578	57240.664	43108.996	36269.294	1.879
Valve diameter(mm):	63	96223.883	88756.625	81512.533	74985.975	67580.133	60729.789	57289.086	43215.082	36284.855	1.844
Valve position:	Open	96379.944	88530.055	81170.544	75227.983	67928.091	60799.383	57428.951	43116.940	36316.617	2.018
Pipe Diameter (mm):	63.08	96287.414	88312.078	81136.516	75171.930	67907.992	60844.820	57603.250	43135.523	36331.445	2.011
Material Type:	Kaolin 13%	96977.727	89283.609	82330.500	75301.352	68170.391	61123.203	57993.382	43207.664	36437.352	2.177
Density(kg/m <sup>3</sup> ):	1219.9	96843.555	89200.867	82489.797	75209.406	68236.555	61126.512	57952.133	43240.994	36482.273	2.177
γ <sub>f</sub> :	35.000	96675.648	89193.766	81947.125	75445.164	68199.984	61003.113	57835.285	43650.348	36517.668	2.255
K:	1.500	96523.730	89570.078	82116.563	75333.516	68428.802	60926.887	57219.331	43644.609	36587.918	2.246
n:	0.500	97165.852	90133.867	82415.695	75836.336	68522.164	61297.266	57660.172	43821.023	36675.535	2.429
		97312.648	90170.391	82549.892	75854.484	68697.992	61185.117	57407.074	43825.238	36688.492	2.416
		97561.039	90218.578	82683.608	76262.891	68691.969	61601.281	57761.418	43974.754	36869.543	2.568
		97711.664	90218.391	82826.094	76568.906	68938.367	61780.516	57998.156	44057.633	36885.516	2.555
		98131.953	90705.555	83528.598	76590.703	68771.133	61975.371	57961.184	44184.137	37079.367	2.703
		98362.664	90990.641	83764.469	76315.975	69111.008	61956.582	58156.762	44249.734	37021.305	2.708
		97912.469	89997.882	82817.664	75977.609	68419.961	61525.418	57608.727	43706.313	36524.938	2.808
		97453.750	90221.289	83094.516	75671.313	68345.938	61372.992	57588.945	43620.723	36539.449	2.804
		97573.477	90393.956	82830.898	75432.656	68292.081	61544.953	57821.488	43642.863	36507.297	3.003
		97708.305	89888.609	82573.453	75811.625	68134.039	61376.305	57794.672	43595.691	36596.359	3.005
		97513.727	90228.754	83082.059	76164.141	68418.969	61512.590	57871.523	43828.965	36508.833	3.072
		98109.016	90440.992	83442.773	76298.016	68433.906	61522.230	57875.734	43808.344	36579.566	3.077
		96187.141	88330.977	81301.031	75799.867	68224.047	60895.348	55301.605	40868.547	33825.461	3.419
		96219.648	88448.102	81236.797	75843.672	68341.906	59215.957	55559.289	41076.129	33817.941	3.408
		96199.781	88359.227	81441.602	75867.570	68248.398	59088.773	55233.961	41007.082	33724.648	3.543
		96421.805	88623.698	81161.117	75556.430	68224.617	59228.793	54989.281	41028.668	34247.215	3.526
		96465.500	88638.961	81478.813	75644.672	68480.500	59148.340	54462.043	40787.703	33683.715	3.988
		96316.164	88973.180	81437.891	75621.203	68395.777	59092.621	53973.414	40283.576	34483.313	3.951
		97567.852	90068.844	82298.852	74890.250	68867.930	59613.328	54468.277	41150.172	33330.254	4.872
		98342.219	90122.896	82791.259	74965.906	67010.938	59802.094	55606.449	40920.228	33897.867	4.845

**Table 55 HGL Test for kaolin 13%**

		Axial distances									
		-4.9725	-4.8855	-2.885	-0.977	0.987	2.978	3.916	8.472	10.156	
		Valve phase									
		Pod 1	Pod 2	Pod 3	Pod 4	Pod 5	Pod 6	Pod 7	Pod 8	Pod 9	Average Flow rate
		Pa	Pa	Pa	Pa	Pa	Pa	Pa	Pa	Pa	[l/s]
27/6/2004											
Valve Type	Diaphragm	97630.273	89567.519	82167.141	74592.339	66703.922	59439.363	51579.426	38222.031	23813.914	5.003
Valve diameter [mm]	63	109131.320	100774.258	92718.500	84622.914	76485.102	68780.789	64829.445	45262.535	41466.256	5.360
Valve position	Open	108463.063	100012.125	92227.977	84007.986	75675.672	67938.773	62933.484	45953.566	40355.847	5.193
Pipe Diameter [mm]	63.08	108464.703	101134.855	93126.339	85136.336	76784.867	68996.123	64501.410	45302.980	41463.590	5.365
Material Type	Kaolin 13%	108515.477	101125.273	93169.787	85127.008	76743.117	69011.086	64681.418	45286.461	41318.664	5.345
Density [kg/m <sup>3</sup> ]	1209.9	108716.078	101280.477	93458.352	85229.063	76990.211	69187.961	64314.320	45324.141	41523.254	4.287
Tp	25.000	108922.331	101388.945	93411.236	85247.313	76885.133	69114.313	63627.984	45853.566	41431.928	4.075
K	1.800	110165.102	101953.945	93639.055	85673.984	77383.156	69227.141	63759.941	45645.141	41543.230	4.261
n	0.500	110669.555	102174.695	93987.406	86015.211	77254.602	69403.305	63719.523	45644.156	41515.813	4.251
		111071.125	102569.305	94568.789	86507.219	77721.422	69862.891	63877.329	45823.529	41829.713	4.398
		111451.352	102824.609	94651.702	86505.195	77718.516	69883.898	63878.079	45844.227	41863.137	4.614
		111695.328	103138.641	94759.148	86532.305	78021.742	70291.531	63962.669	45815.348	41968.967	4.891
		112193.430	103382.622	95200.570	87547.125	78100.867	70229.477	64199.313	45829.626	42187.624	4.881
		112691.789	103622.102	95777.570	88109.461	78333.625	70576.648	64623.445	45822.703	42254.864	5.080
		112840.406	104054.063	96143.891	87813.648	78651.094	70824.961	64719.773	46142.707	42340.469	5.045
		112811.289	103596.227	96654.211	88304.047	79232.456	71140.125	65028.125	46268.125	42430.369	5.202
		112902.734	104638.287	96704.430	88618.227	79254.234	71335.758	66097.766	46159.672	42534.138	5.206
		112946.383	105070.656	96777.172	88634.963	79412.836	71378.928	67433.875	46423.840	42589.694	5.283
		112913.000	105940.247	96957.781	88768.742	79371.898	71099.914	67093.620	46313.328	42478.277	5.158
		104143.602	96658.180	89196.047	81740.802	74084.586	66567.633	62871.141	46879.035	40678.051	2.289
		100343.102	92212.438	84447.766	76887.320	66699.414	61054.584	57387.801	41542.730	34633.273	3.846
		104943.273	93806.719	87842.641	78822.602	71151.070	63422.434	59200.893	42828.488	35122.082	3.418
		105419.227	97186.102	88910.578	80745.945	71934.688	63781.058	55692.178	42029.473	33759.503	5.804
		107034.305	99340.875	90759.859	82272.336	72823.230	63087.801	60882.906	39183.789	35546.787	7.033

**Table 56 HGL Test for kaolin 13%**

		Axial distances									
		-6.012	-4.809	-3.61	-1.609	0.707	3.007	5.273	8.461	9.956	
		Valve phase									
		Pod 1	Pod 2	Pod 3	Pod 4	Pod 5	Pod 6	Pod 7	Pod 8	Pod 9	Average Flow rate
		Pa	Pa	Pa	Pa	Pa	Pa	Pa	Pa	Pa	[l/s]
8/10/2004											
Valve Type	Diaphragm	67586.422	63264.262	62254.563	58483.891	53172.305	46371.793	43473.105	34826.363	31253.180	0.179
Valve diameter [mm]	80	67823.906	63347.945	62022.574	58305.633	53205.375	46381.314	43460.813	36776.898	33361.433	0.272
Valve position	Open	67946.594	63766.438	63173.543	58782.945	53458.273	46614.340	43670.734	36990.830	33728.781	0.546
Pipe Diameter [mm]	80.43	68344.000	63998.703	63452.590	59059.180	53647.270	46766.238	43825.872	37123.402	33819.684	1.390
Material Type	Kaolin 13%	68497.539	64242.148	63637.567	59119.922	53791.884	46899.998	43931.074	37278.863	33862.602	1.275
Density [kg/m <sup>3</sup> ]	1210.2	69060.531	64870.344	64233.602	59540.121	54301.402	47360.699	44322.441	37406.227	34102.586	1.539
Tp	29.000	69235.141	64977.949	64399.313	58423.086	53299.066	46423.895	43298.781	36427.410	33045.449	1.827
K	1.500	69127.227	64637.766	63643.848	58289.805	53518.836	46434.457	43409.582	36391.883	33134.066	2.089
n	0.300	69195.750	64547.996	63703.727	58226.426	53699.348	46396.941	43476.242	36427.324	33143.484	2.318
		69367.766	64951.094	64325.723	58294.652	53872.996	46675.191	43593.770	36598.803	33230.852	2.594
		69826.484	67221.303	64496.402	59188.901	53822.996	46898.164	43806.422	36640.477	33127.063	2.788
		67281.008	67523.781	64938.480	59636.395	54196.387	47007.113	43870.836	36645.109	33029.521	3.088
		70753.633	68203.445	65473.510	60444.844	54528.672	47471.738	44417.933	37023.031	33777.012	3.352
		71590.469	69014.227	66205.984	61362.223	55109.691	48025.020	44537.234	37640.965	34182.223	3.309
		71454.008	68723.023	66064.383	61151.793	54643.473	47568.255	44340.813	37026.578	33849.691	3.803
		71131.180	69112.469	66372.992	61633.895	54849.566	47660.078	44456.988	37118.270	33621.730	4.093
		72049.547	69744.086	66589.578	61654.715	55114.684	47719.255	44609.020	37196.539	33741.402	4.234
		72941.820	70094.711	67069.336	62040.371	55040.025	47858.242	44598.332	37009.938	33604.856	4.462
		73163.656	69740.125	67059.016	62154.254	55364.220	48010.738	45001.519	37217.727	33754.922	4.808
		73303.234	70196.766	67670.561	62039.895	55389.145	47962.398	44719.863	37452.211	33790.762	5.075
		74200.125	71547.236	68498.258	63071.832	55202.488	48022.848	43074.242	37322.742	33669.789	5.526

Table 57 HGL Test for kaolin 13%

		Axial distances									Average Flow rate (m <sup>3</sup> /s)
Valve phase		4.413	4.809	3.41	1.609	0.707	3.907	5.273	9.441	9.936	
		Pod 1	Pod 2	Pod 3	Pod 4	Pod 5	Pod 6	Pod 7	Pod 8	Pod 9	
		Pa	Pa	Pa	Pa	Pa	Pa	Pa	Pa	Pa	
27/9/2014											
Valve Type:	Diaphragm	72457.813	69113.269	66213.263	61237.816	55159.843	47819.263	44674.121	27186.746	23320.078	2.879
Valve diameter(mm):	80	72174.680	68922.477	66101.562	60990.555	55293.664	47719.426	44473.176	26661.122	23475.219	2.843
Valve position:	Open	72321.648	69150.247	66291.827	61547.781	55314.622	47785.839	44387.378	26726.844	23522.023	2.920
Pipe Diameter (mm):	80.43	72382.213	69171.84	66293.243	61384.283	55210.434	47528.949	44396.821	26471.024	23664.273	3.054
Material Type:	Kaolin 13%	72281.303	69149.920	66723.275	61780.875	55300.781	47459.231	44730.945	26499.043	24028.875	3.361
Density(kg/m <sup>3</sup> ):	1200	72297.727	69117.658	67080.383	61443.230	55961.339	47672.247	44582.469	26703.223	23887.015	3.349
Ty:	29.000	72618.211	70854.445	67704.275	67112.484	56261.488	48226.406	44948.819	27394.828	24292.309	3.708
K:	1.500	74111.928	71315.445	68820.703	62220.676	56331.841	48654.738	45393.535	27185.433	25110.207	3.705
tc:	0.300	75410.727	71673.883	68478.738	63925.212	56611.227	49311.906	46347.758	28226.344	24729.043	3.925
		74801.227	71624.594	68873.391	63873.160	56311.207	49430.391	45256.637	28202.637	24549.188	3.920
		73284.156	69233.711	65647.636	61049.222	53870.498	47198.004	44475.840	27075.984	24075.200	4.188
		72213.242	68818.234	65992.406	61232.875	54113.273	47247.901	44399.031	27020.809	23646.236	4.189
		73502.828	69418.758	66715.531	62039.668	55097.363	48093.977	44817.703	27428.293	24021.823	4.301
		72195.602	69649.078	66826.730	61873.864	54934.941	47926.423	44669.914	27195.828	24000.123	4.286
		73154.242	69614.233	67036.509	62030.112	55225.441	47924.156	44626.086	27215.884	23998.528	4.495
		72805.891	69430.873	67014.479	62256.191	55247.066	48021.723	44872.229	27221.082	23724.488	4.522
		73567.600	70119.633	67624.813	62218.245	55227.817	48063.283	44922.245	27413.922	23946.234	4.646
		73119.432	70202.898	67166.294	62178.242	55176.021	48189.297	44988.633	27383.388	23945.283	4.680
		74229.347	70891.969	67521.158	62580.020	54699.220	48261.801	45028.469	27443.469	24028.245	4.836
		73328.430	70493.200	67597.991	62790.426	54475.648	48212.731	44782.426	27426.484	24040.292	4.868
		74566.125	70499.180	67895.266	62634.045	54471.553	48274.883	44923.707	27411.984	23841.859	5.209
		74471.282	70986.203	67692.170	62729.473	54584.074	48128.295	45076.734	27447.000	24344.723	5.210
		75140.812	71629.195	68486.272	62946.926	54971.141	48542.148	45280.070	27781.926	24099.123	5.544
		75166.953	71622.406	68290.328	63778.933	54526.320	48228.328	44990.215	27620.746	24078.449	5.536
		75449.586	71277.844	68561.563	63694.234	54526.773	48248.047	45223.289	27620.291	24049.238	5.702
		75104.477	71718.236	68720.123	63620.176	54526.449	48423.121	45220.160	27704.992	24031.025	5.677
		73161.945	70414.305	67864.245	62993.234	54712.224	47941.586	45003.285	27283.414	23971.208	5.113
		74429.766	70848.922	68000.272	62090.112	53640.426	48189.125	45104.191	27716.551	24010.121	5.084
		73363.992	70527.973	67801.021	62008.814	53467.539	48003.578	44866.414	27616.168	24210.203	4.725
		73882.819	70522.156	67649.636	62826.926	53623.543	48254.265	44819.215	27568.781	24219.773	4.757
		73846.820	70212.203	67214.461	62494.721	53706.490	48023.703	45137.902	27670.015	24146.465	4.413
		74137.461	70118.781	67022.216	62338.228	53540.899	48293.379	44972.563	27726.922	24152.566	4.411
		72599.287	69162.695	66138.742	61728.578	54967.622	47660.282	44713.924	27227.145	23757.379	3.999
		72302.773	69217.586	66344.208	61781.020	55000.969	47819.903	44726.277	27226.300	23798.160	3.978
		70755.742	67418.235	64838.281	60096.223	53843.296	46854.066	43897.318	26643.180	23112.244	3.262
		69498.141	66204.269	63647.379	59120.566	53287.374	46223.719	43229.188	26325.070	22930.227	2.487